DOCTOR OF PHILOSOPHY

Soil erosion and suspended sediment dynamics in intensive agricultural catchments

Sherriff, Sophie C.

Award date:
2015

Doctor of Philosophy

Soil erosion and suspended sediment dynamics in intensive agricultural catchments

Sophie C. Sherriff

Doctor of Philosophy

University of Dundee

December 2015

Table of Contents

List of Figures

List of Tables

Abbreviations

ACP	Agricultural Catchments Programme
ARM	Anhysteretic Remanence Magnetisation
$bIRM_x$	backfield Isothermal Remanence Magnetisation
CAP	Common Agricultural Policy
Cd	Cadmium
Co	Cobalt
Cr	Chromium
Cu	Copper
CV%	Coefficient of Variance (%)
DM	Diffusion and Migration model
EIA	Environmental Impact Assessment
Event-SSC_{fw}	Flow-weighted storm event suspended sediment concentration
FFD	Freshwater Fish Directive
GAEC	Good Agricultural and Environmental Condition
GLAS	Green Low-carbon Agri-environment Scheme
GOF	Goodness of Fit
HI	Hysteresis Index
IRM_x	Isothermal Remanent Magnetisation
LPIS	Land Parcel Identification System
MB2	Mass Balance 2 model
Mn	Manganese
MDA	Multiple Discriminant Analysis
N	Nitrogen
NAP	National Action Programme
Ni	Nickel
NTU	Nephlometric Turbidity Units
P	Phosphorus
Pb	Lead
Q	Discharge
SDR	Sediment Delivery Ratio
SIRM	Saturation Isothermal Remanence Magnetism
SS	Suspended Sediment

SSC	Suspended Sediment Concentration
SSL	Suspended Sediment Load
SSY	Suspended Sediment Yield
ST_{max}	Maximum potential sediment transfer quantity
T	Turbidity
TC	Total Carbon
TN	Total Nitrogen
TOC	Total Organic Carbon
WFD	Water Framework Directive
χ_{HF}	High-frequency magnetic susceptibility
χ_{LF}	Low-frequency magnetic susceptibility
Zn	Zinc
$\%\chi_{FD}$	Frequency dependent magnetic susceptibility

Acknowledgements

Firstly, I would like to thank my supervisory team, Prof John Rowan (University of Dundee), Drs Daire Ó hUallacháin and Owen Fenton (Teagasc), Prof Phil Jordan (Ulster University) and Dr Alice Melland (University of Southern Queensland) who from the start to the very end were the most positive, enthusiastic and supportive team I could have hoped for, and from their knowledge and guidance, I have learned so much.

I am extremely grateful for funding from the Walsh Fellowship Programme (Teagasc). I also acknowledge financial support from the Walsh Fellowship Overseas Travel Award and the Australian Bicentennial Scholarship Fund (Kings College London) for supporting placements to the University of St Andrews and University of Tasmania, respectively. Dr John Walden (University of St Andrews) is thanked for access to the Environmental Magnetism Laboratory and Prof Stewart Franks (University of Tasmania) is thanked for contributing funding, time and expert knowledge on sediment fingerprinting un-mixing models. I am also deeply appreciative for laboratory support from Craig Phillips for radionuclide analysis (University of Dundee), and Linda Maloney-Finn and Carmel O'Connor (Teagasc) for geochemistry and carbon analysis.

I am indebted to the Agricultural Catchments Programme team, who allowed me access to their study sites, equipment, data, and breadth and depth of knowledge. In particular, I thank Dr Per-Erik Mellander for his time and expertise, and John Kennedy and Eddie Burgess for fieldwork support. I would also like to thank the farmers and landowners of the study catchments.

Thanks to all at Teagasc Johnstown Castle who have made my PhD such a positive experience. In particular I thank Noeleen, Mairead, Dominika, Sara, Orlaith, Mary, Leanne, Andrea and all past WMBSoc members for their friendship and culinary talents. Also, many thanks to colleagues in CECHR and the Geography department at the University of Dundee for being so welcoming and inclusive every time I visited. Special thanks go to Sarah, Kelly, Emily, Heather and Jodie whose friendship and laughter made the holidays an enjoyable distraction!

Finally, I thank my family, my parents Sharon and Gary, and sister, Emma, whose love and encouragement have always been an enormous support.

Declaration

The material contained in this thesis has not been previously submitted for a higher degree in this or any other institution. Unless otherwise stated, all references have been consulted by the author. The work of which the thesis is a record has been done by the author except where otherwise acknowledged.

Sophie C. Sherriff

Abstract

Excessive delivery of fine sediment from agricultural river catchments to aquatic ecosystems can degrade chemical water quality and ecological habitats. Management of accelerated soil losses and the transmission of sediment-associated agricultural pollutants, such as phosphorus, is required to mitigate the drive towards sustainable intensification to increase global food security. Quantifying soil erosion and the pathways and fate of fine-grained sediment is presently under-researched worldwide, and particularly in Ireland. This thesis established a sediment monitoring network upon an existing catchment study programme (Agricultural Catchments Programme) in five instrumented catchments (~10 km^2) across Ireland. The research used novel, high quality measurement and analysis techniques to quantify sediment export, determine controls on soil erosion and sediment transport, and identify sediment contributions from multiple sources in different agricultural systems over time to evaluate approaches to fine sediment management.

Results showed suspended sediment measurement using a novel *ex situ* methodology was valid in two of the study catchments against *in situ* and direct depth-integrated cross-section methodologies. Suspended sediment yields in the five intensive agricultural catchments were relatively low compared to European catchments in the same climatic zone, attributed to regionally-specific land use patterns and land management practices expressed in terms of 'landscape complexity' (irregular, small field sizes partitioned by abundant hedgerows and high drainage ditch densities) resulting in low field-to-channel connectivity. Variations in suspended sediment yield between catchments were explained primarily by soil permeability and ground cover, whereby arable land use on poorly-drained soils were associated with the largest sediment yields.

Storm-event sediment export and sediment fingerprinting data demonstrated that sediment connectivity fluctuations resulted from rainfall seasonality, which in turn regulated the contrasting spatial and temporal extent of surface hydrological pathways. Increased transport occurred when and where sediment sources were available as a result of hillslope land use (low groundcover) or channel characteristics. Field topsoils were most vulnerable when low groundcover coincided with surface hydrological pathways; frequently on poorly-drained soils and following extreme rainfall events on

well-drained soils as storage decreased. Although well-drained soils currently demonstrate low water erosion risk, past sugar beet crops exposed freshly drilled soils during periods of greater rainfall risk and soil removal during crop harvesting. Sediment loss from grassland catchments dominated by poorly-drained soils and extensive land drainage (sub-surface and surface) primarily derived from channel banks due to the delivery of high velocity flows from up-catchment drained hillslopes. Catchment specific soil erosion and sediment loss mitigation measures are imperative to cost-effectively preserve or improve soil and freshwater ecosystem quality worldwide.

Published works

The following chapters have been published or under-review in peer-reviewed journals as cited below:

Chapter 3: Sherriff, S.C., Rowan, J.S., Melland, A.R., Jordan, P., Fenton, O, Ó hUallacháin, D. (2015a) Investigating suspended sediment dynamics in contrasting agricultural catchments using ex-situ turbidity-based suspended sediment monitoring, *Hydrology and Earth System Sciences*, 19, 3349-3363. Impact factor: 3.535 – Appendix 1.

Chapter 4: Sherriff, S.C., Rowan, J.S., Fenton, O., Jordan, P., Melland, A.R., Mellander, P.-E., Ó hUallacháin, D. (2016) Storm event suspended sediment-discharge hysteresis and controls in agricultural watersheds: implications for watershed scale sediment management, *Environmental Science & Technology*, 50, (4), 1769-1778. http://pubs.acs.org/doi/abs/10.1021/acs.est.5b04573 Impact factor: 5.330 – Appendix 2.

Chapter 5: Sherriff, S.C., Franks, S.W., Rowan, J.S., Fenton, O., Ó hUallacháin, D. (2015b) Uncertainty-based assessment of tracer selection, tracer non-conservativeness and multiple solutions in sediment fingerprinting using synthetic and field data, *Journal of Soils and Sediments*, 15, (10), 2101-2116. Impact factor: 2.139 – Appendix 3.

Chapter 1. Introduction, Literature Review and Aims

1.1 Introduction

The deterioration of soil and water quality worldwide has been attributed to the intensification and expansion of agricultural land use (Foley *et al.*, 2005; Raymond *et al.*, 2008; Quinton *et al.*, 2010). The growing demand for food due to an increasing global population means the reversion of agricultural land to pre-development conditions to improve the sustainability of land and aquatic ecosystems is largely idealistic and costly (Rickson, 2014). Effective management is, therefore, required to alleviate the negative environmental impacts of pollutant delivery from agricultural land whilst maintaining production.

Soil erosion and enhanced delivery of sediment into channel networks are natural processes enhanced by intensive land uses such as agriculture. Excessive loss of soil from agricultural landscapes preferentially depletes fine sediment, sediment-associated nutrients such as phosphorus (P), and organic matter which are crucial components of healthy soil systems required to sustain agricultural production (Van Oost *et al.*, 2007; Creamer *et al.*, 2010). However, the principal motivation for sediment studies are off-site environmental impacts including impaired chemical, ecological and physical river condition due to accelerated transport and delivery of eroded sediment and associated nutrients into aquatic ecosystems (Kemp *et al.*, 2011; Kjelland *et al.*, 2015).

In Europe, the preservation or improvement of water quality is legislated under the European Union Water Framework Directive (WFD – OJEU, 2000; Ballantine *et al.*, 2009). This requires that water bodies in Member States achieve "good" chemical and ecological water quality compared to an appropriate reference condition. Under the WFD, management of water quality requires a holistic, inter-disciplinary and catchment-based approach which also considers the chemical water quality and hydro-geomorphic condition of river channels. Water quality impacts from agriculture are regulated under the Nitrates Directive (OJEU 1991) within the WFD, however this legislation is focussed on the nutrients nitrogen (N) and P with no reference to sediment. The repealed Freshwater Fish Directive (OJEU, 2006) stipulated an annual average suspended sediment threshold for salmonid habitats. However, to mitigate wider ecological impacts more information is needed on the impacts of suspended and

deposited sediment on a range of aquatic species and their life-stage (Collins *et al.*, 2011). Despite the recognition that fine sediments are the "most widespread and detrimental forms of aquatic pollution" (Jones *et al.*, 2011a; pp. 1055), no sediment thresholds currently exist in European policy (Brils, 2008; Collins and Anthony, 2008). Regulation of sediment delivery in agricultural catchments is, therefore, frequently considered through P which has a high affinity with particulate transport.

Sediment management strategies require robust determination of sediment flux (Navratil *et al.*, 2011), knowledge of the sources and fate of fine sediments within the catchment system (Walling, 2005), and an appreciation of the risks that elevated sediment concentrations present to aquatic ecosystems (Bilotta and Brazier, 2008). In agricultural catchments, the hydrologic and geomorphic responses are intensified by reduced lag times and elevated sediment concentration and flux patterns (Walling and Webb, 1988; Wass and Leeks, 1999) as a consequence of land use (grassland versus arable) and the extent and efficiency of artificial drainage networks (Vought and Lacoursiére, 2010; Shore *et al.*, 2013).Where negative impacts on aquatic ecosystems are identified, remediation must address multiple stressors (Matthei *et al.*, 2010).

Designation of priority sediment management areas in agricultural catchments is challenged by our ability to disentangle the complexity of static and variable environmental and land use processes. The impact of many agricultural land management processes on soil erosion or sediment loss have been measured or approximated at plot and field scales (Boardman and Favis-Mortlock, 2014; Rickson, 2014). However, the resource intensiveness of data collection at the wider catchment management unit and the scale dependency of environmental processes governing the erosion, entrainment, transport and deposition of sediment particles, make the robust and cost-effective determination of sediment sources a continued area of interest in agricultural catchments.

1.2 Literature review

Intensive agriculture has elevated soil erosion and suspended sediment yields throughout Europe (Van Oost *et al.*, 2009; Cerdan *et al.*, 2010; Foucher *et al.*, 2014). In Ireland, over 50% of land is utilised for agriculture (European average 40%), which is primarily permanent pasture based farming enterprises such as grazing for dairy and beef cattle, and sheep (CSO, 2015). Agricultural production from arable systems in the south-east of Ireland and intensive milk production in the south of Ireland are comparable with intensive systems worldwide (Melland *et al.*, 2012a; Murphy *et al.*, 2015) but modelled country-wide soil erosion rates are low compared to elsewhere in Europe (Panagos *et al.*, 2015). There is a paucity of high quality field evidence regarding catchment suspended sediment yields, but where available, suggests rates are similarly low (Melland *et al.*, 2012a; Harrington and Harrington, 2013, Thompson *et al.*, 2014). Recent policy drives to increase production through 'sustainable intensification' (Food Harvest, (DAFF, 2010) and Food Wise (DAFM, 2015)) emphasise the need to better understand the fate of eroded soil across different agricultural landscapes.

1.2.1 Landscape complexity and soil loss in Ireland

Soil erosion by water is suggested to be the principal erosion mechanism in Ireland (Fay *et al.*, 2002; Regan *et al.*, 2012). In agricultural landscapes, ground cover and soil management have significantly altered the soil erosion risk relative to natural and semi-natural vegetation cover. At the plot scale, reduced groundcover increases the exposure of soil surfaces to detachment by raindrop impact and downslope transport by surface runoff, typically a combination of infiltration-excess and saturation-excess flow (Bryan, 2000). Vegetation acts to intercept and dissipate rainfall energy, and increase surface roughness which adds flow resistance, mechanical strength and promotes water infiltration which suppresses entrainment and transport (Rachmann *et al.*, 2003; Zhang *et al.*, 2003). On arable land, periods of low groundcover between cropping cycles or adjacent to row crops such as potatoes and maize are 'windows of opportunity' for soil erosion (Boardman and Favis-Mortlock, 2014; Boardman, 2015). Intensively-managed grasslands are also an increasingly acknowledged sediment source (Bilotta *et al.*, 2010) where high stocking densities increase the likelihood of compaction, mechanical poaching and greater exposure of bare-ground due to over-grazing (Bilotta *et al.*, 2007a)

which increases runoff and the associated transport of particle-bound pollutants, such as P (Haygarth *et al.*, 2006).

At the field-scale, soil properties become increasingly heterogeneous (Figure 1.1) which influences permeability and the distribution of hydrological flow pathways. For example, well-drained soils, such as Brown Earths and Podzols commonly located on hillslopes, contribute sediment predominantly through sub-surface pathways. Conversely, poorly-drained soils, such as Gleys (surface and groundwater) and alluvium, are at greater risk of overland-flow generation and surface soil erosion due to reduced permeability. Micro-topography is also detectable at this scale, acting to concentrate overland flow energy into discrete channels (rill networks) and encourage deposition in hollows (Bryan, 2000; Darboux *et al.*, 2003; Shore *et al.*, 2013).

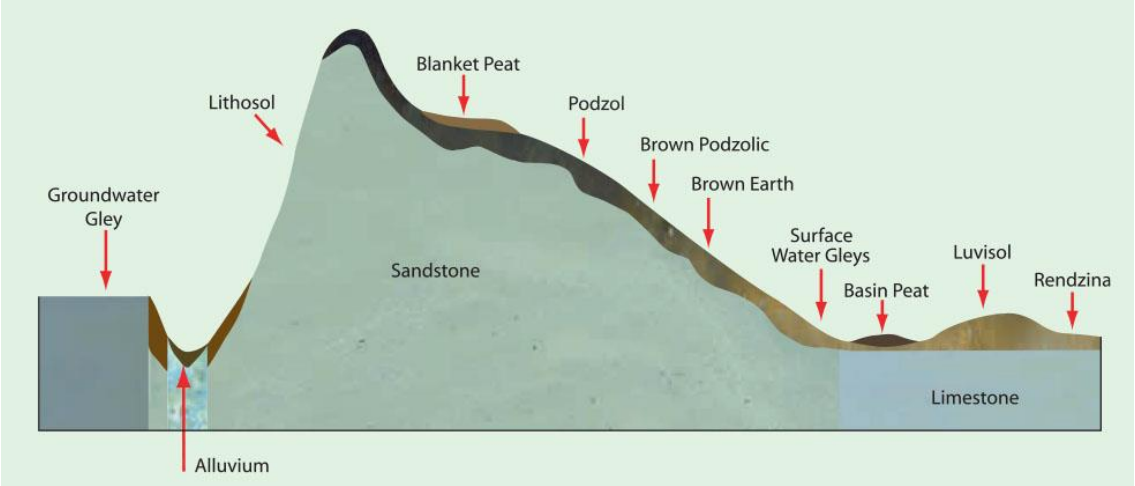

Figure 1.1. Schematic diagram of a typical Irish soil landscapes and resultant soil types. (from: Anon, 2013).

In conventionally ploughed arable systems (as opposed to minimum or no-till systems), tillage erosion redistributes soil downslope within fields (Van Oost *et al.*, 2007; Soane *et al.*, 2012). Without appropriate management, tramline wheelings (Figure 1.2) act as a conduit for flow promoting the initiation of rill networks (Silgram *et al.*, 2010; Rickson, 2014; Boardman, 2015). In grasslands, compacted areas where stock are frequently concentrated (such as near gateways) or areas of congregation such as drinking troughs increase soil erosion risk through degraded soil structures (Bilotta *et al.*, 2007b; Palmer and Smith, 2013). In particular, stock access to areas of high connectivity or direct stream access can contribute to sediment erosion by poaching (Trimble and Mendel, 1995; Evans *et al.*, 2006).

Figure 1.2. Downslope tramlines in arable field in north-east Ireland.

Intensification of arable agriculture across Europe has resulted in significant landscape reconfiguration (Medley *et al.*, 1995; Baessler and Klotz, 2006). Increased field size, utilisable land area, on-field trafficking, stocking densities and artificial drainage reduce landscape complexity and enhance soil erosion and sediment transport (Huang and O'Connell, 2000; Withers *et al.*, 2006; Foucher *et al.*, 2014). Removal of field boundaries and hedgerows reduces interception of surface flow pathways and deposition of sediments in transport (Lacoste *et al.*, 2014). The resulting larger fields have increased hydrological connectivity and slope-length i.e., potential size of rill networks or area susceptible to sheet-flow (Boardman, 2015). In Ireland, however, landscape features have been largely preserved relative to other European countries (Figure 1.3). The dominance of grass based farming enterprises has lessened field amalgamation to accommodate machinery which potentially reduces soil loss risk (Deverell *et al.*, 2009).

Artificial drainage, through surface (ditches) and sub-surface drainage (drains), installed to enhance production from low permeability soils, is widespread across agricultural areas in Ireland (O'Sullivan *et al.*, 2015). As a result, natural flow pathways and connectivity are modified (Ibrahim *et al.*, 2013; Shore *et al.*, 2013). Drainage emplacement and maintenance, for example, can result in faster quick-flow, resulting in an increased likelihood of more frequent, higher magnitude and short duration sediment transfers associated with storm runoff (Wiskow and van der Ploeg, 2003; Deasy *et al.*, 2009; Florsheim *et al.*, 2011). Ditches and river channels have also been suggested to facilitate sediment deposition and storage (Rehg *et al.*, 2005; Duerdoth *et al.*, 2015;

Figure 1.3. Aerial imagery of intensive agricultural systems at identical scales in a) Ireland, b) the United Kingdom and, c) the Netherlands. Source: Google Maps.

Shore *et al.*, 2015). Eroding channel banks, with high and consistent hydrological connectivity, and increased erosion sensitivity due to shallow topsoil root networks, low vegetation cover, natural bank erodibility and/or acceleration by stock or vehicle access are also important sediment sources in agricultural catchments (Figure 1.4 – Lefrançois *et al.*, 2007; Lamba *et al.*, 2015). Other potential sediment sources include un-metalled farm tracks (compacted and un-vegetated areas for vehicle or stock trafficking which act as conduits for excess surface water) or grass road verges damaged by vehicle wheels on narrow roads (Collins *et al.*, 2010a; Boardman, 2013).

Figure 1.4. Acceleration of bank erosion by poaching.

Sediment loss from individual sources at specific scales may be measured with a reasonable level of certainty (Regan *et al.*, 2010; Veihe *et al.*, 2011). However, sediment delivery at the catchment scale is related to the efficacy and capacity of hydrological routing dynamics. Surface flow pathways dominate particulate transport (Walling *et al.*, 1999; Mellander *et al.*, 2015) although significant losses can be attributed to sub-surface pathways in catchments with extensive artificial sub-surface drainage (Deasy *et al.*, 2009). Surface flow primarily results from saturation-excess overland flow in temperate climates where received moisture (from groundwater, upslope or rainfall) exceeds the water holding capacity of a soil (Kirkby, 1978). Surface and sub-surface hydrological pathways are spatially and temporally variable and are only significant for sediment delivery where and when they are hydrologically connected to the channel network (Fryirs *et al.*, 2007; Shore *et al.*, 2013). Bracken and Croke (2007) described attributes of structural connectivity to comprise stable landscape components such as slope lengths, form and soil drainage, and dynamic connectivity

comprising variable landscape components such as land use, antecedent conditions and rainfall event characteristics. Where sediment availability and hydrological connectivity coincide, critical source areas are established, which are responsible for a disproportionately larger sediment supply compared to the rest of the catchment (Thompson *et al.*, 2013b).

Figure 1.5. Saturation excess sediment-laden runoff connecting with main stem channel flow during extended storm event (Grassland B).

1.2.2 Erosion and sediment delivery in heterogeneous (complex) agricultural agro-ecosystems

Agro-ecosystems focussed on food production can be defined by a modification gradient. These span from unenclosed, low intensity grazing regimes to intensive grassland/arable systems with a myriad of irregularly sized and shaped fields (bounded by walls, fences, hedgerows and ditches) which create complex and fragmented land cover patterns. Erosion and sediment delivery processes in the latter are intrinsically more complex and present greater challenges to measure and model erosion rates and sediment delivery. Responding to the need for high resolution field data, recent developments have involved out-of-channel monitoring kiosks capable of high resolution measurements of water quality parameters (Jordan and Cassidy, 2011; Wall *et al.*, 2011; Owen *et al.*, 2012). Such approaches are designed to overcome common pitfalls of sediment estimation such as inconsistency of power supply, bio-fouling and

inaccurate data recording due to in-stream debris (Wass and Leeks, 1999; Jordan *et al.*, 2007). Validation of novel methodologies alongside established 'gold standard' approaches is imperative to assure robust estimation of pollutant fluxes but are absent to date.

Catchment management plans aiming to reduce contemporary suspended sediment yields (SSYs) typically bench-mark against pre-agricultural base line fluxes approximated by paleolimnological reconstruction (Walling *et al.*, 2007; Foster *et al.*, 2011). Studies reconstructing SSYs in Ireland are limited in number; Huang and O'Connell (2000) estimated yields of 14 t km^{-2} yr^{-1} during a phase of agricultural quiescence from 1898-1973 in north-west Ireland (maximum rate 58 t km^{-2} yr^{-1} from 1835-1850 attributed to population increases) and 25 t km^{-2} yr^{-1} from 1973-1991 (Figure 1.6). Jordan *et al.* (2002), however, reported more consistent yields of roughly 10 t/km^2/yr from 1915-1995 in north-east Ireland. Contemporary yields vary between 3 and 44 t km^{-2} yr^{-1} (Melland *et al.*, 2012a; Harrington and Harrington, 2013; Thompson *et al.*, 2014), the range attributed to catchment sizes, shapes and land uses. Simultaneous multi-catchment studies offer unique opportunities to investigate the impacts of climate and land use disturbances on sediment exports. A dedicated assessment of the influence of contrasting agricultural systems on sediment dynamics has not been assessed to date in Ireland but is essential to target cost-effective sediment management strategies.

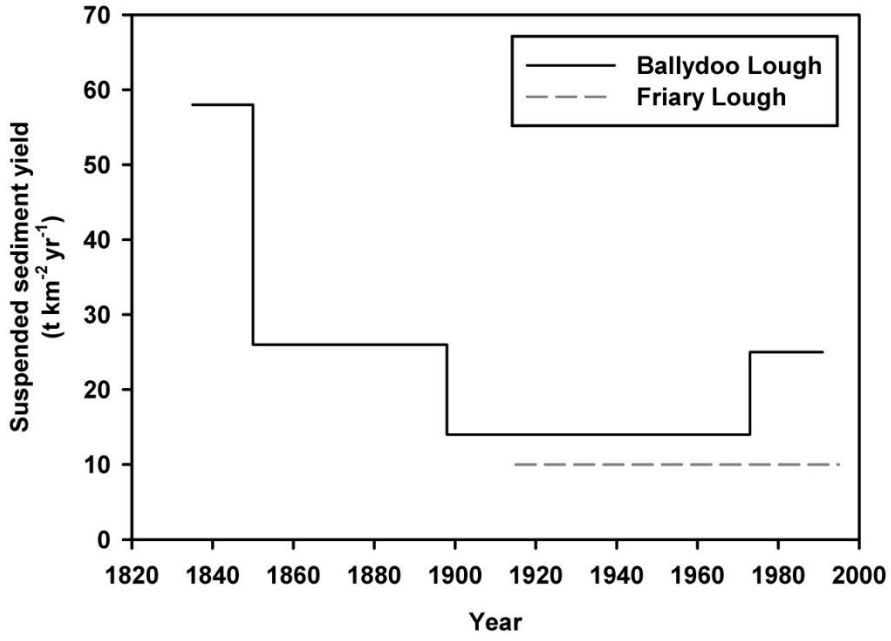

Figure 1.6. Reconstructed suspended sediment yields from two lakes in Ireland. Redrawn from Huang and O'Connell (2000) – Ballydoo Lough, and Jordan *et al.*, (2000) – Friary Lough

Attributing specific land management practices to sediment export at the catchment scale requires high resolution sediment flux assessment. Storm-event scale sediment transfers have attracted significant attention as the hysteretic response of suspended sediment concentration and discharge data provide insights into sources and likely transport pathways (Williams, 1989). The technique has been widely applied in agricultural catchments, but only rarely used to investigate the inter-catchment impact of land uses (Baca 2008; Eder *et al.*, 2010; Gellis, 2013; Onderka *et al.*, 2014; Perks *et al.*, 2015). Considerable opportunity may be afforded from novel application of existing hysteresis methodologies for greater understanding of short-term catchment sediment dynamics and as a validation tool for other methodological approaches to inform sediment management strategies. Challenges in suspended sediment flux measurement and the processes controlling catchment sediment loss occur in addition to the uncertainty in prediction of fine sediments impacts ecology; the former are of relevance here.

1.2.3 Focussing catchment sediment management strategies

With 53% of pollution cases from 2010-2012 in Irish rivers and canals attributed to agriculture (Bradley *et al.*, 2015), targeting catchment management resources is a priority. Catchment 'walkovers' and fluvial audits are methods used to determine sediment sources (Collins and Walling, 2004; Walling and Collins, 2007). In particular, sediment budget investigations can offer valuable information on erosion rates and delivery mechanisms to estimate a catchment sediment delivery ratio (catchment-SDR). The resource intensiveness of data collection and limited ability to detect short-term sediment source fluctuations, however, restricts the suitability of walkover and sediment budget approaches for simultaneous multi-catchment investigations. Sediment fingerprinting is an alternative approach to quantify relative contributions (and commonly accompanied with uncertainty estimates) from a range of potential sediment sources. Using this method, 'end-member' upstream sources are sampled along with downstream 'target' sediments obtained from the respective catchment outlet. The relative contribution of sources is inferred using physico-chemical characteristics and a statistical un-mixing model. The technique has been applied over a range of spatial scales from headwater systems to macro-catchments ($0.5 – 10^4$ km^2) and over timescales spanning storm-events to multi-decadal (Collins *et al.*, 2010b; Rowan *et al.*, 2012; Collins *et al.*, 2013; Belmont *et al.*, 2014; Cooper *et al.*, 2014).

Current sediment fingerprinting research broadly addresses two priorities: application based investigations using sediment fingerprinting as a catchment management tool to inform policy level decisions (*cf.* Rowan *et al.*, 2012; Thompson *et al.*, 2013; Lamba *et al.*, 2015), and assessment of approaches to the sediment fingerprinting methodology. Investigations to the latter include demonstrating the impact of un-mixing model selection on result accuracy, assessment and reduction of uncertainty envelopes, incorporation of novel tracers, environmental significance of employed tracers and the suitability of numeric approaches to represent complex environmental processes (Blake *et al.*, 2012; Koiter *et al.*, 2013a; Smith and Blake, 2014; Palazón *et al.*, 2015; Pulley *et al.*, 2015). Identification and assessment of uncertainty components and their impact upon the reliability of un-mixing results require greater exploration, in particular, the selection of appropriate tracers. Application of catchment sediment fingerprinting studies is frequently used as a diagnostic tool, however, simultaneous investigations in multiple study catchments are essential for development of conceptual models of sediment transfer and delivery to aquatic ecosystems.

1.2.4 Soil erosion, sustainability and policy

Sustaining soil health to provide multiple 'soil functions', including supporting intensive agriculture, is increasingly recognised as a management priority (Schulte *et al.*, 2014). Sustainable intensification is the motivation for strategic agendas such as Food Harvest 2020 which aims to achieve 50% and 33% increases in milk yield and primary agricultural output, respectively (DAFF, 2010), and a subsequent Food Wise 2025 strategy aiming to increase agri-food exports, value added to agri-food products, and primary productivity by 85%, 70% and 65%, respectively (DAFM, 2015). Soil erosion is one of many potential threats which also include nutrient depletion, loss of soil organic carbon, compaction and contamination (Creamer *et al*., 2010). Quantity and provenance assessment of delivered sediment load at the catchment outlet (although applicable to water quality motivated management strategies) may underestimate the extent and magnitude of hillslope soil erosion as the catchment retains sediment through storage in hillslope, fluvial or channel systems. The lack of field-scale soil erosion data in Ireland is of considerable importance for policy makers, particularly in high-risk intensive arable catchments to assess the impact of mitigation measures.

Policy measures aimed at reducing N and P, promoting biodiversity and soil sustainability, and preserving rural farming landscapes may reduce soil erosion risk. Nitrates Directive restrictions on stocking rates (equivalent to 2 dairy cows ha^{-1} or 170 kg organic N ha^{-1} yr^{-1}) and deadlines for green cover establishment after harvest on arable land (to minimise the losses of N and P from the landscape) are regulated in Ireland with the intention of reducing soil erosion from bare and overgrazed land (OJEU, 1991). Other regulated measures such as the Good Agricultural and Environmental Conditions (GAEC – Teagasc, 2015) promote soil protection by preventing overgrazing and poaching and the retention of landscape features (e.g. hedgerows and ditches). Newly introduced 'Greening' measures (worth 30% of pillar one payments under CAP (Common Agricultural Policy) to farmers) promote arable crop diversification, maintenance of permanent pasture and generation of Ecological Focus Areas (EFAs) on farms, aimed at mitigating climate change, conserving biodiversity and improving water quality (EEA, 2014). Reductions in soil erosion risk are likely from permanent pasture where ground cover is maintained; however, crop diversification may increase soil erosion where high risk row crops are introduced to crop rotations.

Voluntary agri-environment schemes such as the Green Low-carbon Agri-environment Scheme (GLAS), part of the EU Rural Development regulation (OJEU, 2013), promotes the use of minimum tillage, arable grass margins, riparian margins, planting hedgerows and excluding cattle from watercourses, all of which are likely to reduce sediment loss risk through interception of transport pathways and preservation of good soil structure. Environmental Impact Assessments (EIAs) seek to regulate the impact of short-term but high soil erosion or sediment transport magnitude risk due to agricultural modifications such as reconfiguration or removal of field boundaries, conversion of marginal land to intensive agriculture and installation of sub-surface drains or edge of field open drains.

1.3 Aims and objectives

The review of literature on soil erosion and sediment dynamics in agricultural catchments established multiple knowledge gaps which are summarised below as research objectives for this thesis:

1. Evaluate novel suspended sediment flux estimation methods and quantify suspended sediment fluxes from multiple Irish agricultural catchments over a gradient of land uses;
2. Investigate event-scale suspended sediment delivery in relation to land use and hydrological controls in intensive agricultural catchments;
3. Investigate novel approaches to reduce uncertainty and assess multiple solutions in sediment fingerprinting un-mixing models;
4. Identify suspended sediment sources over time in multiple intensive agricultural catchments with a gradient of land uses;
5. Explore the impact of soil erosion on the sustainability of soil resources in a highly productive arable catchment.

1.4 Project format

The format of this thesis is illustrated in Figure 1.7 whereby five experimental chapters (Chapters 3 – 7) directly address each of the identified research objectives in the previous section.

Chapter 2 summarises the physical (geology, physiography, soils, landscape, river and artificial drainage network), land use patterns, including proportion of grassland and arable crops, farming enterprise, stocking density, dominant arable crop cycles, and climatic characteristics of the five study catchment investigated in this thesis.

Chapter 3 investigates the accuracy of *ex situ* suspended sediment monitoring methodologies and assesses sediment dynamics by estimating suspended sediment fluxes and yields in five study catchments. Firstly, sediment yields are discussed within the context of published literature to assess the extent of sediment loss in Ireland. Sediment dynamics are then compared to conceptualise the controls on sediment loss based on contrasting catchment characteristics.

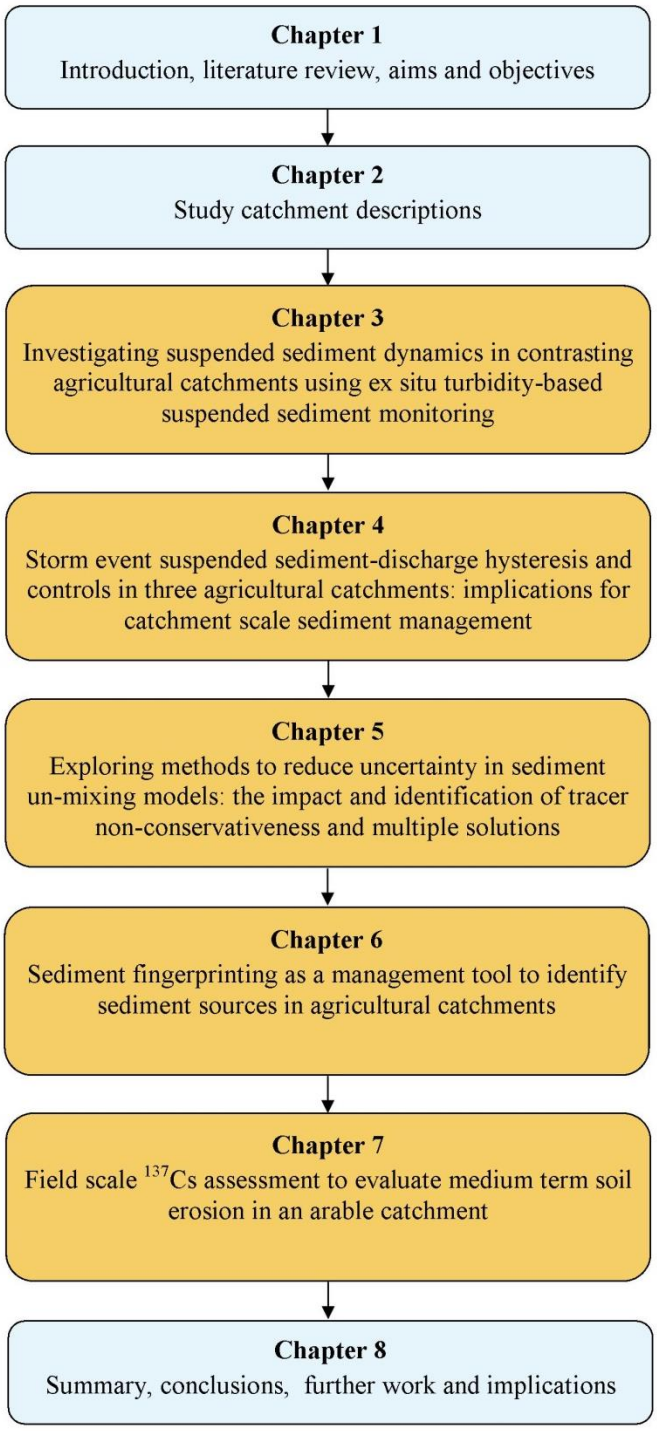

Figure 1.7. Flow chart summary of thesis chapters.

In Chapter 4, an existing storm-event sediment hysteresis metric is used to infer catchment sediment sources and transport pathways for all storm events in three of the five study catchments over two years to investigate the seasonality of sediment dynamics. Seasonal trends are interpreted according to the structural and functional connectivity resulting from catchment soil type and ground cover attributes and antecedent and storm specific rainfall.

In Chapter 5, innovative approaches to reduce uncertainty and improve accuracy of sediment fingerprinting results due to tracer non-conservativeness and tracer selection strategies are presented and a method to identify multiple solutions is assessed using a Monte-Carlo un-mixing model. These methodologies are trialled on synthetic data and a sub-set of field data collected from one catchment.

Chapter 6 explores the application of sediment fingerprinting in three study catchments (consistent with those in Chapter 4) to investigate the provenance of sediments collected at respective catchment outlets. Uncertainty-inclusive sediment provenance is assessed using multiple time integrated samples throughout two monitoring years. In addition to using sediment fingerprinting as an approach to robustly identify sediment sources to inform cost-effective management strategies, results seek to confirm the earlier application of event scale sediment transfer analysis to identify sediment sources and transport pathways.

Chapter 7 quantifies medium-term field-scale soil erosion rates in an intensively cultivated catchment with high-permeability soils. The likely impact of different soil erosion mechanisms (water, tillage etc) and the hillslope component of the catchment sediment budget are discussed. Soil organic carbon and the organic carbon losses attributed to soil erosion were also estimated to indicate the sustainability of soil resources.

Chapter 8 summarises the main findings from the experimental chapters and evaluates them in the wider context of sediment dynamics research and in particular impacts of intensive agricultural catchments on water quality. Opportunities for further research are discussed along with implications for catchment management and policy in terms of agricultural intensification and climate change.

Chapter 2. Study sites

2.1 The Agricultural Catchments Programme

The Agricultural Catchments Programme (ACP) was established to fulfil the monitoring and evaluation requirements of the Nitrates Directive for Ireland (OJEU, 1991) which is regulated as a part of the WFD (Wall *et al.*, 2011). Scientific and socio-economic approaches were used to investigate the combined focusses of profitable farming and good environmental quality and to provide an evidence base against which National Action Programme (NAP) measures for the mitigation of N and P can be measured. The mini-catchment scale (approximately 10 km^2) was deemed appropriate to effectively monitor the nutrient transfer continuum: source, mobilisation, transfer, delivery and impact (Haygarth *et al.*, 2005) and the influence of land management.

Study catchments, selected by the ACP according to size, principal land use type after minimising non-agricultural land uses (such as urban, woodland and peat soils), assessed the combined soil and geological hydrological controls on N and P loss risk (Fealy *et al.*, 2010). The risk of sediment loss in these catchments is aligned with P risk associated with overland flow transfers. Six catchments in total were selected to represent the range of agricultural land use types in Ireland for ACP research.

2.2 Catchment descriptions

Five of the six ACP river monitoring catchments were selected for this study (Figure 2.1). Catchments were chosen to represent the main intensive agricultural land use types in Ireland, with contrasting hydrological flow pathways at a scale where the detection of headwater to channel hydrological processes are detectable (Fealy *et al.*, 2010). One low-relief karst catchment was omitted from this study due to intermitted runoff and very low suspended sediment (SS) contributions (*cf.* Mellander *et al.*, 2012). All catchments had identical meteorological and stream hydrology instrumentation installed. The physical, land use and climate characteristics of each catchment are shown in Figure 2.2 (geology), Figure 2.3 (soils), Figure 2.4 (topography, river network and instrument installation locations), and Figure 2.5 (land use), Table 2.1 and are summarised below:

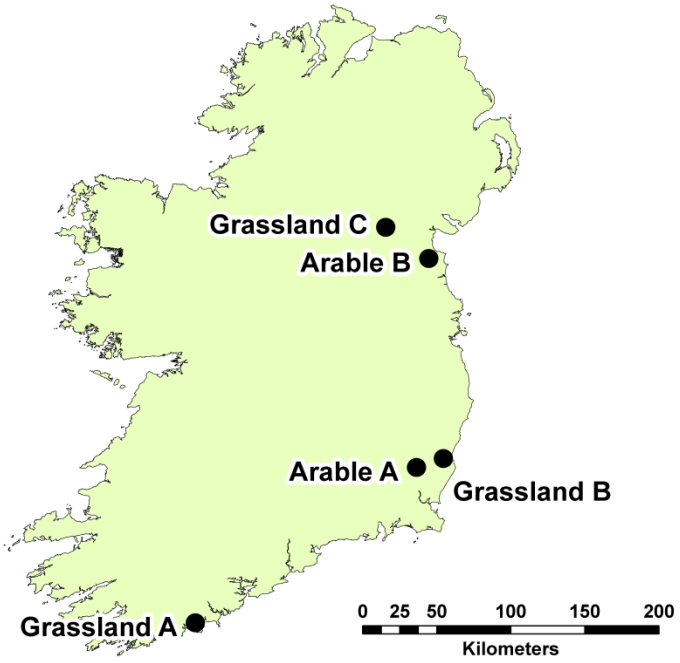

Figure 2.1. Location of five study catchments across Ireland.

Grassland A catchment (7.9 km^2) is located in south-west Ireland (51°38'N 8°47'W). Catchment soils are predominantly shallow well-drained Brown Earths and Podzols on hillslopes with smaller areas of poorly-drained Surface Water Gleys at the base of hillslopes. Loam dominates the texture of A- and B- horizons, where soils have evolved from Quaternary drift deposits creating a coarse loamy with siliceous stones textured subsoil. Devonian old red sandstone and mudstone geology from the Toe Head and Castlehaven formations (Sleeman and Pracht, 1995) underlie soils which form an unconfined productive aquifer (Mellander *et al.*, 2014). The dominance of high permeability soils on moderately permeable bedrock results in predominantly sub-surface hydrological pathways.

The main stream flows from west to east exiting the catchment as a second order watercourse. Artificial drainage ditches, defined as edge-of-field open drains (Shore *et al.*, 2013) are present at a catchment average density of 1.7 km km^{-2} (Sherriff *et al.*, 2015a) mainly concentrated in lowland areas of poorly-drained soils. Ninety per cent of the catchment is utilised for agriculture; 75% for grassland and 15% for arable land use (Murphy *et al.*, 2015). Grassland is predominantly grazed by cattle for intensive dairy production and smaller areas of beef production, with an average catchment stocking rate of 1.98 livestock units (LU) ha^{-1}. Minor areas of arable land use are used for maize and spring cereals (Murphy *et al.*, 2015). Fields are on average 2.0 ha in size (national

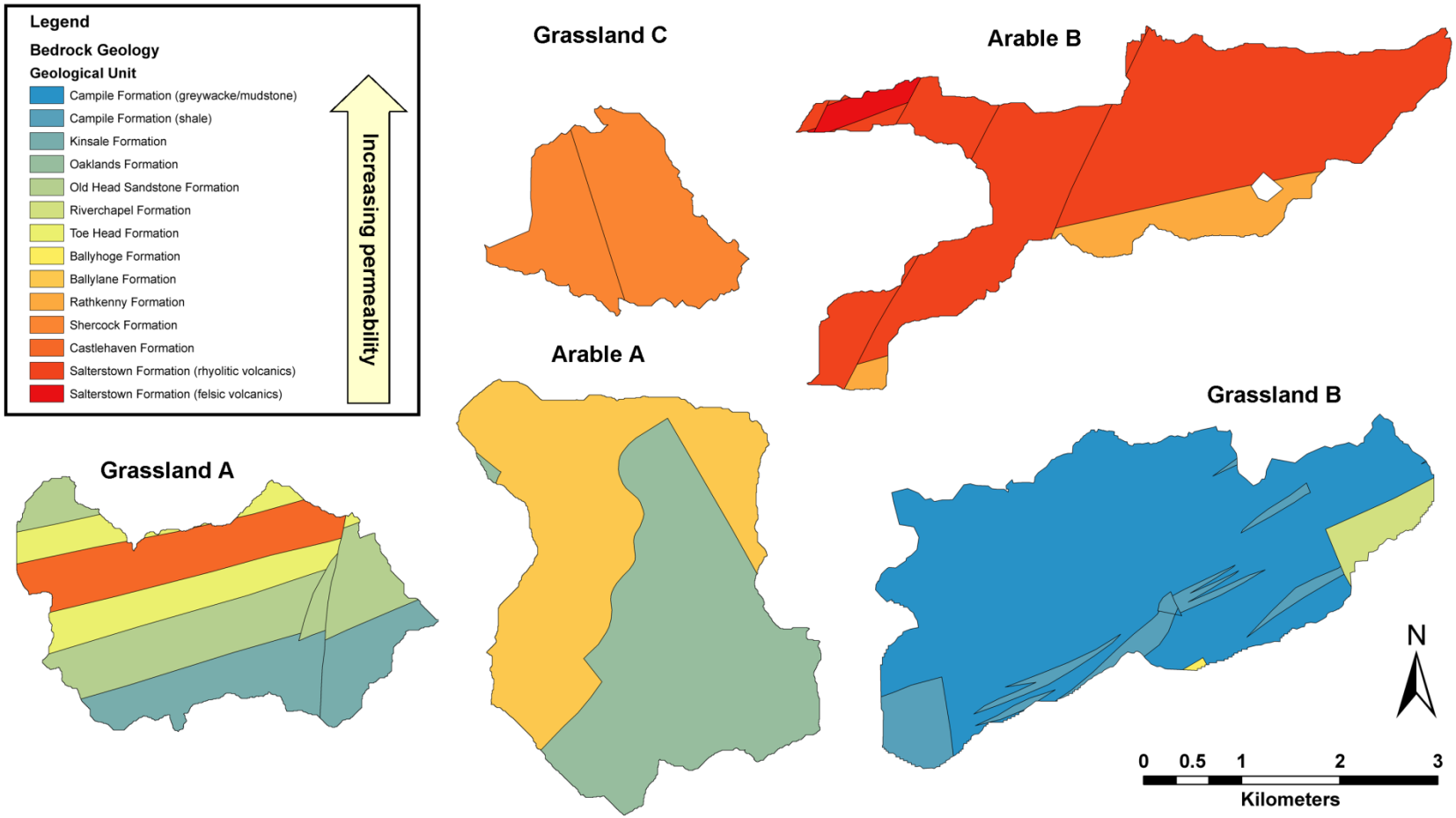

Figure 2.2. Bedrock geology in five study catchments.

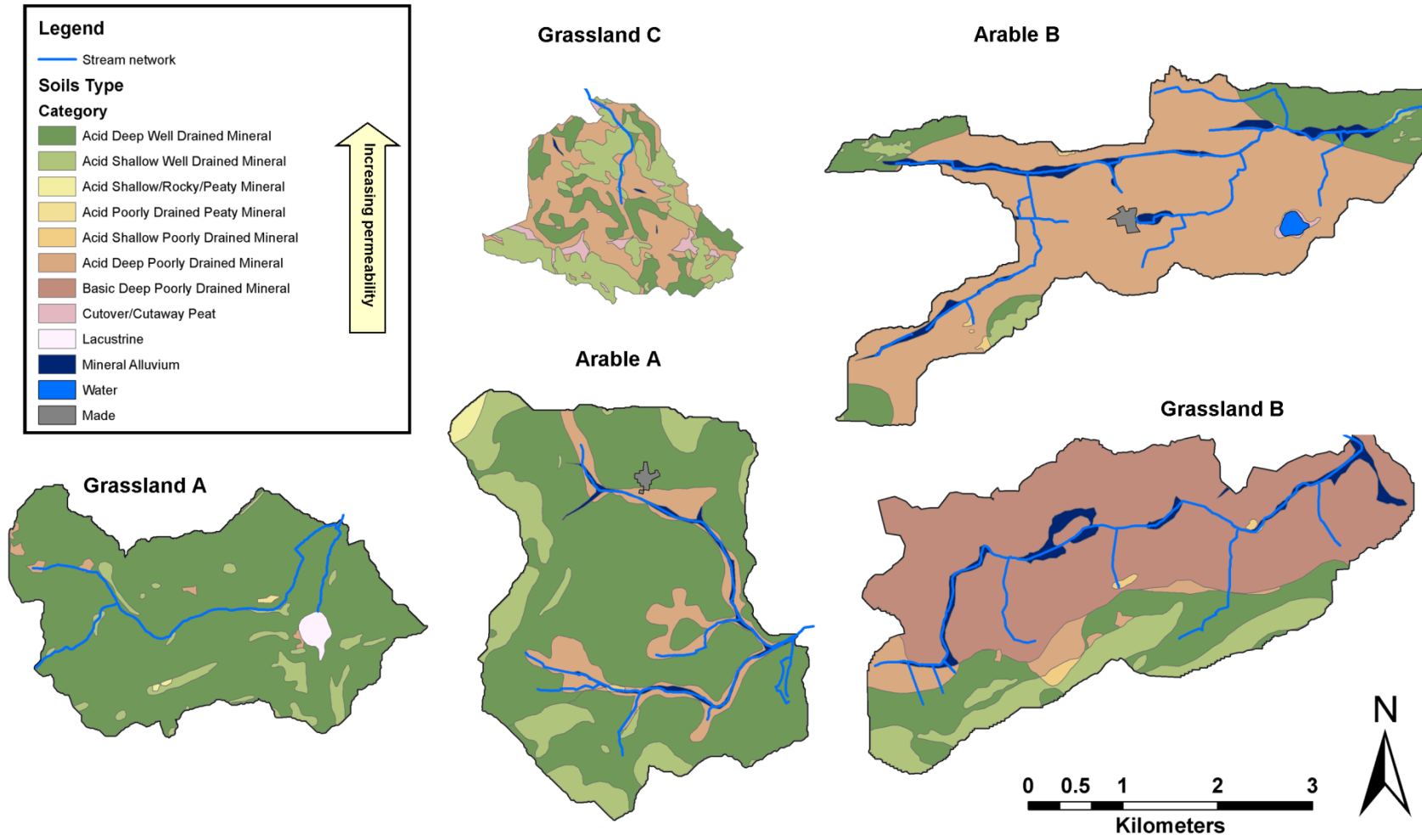

Figure 2.3. Soil type categories in five study catchments.

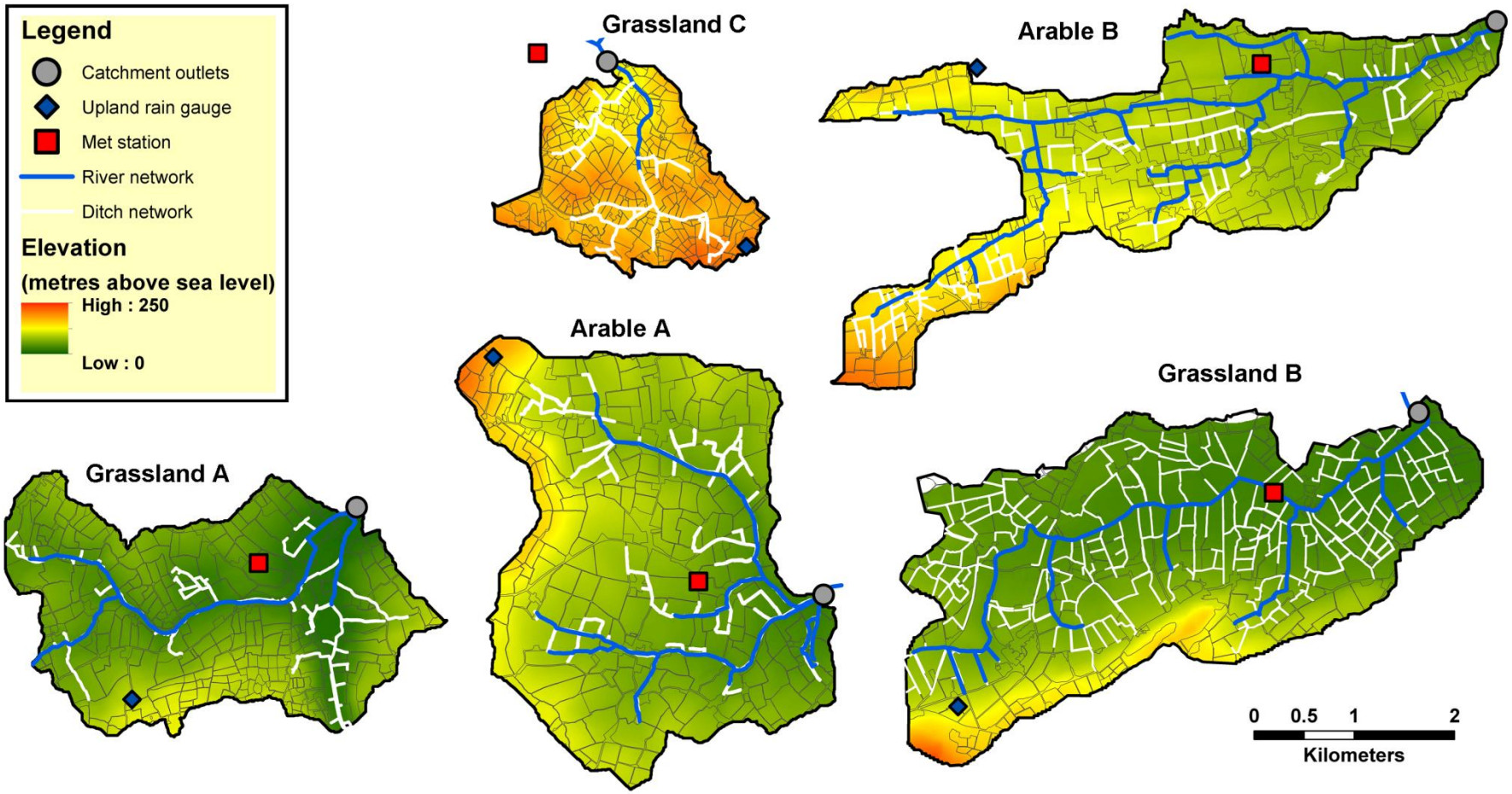

Figure 2.4. Elevation, instrumentation, and river and ditch networks in five study catchments.

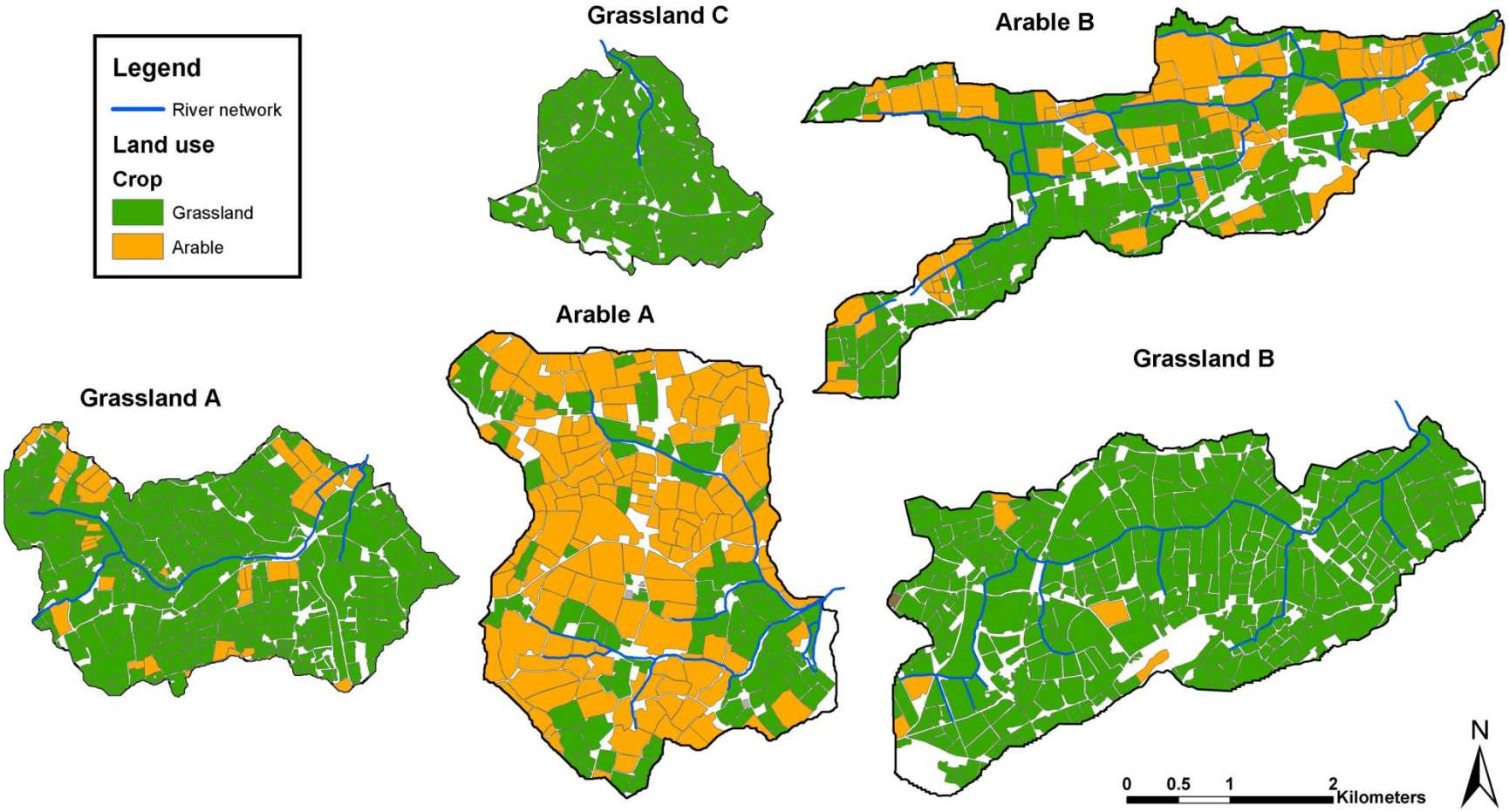

Figure 2.5. Field-scale land use maps for five study catchments. Note: blank areas comprise forests, roads, gardens and urban land uses.

Table 2.1. Summary of five study catchment characteristics.

Catchment	**Size (km^2)**	**30-year average rainfall[a] ($mm\ yr^{-1}$)**	**Median slope (°)**	**Dominant soil drainage class / *flow pathway***	**Land-use**	**Landscape complexity features**			
						Field size (ha)	Average maximum down-slope length (m)	Hedgerow density ($km^2\ km^{-2}$)	Ditch density ($km\ km^{-2}$)
Grassland A	7.9	1228	4	Well-drained *Sub-surface*	89% grassland predominantly for dairy cattle; 5% arable	2.00	170	0.061	1.7
Grassland B	11.5	906	3	Poorly-drained *Surface*	77% grassland for dairy cattle, beef cattle and sheep; 12% spring crops 2% winter crops	3.04	189	0.011	5.7[b]
Grassland C	3.3	960	6	Moderately- to poorly- drained *Surface*	94% grassland for beef cattle, dairy cattle and sheep	1.12	114	0.044	2.6
Arable A	11.2	906	3	Well-drained *Sub-surface*	54% arable predominantly spring crops; 39% grassland mainly for beef cattle and sheep	3.32	194	0.011	1.3[b]
Arable B	9.4	758	3	Poorly- drained *Surface*	42% arable crops; 29% grazing for beef cattle and sheep; 19% dairy cattle grazing	2.70	200	0.011	2.3

average 3.9 ha for grassland and 5.2 ha for arable fields – Deverell *et al.,* 2009), an average maximum downslope length of 170 m and frequently bordered by hedgerows at a density of 0.061 km^2 km^{-2} (Sherriff *et al.,* 2015a). The 30-year average annual rainfall (1981-2010) was 1228 mm from the nearest synoptic station at Cork Airport (51º51'N, 8º29'W).

Grassland B catchment (11.0 km^2) is located in south-east Ireland (52°36'N, 6°20'W). Soil type is predominantly poorly-drained Groundwater Gleys (but occasionally well-drained where antecedent soil moisture is low) in the catchment lowlands with a clay loam texture in A- and B-horizons resulting from a clayey calcareous Irish Sea till subsoil. The uplands contain smaller areas of well-drained Brown Earths, these soils are underlain by drift deposits with siliceous stones. The underlying geology is permeable, dominated by Ordovician volcanics and metasediments of the Campile formation (Tietzsch-Tyler *et al.,* 1994), which form a productive aquifer with faults (Mellander *et al.,* 2012). The dominance of low permeability soils result in surface hydrological pathways except for the small areas of high permeability soils in the uplands where sub-surface pathways occur (Mellander *et al.,* 2012; Shore *et al.,* 2013).

The second order main stream flows west to east with two tributaries from the southern hillslopes. Artificial drainage is widespread including ditches (density 5.7 km km^{-2}), and closed, sub-surface piped drains (Sherriff *et al.,* 2015a) on lowland, poorly-drained soils. High agricultural utilisation (97%) is predominantly grass-based (77%) for dairy and beef cattle grazing, and also sheep enterprises (Shore *et al.,* 2013) with stocking rate of 1.04 LU ha^{-1} (Mellander *et al.*, 2015). Arable crops such as spring barley comprise roughly 14% of the catchment, most common on well-drained upland soils. On average fields are 3.04 ha in size, an average maximum downslope length of 189 m and frequently bordered by hedgerows at a density of 0.011 km^2 km^{-2} (Sherriff *et al.,* 2015a). The 30-year annual average rainfall (1981-2010) was 906 mm (Shore *et al.,* 2013).

Grassland C catchment (3.3 km^2) is located in north-east Ireland (54°01'N, 6°51'W). Soils are mainly deep and moderate- to poorly-drained, characterised by a loam A-horizon texture and clay loam B-horizon, and areas of shallow well-drained soils in the upper catchment areas underlain predominately by Lower Palaeozoic shale tills. The geology is Silurian metasediments and volcanics of the Shercock Formation (Geraghty

et al., 1997), which create an unproductive aquifer. Overland flow and near-surface pathways are, therefore, dominant here due to low permeability soils and low permeability geology.

The stream is one main second order channel flowing south-east to north-west with one small tributary and further artificial drainage ditches at a density of 2.6 km km^{-2} on poorly-drained soils at lower elevations (Sherriff *et al.,* 2015a). Agriculture comprises 94% of the catchment land use and is principally grass-based for dairy cattle, sheep and beef cattle grazing at a stocking rate of 1.00 LU ha^{-1} (Sherriff *et al.,* 2015a). The average field size and average maximum downslope length is the smallest of all catchments at 1.12 ha and 114 m, respectively. Hedgerows occur at a density of 0.044 km^2 km^{-2}. The 30-year annual average rainfall was 960 mm at the nearest synoptic weather station at Clones, Co. Monaghan (54º11'N, 07º54'W)

Arable A catchment (11.2 km^2) is located in south-east Ireland (52°34'N, 6°36'W). Soils are predominantly shallow well-drained Brown Earths with loam texture dominating the A- and B-horizons, and limited areas of poorly-drained Groundwater Gleys around the stream corridor to the east of the catchment (Melland *et al.,* 2012a). Subsoils predominantly comprise fine loamy drift with siliceous stones over slate and silt stones of the Oaklands Formation (Tietzsch-Tyler *et al.,* 1994), which produces a poorly-productive aquifer. The high permeability soil and geology result in below-ground hydrological transfers, particularly bedrock fissure-flow (Mellander *et al.,* 2012).

The stream network comprises two main tributaries flowing west-east and north-south which join approximately 0.3 km upstream of the catchment outlet, where the stream becomes third order. Artificial drainage is limited to the poorly-drained soil areas and comprises of open ditches (density 1.3 km km^{-2}) and sub-surface piped drainage predominately on low permeability soils in the riparian corridor (Shore *et al.,* 2013; Sherriff *et al.,* 2015a). Ninety-three per cent of the catchment is utilised for agriculture which is predominantly spring barley (54% – Shore *et al.,* 2013). Areas of permanent grassland for beef cattle and sheep grazing occur in more poorly-drained areas (Melland *et al.,* 2012a) at an intensity of 0.40 LU ha^{-1}. Larger average field sizes (3.32 ha) result in lower hedgerow densities (0.011 km^2 km^{-2}) and larger average maximum downslope

length (194 m) than grass-dominated catchments (Sherriff *et al.,* 2015a). The 30-year annual average rainfall (1981-2010) was 906 mm (Shore *et al.,* 2015).

Arable B catchment (9.5 km^2) is located in north-east Ireland (53°49'N, 6°27'W). The soil type is a complex pattern of poor- to moderately-drained soils (Melland *et al.,* 2012a). Loam soil texture dominates the A-horizon and clay loams are dominant in the B-horizon. Subsoil is dominated by fine till containing siliceous stones with fluvioglacial sediments located near-channel. Soils are underlain by calcareous greywacke and banded mudstone geology (McConnell *et al.,* 2001) and produce a poorly productive aquifer (Mellander *et al.,* 2012). Hydrologically, surface pathways dominate due to low permeability soils; however, below-ground pathways may also be important especially during winter in areas of moderate soil permeability (Melland *et al.,* 2012a; Mellander *et al.,* 2012).

The third order stream flows west-east with tributaries from both the north and south of the catchment. Artificial drainage is widespread at 2.3 km km^{-2}, particularly in the poorly-drained catchment areas (Sherriff *et al.,* 2015a). The catchment is 90% utilised for agriculture, 48% of which for grassland and 42% for arable land use (Sherriff *et al.,* 2015a). Arable land is dominated by winter-sown cereals, but also comprises maize and potatoes (Melland *et al.,* 2012a). These areas are unmanaged between cropping cycles; however, crop rotation is more common than at Arable A due to the greater range of crop types. Areas of permanent grassland are utilised for dairy cattle, beef cattle, and sheep grazing at an intensity of 0.77 LU ha^{-1} (Sherriff *et al.,* 2015a). Fields are, on average, 2.7 ha in size, have a maximum downslope length of 200 m and the catchment hedgerow density is 0.0101 km^2 km^{-2}. The 30-year annual average rainfall from the nearest synoptic station at Dublin Airport (53º25'N, 6º14'W) from 1981-2010 was 758 mm.

Chapter 3. Investigating suspended sediment dynamics in contrasting agricultural catchments using ex situ turbidity-based suspended sediment monitoring

3.1 Introduction

Accurate sediment yield estimation is important in complex and dynamic agricultural catchments. Measurement programmes require three considerations. Firstly, robust flow and sediment concentration data capable of accurately describing short-term fluxes (Navratil *et al.,* 2011). Secondly, the duration of the measurements must be sufficiently long to be 'representative' of either stationary long-term averages (inclusive of natural variability), or to reveal temporal trends of increasing or decreasing loads or concentrations. Capturing crucial high magnitude, low frequency events is, therefore, vital to generating meaningful flux determinations (Walling and Webb, 1988; Wass and Leeks, 1999). Thirdly, monitoring programmes need to be operationally cost-effective.

Sediment load estimation based on suspended sediment concentration (SSC) to discharge rating curves has been widely superseded by catchment outlet, near-continuous turbidity monitoring (Lewis, 2003; Jarstram *et al.*, 2010; Melland *et al.,* 2012a). The latter requires turbidity sensors, loggers and infrastructure that cope with issues such as debris interference, bio-fouling, power outages and equipment/data security (Wass and Leeks, 1999; Jordan *et al.*, 2007; Owen *et al.,* 2012). Assessment of new monitoring strategies, compared to traditional *in situ* turbidity-SSC monitoring programmes, is essential to assess improvements, limitations, and validate their implementation.

The aims of this chapter were to:

- Assess the efficacy of a novel *ex situ* SS monitoring technique against *in situ* and direct SS monitoring methods in two study catchments for method validation (Grassland B and Arable B);
- Investigate annual average sediment concentrations and yields in relation to land use and physical characteristics in five monitored catchments using *ex situ* SS monitoring.

3.2 Methodology

3.2.1 Suspended sediment monitoring

Turbidity (T) data were collected using a turbidity sensor (Solitax, Hach-Lange, Germany; range 0-4000 NTU; factory calibrated to 1000 NTU) and SC1000 controller at 10 min intervals. The sensors were located out-of-stream (ex situ) in a rapidly and continuously circulating header tank with river water delivered from the channel by an in-stream pump (30 m^3 hr^{-1}) located on the channel bed (Figure 3.1). The instrument tank was assumed well-mixed as no particulate deposition occurred. Turbidity probes were fitted with wipers to prevent biological fouling, and checked monthly against deionised water (0 NTU) and a 20 NTU Formazin turbidity standard. Synchronised discharge data (Q – m^3 s^{-1}) were calculated from vented pressure-transducer stage measurements (OTT Orpheus-mini; OTT Germany). Stage height was converted to Q using velocity-area measurements (OTT Acoustic Doppler Current meter; OTT Germany) collected over non-standard flat-v weirs (custom made, Corbett Concrete, Ireland) and WISKI-SKED software (Grassland A, R^2=0.96, n=272; Grassland B, R^2=1, n=166 (Mellander *et al.*, 2015); Grassland C, R^2=0.95 and 0.97, n=316; Arable A, R^2=1, n=376 (Mellander *et al.*, 2015); Arable B, R^2=0.94 and 1, n=493). Both Grassland C and Arable B had changing controls at higher discharges and WISKI-SKED provided two parts to the curves with two R^2 coefficients.

Turbidity units (NTU) were field-calibrated to SSC (mg L^{-1}) using a combination of regular low-flow samples (at least fortnightly since programme initiation) and intensive sampling during high magnitude flow events with elevated SSCs. In all cases, water samples were collected from the instrument tank either manually, or using a programmable automatic water sampler (ISCO 6712; ISCO Inc. USA) with 1 m pumping tube (pump capacity ~0.9 m s^{-1}) at predefined intervals of 30- or 60-mins according to the specific storm characteristics. High SSC data capture was further targeted in Grassland B and Arable B using a turbidity-stratified sampling programme, whereby collection of 1000 ml samples were triggered when T measurements were within threshold turbidity bands of 140 to 160 NTU, 240 to 260 NTU, 480 to 530 NTU and 700 to 800 NTU. This circumvented the need to pre-set water samplers according to forecasted event characteristics. Water samples were stored at 4ºC on return to the laboratory before a sub-sample (minimum 100 ml) was processed for SSC. Whatman

Figure 3.1. Photographs from study site showing catchment outlet suspended sediment estimation; flow and in-situ and ex-situ turbidity equipment.

GF/C glass-fibre filter papers (1.2 µm) were pre-dried at 105ºC for 1 hr, cooled in a desiccator and weighed before being used for vacuum filtration. Sediment concentrations were calculated from the weight of residue retained on the filter post-filtration once dried >12 hr at 105ºC and cooled in a desiccator.

3.3 Method comparison

In order to compare the *ex situ* sampling methodology described above with the conventional *in situ* monitoring approach, additional instrumentation to measure T was installed in Grassland B and Arable B from September to December 2012, and December 2012 to March 2013 respectively. A turbidimeter (T_{IN}) (Analite, McVan, Australia, range 0-1000 NTU) fitted with a wiper blade to prevent biological fouling and automatic pumping sampler ($ISCO_{IN}$) intake were positioned *in situ*, adjacent to the channel edge, in proximity to the bankside analyser pump intake (1 m and 4 m upstream, respectively in both catchments), but sufficiently distant not to affect, or to be affected by the *ex situ* instrumentation (Figure 3.1). The turbidity sensor T_{IN} and the $ISCO_{IN}$ intake at Grassland B were approximately 20 cm above the channel bed and 15 cm from the bank edge. At Arable B, T_{IN} and the $ISCO_{IN}$ intake were positioned approximately 10 cm from the bank edge and 10 cm above the channel bed. T_{IN} and $ISCO_{IN}$ sample collection was synchronised to replicate the *ex situ* turbidity sensor (T_{OUT}) and pumping sampler ($ISCO_{OUT}$) programme as described above. T-SSC rating curves were developed for each sensor using water samples collected at the respective positions ($ISCO_{OUT}$ and $ISCO_{IN}$) and applied to the raw turbidity set. Low quality data capture attributed to spurious readings (a short-term increase in T output not associated with a known environmental process such as accompanying rise in Q or equipment maintenance), saturation of the T_{IN} sensor or missing data at T_{OUT} due to delivery system blockages did not undergo correction such that comparisons between methodologies could be made. Five storm-flow events were captured in Grassland B and two in Arable B for T-SSC calibration. Due to the location settings, the *in situ* automatic water sampler was fitted with a 7 m long intake tube in both catchments.

Depth integrated water samples were manually collected (n=171) from a bridge over each investigated channel during flood events, using a depth-integrating SS sampler (US DH-48, Rickly Hydrological; USA). These samples were used firstly to investigate the cross-sectional variability in sediment transportation, and secondly to provide a

validation dataset to assess and compare the efficacy of estimated SSC using at *in situ* and *ex situ* T sensors. Samples were collected using two strategies; 1) depth-integrated samples taken at 20 cm intervals across the channel width in rapid succession, and 2) samples taken at coarser widths roughly 1 m intervals. All samples were processed for SSC as described above. Due to the sampling approach used, consecutive depth-integrated samples reflected the event trend (either the rising or falling sedigraph limb) plus the cross-sectional trend. The event effect was de-trended using SSC estimated from the *ex situ* turbidimeter. The average change in SSC during transect sampling at $T_{OUT,}$ or the event trend, was 9% (range 1% at 175 mg L^{-1} to 19% at 442 mg L^{-1}), average transect time was 22 mins.

Where sufficient sample volume and sediment concentration existed, samples were analysed for particle size distribution using laser diffraction (Malvern Mastersizer 2000G, Malvern, UK). Samples were circulated for 2 min (pump speed 2000 rpm, stirrer speed 800 rpm) before analysis with no pre-treatment, i.e., physical or chemical dispersant, to broadly replicate the 'effective particle size' measured by the turbidity sensor. To assess the effect of automatic sampler tube length, laboratory prepared SSC samples were collected using the two intake pump lengths (1 m and 7 m) used in-field. Ten 500 ml sub-samples (at 5-, 10-, 25-, 50-, 100-, 250-, 500-, 750- and 1000-mg L^{-1}) were collected from homogenised 10 litre mixtures using each pump length and processed for SSC. A non-parametric Mann-Whitney U-test was conducted to compare SSC values collected at $ISCO_{IN}$ (SSC $ISCO_{IN}$) and $ISCO_{OUT}$ (SSC $ISCO_{OUT}$), and particle size characteristics at the two study sites.

3.3.1 Suspended sediment rating curve construction

Data pairs for T-SSC calibration for each individual site (each catchment outlet over complete time series) and method comparison investigations were statistically assessed using SAS 9.3 (SAS Institute Inc., USA). Two regression equations; power (Eq. 1) and two-section linear split at a threshold T' (Eq. 2), were assessed using the mean square error (MSE) of the SSC predictions.

Power $$SSC = aT^b$$

Equation 3.1

Split linear $$SSC = aT \;\; Where\, T < T'$$

$$SSC = c(b_1 - b_2) + b_2 T \;\; Where\, T > T'$$

Equation 3.2

The intercept was set at zero for all regressions and was considered not to compromise fit at the upper end of the dataset (*cf.* Thompson *et al.*, 2014). Power relationships provided the best fit in Grassland A, Grassland B, Grassland C and Arable A, whereas the split linear relationship considerably improved fit at Arable B (Table 3.1). Using the selected curves, continuous turbidity measurements were computed to SSC and, using discharge data, were converted to instantaneous sediment load (SSL – t s^{-1}) and yield (SSY – t km^{-2} yr^{-1}).

Table 3.1. Turbidity-suspended sediment calibration data-set summary and rating curve equations and fit parameters

Catchment	Data points	Calibrated turbidity range (NTU)	Maximum measured turbidity in NTU (number of data points outside calibrated range)[a]	Calibration equation	MSE
Grassland A	247	0-725	1074 (n=7)	$SSC=0.6636T^{1.1045}$	495
Grassland B	443	1-577	1179 (n=37)	$SSC=0.5657T^{1.1109}$	580
Grassland C	339	1-154	1225 (n=207)	$SSC=0.4341T^{1.2148}$	38
Arable A	231	1-767	2730 (n=30)	$SSC=0.4119T^{1.1456}$	891
Arable B	242	1-1853	1853 (n=0)	Where T<432.2 SSC=1.1320T Where T>432.2 SSC=0.5288+0.6032T	1335

3.4 Results and discussion

3.4.1 Method comparison

Dataset completeness was similar in both T records (98-99%); however, the timing and nature of spurious and/or missing T data were dissimilar (Figure 3.2). Spurious data at T_{IN} coincided with random peaks possibly relating to local debris interference around the sensor which is a frequent problem in T analysis (Lewis and Eads, 2001). This effect was not recorded at T_{OUT}, suggesting that the *ex situ* approach was less vulnerable to local in-stream debris interference (Jansson, 2002). Missing data at T_{IN} during periods

of high sediment concentration was attributed to sensor saturation at Arable B. The T_{OUT} probe estimated 5% of the total sediment load was delivered whilst T_{IN} was saturated. Sporadically, pump blockages occurred in T_{OUT} at Arable B due to extreme debris transport in the channel (Melland *et al.,* 2012b), data collection was ordinarily restored in less than 2 hr. At T_{IN} 6% of the total load was delivered during this period. The *ex situ* turbidity monitoring may be at greater risk of delivery system blockages, especially during key periods of elevated turbidity and sediment transfer. These short periods are critical for sediment transport as they are responsible for the majority of the annual sediment load (Walling and Webb, 1988; Lawler *et al.,* 2006; Estrany *et al.,* 2009; Navratil *et al.,* 2011). Other key issues such as bio-fouling trends were not found in either dataset, reflecting the sub-weekly frequency of maintenance at these sites.

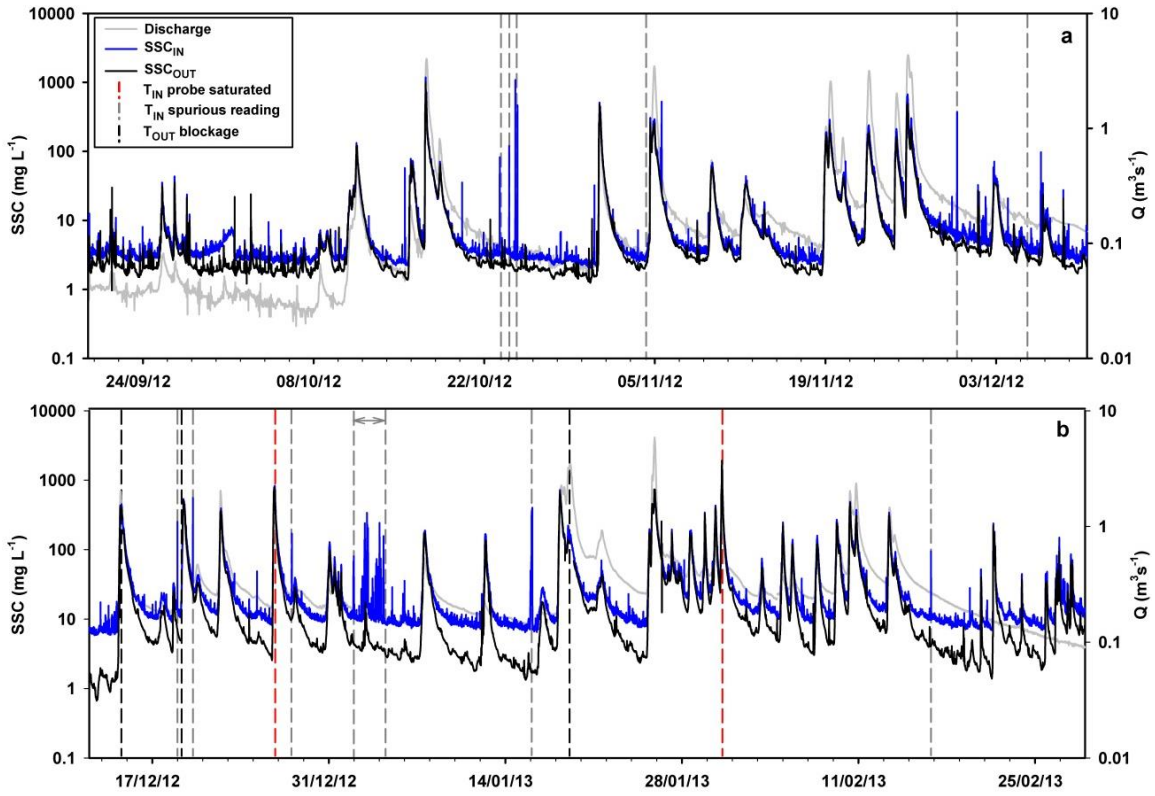

Figure 3.2. Raw turbidity output of T_{IN} and T_{OUT} sensors (converted to SSC) and discharge at, a) Grassland B and, b) Arable B. Periods of missing data are annotated with dashed lines.

Estimated sediment metrics during both monitoring periods showed discrepancies between the two measurement locations (

Table 3.2). Suspended sediment load estimated by *ex situ* equipment was 83% and 91% of *in situ* at Grassland B and Arable B, respectively, and mean SSC at SSC_{OUT} was 85% of SSC_{IN} at both locations. Differences in raw T output between the sensors were

negated by calibration with SSC; however, the SSC of water samples from *in situ* (SSC $ISCO_{IN}$) and *ex situ* (SSC $ISCO_{OUT}$) measurement locations showed consistent differences. Samples at SSC $ISCO_{OUT}$ were 90% and 94% of SSC $ISCO_{IN}$ at Grassland B and Arable B catchments, respectively. The differences in SSC and loads between the two approaches was not statistically significant, as confirmed by the non-parametric Mann-Whitney between SSC $ISCO_{OUT}$ and SSC $ISCO_{IN}$ ($p>0.05$).

Table 3.2. Suspended sediment metrics estimated using *in situ* and *ex situ* turbidity-based SSC estimation methods.

Catchment	**Total load (t)[a]**		**Mean concentration (mg L^{-1})**		**Max concentration (mg L^{-1})**	
	SSL_{OUT}	SSL_{IN}	SSC_{OUT}	SSC_{IN}	SSC_{OUT}	SSC_{IN}
Grassland B	128±28	154±35	14	16	1010	1188
Arable B	225±54	248±52	29	34	2043	823[b]

[a] confidence intervals are the coefficient of variance of the mean prediction
[b] T_{IN} sensor saturated at 1000 NTU

Particle size analysis of event samples showed that the proportion of silt and sand particles changed through the events, whereas clay remained consistent. The greater density of sand particles compared to silts and clays can impact SSC and be oversampled by pumped samples such as the $ISCO_{IN}$ approach, depending on the position of the intake and the effectiveness of mixing in the water column (Horowitz, 2008). The percentage of sand (or sand-sized aggregates) between SSC $ISCO_{IN}$ and SSC $ISCO_{OUT}$ did not differ significantly ($p>0.05$). Additionally, the ratio of the sand-sized fraction between simultaneous samples at $ISCO_{IN}$ and $ISCO_{OUT}$ showed no consistent evidence of over- or under-collection by either collection method. The hypothesis that inadequate sample collection could affect the differences between SSCs at $ISCO_{IN}$ and $ISCO_{OUT}$ is unlikely, as contrasts between the sand-sized fractions seemed to be event specific.

Differences between SSC $ISCO_{IN}$ and SSC $ISCO_{OUT}$ could not be directly attributed to diverging particle-size of the collected samples ($p>0.05$), or the pump length of the water sample collection ($p>0.05$ – Figure 3.3).

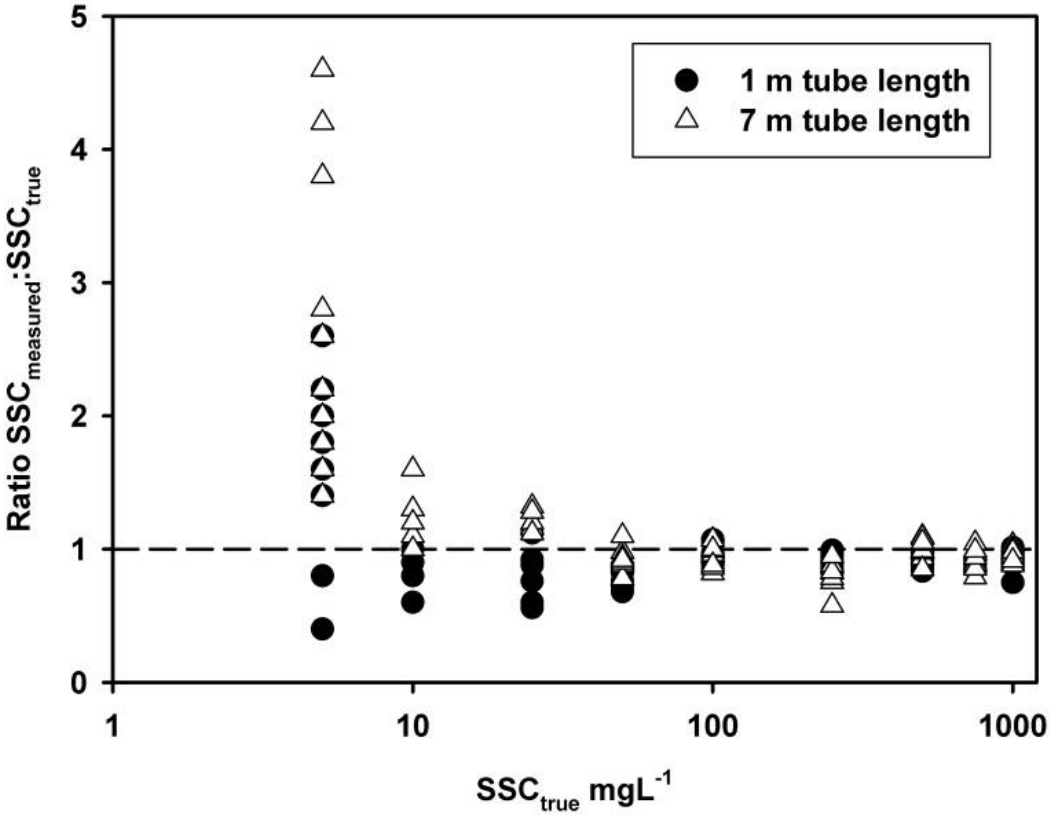

Figure 3.3. Suspended sediment concentration of samples collected from known concentrations (SSC_{true}) using ISCO water samplers with 1 and 7 m tube lengths.

The position of the sample intake within the cross section could also not be shown to cause differences in SSC $ISCO_{IN}$ and SSC $ISCO_{OUT}$ SSC (Figure 3.4). It is possible that the proximity of the $ISCO_{IN}$ pump intake to the channel bank could influence the relationship; however, differences could additionally result from methodological dissimilarities which could not be tested in isolation, i.e., the piped-delivery of river water to the *ex situ* instrument tank. The impact of elevated SSCs from $ISCO_{IN}$, compared to $ISCO_{OUT}$ on the calibration of turbidity sensors T_{IN} and T_{OUT}, and the consequential prediction of high-resolution turbidity-based SSC record is discussed below.

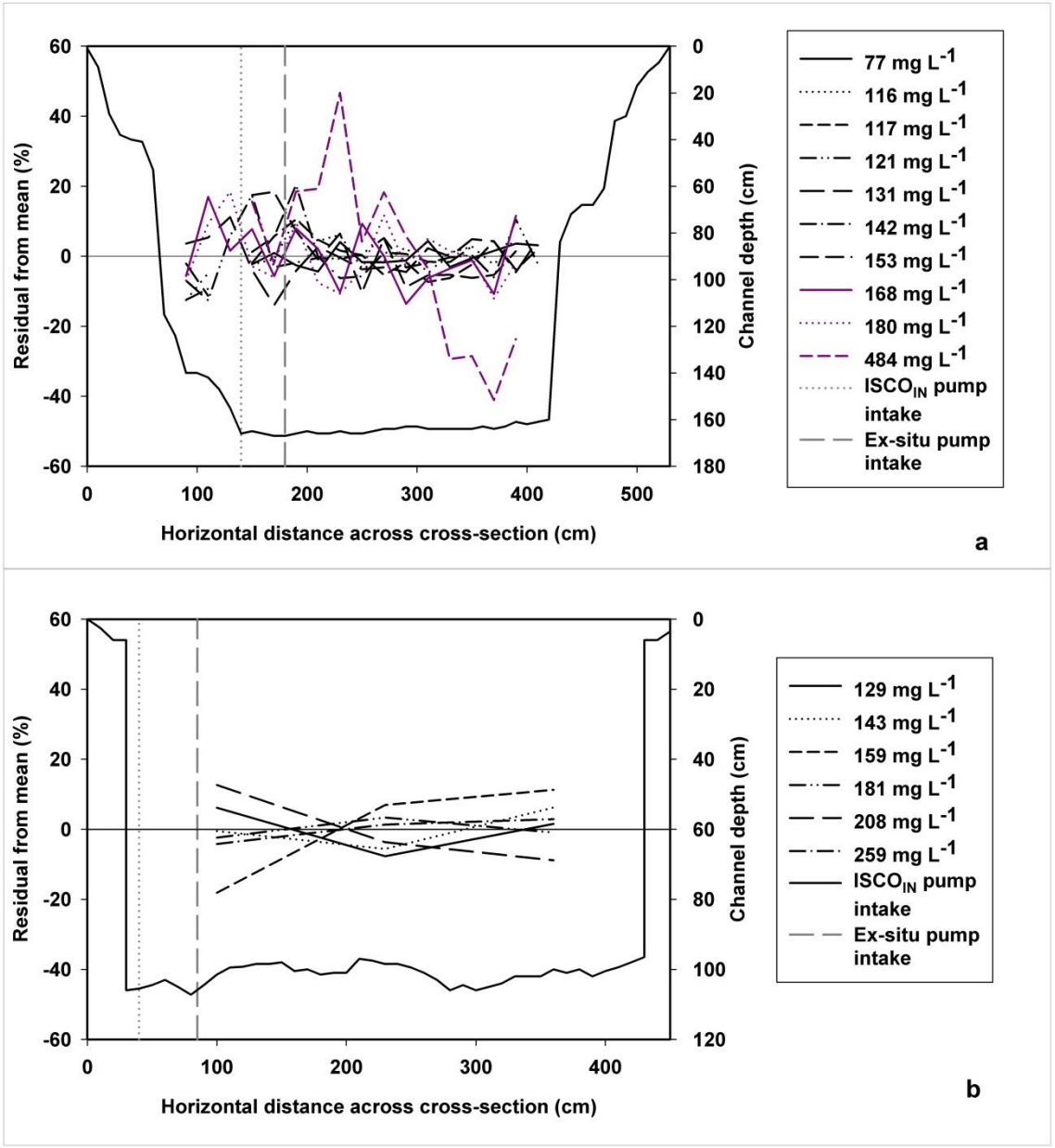

Figure 3.4. Variability of instantaneous depth-integrated SSC measurements across the channel cross section compared to the mean transect SSC using a US DH-48 sediment samplers at, a) Grassland B and, b) Arable B.

3.4.2 Method validation

Samples collected from the channel cross-section were used to test the accuracy of predicted SSC using calibrated turbidity sensors at *in situ* and *ex situ* locations. The average SSC from each cross-sectional, depth-integrated set of measurements was plotted onto the rating curve over the method comparison monitoring period (Figure 3.5).

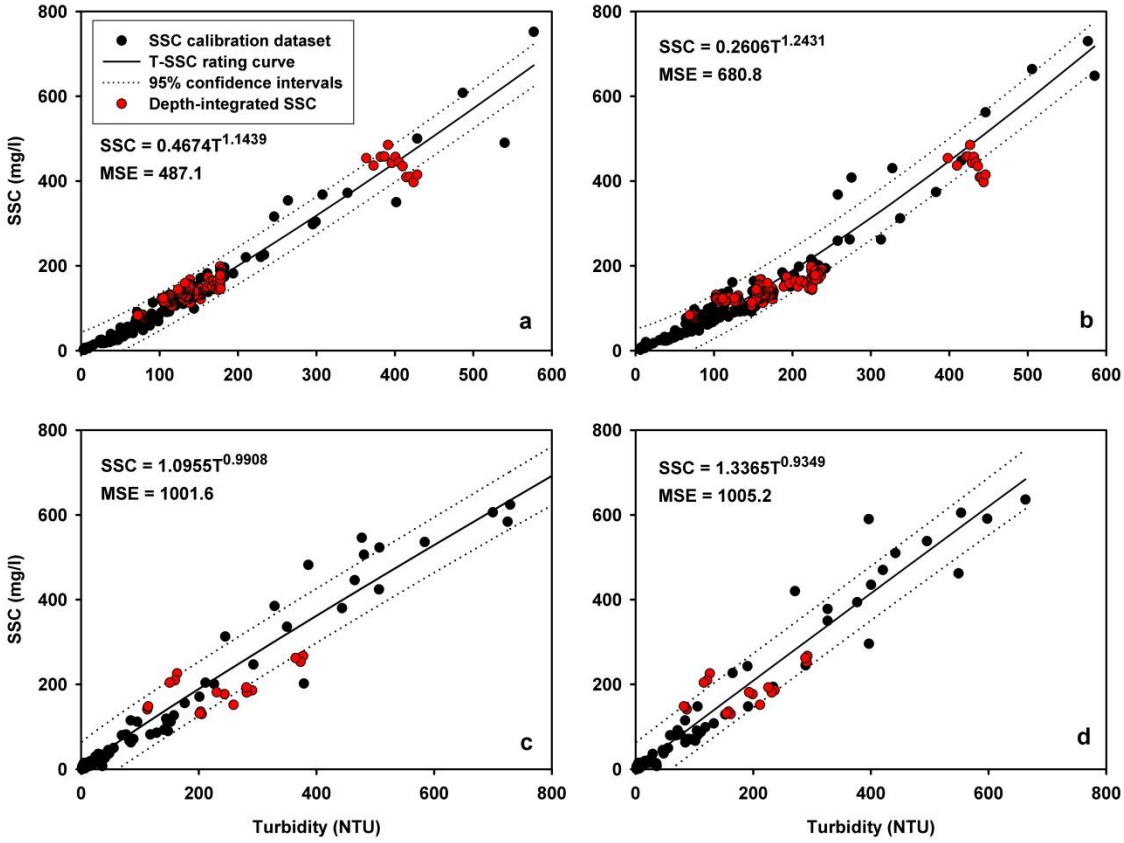

Figure 3.5. Turbidity-suspended sediment concentration rating curves, confidence intervals, calibration data and cross-sectional depth-integrated suspended sediment concentrations samples for, a) Grassland B T_{OUT}, b) Grassland B T_{IN}, c) Arable B T_{OUT}, and, d) Arable B T_{IN}.

At Grassland B, measured SSCs plot within the 95% confidence intervals of predicted SSC from both methodologies using the simultaneous T values. This trend is repeated for the majority of samples at Arable B; however, some data points plot outside of the 95% confidence intervals for both *in situ* and *ex situ* method datasets. In the case that these out of range values were consistently higher or lower than the predicted values, this may suggest a systematic error due to sampling strategy; however, both upper and lower confidence limits were exceeded by the SSC values (Figure 3.5). Therefore, the error associated with the measurement method was generally less than that encapsulated within the 95% prediction intervals of the T to SSC calibration curve and consequently, both measurement approaches can be accepted as accurate for the estimation of SS metrics in these catchments. The suitability of *ex situ* water monitoring equipment installation must consider programme specific research objectives. Melland *et al.* (2012b) stated that for policy evaluation studies including multiple water quality parameters in addition to SSC, the improved resolution, accuracy and precision, in

particular for hydrologically dynamic catchments, justified the increased financial costs of initial installation of *ex situ* instrumentation.

3.5 Suspended sediment metrics in five agricultural catchments

High magnitude SSCs were of short duration in all five catchments (e.g. Figure 3.2 for Grassland B and Arable B), but such periods are typically critical to cumulative annual SSY (Figure 3.6 – Walling and Webb, 1988; Navratil *et al.*, 2011). Grassland B and Arable B had a large proportion (80% of the monitoring period) of sediment transported at SSCs between 1 and 10 mg L^{-1}, and shorter periods of concentrations ≥10 mg L^{-1} for 15% and 20% of the monitoring period respectively (Figure 3.6).

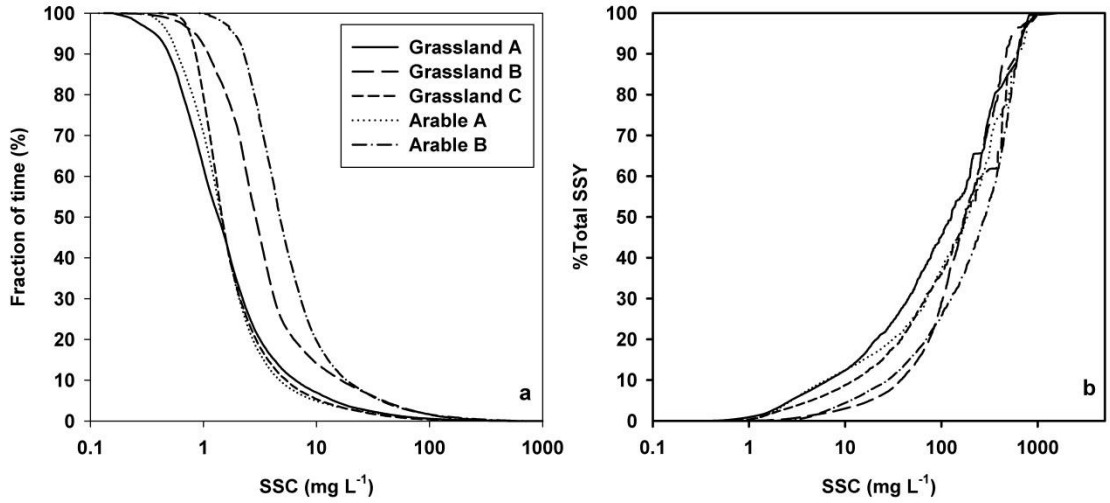

Figure 3.6. Frequency-duration graphs of, a) suspended sediment concentration exceedance with time and, b) cumulative percentage of suspended sediment yield with exceedance of suspended sediment concentration.

In the remaining catchments, low concentrations of <1 mg L^{-1} were more common and occurred between 25 and 40% of the time. High concentrations (≥10 mg L^{-1}) were limited to less than 10% of the monitoring period. Overall, however, the Freshwater Fish Directive (FFD) average annual SSC guideline was not exceeded in any monitoring year in any of the catchments (Table 3.3). The highest mean SSCs were recorded at Grassland B (up to 14 mg L^{-1}) and Arable B (up to 17 mg L^{-1}) and the remaining catchments reported very low values of <6 mg L^{-1}. Accordingly, the instantaneous exceedance of the FFD guideline (Table 3.3) occurred during extremely short time periods (1-11% of sampled time per year). The values here are similar to those reported by Thompson *et al.* (2014) in two other intensively managed grassland

catchments in Ireland; 8% exceedance was reported in a moderately-drained catchment in Co. Down and 18% exceedance in a poorly-drained catchment in Co. Louth. Although the instantaneous exceedance of the FFD metric have been reported in other sediment studies (Glendell *et al.,* 2014; Peukert *et al.,* 2014; Thompson *et al.,* 2014), the transferability of this coarse threshold (compliance to which requires an undefined annual sample number) to high-resolution SS data is questionable.

Average SSYs in the five catchments were 9, 25, 12, 12 and 24 t km^{-2} yr^{-1} at Grassland A, Grassland B, Grassland C, Arable A and Arable B respectively. Figure 3.7 illustrates average annual SSYs from Ireland, the United Kingdom (UK) and the wider Atlantic climatic region of Europe (Vanmaercke *et al.,* 2011). The variability of average SSYs may be partly described by catchment size (x axis) along with site specific variations in slope angles, slope length and soil types which further influence erodibility. Values from catchments assessed in this study align with existing data on SSY in Ireland (*cf.* Huang and O'Connell, 2000; Jordan *et al.,* 2002; Harrington and Harrington, 2013; Thompson *et al.,* 2014), and are consistently low compared with the UK and Europe. Considering the agricultural intensity of these catchments, illustrated by the fact that Grassland A is in region of the highest milk yield in Ireland (Läppe and Hennessy, 2012), and crop yields across Ireland are internationally high (Melland *et al.,* 2012a)), these values are particularly low.

Table 3.3. Annual rainfall, discharge and suspended sediment flux summary for five catchments.

	Grassland A			Grassland B				Grassland C				Arable A				Arable B			
Year	2010	2011	2012	2009	2010	2011	2012	2010	2011	2012	2009	2010	2011	2012	2009	2010	2011	2012
Rainfall (mm yr^{-1})	1045	1139	1097	1278	800	1155	920	965	1234	969	1240	763	1102	827	896	742	1049	844
Runoff (mm yr^{-1})	443	633	608	643	330	504	382	424	727	575	750	366	517	473	383	319	521	542
Mean SSC (mg L^{-1})	5	4	5	14	5	8	12	4	4	3	6	3	4	6	9	10	10	18
Max SSC (mg L^{-1})	707	467	966	1020	426	882	707	419	813	462	773	224	737	2141	494	707	688	1120
>25 mg L^{-1} (% of ST*)	3	2	3	11	5	6	8	2	2	2	4	1	2	3	6	6	6	11
SSY (t km^{-2} yr^{-1})	3.95	6.61	14.92	48.39	6.65	13.46	30.08	6.07	22.28	6.52	17.44	2.11	5.22	23.10	15.59	15.97	24.20	41.81

*ST: % of sampled time

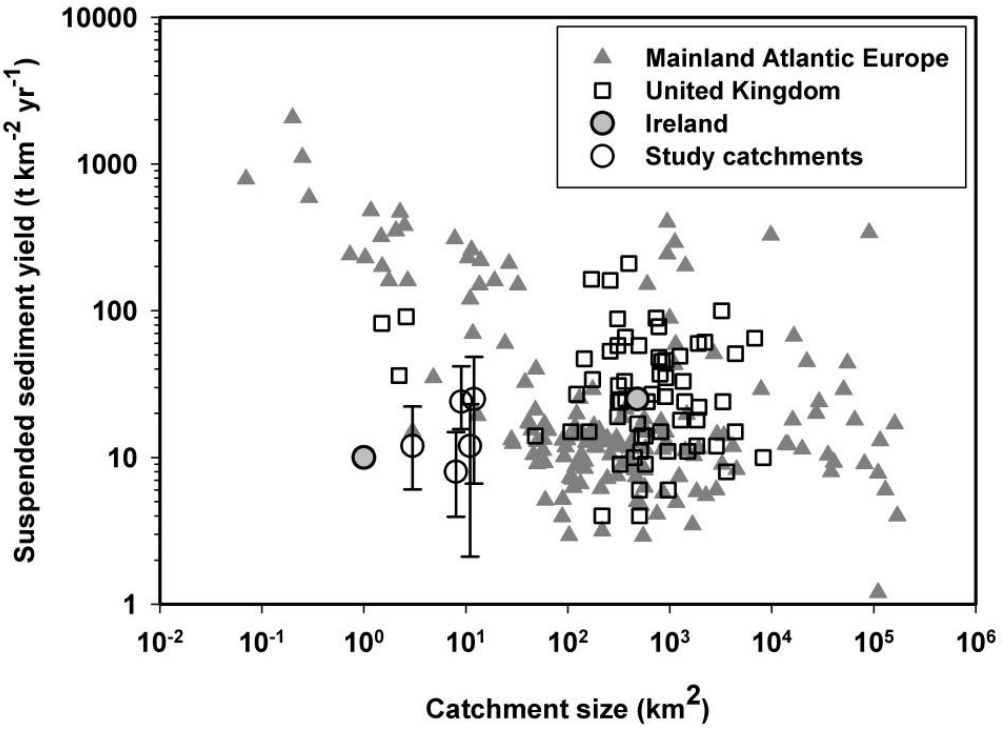

Figure 3.7. Catchment size and suspended sediment yield of European river catchments; study catchments displayed with inter-annual range. Sources: Foster *et al.* (1986); Milliman and Syvitski (1992); McManus and Duck (1996); Wass and Leeks (1999); Huang and O'Connell (2000); Verstraeten and Poesen (2001); Jordan *et al.* (2002); Walling *et al.* (2002); Harlow *et al.* (2006); Oeurng *et al.* (2010); Zabaleta *et al.* (2007); Gay *et al.* (2014).

Catchment observations suggest high land cover complexity, comprising small and irregularly shaped fields, separated by a dense network of hedgerows and vegetated ditches (Table 2.1) reduced water and sediment connectivity between hillslopes and the channel network. Efficient drainage can also reduce the spatial extent and temporal stability of connected areas and, considering the over-engineered nature of these ditch networks, encouraged sediment deposition (Shore *et al.*, 2014). Furthermore, lower slope-lengths reduce the hillslope erosion potential (Lal, 1988), and sediment trapping and soil erosion prevention by root binding of hedgerows was observed. However, at the catchment scale, greater efficiency of hillslope drainage can increase the erosivity of streams in turn accelerating erosion from in-channel sources such as channel banks (Belmont *et al.*, 2011; Massoudieh *et al.*, 2013).

In the UK, Cooper *et al.* (2008) suggested annual average 'target' and threshold 'investigation' SSY values be based upon drainage class and catchment terrain characteristics. Grassland A and Arable A qualify as lowland well-drained catchments and, on average, fall well below target and investigation SSY of 20 and 50 t km^{-2} yr^{-1} respectively. Grassland B, Grassland C and Arable B, categorised as lowland

predominantly poorly-drained catchments, on average, fall below target and investigation thresholds of 40 and 70 t km^{-2} yr^{-1}, respectively. Total SSY data for individual years (Table 3.3), however, indicate variability and exceeded respective SSY target values at Grassland B in 2009, Arable A in 2012 and Arable B in 2012.

Higher average SSC, intra-annual period of FFD exceedance, and average SSY in catchments Grassland B and Arable B are suggested to result from poorer soil drainage. During rainfall events, soils are rapidly saturated and critical overland flow pathways established, and consequently, eroded particles within these connected areas are transported through the catchment (Mellander *et al.,* 2012; Shore *et al.,* 2013). The SSC responses here suggest, as in other catchments with impeded drainage, that high overland-flow potential is also associated with a notable proportion of sediment delivered at lower concentrations over a longer period, through surface and sub-surface flow pathways such as through macropores and tile drains (e.g., Deasy *et al.,* 2009; Melland *et al.,* 2012a; Ibrahaim *et al.,* 2013; Mellander *et al.,* 2015) resulting in increased average SSCs. In catchments Grassland A and Arable A, sub-surface flow pathways dominate, due to well-drained soils reducing the likelihood of overland flow and consequently surface soil losses. Furthermore, at Arable A, Mellander *et al.* (2015) found weathered bedrock formed groundwater pathways further decreasing surface pathway initiation. Consequently, SSCs, intra-annual period of FFD exceedance, and SSYs were low. Conversely, Grassland C more accurately reflects the sediment characteristics of the well-drained catchments despite the moderate- to poorly-drained soils. Near complete cover of permanent pasture here was considered to sufficiently reduce sediment source availability and transport of sediment to the watercourse.

Generalisations can be made in relation to the overriding controls on SSY across the monitored catchments (Figure 3.8). Inter-catchment comparisons here used data from hydrological years 2010 to 2013, where data were available for all five catchments. Sediment delivery was enhanced by the combined effect of an overland-flow dominated transport system (poorly-drained soils) and, to a lesser extent, source availability (arable soils with potentially lengthy periods of bare ground cover (Regan *et al.,* 2012) or seasonally thinly vegetated grassland soils (cf. Bilotta *et al.,* 2010)). Catchments that possess better drainage characteristics and/or permanent crop cover have greater resilience to extreme sediment losses. In catchments such as Arable A, where good-

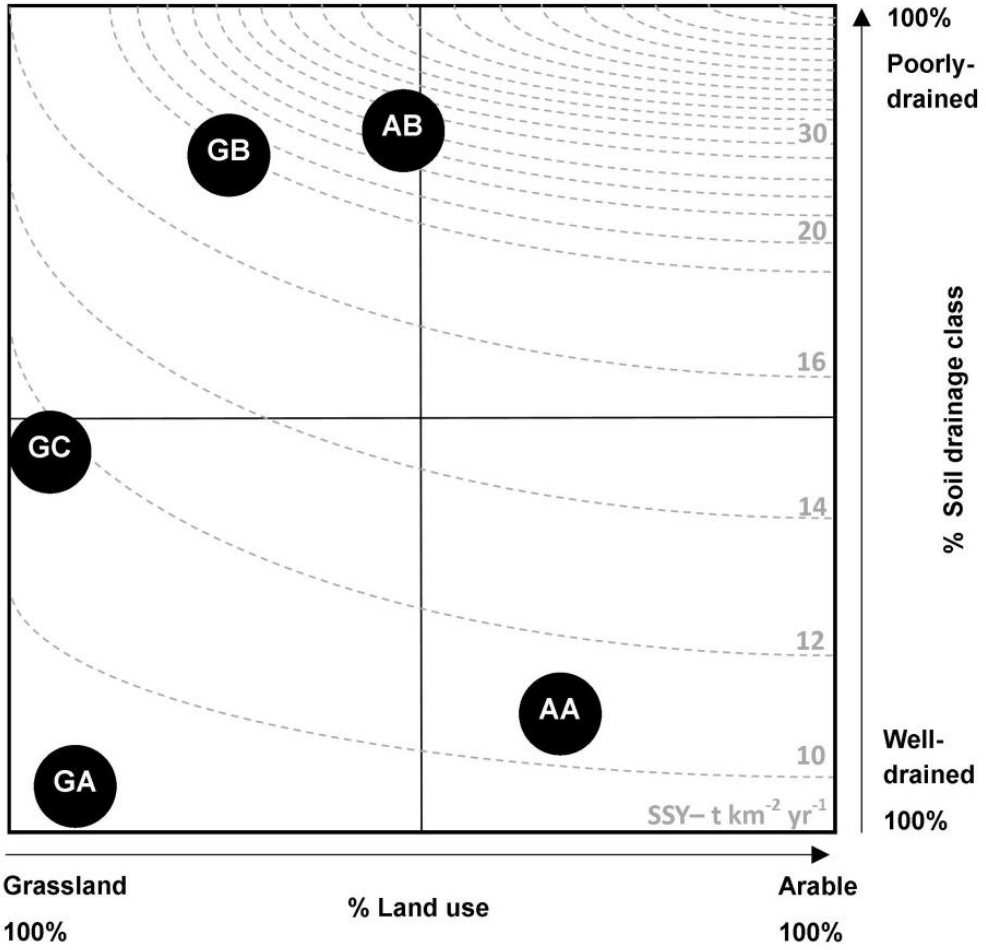

Figure 3.8. Conceptual diagram of suspended sediment yield as represented by iso-lines according to land use and dominant soil drainage class. Abbreviations: GA - Grassland A; GB - Grassland B; GC - Grassland C; AA - Arable A; AB - Arable B.

drainage is combined with high source availability, the risk associated with sediment transport during extreme rainfall events and years was, nevertheless, high. Similarly, poorly-drained soils stabilised by permanent pasture should be maintained and periods of bare cover should be avoided.

High inter-annual variability was evident, particularly with regard to SSY (Table 3.3). The annual SSY coefficient of variation (CV%) were 67%, 76%, 79%, 83% and 50% in Grassland A, Grassland B, Grassland C, Arable A and Arable B, respectively. Notably, in Grassland B and Arable B catchments, the inter-annual SSY ranges of 42, and 26 t km^{-2} yr^{-1}, respectively, were greater than average annual inter-catchments SSY of approximately 24 t km^{-2} yr^{-1} for both sites. The variability found within each of the five monitoring catchment was comparable to the results of Vanmaercke *et al.* (2012) who reported CV% ranging from 6-313% (median 75%) in 726 catchments worldwide. The

catchment with the lowest inter-annual SSY (11 t km^{-2} yr^{-1}), Grassland A, received the least variable rainfall input and total discharge.

Inter-annual SSY variability results from strong seasonality due to the timing and character of rainfall events, soil moisture deficit and land management which conditions sediment availability in critical source areas. Analysis of shorter term sediment losses i.e., at seasonal, monthly and event scales would also provide empirical evidence to inform both high level policy considerations and local decision making. Additionally, assessment of seasonal transfers are likely to have greater ecological significance as mean annual thresholds such as SSC (through the FFD), and SSY may underestimate the seasonal fluctuations of risk of sediments to aquatic ecosystems (Thompson *et al.*, 2014). Sensitivity to sediment is species-specific and dependent upon life stage (Collins *et al.*, 2011); therefore, shorter-term metrics such as the timing, magnitude, duration and frequency of sediment transfers are important concepts to consider. Existing static thresholds may, therefore, be considered ecologically irrelevant, particularly when utilised as an instantaneous threshold for high-resolution data. Future discussion regarding sediment targets requires an assessment of multiple species and habitat quality. This task is particularly complicated where ecological condition is subject to multiple-stressors such as nutrients (Bilotta and Brazier, 2008), bed substrate quality (Kemp *et al.*, 2011) and time lag of water quality response to pollutant mitigation measures (Fenton *et al.*, 2011; Vero *et al.*, 2014).

Overall, annual average sediment metrics from the study catchments (~10 km^2) with land uses broadly representative of agricultural practices across Ireland were relatively low in international terms. Considering the extent and intensity of agricultural land use and high effective rainfall in the study catchments, this is perhaps unexpected considering the small scale of study. As previously discussed, the complexity of landscape features (e.g., fields, hedgerows, ditches), representative of the wider Irish agricultural landscape (Deverell *et al.*, 2009), can be expected to reduce sediment connectivity and thus decrease the likelihood of field-scale soil erosion and promote the resilience of agricultural soils to soil loss. Preservation, restoration or establishment of landscape features may be an important mitigation strategy to support the sustainable intensification of catchment agro-ecosystems worldwide.

However, even with modest SSY, the potential for off-farm risks to ecologically sensitive aquatic habitats, for example, from SS deposition in rivers, and the potential for channel network sediment storage to moderate or accelerate sediment yields requires further consideration. Therefore, identification of the specific mechanisms promoting soil conservation or sediment retention in multiple catchments with contrasting physical and land use characteristics is important. This is particularly relevant for water and agricultural policy, as the prevention of environmental degradation and maintenance and/or sustainable intensification of agricultural production are simultaneously considered. Furthermore, other sediment sources, for example, from channel banks and road networks may contribute significant proportions of the annual load (Rowan *et al.,* 2012; Collins *et al.,* 2013; Sherriff *et al.,* 2014) particularly where strategies to reduce sediment loss on the hillslope scale such as sub-surface drainage may accelerate losses from channel sediment sources at the catchment scale. Assessment of such sources could be a useful insight to prioritise sediment management strategies (Wilson *et al.,* 2008).

3.6 Conclusions

This study assessed the accuracy and reliability of an *ex situ*, turbidity-based methodology to estimate suspended sediment fluxes in multiple monitored catchments. Applying the method, annual SSC, FFD exceedance and SSY data in five catchments were further investigated in relation to physical catchment characteristics and land management. The key findings are:

- Suspended sediment metrics between *in situ* and *ex situ* methodologies were not significantly different from in-stream cross-sectional, depth-integrated samples in two monitoring catchments;
- The *ex situ* methodology reported less sensitivity to spurious data peaks; however, periods of extreme large debris transport increased the sensitivity of the *ex situ* instrumentation to short-term blockages;
- All catchments reported mean annual SSCs of less than the FFD threshold of 25 mg L^{-1} and short-term exceedance of 1-11% of sampled time;
- Inter-annual variability of SSY was strong due to the timing and character of rainfall events in relation to land management;

- Average annual SSYs in all five Irish catchments reported here were low in comparison to similar catchment and landscape settings elsewhere in Europe. Farming practices favouring relatively small fields, a high density of field boundaries including ditches, with low consequent connectivity are likely to explain this;
- Within the study catchments, SSY was higher in catchments dominated by poorly-drained soils than those with well-drained soils. Furthermore, on poorly-drained soils, catchments with a greater proportion of arable land use reported the highest annual average SSY;
- Well drained soils dominated by arable crops did, however, show the potential to supply significant quantities of sediment;
- Complexity of landscape features (hedgerows, drainage ditches and irregular field sizes) may provide resilience to hillslope soil erosion and/or sediment transport despite spatial dominance and intensity of agriculture and these will be important considerations for future management (such as sustainable intensification) and/or SS mitigation in Ireland and elsewhere.

3.7 Summary

These findings illustrate, using high-quality and high-resolution suspended sediment dataset, that interaction between climate, catchment characteristics and land use regulate the supply of sediments from agricultural catchments. The low suspended sediment yields reported from these catchments, relative to other international studies, are justified by the reduced connectivity resulting from complex patterns of landscape features (hedgerows, drainage ditches, small field sizes) and land management. These findings have international significance for protecting water quality (for sediments and other agricultural pollutants with a high affinity with particulate transport) from agro-ecosystems driving towards sustainably intensifying to meet global food demands.

Finer resolution seasonal and storm-event scale sediment transfers may better inform erosion risk due to better detection of sediment pulses moving into the channel network particularly within ecologically sensitive periods. Further to this, the assessment of seasonal sediment provenance and field-scale soil loss assessments within this land management and landscape framework are crucial to quantify the contributions made from specific agricultural and other sediment sources.

Chapter 4. Storm-event suspended sediment-discharge hysteresis and controls in three agricultural catchments: implications for catchment scale sediment management

4.1 Introduction

Understanding patterns and rates of erosion at the catchment scale which supply suspended sediment (SS) into the channel network is a key element in sustainable catchment management planning (Rowan *et al.*, 2012). Annual SS metrics are useful for prioritising management strategies between basins; however, they provide limited understanding of internal sediment delivery mechanisms (Sherriff *et al.,* 2015a). Methodologies such as sediment fingerprinting (Rowan *et al.,* 2012; Koiter *et al.,* 2013; Thompson *et al.,* 2013; Belmont *et al.,* 2014; Smith and Blake, 2014), sediment budgets (Walling *et al.,* 2002; Wallling and Collins, 2008; Minella *et al.,* 2014) and modelling (Collins *et al.,* 2007) are used to target sediment sources in agricultural catchments. However, the resource intensiveness of field data collection and model validation can restrict multi-catchment and high temporal resolution investigations. Analysis of catchment SSC and discharge (Q) hysteresis following rainfall-runoff are, however, inherently high-resolution. Diagnostic analysis of SS-Q hysteresis relations following a rainfall event can be used to elucidate the interactions between flow pathways and sediment yield, and gain insights into sediment source availability, sediment storage and hydrological pathways (Williams, 1989; Duvert *et al.,* 2010; Vongvixay *et al.,* 2010).

The use of SSC-Q hysteresis as a sediment management tool has been limited by the inconsistent use of qualitative hysteresis categories, the difficulty of interpreting sediment pathways for complex hysteresis storms, and the scale-dependency of sediment pathways in relation to catchment size (Gao and Josefson, 2012). Recent developments in quantitative hysteresis parameters e.g., the Hysteresis Index (HI – Langlois *et al.,* 2005; Lawler *et al.,* 2006; Aich *et al.,* 2014) and the availability and improved reliability of high resolution SS datasets facilitates the analysis of consecutive events in multiple catchments over time (Sherriff *et al.,* 2015a). Long-term event-scale monitoring is commonly analysed using multivariate statistics to attribute sediment response (either hysteresis type or numeric sediment metrics such as event SS yield, maximum SSC, mean SSC) to potential rainfall, discharge and antecedent soil condition

controls (Zabaleta *et al.,* 2007; Estrany *et al.,* 2009; Duvert *et al.,* 2010; Oeurng *et al.,* 2010; Giménez *et al.,* 2012; Perks *et al.,* 2015). The evolution of HI over time, however, has the potential to indicate seasonal variability thus facilitating a dynamic understanding of catchment sediment dynamics, in terms of structural and functional hydrological connectivity (Bracken *et al.,* 2013), transport pathways and sediment availability. Such information is critical, particularly in agricultural catchments, to improve knowledge of diffuse pollutants under a range of flow conditions to rigorously assess the causes of sediment export (Bowes *et al.,* 2005; Bende-Michl *et al.,* 2013).

The aim of the study was to develop conceptual models of SS transfer dynamics across and within multiple intensively managed agricultural catchments to increase understanding and aid with catchment management. The objectives were to:

- Develop an understanding of dominant hydrology and sediment pathways using storm resolution SS and Q data;
- Investigate the temporal evolution of catchment sediment transport processes and contributing areas through SSC-Q hysteresis loop analysis;
- Estimate the quantity of readily available and total channel bed sediment storage to determine the likely impact of channel sediment storage on hysteresis responses.

4.2 Methodology

4.2.1 Data collection

Suspended sediment data were collected at each catchment outlet using high-resolution (10 min) T and Q measurements – Section 3.2.1. Meteorological data were collected from a weather station in the lowlands of each catchment (BWS200, Campbell Scientific) measuring 10 min resolution rainfall, air temperature, relative air humidity, radiation and wind-speed. Higher-altitude rainfall amount and rainfall intensity were also measured with an additional rain gauge in the uplands of each catchment. Ground cover of dominant crop types in each catchment were estimated using monthly observations from multiple locations and 70% ground cover was defined as the threshold required to reduce soil erosion risk (Sanjari *et al.,* 2009).

4.2.1.1 Channel bed sediment storage

Fine sediment storage in the river channel was estimated using the re-suspension method (Lambert and Walling, 1988). The network length was divided into multiple reach types based on a visual assessment of channel dimensions, catchment position and bank stability (Table 4.1). A representative location within each reach was selected for bed sediment sampling in December 2013, May 2014 and August 2014 (Figure 4.1). Samples were collected from within a metal cylinder (diameter 0.4 m) pushed into the stream bed (to approximately 5 cm depth) at three locations within each reach (assumed high, medium and low storage). The depth of water enclosed in the cylinder was recorded and a cordless power drill with stirrer attachment used to agitate fine sediments (approximately 60-90 seconds) from which a water sample was collected (up to 1 litre). Firstly, only the water was agitated to determine the readily available fine sediment concentrations. Secondly, a sample was taken after full agitation of sediments in the upper 5 cm of the channel bed. Low water levels, channel bed vegetation, or impeded access occasionally prevented sample collection as did absence of storage in the lower reaches of Arable B. To account for limited storage in Arable B, the proportion of fine sediment cover was recorded which was used in later calculations.

Samples were refrigerated (3ºC) on return to the laboratory before subsequent sample preparation and analysis. Samples of the readily available fraction were measured for suspended sediment concentration using the method described in Chapter 3. For full agitation samples, total sample volume was recorded and the contents were transferred to a pre-weighed plastic tray. Samples were oven dried at <40ºC (approximately 72 hours) and re-weighed to determine the total solid content of samples. Samples were dry-sieved to 125 μm, to retain the finer fraction and weighed to determine sample quantity. Bed sediment concentrations (C_{bs} – g m^{-2}) for readily dispersible or full agitation samples were determined using the following equation:

$$C_{bs} = \frac{V_c \times SSC}{A_c}$$

Equation 4.1

Where V_c is the cylinder volume (litres), *SSC* is the sediment concentration in (g L^{-1}) and A_c is the area sampled (m^2).

Table 4.1. Channel reach descriptions for Grassland B, Arable A and Arable B.

Reach	Description
Grassland B	
1	Wide >2 m, deep >1.5 m bankfull depth, trees along one bank only, stock access on opposite bank
2	Same as reach 1 but with trees vegetation both banks
3	Smaller tributary and ditch channels with little or no evidence of disturbance, channel dimensions <1 m deep, <1 m wide
4	Smaller channels with noticeable disturbance, i.e., post-management, low vegetation cover on banks or evidence of channel bank erosion due to flow
5	Approximately 1.5 m width, 1.5 m bankfull depth with tree vegetation present on both banks
6	Bankfull depths frequently ca. 2 m, some areas of stock access
7	Bankfull depth approximately 1 m and 1.5 m depth, vegetation present on both banks and no stock access
8	Similar to reach 5 but with greater sinuosity
9	Upland woodland river section with large boulders on bed, channel dimensions 1 m depth, 1-1.5 m width, vegetation cover is variable on one side (range: grass only to woodland species)
Arable A	
1	Small channel approximately 1 m width and 1.5 m bankfull depth in established riparian woodland
2	Meandering main river channel >2 m wide and 1 m bankfull depth in established riparian woodland
3	Narrower tributary, 1-1.5 m width and 1 m depth with established riparian woodland corridor and few stock access points for drinking water
4	Channels 1.5 m wide and <1.5 m bankfull depth with evidence of removal large vegetation removal from one bank to facilitate channel management. Other (field boundary) side features established woodland species.
5	Smaller tributary and ditch channels with little or no evidence of disturbance, channel dimensions <1 m deep, <1 m wide
6	Bankfull depths 0.5-1 m, width 1-1.5 m, stock access but tree species along both channel banks
7	Bankfull depth approximately 1 m, width 1.5 m, tree species along one channel bank and stock access on opposite bank
Arable B	
1	Wide >2.5 m, 1-1.5 m bankfull depth with bedrock substrate and established riparian corridor with woodland species
2	Channel width 2 m but similar depth to reach 1, woodland riparian corridor and a few stock access points
3	Smaller channels (approximately 1 m x 1 m) open to stock access and considerable fine sediment visible on channel bed
4	Smaller channels (approximately 1 m x 1 m), no stock access, often woodland species on one bank and less established vegetation on opposite bank
5	Channel dimensions approximately 1.5 x 1.5 m with woodland tree species on one bank but less established vegetation on opposite bank
6	Little established vegetation on either banks and evidence of channel management, channel dimensions approximately 1.5 x 1.5 m.
7	Channels show evidence of management but not the riparian zone, 1.5 m deep, 1 m wide, one bank has trees present
8	Wide and shallower channel section (2 m x 1 m, respectively), established vegetation on both channel banks and no stock access

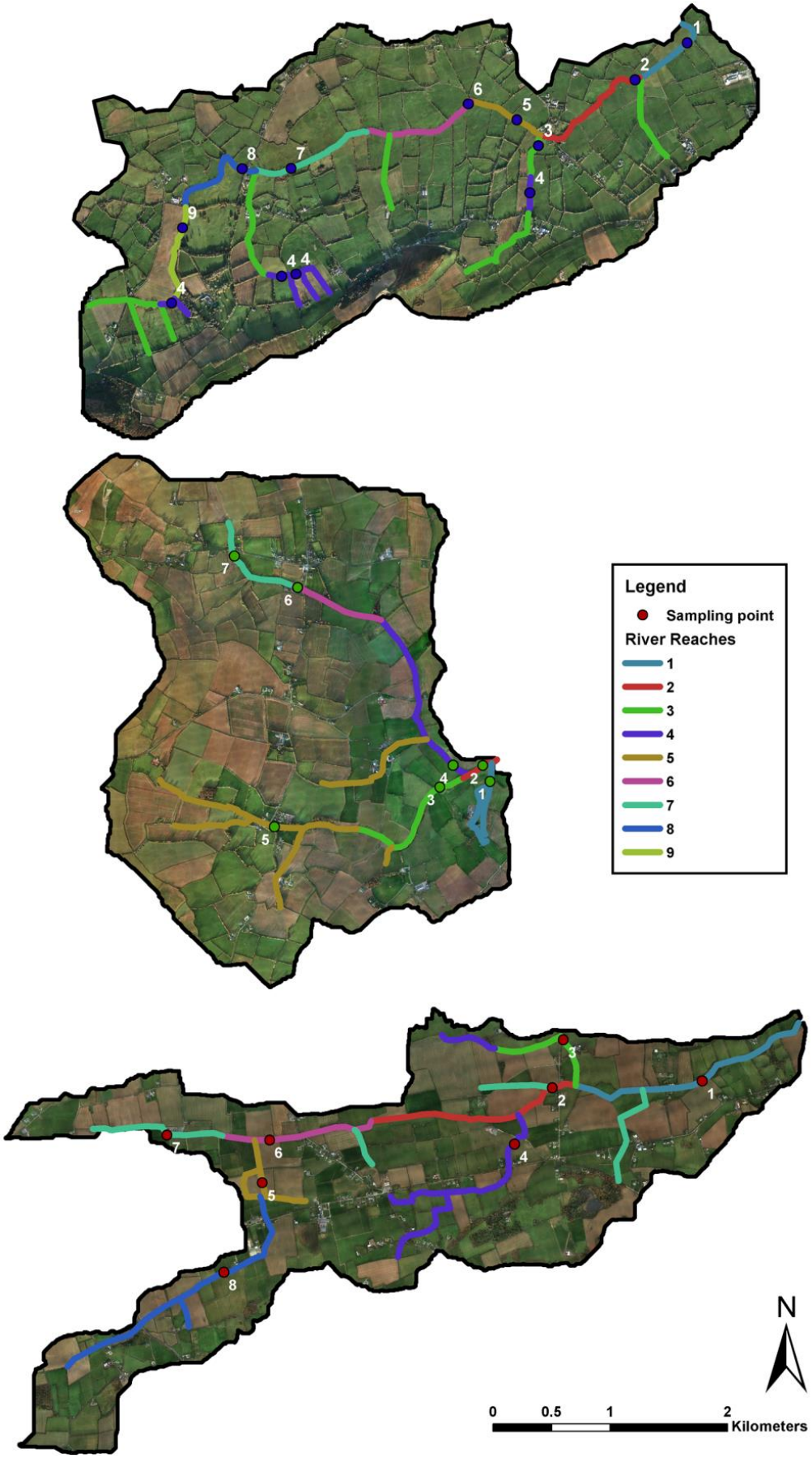

Figure 4.1. Location of study reaches and sampling points in Grassland B, Arable A and Arable B.

4.2.2 Data analysis

4.2.2.1 Event analysis

Individual storm events from October 2011 to September 2013 were extracted according to catchment specific hydro-sedimentary characteristics (Zabaleta *et al.*, 2007). In Grassland B, storm event initiation was defined where the rate of change between consecutive 10-min measurements of Q and SSC exceeded 0.005 m^3 sec^{-1} and 2 mg L^{-1}, respectively, and consistent decreases between consecutive 10-min measurements in Q of <0.012 m^3 sec^{-1} and SSC of 1 mg L^{-1} defined event termination. In Arable A, event initiation was defined where Q increased by >0.003 m^3 sec^{-1} and SSC by 2 mg L^{-1} between consecutive 10-min measurements, and termination where Q decreased by <0.007 m^3 sec^{-1} and SSC by 1 mg L^{-1}. In Arable B, event initiation was defined where Q increased by >0.005 m^3 sec^{-1} and SSC by >2 mg L^{-1} and termination where Q decreased by <0.003 m^3 sec^{-1} and SSC by <1 mg L^{-1} between consecutive 10-min measurements. Where multiple SSC and Q peaks in the stream record could be related to separate rainfall bands they were divided and assessed as single events. Grassland B, Arable A and Arable B comprised 88, 67 and 90 storm events over the study period, respectively.

Events were classified according to hysteresis categories (Williams, 1989) and a HI (Lawler *et al.*, 2006). Bi-plots of Q and SSC indicated the hysteresis loop direction to qualitatively assign hysteresis type; clockwise where SSC peaks before Q, anti-clockwise where Q peaks before SSC, no hysteresis where peaks are simultaneous, Figure-8 which feature both clockwise and anti-clockwise characteristics and complex hysteresis where a clear relationship between SSC and Q is difficult to define.

The HI is a numerical indicator of hysteresis (Lawler *et al.*, 2006) which is calculated using Q and SSC data from each storm event; firstly the mid-point of Q (Q_{mid}) must be determined:

$$Q_{mid} = 0.5(Q_{max} - Q_{min}) + Q_{min}$$

Equation 4.2

where Q_{min} is the discharge at the initiation of the event. The corresponding SSC values at Q_{mid} on the rising (SSC_{RL}) and falling (SSC_{FL}) hydrological limbs are then assessed:

Where $SSC_{RL} > SSC_{FL}$:

$$HI = (SSC_{RL}/SSC_{FL}) - 1$$

Equation 4.3

And where $SSC_{RL} < SSC_{FL}$:

$$HI = (- 1/(SSC_{RL}/SSC_{FL})) + 1.$$

Equation 4.4

Higher magnitudes of HI in either direction indicate greater asynchronous behavior between SSC and Q. Positive HI values indicate clockwise hysteresis, where HI~0 hysteresis is absent and a simultaneous SSC and Q response occurs, and negative HI values indicate anti-clockwise hysteresis. The HI, calculated at a single Q value, i.e., Q_{mid}, cannot reveal figure-8 and complex hysteresis categories. To aid further discussion, clockwise responses and positive HI metrics are referred to as a 'proximal' response and are broadly defined as sediment derived from sources local to the monitoring point and/or subject to a rapid transport pathway. Negative HIs and hysteresis categories are referred as 'distal' sediment responses may conversely indicate a spatially distal sediment source, and/or subject to a delayed transport mechanism.

Data were separated by hysteresis category (clockwise, anticlockwise, no hysteresis, figure-8 and complex) to investigate controls in each catchment (Williams, 1989). Eighteen potential hydrological event controls were collated for each event. Stream discharge parameters: maximum discharge ($m^3\ sec^{-1}$), total event discharge (m^3), event duration (min), flood intensity ((maximum Q – minimum Q)/time of rise) and runoff ratio (total discharge/total rainfall (%). Precipitation amount parameters: total event precipitation (mm), duration of rainfall event (min). Precipitation intensity parameters: maximum 10 min and 30 min precipitation intensity (mm hr^{-1}), and average precipitation intensity (mm hr^{-1}). Antecedent parameters: antecedent rainfall at 1, 3, 5 and 10 days before an event initiation (mm) and antecedent soil wetness at 1, 3, 5 and 10 days before event initiation (mm). Soil wetness was calculated using the effective drainage component of a soil moisture deficit (SMD) model which represents infiltration and runoff components calculated by subtracting the surplus rainfall after actual evapotranspiration and filling of a typical soil moisture profile (Schulte *et al.*, 2005). A conceptual framework for interpretation of potential controls is illustrated in Figure 4.2.

The event-SSC_{fw} (total event SS load divided by total event Q – mg L^{-1}) was selected as the sediment response variable. Flow-weighted concentration metrics are more indicative of source availability by reducing the influence of contrasting catchment hydrology (Jordan *et al.*, 2005) and also removes any potential auto-correlation with the discharge parameters used to calculate SSC. Principal components analysis was performed (SAS JMP v9) and dominant controls were defined as those occupying a similar area of the loading plot to event-SSC_{fw}.

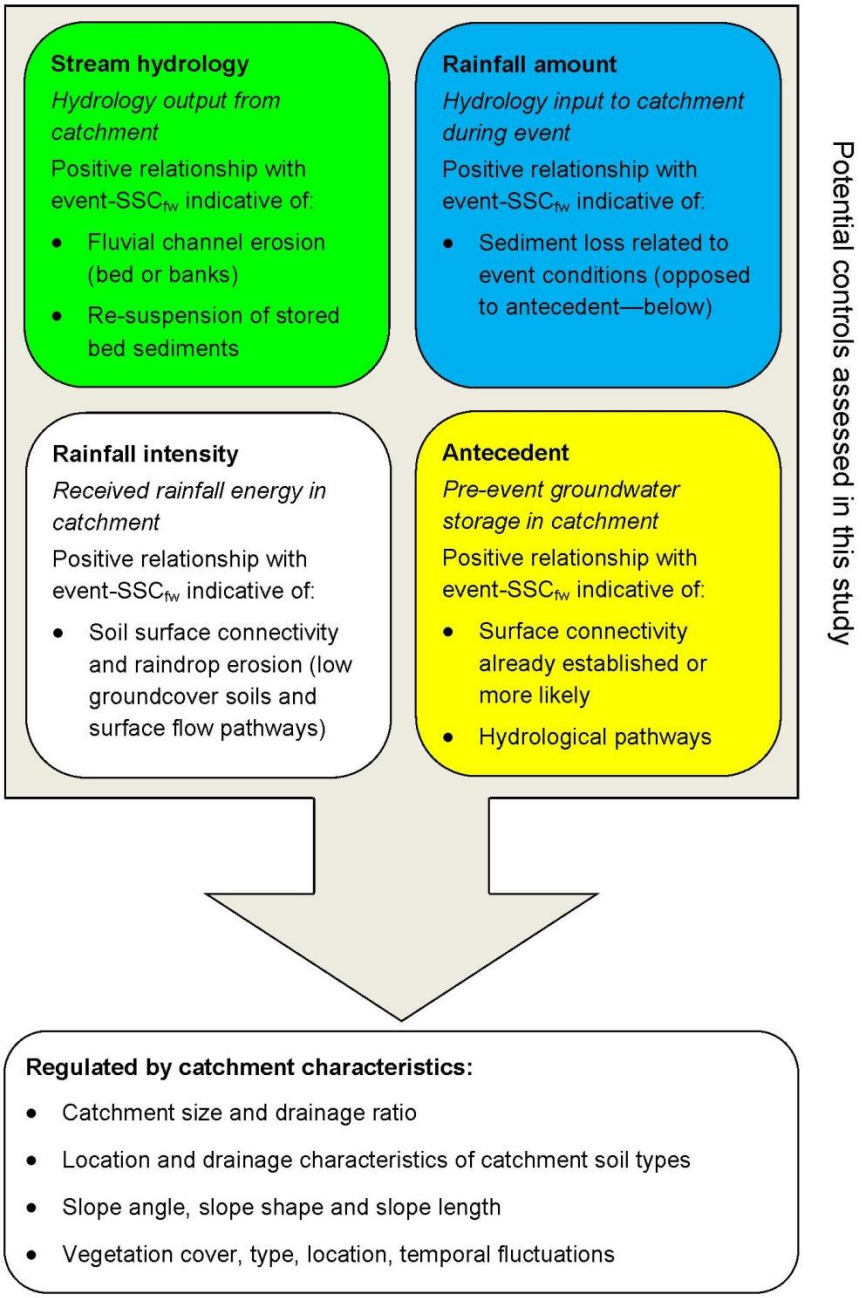

Figure 4.2. Conceptual diagram of potential event controls assessed in this chapter and other influencing controls (considered in the discussion section).

4.3 Results

4.3.1 Storm-event hysteresis

The HI showed events had positive, negative and no hysteresis in all three catchments (Figure 4.3). Events in Grassland B were predominantly positive and these exported greater event-SSC_{fw} compared to events where HI≤0. One event in Grassland B had an extremely negative HI (-71.1) and high magnitude SSC_{fw}. In Arable A, more positive events occurred than negative and event-SSC_{fw} were largest where HI was further from zero (positive or negative) except for one event at HI~0 which reported the highest value (1256 mg L^{-1}) for any catchment. Arable B had the largest HI range but was overall dominated by negative HI events which exported greater sediment quantities. All catchments had lower event-SSC_{fw} during spring/summer than autumn/winter.

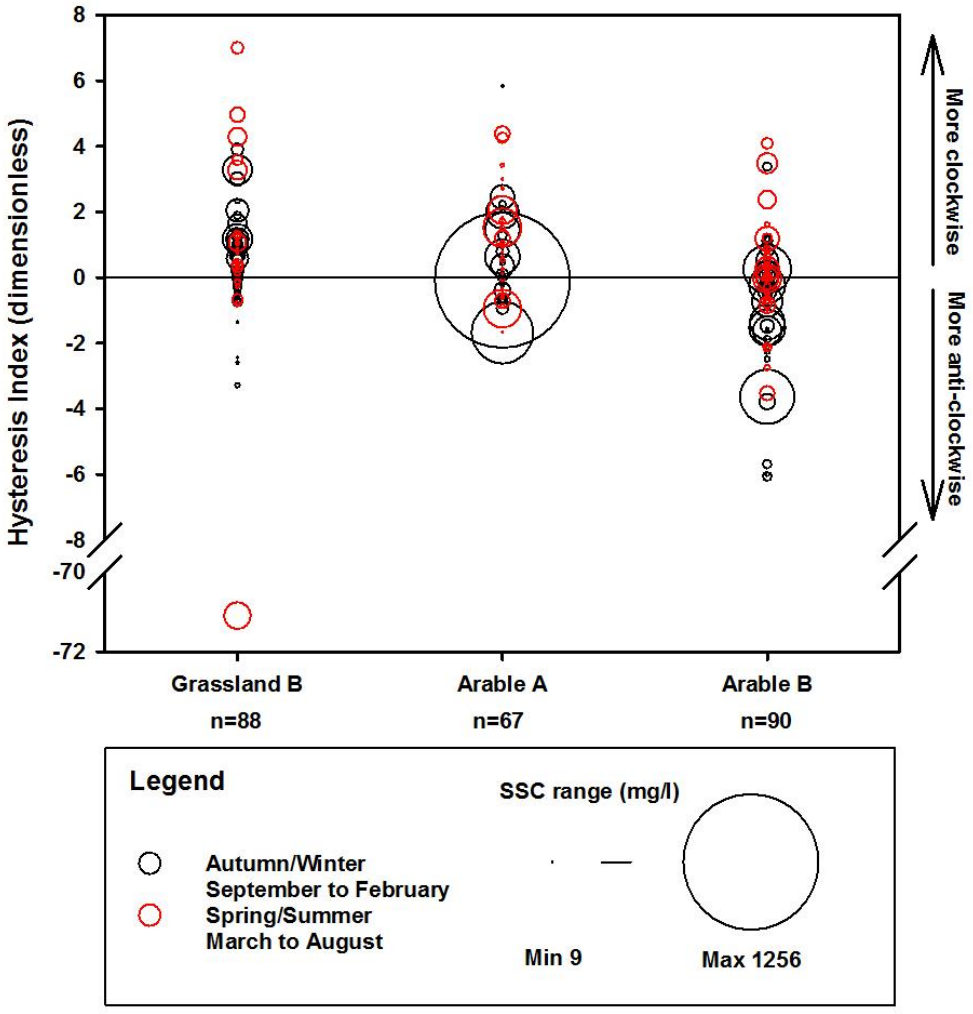

Figure 4.3. Flow-weighted event suspended sediment concentration and hysteresis index for hydro-sedimentary events during spring/summer (March to August) and autumn/winter (September to February) in Grassland B, Arable A and Arable B catchments. The circle size indicates the magnitude of the flow-weighted suspended sediment concentration.

Fluctuations of HI show contrasting seasonal trends between catchments (Figure 4.4). In Grassland B where high (>70%) ground cover was maintained throughout the monitoring period, negative HIs corresponded to periods of lower weekly rainfall values (January to March 2012 and June to July 2013). Periods of high weekly rainfall had positive HI, although scatter is greater at these times. Switches in HI direction (positive to negative or vice versa) occurred in Jan 2012 and May 2012. Arable A showed that, during wetter periods April 2012 to January 2013, positive HI was more common but, similarly to Grassland B, the magnitude of positive HIs decreased as such conditions continued. Decreasing weekly rainfall totals (November 2011 to April 2012) coincided with a negative to positive HI switch. Event-SSC_{fw} was larger where ground cover was less than 70% in the arable catchments ($p<0.05$). Consistently high weekly rainfall totals corresponded with a change in direction from positive to negative HI in Arable B (April 2012 to September 2012) and as wet conditions continued until February 2013, negative HI was sustained. Increased weekly rainfall then decreased from March 2013 onwards coinciding with HI returning towards zero.

Examples of all qualitative hysteresis categories were displayed in the three catchments (Figure 4.5), however, 'no hysteresis' events could not be analysed in Grassland B and Arable B as they were too infrequent (n=1 and n=2, respectively). The contribution of each event hysteresis type to the total event load was not dependent upon the frequency that type of hysteresis occurred in any catchment. In Grassland B, clockwise hysteresis was the most frequent (60%) and contributed the greatest proportion (59%) of the total event SS load. Anti-clockwise hysteresis occurred for 14% of events, but only contributed to 2% of the event SS load. The total SS event load at Arable A is dominated by events with no hysteresis (47%) but this hysteresis type occurred only 11% of the time. Similarly to Grassland B, clockwise is the dominant hysteresis type in Arable A (39%) and has a similar proportion of SS load contribution (35%). At Arable B, anti-clockwise was most frequent (36%) but contributed 23% of the total event SS load. Contrastingly, figure-8 events comprise 21% of events are Arable B but contribute 43% of the total event SS load.

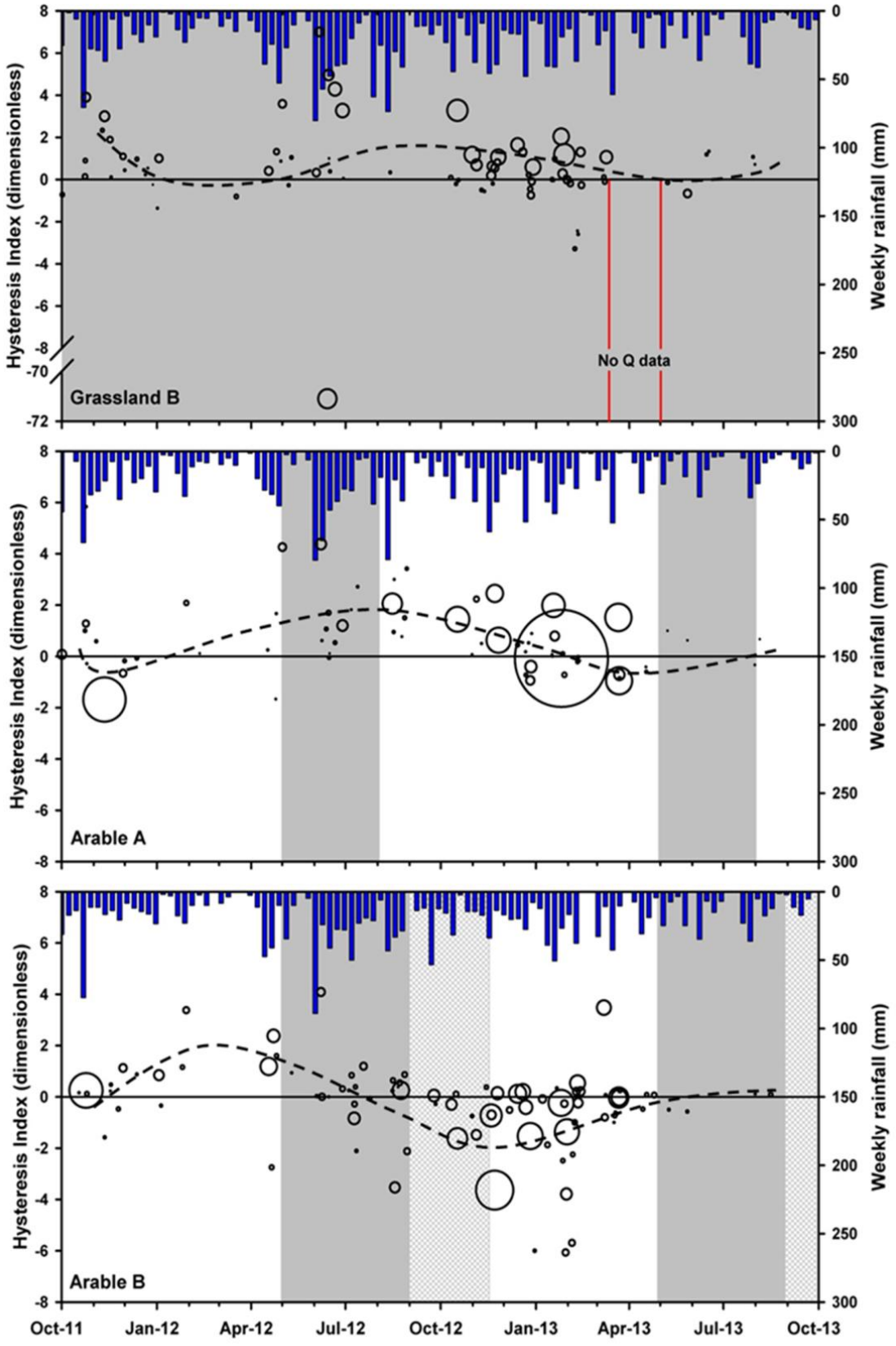

Figure 4.4. Hysteresis index, weekly rainfall and magnitude of flow-weighted suspended sediment concentration response (indicated by size of circle) over monitoring period. Grey panel: high groundcover (>70%), grey-white panel: a reduced proportion of fields possessed high ground cover, dashed line indicates seasonal trend.

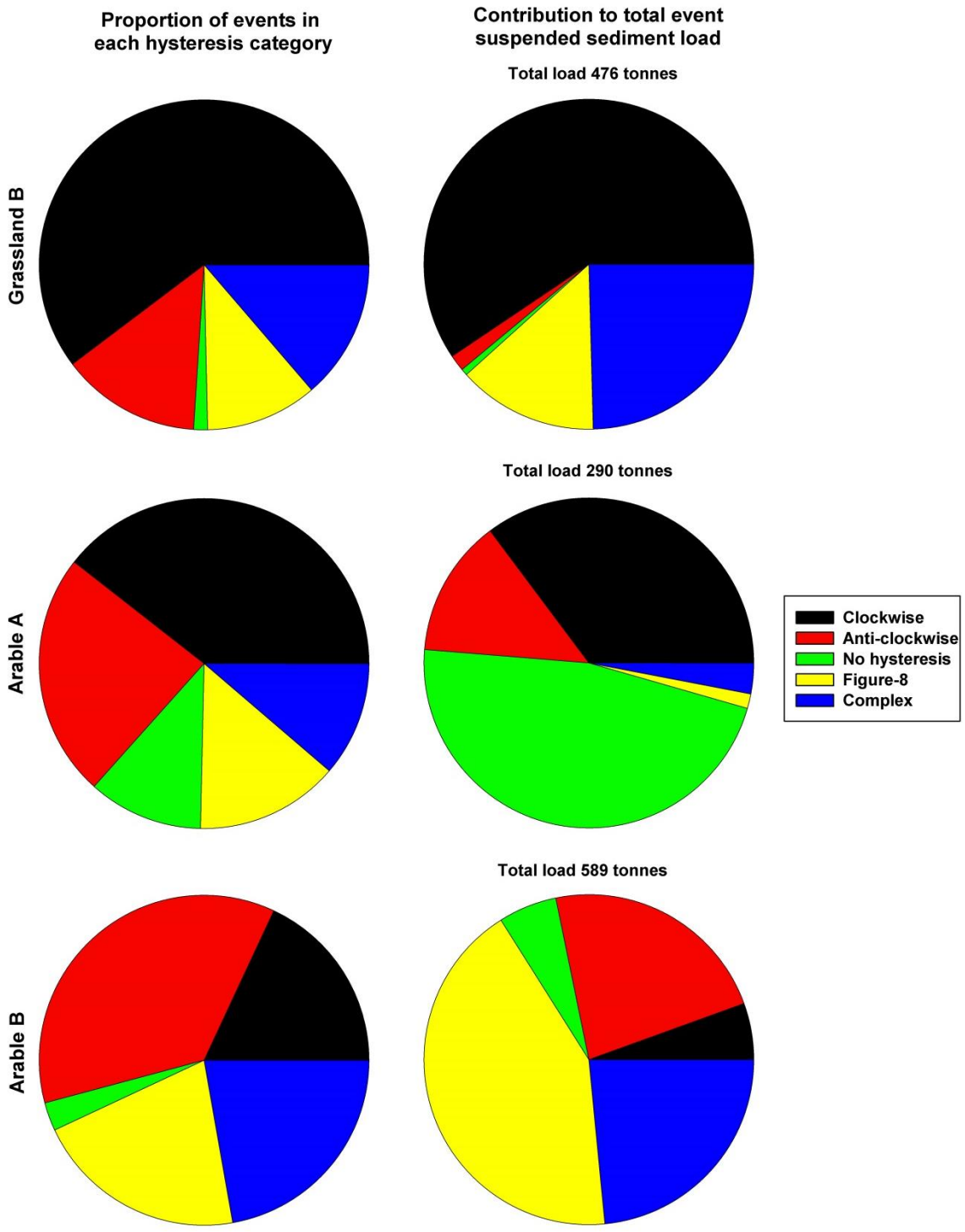

Figure 4.5. Proportion of events categorised by hysteresis type (left), and the contribution of hysteresis type to total event load over monitoring period (right).

4.3.2 Storm-event controls

The results of PCA analysis showing relationships between potential controlling variables and event-SSC_{fw} ($p<0.05$) for each hysteresis category are illustrated in Figure 4.6 (Grassland B), Figure 4.7 (Arable A) and Figure 4.8 (Arable B). Events with clockwise hysteresis in Grassland B showed event-SSC_{fw} was most strongly related to discharge parameters, total precipitation and 30-min precipitation intensity. Event-SSC_{fw} from clockwise events in Arable A were controlled by the same discharge variables and total precipitation but also precipitation duration. In Arable B, clockwise event-SSC_{fw} was controlled by precipitation total and precipitation intensity variables only. Event-SSC_{fw} from anti-clockwise hysteresis events were primarily related to discharge and rainfall intensity variables in catchments Arable A and Arable B. Grassland B anti-clockwise events showed event-SSC_{fw} was most strongly related to discharge and rainfall total variables but also 3-5 day antecedent rainfall and soil wetness. During figure-8 hysteresis events, event-SSC_{fw} was controlled by discharge and precipitation factors in the arable catchments which reflected the combined variable list for clockwise and anti-clockwise hysteresis. Grassland B did not report the same trend; variables related to event-SSC_{fw} for figure-8 hysteresis events were discharge, precipitation amount and precipitation intensity. Complex hysteresis events in Grassland B showed discharge, precipitation and 10-day antecedent precipitation and soil wetness variables were most strongly related to event-SSC_{fw}. Similarly in Arable B, discharge variables and total were best correlated to event-SSC_{fw} during complex hysteresis events; however, Arable A did not show any clustering. Events with synchronous SSC and Q response at Arable A showed strongest relationships between event-SSC_{fw} and discharge, precipitation total and precipitation intensity variables.

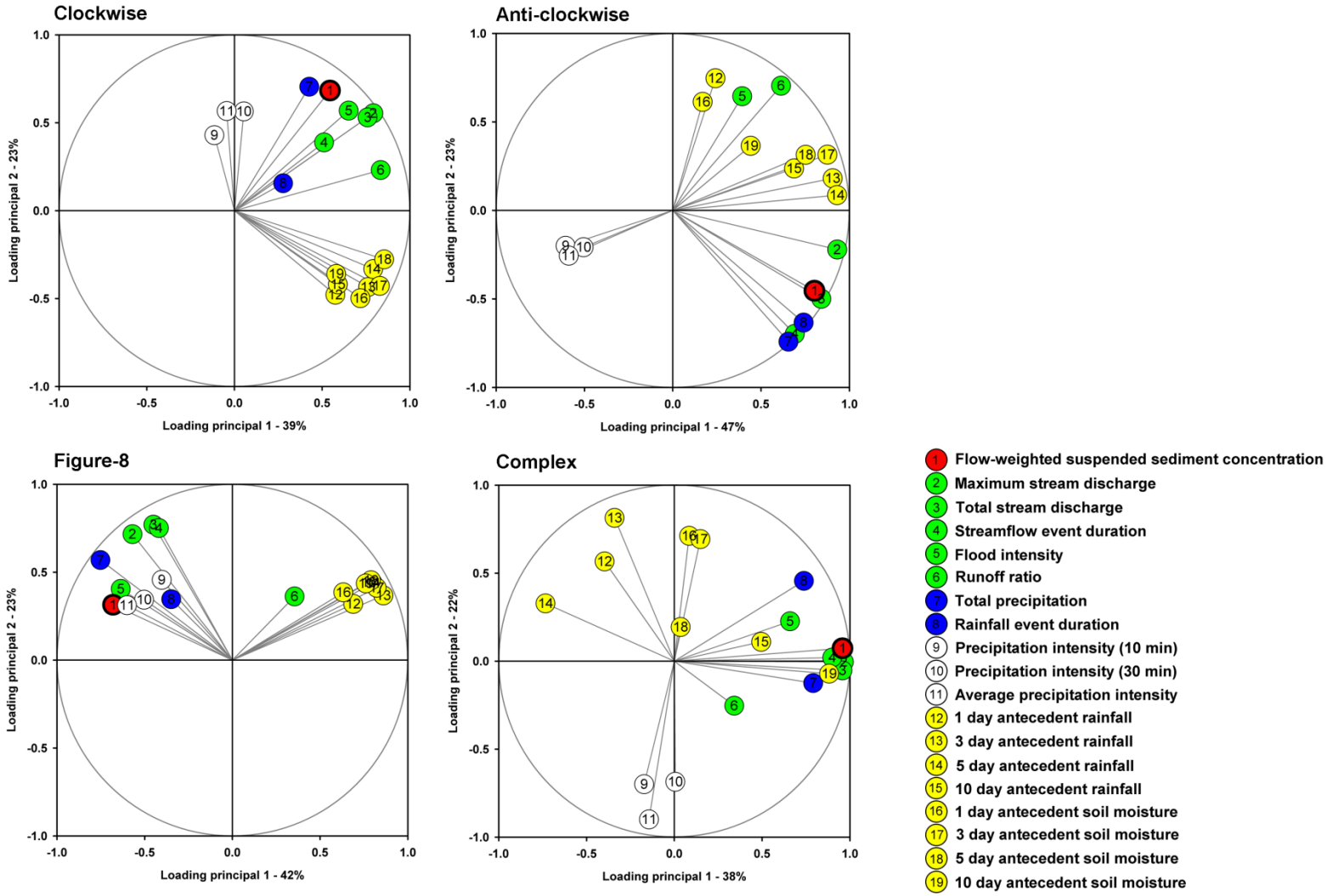

Figure 4.6. PCA loading diagrams of potential event controls and the sediment response variable (event-SSC_{fw}) in Grassland B for separated hysteresis categories.

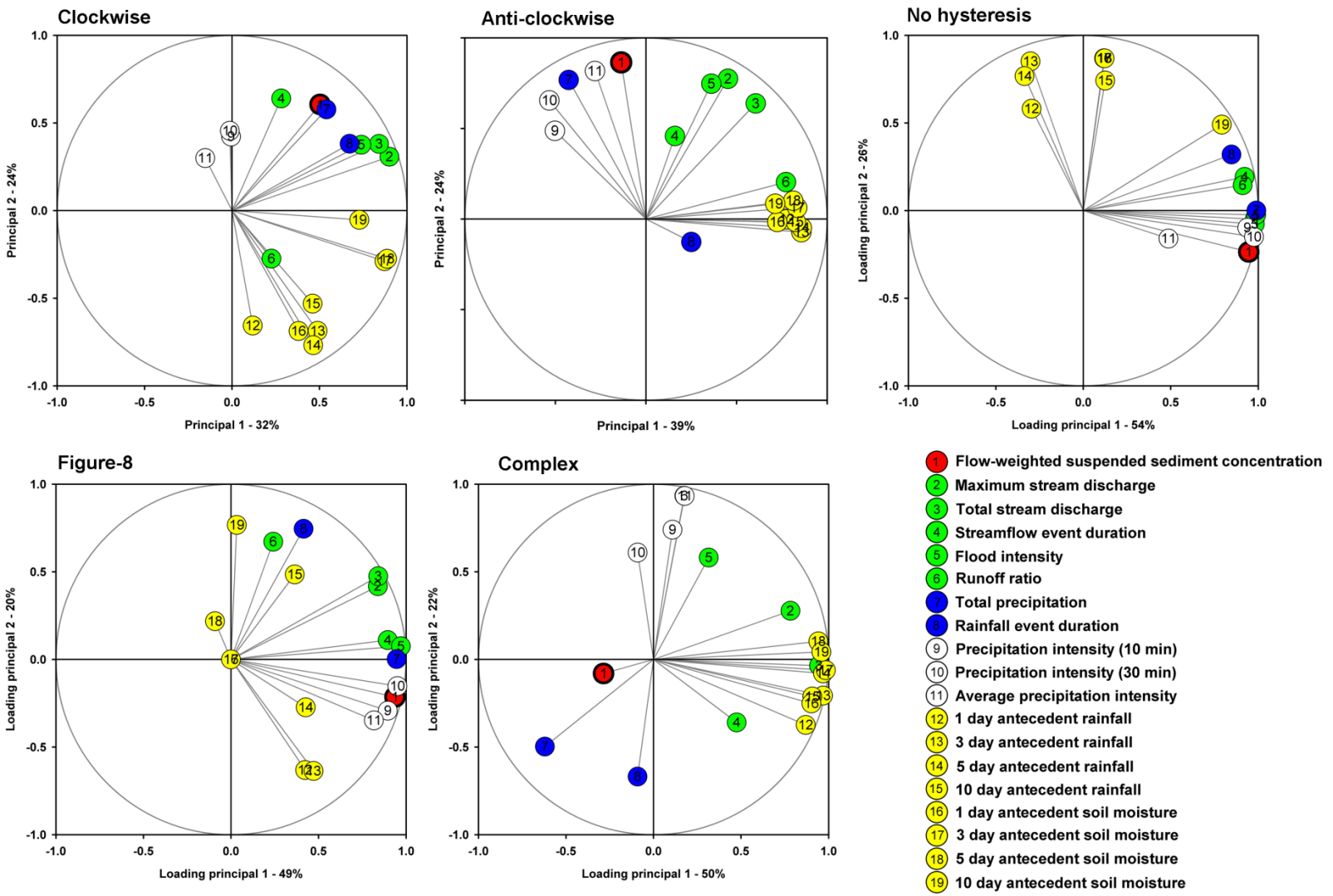

Figure 4.7. PCA loading diagrams of potential event controls and the sediment response variable (event-SSC_{fw}) in Arable A for separated hysteresis categories.

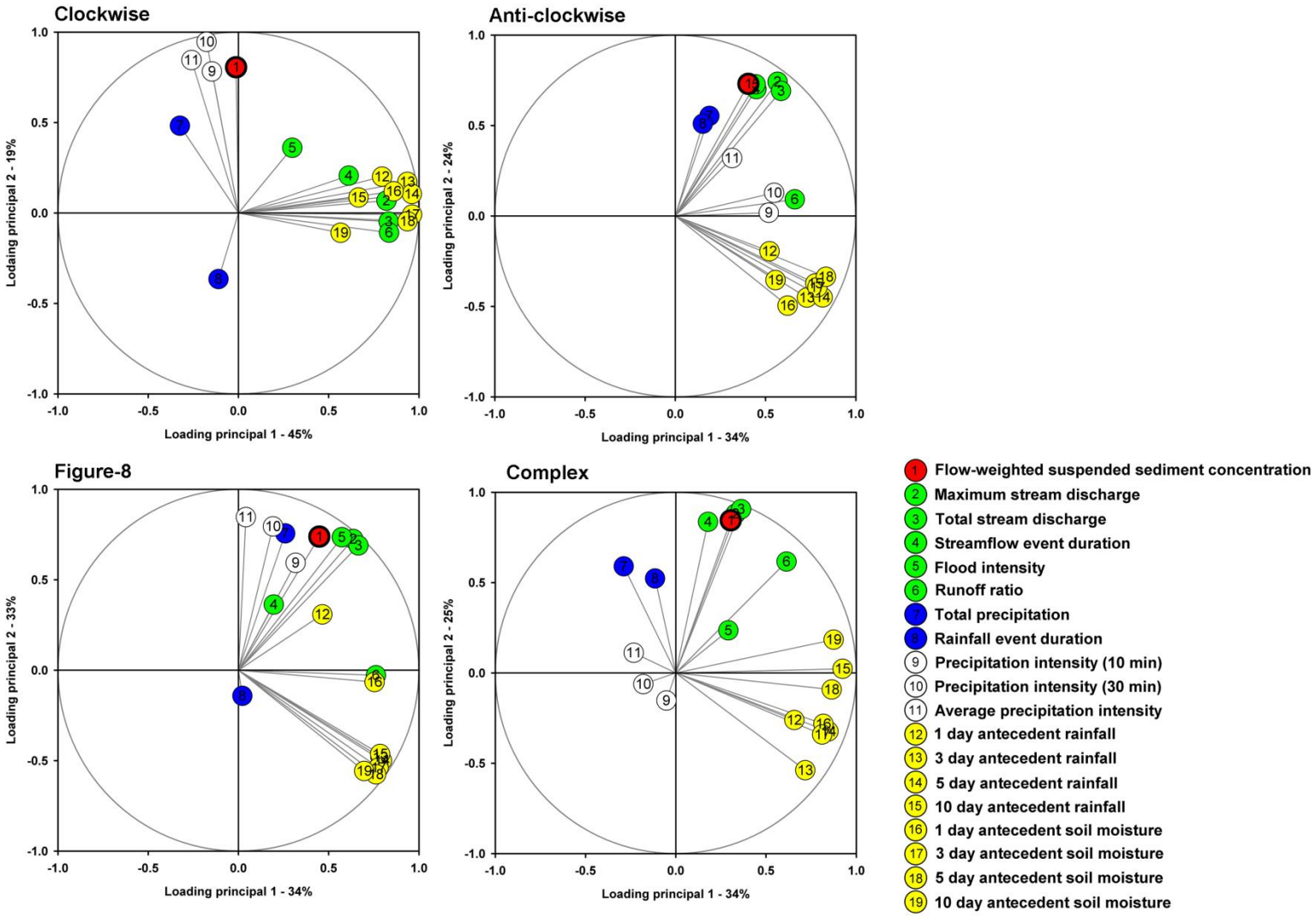

Figure 4.8. PCA loading diagrams of potential event controls and the sediment response variable (event-SSC_{fw}) in Arable B for separated hysteresis categories.

4.3.3 Channel bed sediment storage

Fine sediment concentrations of readily available and total sediment storage were similar in the three study catchments and showed limited variability between sample dates (Table 4.2 and Table 4.3). Greater storage of readily available sediment occurred in Arable A and Arable B (reach 3 in both cases). Total readily available sediment channel storage was on average 0.98 t (0.70 – 1.22), 1.55 t (0.81 – 2.43) and 0.8 t (0.93 – 1.48) in Grassland B, Arable A and Arable B, respectively. No consistency in seasonal pattern of readily available channel sediment occurred between the catchments. Total sediment storage was greater in smaller channels where channel vegetation was limited (Grassland B reach 4, Arable B reach 7) or accessible to stock (Arable B reach 3). Fine sediment storage was on average 90 t (75 – 101 t), 128 t (83 – 171) and 286 t (120 – 504 t) in Grassland B, Arable A and Arable B, respectively. Total reach storage per unit length was generally higher in December than May and August.

Table 4.2. Bed sediment data for readily available sediment fraction samples from December 2013, May and August 2014 in Grassland B, Arable A and Arable B and approximated storage rates.

	Bed sediment storage (g m^{-2})			**Total reach storage (t)**			**Reach storage per unit length (t km^{-1})**		
	Dec	*May*	*Aug*	*Dec*	*May*	*Aug*	*Dec*	*May*	*Aug*
Grassland B									
1	129	170	165	0.19	0.25	0.24	0.26	0.34	0.33
2	132	67		0.29	0.15		0.26	0.13	
3	32	27		0.13	0.11		0.03	0.03	
4	139	78	92	0.22	0.12	0.15	0.09	0.05	0.06
5	35	66	98	0.03	0.07	0.10	0.05	0.10	0.15
6	73	65	8	0.11	0.10	0.01	0.11	0.10	0.01
7	53	80	66	0.09	0.13	0.11	0.08	0.12	0.10
8	40	48	35	0.05	0.06	0.04	0.06	0.07	0.05
9	126	22	56	0.11	0.02	0.05	0.13	0.02	0.06
			Sum	1.22	1.01	0.70			
Arable A									
1	37	67	71	0.02	0.05	0.05	0.07	0.13	0.14
2	23	52	201	0.03	0.07	0.26	0.02	0.05	0.20
3	403	42	434	0.77	0.08	0.82	0.60	0.06	0.65
4	67		275	0.16		0.67	0.10		0.41
5	11	80	94	0.05	0.36	0.42	0.01	0.08	0.09
6	262	21	69	0.33	0.03	0.09	0.39	0.03	0.10
7	35	273	140	0.03	0.24	0.12	0.03	0.27	0.14
			Sum	1.40	0.81	2.43			
Arable B									
1[a]	127	693	16	0.07	0.38	0.01	0.03	0.17	0.00
2[a]			100			0.06			0.03
3	538	69	442	0.69	0.09	0.57	0.54	0.07	0.44
4	15	31		0.04	0.08		0.02	0.03	
5	70	19	48	0.09	0.03	0.06	0.07	0.02	0.05
6	74	89	15	0.15	0.18	0.03	0.11	0.13	0.02
7	13	27	47	0.04	0.08	0.14	0.01	0.03	0.05
8	148	60	22	0.41	0.17	0.06	0.15	0.06	0.02
			Sum	1.48	0.99	0.93			

[a]a proportion factor (0.1 and 0.15 in reach 1 and 2, respectively) accounted for proportion of fine sediment cover on channel bed.

Table 4.3. Bed sediment data for full agitation samples from December 2013, May and August 2014 in Grassland B, Arable A and Arable B and approximated storage rates.

	Bed sediment storage (g m^{-2})			**Total reach storage (t)**			**Reach storage per unit length (t km^{-1})**		
	Dec	*May*	*Aug*	*Dec*	*May*	*Aug*	*Dec*	*May*	*Aug*
Grassland B									
1	6219	16759	13247	9.2	24.9	19.7	12.4	33.5	26.5
2	8005	5867		17.5	12.8		16.0	11.7	
3	2442	5465		9.8	21.9		2.4	5.5	
4	14588	8107	7657	23.0	12.8	12.1	9.3	5.2	4.9
5	8979	7594	17317	9.0	7.6	17.3	13.5	11.4	26.0
6	5859	2188	6977	8.9	3.3	10.6	8.8	3.3	10.5
7	4972	1259	3803	8.1	2.1	6.2	7.5	1.9	5.7
8	8364	4800	4522	10.3	5.9	5.6	12.6	7.2	6.8
9	5696	2848	4085	4.9	2.4	3.5	5.7	2.9	4.1
			Sum	101	94	95			
Arable A									
1	15838	16070	11173	10.6	10.7	7.5	31.7	32.1	22.4
2	3269	8465	10433	4.2	10.8	13.3	3.3	8.5	10.4
3	7848	7556	47826	14.9	14.4	90.9	11.8	11.3	71.8
4	6971		3476	17.0		8.5	10.5		5.2
5	13627	5636	6858	61.0	25.2	30.7	13.6	5.6	6.9
6	11023	7275	11124	13.9	9.2	14.0	16.5	10.9	16.7
7	10507	15316	7135	9.1	13.2	6.2	10.5	15.3	7.1
			Sum	131	83	171			
Arable B									
1[a]	24120	7608	18470	19.8	6.2	15.2	6.03	1.90	4.62
2[a]		67860	5312		38.1	3.0		20.4	1.6
3	142013		135526	253.4		241.8	142.0		135.5
4	38520	6311		76.0	12.5		38.5	6.3	
5	5030	9533	4516	6.6	12.5	5.9	5.0	9.5	4.5
6	14535	3630	4104	28.8	7.2	8.1	21.8	5.4	6.2
7	31920	4882	4038	96.1	14.7	12.2	31.9	4.9	4.0
8	29547	10278	7780	81.5	28.3	21.4	29.5	10.3	7.8
			Sum	504	121	235			

[a]a proportion factor (0.1 and 0.15 in reach 1 and 2, respectively) accounted for proportion of fine sediment cover on channel bed.

4.4 Discussion

4.4.1 Structural connectivity and dominant sediment pathways

In Grassland B, predominantly positive HIs (aligned with clockwise hysteresis) were primarily controlled by stream hydrology, suggesting sediments were primarily channel derived despite good surface hydrological connectivity (Mellander *et al.,* 2012) driven by perched groundwater on poorly-drained lowland soils (Mellander *et al.,* 2015). Permanent grassland likely limits sediment availability (and sediment connectivity) from hillslopes resulting in infrequent and lower yielding distal sediment hysteresis responses. Availability of sediment in- or near- channels was confirmed by observed channel bank erosion, sediment storage in lower stream reaches where the readily available sediment storage is largest in Grassland B, and sediment fingerprinting data (Sherriff *et al.,* 2014). High energy surface runoff from lowland soils and emergent flow from well-drained upland soils is rapidly diverted through extensive sub-surface and surface (drainage ditch) artificial drainage networks (Mellander *et al.,* 2015; Glendell and Brazier, 2014; Shore *et al.,* 2015). In agricultural catchments, channels are artificially straightened, deepened and widened; subsequently increasing the magnitude and erosivity of high flows and reduces base flows which encourage sediment deposition (Vought and Lacoursiére, 2010). Channel bed sediment storage is greater in the upper catchment where channels are widened and deepened and reaches where the channel cross-section is less stable (stock access, low vegetation, maintained to increase width and depth) which confirms the importance of interactions between channel dimensions and hydraulic potential of flow.

In Arable A, sub-surface hydrological pathways resulting from infiltration dominated well-drained soils overlain upon fractured bedrock reduces surface hydrological connectivity (Mellander *et al.,* 2015). This structural dis-connectivity on hillslopes effectively reduces soil loss risk where the spatial and temporal sediment risk is greatest (catchment features the highest proportion and longest period of low ground cover). Proximal sediment hysteresis, controlled predominantly by stream hydrology, was therefore most frequent but unlike Grassland B, riparian woodland at lower stream reaches likely increased channel bank stability. In- or near- channel storage, therefore, likely controlled this response, influenced by the accumulation of intermediate sub-surface storage due to inefficient particulate transport through well-drained soils

(Warsta *et al.,* 2013), and rapid flood recession causing deposition of entrained sediment. This is shown by greatest bed sediment storage in lower reaches closest to the catchment outlet monitoring point. Channel and subsurface sediment stores were likely re-suspended and entrained where flow transport capacity was sufficient, resulting in the predominantly proximal response (Oeurng *et al.,* 2010). This may also be responsible for reduced reach storage nearer to the outlet monitoring location (reach 2) in December (when events can be assumed more frequent) compared to May and August which are relatively more hydrologically quiescent.

A wider HI range in Arable B likely resulted from the complexity of soil types and consequential variability of hydrological flow pathways. Moderate- to poorly- drained soils, featuring low storage capacities, increase the likelihood of surface flow pathways upslope of the channel network and result in surficially derived sediments (indicated by rainfall erosivity parameters) in all hysteresis categories (Duvert *et al.,* 2010). The absence of hydrological controls for positive (or clockwise) events and lower event-SSC_{fw} is supported by low concentrations of sediment storage in channel reaches closer to the outlet monitoring station (readily available or total storage) and limited bank erosion due to a riparian woodland corridor along lower stream reaches. Near-channel poached areas may, therefore, regulate the proximal response (Bilotta *et al.,* 2007b; Mano *et al.,* 2009; Oeurng *et al.,* 2010) or highly connected features such as un-metalled roads (Collins *et al.,* 2010a). The high density of agricultural drains (length per unit area) is likely to reduce the hillslope to stream transit time and increase the proportion of the drainage network contributing to proximally derived sediment responses (Gao and Josefson, 2012).

4.4.2 Temporal hysteresis evolution, functional connectivity and sediment availability

Seasonality of the hysteresis response was revealed using the HI to indicate the influence of dynamic pathways on sediment export. In Grassland B, the onset and continuation of wetter periods switched to and sustained positive HIs which exported the greatest proportion of sediments. Under these conditions, channel banks were repeatedly exposed to elevated stream flows and velocities and likely exacerbated by pressure gradients in confined groundwater conditions causing channel bank seepage (Fox *et al.,* 2007). This is consistent with other regions characterised by poorly-drained

soils such as the US Midwest where flat topography, and therefore, reduced surface runoff enhances lateral groundwater pressure gradients on channel banks (Lenhart et al., 2012). Successive events decreased HI magnitude suggesting depletion (exhaustion) of immediately proximal sediment sources (likely channel storage – Giménez *et al.,* 2012). Seasonal channel vegetation is also likely to stabilise channel bed sediments reducing source availability in summer months (Steegen *et al.,* 2000; Perks *et al.,* 2015). Ditch channels (open drains) were more vegetated and had a higher coverage of fine sediment than channel beds (Shore *et al.,* 2013); this may explain the increased HI magnitude during summer months should the longitudinal connectivity of the channel network be impacted. An extreme negative hysteresis event, attributed to a localised upland rainfall event exported a high event-SSC_{fw}, therefore, the activation of distal sources in Grassland B cannot be neglected.

In Arable A, the onset of wetter conditions coincided with high ground cover which continued the proximal hysteresis response as distal sediments were unavailable. Where land management reduced groundcover on arable soils during continued high rainfall conditions sediment export was increased but the hysteresis response was gradual. Although surficial sediment sources were not indicated by rainfall erosivity controls on clockwise hysteresis events in Arable A, attenuation of surface pathways sediment response from small areas of poorly-drained soils near the channel network may occur due to the dominance of well-drained soils characterised by infiltration and sub-surface pathways. Similar attenuation was attributed to a large catchment in Spain (Zabaleta *et al.,* 2007). Events with distal sediment components (anti-clockwise and figure-8) were surficially derived but did not necessarily yield a higher proportion of sediments as widespread connectivity of well-drained hillslope soils was unlikely. The greatest SSC_{fw} occurred at Arable A where an extreme rainfall event (31 mm total rainfall, 2.11 mm hr^{-1} average precipitation intensity) resulted in an intense (0.57 m^3 sec^{-1} discharge increase per hour of rising event limb) and long duration (13 hr) stream hydrology event and coincided with low ground cover. Simultaneous sediment and discharge peaks suggested a large proportion of both poorly-drained and well-drained soils were connected resulting in large sediment export; here defined as the maximum sediment transfer potential (ST_{max}).

Contrastingly, the dominance and increasing magnitude of negative HIs (distal sources) during sustained wetter conditions in Arable B suggested increasing hydrological connectivity of the landscape in response to antecedent soil wetness (Duvert *et al.*, 2010). Surface pathways were likely established here and during low ground cover, larger proportions of sediment were exported and the ST_{max} is achieved more frequently than at Arable A as connectivity is maintained. Greater ground cover reduced sediment export but not the HI trend, suggesting that distal, near-channel sediments or rapidly connected soils such as poached and compacted intensive grassland soils (Bilotta *et al.*, 2007) and tramlines or field margins in arable fields (Zabaleta *et al.*, 2007; Mano *et al.*, 2009; Silgram *et al.*, 2010; Regan *et al.*, 2012) were available throughout the year. In addition, channel bed sediment storage was greater in areas spatially more distal from the monitoring point which may have further contributed to delayed sediment responses. During drier conditions hillslope connectivity was reduced and near-channel surface sources remained active.

The availability of sediments across each and the catchment and variability of flow pathways likely caused the range of hysteresis types and the importance of proximal and distal categories (anti-clockwise, figure-8 and complex) to the sediment export contribution. Scatter around the seasonal trend in all catchments likely results from shorter-term fluctuations in connectivity, depletion of available sources, inter-event sediment accumulation, event specific characteristics (rainfall intensity and duration) and the spatial variability of rainfall catchments (Walling *et al.*, 1988; Steegen *et al.*, 2000; Boardman *et al.*, 2009; Oeurng *et al.*, 2010). Readily available sediment from channel storage were low in quantity and showed limited fluctuations but the total sediment storage from full agitation of the channel bed showed 31%, 95% and 127% of the annual average sediment yield is stored in Grassland B, Arable A and Arable B, respectively.

4.4.3 Management of sediment sources and pathways

Reduction of soil loss and sediment yield requires catchment specific management strategies dependent upon the spatial source availability and landscape connectivity; however, the sediment contribution rather than the frequency of hysteresis type must be used to prioritise management strategies. In Grassland B, the poorly-drained grassland catchment, sediment loss from lowland hillslope overland flow pathways are effectively

reduced by permanent crop cover and thus current land management practices must be maintained to prevent activation of distal sources. Channel bank erosion results from high flow energy in the channel network, therefore, dissipation of flow velocities through improving lateral connectivity (reduction of channel side slope gradient, establishing riparian wetlands), introducing channel geomorphic complexity (construction of artificial riffle-pool sequences and re-meandering) and establishing woodland riparian corridors to stabilise banks are management options (Vought and Lacoursière, 2010; Ockenden *et al.,* 2014). Management of the stream corridor will likely reduce the magnitude of positive hysteresis responses and sediment loss.

Conversion of arable soils to permanent grassland in Arable B will effectively reduce hillslope source availability. However, post-conversion, increased channel flow velocities as in Grassland B may result as less energy is expended on the erosion and transport of hillslope particulates. The sediment loss risk may consequently be offset particularly in upland and mid-channel reaches where no woodland riparian corridor is present. Reducing hillslope connectivity by increasing sub-surface pathways through appropriate sub-surface drainage (Tuohy *et al.,* 2015) or increasing soil water storage capacity by aeration (Perks *et al.,* 2015) may reduce surface flows but efficacy over time is spatially variable (Tuohy *et al.,* 2015). Interception of surface pathways through buffer strips encourage deposition of sediments and reduction of flow pathways, but can require agricultural land to be set-aside (Ockenden *et al.,* 2014), therefore, Rural Sustainable Drainage Systems (RSuDS) are a viable alternative to reduce surface flow energy and minimise the area set-aside where land use pressure exists (Owens *et al.,* 2007).

Natural dis-connectivity in Arable A effectively reduces soil loss risk from low ground cover on hillslopes. Extreme rainfall was capable of exceeding infiltration capacities (infiltration excess), activating surface pathways and exporting large sediment quantities but was infrequent. Temporary sediment control measures such as sediment fences (Vinten *et al.,* 2014) may be a more practical solution on fields with a high soil erosion risk when extreme rainfall events are predicted. Large scale conversion to grassland is unlikely to reduce sediment export effectively and would be impractical where maintenance of agricultural productivity is an objective (Boardman *et al.,* 2009).

Climate change projections suggest increased winter and reduced summer rainfall and streamflow (Steele-Dunne *et al.,* 2008). The assessment of hysteresis dynamics over time encapsulates dynamic and complex system functions such that impacts on hydrological and sediment pathways can be projected in the study catchments. Natural dis-connectivity in Arable A is likely to more frequently exceeded in winter increasing hillslope connectivity and the achievement of ST_{max} during low ground cover periods. Surface sources will continue to dominate in Arable B with more frequent and higher magnitude distal responses and greater sediment export during low groundcover periods. In Grassland B the dominant hysteresis response would likely be unchanged but, similarly to Arable B the magnitude, in this case of the proximal response (and associated sediment export) will likely increase as stream channels are more frequently inundated. Intermittent negative hysteresis may become more frequent as well-drained upland soils are connected following prolonged wet conditions.

Management of hydrological connectivity is becoming more widely recognised as an effective approach to catchment pollutant management strategies. Novel analysis using high-resolution, robust suspended sediment estimation techniques in this study provides a framework to assess sediment connectivity fluctuations over time using event data as 'snapshots' to interpret catchment behaviour. As a result, valuable information for catchment managers has been unearthed, i.e., reducing sediment loss risk by managing fluctuating sediment connectivity. This approach is valid in catchments with contrasting physical catchment conditions, land use and land management pressures, and facilitates projections sediment connectivity variations through climate change. Consequently, measures to support sustainable intensification of agricultural systems can be more robustly and cost-effectively designed to mitigate current and future sediment loss risk.

4.5 Conclusions

This study has highlighted the potential for a two-year storm-event discharge and suspended sediment hysteresis dataset to indicate sediment dynamics in three catchments with contrasting agricultural land uses and dominant soil drainage types. Combined use of a hysteresis index, flow-weighted sediment concentrations and multivariate analysis of event controls was an effective assessment tool to infer sediment sources and transport mechanisms. Recommendations for approaches to

sediment management in terms of sediment connectivity have significance for global mitigation measures. Key conclusions are:

- Catchments with impeded drainage (moderate- or poorly-drained soils) and, therefore, high surface connectivity had contrasting hysteresis responses due to the location of available sources (hillslope versus channel bank);
- The well-drained catchment exported less sediment overall as soil properties reduced surface hydrological connectivity but, when catchment connectivity was established, the largest event sediment load of all catchments occurred;
- Event sediment export was elevated in arable catchments when low groundcover was coupled with high connectivity, whereas in the grassland catchment, export was attributed to periods of increased rainfall only;
- Seasonality of hysteresis response and sediment export quantity reflected the connectivity of flow pathways due to antecedent soil moisture, connectivity resulting from event rainfall characteristics, and fluctuations in the availability of dominant sources;
- Evaluation of hysteresis in light of interpreted dominant flow pathways and agricultural land use pressures informed the conceptual understanding of sediment transport dynamics to a catchment outlet;
- Considerable short-term scatter in catchment hysteresis index suggests sediment management strategies based on a limited number or selected events may not be indicative of longer-term catchment dynamics.

4.6 Summary

Novel application of an existing hysteresis index using high-resolution suspended sediment and discharge datasets has provided insights into SS dynamics in multiple agricultural catchments with contrasting physical characteristics and land use pressures. This is the first evidence-led approach to estimate fluctuations in sediment connectivity over two-years and has considerable utility for cost-effective monitoring of sediment dynamics. The methodology employed here may similarly be considered for other agricultural catchments and pollutants such as phosphorus and nitrates. However, inferences using high-resolution SS-Q hysteresis require confirmation using robust sediment provenance methodologies; this will be completed in the Chapter 6.

Chapter 5. Exploring methods to reduce uncertainty in sediment un-mixing models: the impact and identification of tracer non-conservativeness

5.1 Introduction

Predictions of sediment source contributions using sediment fingerprinting methodologies are accompanied by an inherent uncertainty; a consequence of multiple uncertainty components such as the number of tracers, dimensionality, intra- versus inter- source variability and tracer analytical uncertainty (Franks and Rowan, 2000; Small *et al.,* 2002; Small *et al.,* 2004). The propagation of uncertainties through to the result prediction is made possible by Monte-Carlo based modelling techniques (Franks and Rowan, 2000; Cooper *et al.,* 2014). The recognition of, and capacity to fully assess these components of uncertainty has encouraged discussion and evaluation of research priorities to improve robustness of un-mixing results (Rowan *et al.,* 2012; Nosrati *et al.,* 2014; Laceby and Olley, 2015). Two outstanding uncertainty components are the identification of an optimal tracer set for un-mixing and the impact of multiple solutions within a tracer set on source predictions.

The array of tracers available to a sediment fingerprinting application has increased as a result of improved analytical capabilities (more samples can be analysed for a greater number of tracers more rapidly), the benefit of using a multi-parameter approach and the endeavour to develop new tracer properties to improve source resolution (Walling *et al.,* 1993; Walling, 2013; Martinez-Carreras *et al.,* 2010; Blake *et al.,* 2012). Selection of the most valuable tracers (based on their physical relevance between source groups and reliability over the scale of assessment) offers opportunities to improve the cost-effectiveness of sediment fingerprinting and, hence, validate it as a routine management tool. Tracer generation, transport and conservativeness are, however, largely catchment specific and to date this has encouraged the use of statistical tracer reduction techniques to select an optimal un-mixing tracer set.

A widely adopted two-step tracer selection approach defines an ‘optimal’ tracer set for un-mixing based on source data (Collins *et al.,* 1997). Firstly, the capacity of an individual tracer to differentiate between sources is statistically verified using, for example, the Kruskal Wallis test. Furthermore, discriminant analysis determines the

discrimination potential of multiple tracers to optimise the tracer set. Such statistical approaches have been criticised due to their statistical reliability and lack of physical relevance (Koiter *et al.,* 2013b), however, remain an integral component of tracer selection strategies. Source optimisation does not assess target tracer values and are, therefore, at risk of being significantly impacted by non-conservative tracer issues. The veracity of source group contributions and associated uncertainty may, therefore, be negatively impacted.

Non-conservativeness between tracer values in sources compared to downstream target sediments can be separated into two categories. The first arise from particle-size effects involving both selective entrainment of fines and preferential deposition of the coarser fraction along the transport pathway and, therefore, incur no bio-geochemical alteration of tracer concentrations (Davis and Fox, 2009; Koiter *et al.,* 2013a; Walling, 2013). The second equates to a true non-conservativeness whereby biogeochemical processes alter the tracer concentration associated with particles (Mukundan *et al.,* 2012). Physical processes, such as erosion and transport of particles, can selectively transport specific particle size classes and organic matter. Due to the greater specific surface area of finer particles and organic substances, these fractions are chemically more reactive and, therefore, can contain higher tracer concentrations. This has been highlighted for certain geochemical (Horowitz, 1991), mineral magnetic (Foster *et al.,* 1998; Hatfield and Maher, 2009) and radionuclide properties (Wilkinson *et al.,* 2009; Parsons and Foster, 2011).

In many studies tracer signal integrity is assumed providing the underlying selectivity processes can be quantified (Foster and Lees, 2000). The impact of particle size selectivity is commonly reduced by restricting the particle size distribution (e.g. to <63 µm) by sieving to exclude the coarsest fraction. Uncertainty-based assessment by Small *et al.,* (2004) determined the effect of particle size enrichment/depletion on individual tracer concentrations between source and target sediment samples, and tracer values were corrected according to tracer specific surface area associations. Other studies have targeted specific particle size classes (Hatfield *et al.,* 2008, Wilkinson *et al.,* 2009) or chosen tracers which show less particle size dependency. While such investigations have contributed important insights into uncertainty reduction, their application has been limited by the comparative simplicity of linear correction factors (Collins *et al.,*

1998) despite debates surrounding their appropriateness (Russell *et al.,* 2001; Motha *et al.,* 2004; Small *et al.,* 2004; Smith and Blake, 2014).

Biogeochemical transformation of tracers or 'true' non-conservativeness is suggested to introduce further uncertainty into source predictions. The likelihood of a tracer to undergo transformation is dependent upon its reactivity to biogeochemical processes e.g., sorption, dissolution, precipitation, oxidation, reduction, and the presence of environmental conditions facilitating transformation. Highly reactive elements, such as phosphorus and nitrogen, are readily cycled and/or subject to human amendments and are consequently unsuitable tracers. Robust, conservative tracers such as heavy metals are less susceptible to biogeochemical transformations, therefore, are more reliable tracers. A review of the processes underlying tracer transformations by Koiter *et al.,* (2013a) highlighted the catchment and environment specific nature of tracer generation and transformation potential, and therefore, the difficulties involved in assessing tracer data at the catchment scale. Additionally, Smith and Owens (2014) detected non-conservative behaviour of As and Se in sediments collected using time-integrated sediment samplers relative to local bed sediment samples. It is clear that the detection of non-conservative behaviour is problematic but of great importance to confidently determine sediment sources.

Existing approaches to identify non-conservative tracer behaviour compare target tracer values to source data. Target values have been assumed non-conservative where they fall outside of the range of individual source sample values (Mukundan *et al.,* 2010; Smith and Blake, 2014). A more stringent test by Collins *et al.* (2010b) required target values to be within the range of mean source values. Similarly Collins *et al.,* (2013) required target values, which had been pre-corrected for tracer discriminatory power, to lie within median source values. Additional limitations include the requirement for average tracer values, where multiple targets have been collected, to be contained by mean source values (Wilkinson *et al.,* 2013). Smith and Blake (2014) removed tracers from analysis based on target tracer values exceeding the range of source tracer values. These non-conservative tracers were attributed to organic enrichment resulting from peaty soils and in the case of Fe, Mn and Zn, to contamination from mining activity. The suitability of these methods is, however, unknown as it is plausible that non-conservative behaviour remains where tracers have been modified by an unquantifiable

process, are uncorrected or wrongly corrected, or are affected by an undetectable error, i.e. analytical or sample contamination.

Franks and Rowan (2000) introduced a permutation algorithm based on Bayesian principles to identify non-informative tracers within a solution set. Tracers were considered non-informative or 'corrupt', where they did not contribute to a constrained solution, therefore, it considers uncertainty of the source predictions as well as model fit to select the most informative tracers. The procedure was applied to a synthetic dataset whereby a target tracer value was artificially corrupted (to replicate random tracer non-conservative behaviour), successfully detected by the model, and subsequently rejected by the user as a non-informative tracer. Krause *et al.,* (2003) later applied the model to field data whereby three tracers (Pb, Mn and Fe) were rejected by the model and determined non-conservative. Despite the dependence upon statistical methods, the rejection or inclusion of a tracer is user dependent, therefore, tracers identified for rejection can be assessed according to potential underlying physical processes or transformations. The utility of this algorithm for the detection of tracer non-conservativeness has since received little attention, however, but has potential to benefit tracer selection routines.

The permutation approach also provides an opportunity to assess the range of predictions possible within a large tracer set. The over-determined nature of un-mixing models means that sub-sets of the original tracer set provide multiple potential solutions. The uncertainties present in each tracer may result in multiple and equally likely sub-sets (i.e. similar model fit, or similarly constrained results) but contrasting solutions (Rowan *et al.,* 2000). These non-unique (also referred to as equifinal) solutions, present the user with the need to justify the content of a tracer solution set and validate the predicted solution. Many authors have advocated the need to increase the number of tracers employed in un-mixing models (Small *et al.*, 2004; Martinez-Carreras *et al.,* 2008), which may require multiple solutions arising to be considered. The investigation of multiple solutions has not been approached systematically to date.

In this study we use the FR2000 un-mixing model and the permutation algorithm (Franks and Rowan, 2000) to determine the impact of non-conservative tracers on source predictions and uncertainty, and assess tracer optimisation approaches. A methodology is also introduced to identify multiple solutions, and to determine the

impact of these on predictions of source contributions and associated uncertainty. Firstly, this was completed using a constrained synthetic dataset and, secondly, using field data.

5.2 Methodology

5.2.1 FR2000 un-mixing model

The FR2000 algorithm un-mixing approach is summarised as:

$$\begin{bmatrix} \hat{\bar{x}}_{1,1} & \hat{\bar{x}}_{1,2} & \dots & \hat{\bar{x}}_{1,n} \\ \hat{\bar{x}}_{2,1} & \hat{\bar{x}}_{2,2} & \dots & \dots \\ \dots & \dots & \dots & \dots \\ \dots & \dots & \dots & \dots \\ \hat{\bar{x}}_{m,1} & \dots & \dots & \hat{\bar{x}}_{m,n} \end{bmatrix} \begin{bmatrix} A_1 \\ A_2 \\ \vdots \\ A_n \end{bmatrix} = \begin{bmatrix} X_1 \\ X_2 \\ \vdots \\ \vdots \\ \vdots \\ X_m \end{bmatrix} + \begin{bmatrix} \varepsilon_1 \\ \varepsilon_2 \\ \vdots \\ \vdots \\ \vdots \\ \varepsilon_m \end{bmatrix}$$

Equation 5.1

and constrained by:

$$\sum_{j=1}^{n} A_j = 1 \qquad \text{Where } 0 \leq A_j \leq 1$$

Equation 5.2

where $\hat{\bar{x}}_{ij}$ is the estimated population mean, i is the trace property, j is the source group, n is the number of sources and m is the number of tracers. A_j is the fractional contribution of each source group, and ε_i is the sum of the least squares error associated with the prediction of the mixture tracer characteristic, X_i. Equation 2 constrains the solution such that individual source contribution (A_j) must between 0 and 1, and all sources sum to 1.

The uncertainty in estimation of source contributions was described by the variance component of the Student's t-distribution ($\hat{\sigma}^2$),

$$\hat{\sigma}^2 = \left(\frac{S}{\sqrt{d}}\right)^2$$

Equation 5.3

where S is the sample standard deviation and d is the number of independent samples.

Uncertainties of sample means were propagated using Monte Carlo sampling. A mean probability distribution for each tracer value in the source groups and target sediment were derived from the input dataset. Source contributions were solved using the source and target probability distributions and solved using a least-squares SIMPLEX optimisation routine for 1000 realisations to obtain an optimised source group prediction distribution. The median source contribution was estimated and 95% confidence intervals were calculated from the optimised frequency distribution.

5.2.2 FR2000 permutation algorithm

Identification of optimal tracer solution sets were approached using a permutation version of the FR2000 model. All possible tracer combinations that satisfy the minimum tracer number requirement, m≥n-1, where m is the number of tracers required and n is the number of source to be un-mixed, were calculated within the algorithm. In the previous development of the tracer selection algorithm (Franks and Rowan, 2000; Krause *et al.*, 2003), all potential tracers were included in the first model permutation. Repetition of the algorithm with the sequential removal of each tracer, i.e. all combinations of m-1 tracers, was evaluated according to the sum of least squares error components of all realisations within a permutation,

$$\varepsilon_R = \sum_{i=1}^{m} \varepsilon_i \text{ where } \varepsilon_P = \sum_{k=1}^{K} \varepsilon_R$$

Equation 5.4

where ε_R is the total error of a realisation. εi is the sum of the least squares error for each sediment trace property, and ε_P is the error associated with a specific permutation where K is the number of realisations. The preferential solution within a permutation realises the lowest ε_R. Consequently, the removal of the tracer which afforded this reduction is a candidate tracer for removal resulting from an improved least squares fit.

Comparison of solutions derived using tracers sets with decreasing tracer numbers is problematic because as error term is not comparable between permutations with different numbers of tracers; consequently an uncertainty index was developed to assess the relative uncertainty (U) of the derived source predictions for different tracer permutations:

$$U = \sum_{j=1}^{m}((1 + q^{j}_{1-(0.5\propto)}) - (1 + q^{j}_{(0.5\propto)}))/(1 + q^{j}_{0.5})$$

Equation 5.5

Where $q^{j}_{1-(0.5\propto)}$ and $q^{j}_{(0.5\propto)}$ are the (1-α)% upper and lower confidence quantiles, and $q^{j}_{0.5}$ is the median quantile of predicted source contribution A_j. A constant is added to each quantile to negate the inflation of U where the median value approaches zero. Where U is reduced due to the removal of a tracer, the result is more constrained, and the tracer is permanently removed. If U increases due to the removal of a tracer, the result is less constrained and therefore the tracer cannot be rejected from the solution set. The process is repeated with m-2, m-3… tracers until U no longer decreases; this is the optimum tracer set.

In this study, the metrics first defined by Franks and Rowan (2000) were approached in a reversed structure. The first permutation included the minimum possible number of tracers to define the sources (m) with additional tracers sequentially added (m+1) into the solution set. Improvement on model fit (ε_P) and consequential impact on the uncertainty of target sediment estimations (U) were used for verification, consistent with the previous approach. Where an added tracer contributed to a solution with the lowest mean square error, and U is reduced as a result of its addition, it was retained. Subsequent permutations increase tracer number (m+2, m+3…) until the result possessed the lowest constraint, i.e. the addition of further tracers cause U to increase. Tracers not included in the optimal solution set were considered as 'corrupt' as they contributed additional uncertainty to the solution set. The cause of this uncertainty could be further explored in relation to source characteristics or non-conservative behaviour.

5.2.3 Synthetic datasets

An input dataset comprising 50 tracers was synthetically assembled (Table 5.1). A range of mean source values (minimum and maximum) were entered into a random number generator, four random numbers within this range were assigned as the mean values for four sources respectively. Similarly the CV% was randomly allocated within a range of values from 8-73% (average 36%). Normal Gaussian distributions describing the relevant mean and CV% were used to create individual samples. This normality assumption, although not realistic of sampled data in the majority of existing sediment

Table 5.1. A fifty tracer synthetic dataset of randomly assigned mean source and coefficient of variance (CV%) values, perfect target tracer values and corrupted tracer value (tracer 3). Testing of dataset with three tracers refers to tracer 1-3, five tracers 1-5, eight tracers 1-8 etc.

Tracer	**Source 1** Mean	CV%	**Source 2** Mean	CV%	**Source 3** Mean	CV%	**Source 4** Mean	CV%	**Perfect target value (corrupt)**
1	0.1	60.1	0.1	29.1	0.1	26.6	0.3	61.0	0.1
2	336.8	52.6	131.6	16.5	283.4	35.2	146.9	43.8	250.1
3	1.6	20.3	3.9	29.5	3.5	39.5	2.8	48.0	2.8 (3.1)
4	12.8	26.8	5.2	38.3	14.1	11.4	10.6	24.8	112.0
5	1127.3	38.5	281.6	29.0	486.4	27.1	1187.1	40.7	819.7
6	32.9	26.3	30.6	33.7	41.5	49.0	37.5	55.5	36.8
7	7.7	16.5	5.1	43.7	3.4	19.4	3.3	56.7	4.8
8	7.9	32.4	1.2	28.2	0.2	35.5	2.1	31.8	1.8
⋮	⋮	⋮	⋮	⋮	⋮	⋮	⋮	⋮	⋮
48	26.9	31.9	40.6	51.9	16.4	31.6	22.6	58.1	23.5
49	1.2	41.7	1.0	23.2	1.0	19.6	0.8	33.9	1.0
50	47.7	29.5	50.6	33.6	16.2	57.6	21.9	54.2	30.5

fingerprinting studies, was considered as suitable to test model function with controlled input data. The number of samples at each source was similarly variable; sources 1-4 comprised 10, 21, 18 and 15 samples respectively. Target values for each tracer were calculated according to pre-determined synthetic contributions; A_1=30%, A_2=10%, A_3=35% and A_4=25% and average source values according to Eq. 1. The un-mixing model, FR2000, was run multiple times employing initially three tracers and gradually increasing the number of tracers to the maximum number of 50 tracers with a 'perfect' solution. The target tracer value of one random tracer was subsequently 'corrupted', i.e. artificially modified to represent falsely corrected, or an uncorrected non-conservative tracer within the range of the relevant mean source tracer values and the un-mixing repeated.

A smaller dataset, comprising eight of the above 50 tracers, was processed using the permutation algorithm to determine the ability of the algorithm to detect non-conservative behaviour. The value of one tracer at the target was sequentially corrupted in steps of 5% in positive and negative directions. The minimum and maximum level of corruption was constrained by the range of mean source values, i.e. where other techniques would be capable of detecting the non-conservative behaviour (Collins *et al.*,

2010b). Consequently the range of corruption was -90% to +155% of the original tracer value. For each result the 'optimum' solution and associated uncertainty were recorded. The goodness of fit (GOF) was calculated for each corruption step using Eq. 6.3:

$$GOF = \left\{1 - \left(\left|C_i - \sum_{s=1}^{m} P_s S_{si}\right|\right)/C_i\right\} * 100$$

Equation 5.6

The tracer selection procedure proposed by Collins *et al.* (1997) was additionally performed on the eight tracer dataset (with corrupted target tracer) and using the FR2000 methodology and to achieve the 'optimum' tracer set. The Kruskal-Wallis H-test (SPSS v22) examined the discrimination capabilities of each tracer to distinguish between sources. Tracers that exceeded a critical H-value of 7.598, dependent upon the number of sources and confidence interval, were retained for further statistical verification. Multiple Discriminant Analysis (MDA), step two, was performed on the remaining seven tracers passing stage one (SPSS v22). The stepwise test obtains an optimum set of tracers by minimising Wilks' Lambda. Default values were used for the partial-F inclusion 3.84 and removal 2.71. The procedure continues until the maximum amount of discrimination can be obtained from the input tracers. Those retained are deemed the 'optimal' tracer solution set for subsequent un-mixing.

5.2.4 Multiple solution methodology

Multiple solutions were explored using a simplistic four source, eight tracer synthetic dataset. In order to test the permutation algorithm two solution sets were predetermined; solution one, relating to tracers 1 to 4 had target values calculated according to contributions A_1=40%; A_2=15%; A_3=30%; A_4=15%; and solution two, relating to tracers 5-8 and target values were calculated according to contributions A_1=15%; A_2=35%; A_3=20%; A_4=30% (Table 5.2). Each source contained ten samples from a Gaussian distribution (CV=10%).

Table 5.2. Synthetic dataset with two pre-determined solutions. Source values are true population means, target tracer valies are calculated according to pre-determined contribution ratios: solution one (tracers 1-4), solution two (tracers 5-8).

Tracer no.	Source 1	Source 2	Source 3	Source 4	Target
Sub-set 1	40%	15%	30%	15%	
1	0.49	0.22	0.33	0.13	0.35

2	1.95	1.21	0.76	1.61	1.43
3	5.57	2.19	8.72	4.03	5.78
4	42.98	49.63	39.88	73.16	47.57
Sub-set 2	15%	35%	20%	30%	
5	27.40	15.74	10.99	24.41	19.14
6	610.21	215.07	296.38	1172.45	577.82
7	50.11	17.54	33.47	26.80	28.39
8	118.30	178.90	128.44	163.20	155.01

All potential multiple solution combinations, assuming a maximum of two solutions, were explored. Each solution set must qualify against the minimum tracer requirement for source definition, i.e. $m \geq n-1$ (Table 5.3) and each tracer can only belong to one solution set. Combinations of multiple solutions were judged according to the combined solution error ε_S, i.e., the sum of error (ε_P) for each solution. Consistent with the FR2000 method, the combination with the lowest combined error is deemed the candidate multiple solution arrangement. By ensuring the combined error is the lowest, the model fit is preserved.

Source prediction results using each multiple solution and the single solution (prediction reported by using all available tracers) were compared. Tracer sub-sets which reported contrasting source prediction from each other and the single solution were accepted as containing multiple solutions. Where these conditions are not met, i.e., both tracer sub-sets report similar source predictions to each other and the all tracer solution, the tracers can be assumed to be in agreement and therefore the single solution accepted as the most appropriate array of tracers.

Table 5.3. Examples of tracer sub-group combinations for common source and tracer numbers in un-mixing applications.

		Tracers			
		6	7	8	9
Sources	3	3+3	3+4	4+4	4+5
	4	3+3	3+4	4+4	4+5

5.2.5 Field data

A sub-set of data was selected to explore potential non-conservative tracers and multiple solutions using the FR2000 permutation algorithm. Samples were collected from the Grassland B catchment (Section 2.2), sampling methods as summarised in Section 6.2.1. Target (river sediment) samples from May 2012 to June 2013 (collected in Jul-12, Sep-12, Jan-13, Feb-13, Apr-13, May-13 and Jun-13) were selected and a sub-set of source samples topsoils (n=34), subsoils (n=32), eroding channel banks (n=59), eroding open field drains (n=4), damaged road verges (n=43) and farm tracks (n=6).

5.2.6 Laboratory analysis

Soil samples were oven dried at <40ºC and dry-sieved to broadly replicate particle size between soils and in-stream sediments (Walling *et al.*, 2002). Particle size data from a selection of river sediments collected by the TISS devices reported a 90th percentile frequently greater than 63 μm, therefore, the larger 125 μm aperture was used. River sediment samples were refrigerated at 3ºC for a minimum of 72 hours to ensure settling of particles before water was siphoned. Samples were subsequently oven dried at <40ºC and gently disaggregated with a pestle and mortar before subsequent analysis.

For mineral magnetic analysis, samples were immobilised in 10-cc plastic containers using cling film and cotton wool. Magnetic susceptibility (χ, or concentration of magnetic minerals, was measured using a Bartington MS3B Dual Frequency sensor (Oxford, UK) at low (0.47 kHz) and high (4.65 kHz) frequency to report the mass-specific low field susceptibility (χ_{LF} – 10^{-6} m^{-3} kg^{-1}), high field susceptibility (χ_{HF} – 10^{-6} m^{-3} kg^{-1}), respectively. The frequency-dependent susceptibility ($\%\chi_{FD}$) was calculated ($(\chi_{HF} - \chi_{LF})/\chi_{LF} * 100$). Anhysteretic remanent magnetisation (ARM) was induced using a Molspin AF demagnetiser (Newcastle, UK) with ARM attachment. Isothermal remanent magnetisation (IRM) was induced using a Magnetic Measurements 10 T Pulse Magnetiser (Aughton, UK) at a forward field of 1 T, here defined as the saturation isothermal remanent magnetisation (SIRM) and reverse fields of 40 mT ($bIRM_{40mT}$) and 300 mT ($bIRM_{300mT}$). Samples for ARM and IRM were subsequently analysed using a Molspin 1A fluxgate magnetometer (Newcastle, UK) and converted to mass-specific units of IRM (10^{-5} Am^2 kg^{-1}) and χ_{ARM} (10^{-7} Am^2 kg^{-1} – once normalised by the biasing field 31.84 Am^{-1}), respectively. Ratios between bIRMs and the SIRM were used to calculate IRM_{soft} (using the 40 mT field) and IRM_{hard} (using the 300 mT field) and were

transformed to ensure all data were positive before statistical analysis. Further ratios of parameters SIRM/χ_{LF}, SIRM/χ_{ARM}, χ_{ARM}/χ_{LF} and the H-ratio (0.5 * (SIRM-bIRM$_{40}$)) were calculated to explore magnetic grain size characteristics. Geochemical elements cadmium (Cd), cobalt (Co), chromium (Cr), copper (Cu), manganese (Mn), nickel (Ni), lead (Pb) and zinc (Zn) were analysed using an Agilent ICP-OES (Santa Clara, US) following microwave assisted acid digestion (USEPA, 1996) to obtain total concentration (mg kg^{-1}).

5.3 Results and discussion

5.3.1 Impact of tracer non-conservativeness

Predicted source contributions, represented by the median and 95% confidence intervals in 'perfect' and 'corrupted' synthetic datasets are shown in Figure 5.1. Where tracer numbers are limited, inaccurate predictions are reported for all four source groups for 'perfect' and 'corrupted' datasets. Predicted source contributions converge towards the pre-determined source proportions (represented by the dashed line) due to the increasing number of tracers used for un-mixing. In the 'perfect' dataset, the uncertainty in the result prediction is solely a consequence of the source tracer data. As target tracer values were calculated as an exact value, additional uncertainty components e.g. target variability or non-conservative tracer behaviour, were eliminated. The addition of further tracers, therefore, improves source dimensionality and definition which is beneficial to reduce prediction uncertainty (Small *et al.*, 2004; Martinez-Carreras *et al.*, 2008).

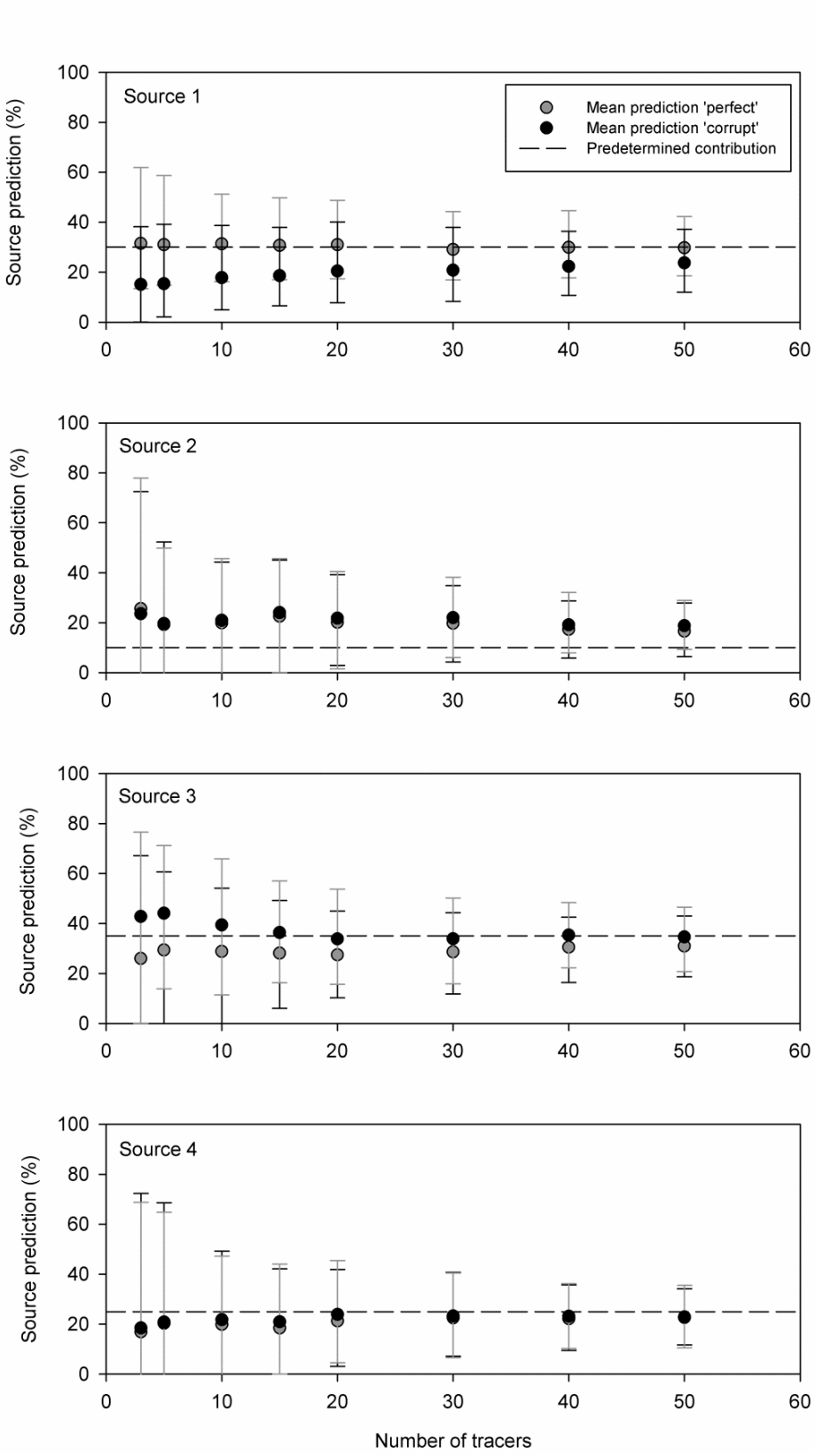

Figure 5.1. Result predictions and 95% confidence intervals for 'perfect' and 'corrupted' datasets using the FR2000 un-mixing model

Confidence intervals of ‘perfect’ and ‘corrupt’ datasets at a specific tracer number indicate that the inclusion of a single corrupt tracer, even in large datasets, does not substantially increase uncertainty. The cumulative uncertainty of all sources does increase despite individual sources showing more constrained solutions for the corrupt dataset compared to the perfect result. The median source predictions between ‘perfect’ and ‘corrupted’ datasets differ greatly at sources one and three which possess the largest proportion of the target sample. The impact of these results in a sediment management context should also be considered. Source 1, pre-determined to be the dominant sediment source was suggested to have a lesser contribution than all other sources until over 30 tracers (29 correct and one corrupt) are used. A ‘corrupted’ ten tracer dataset would indicate that sources two and three are priority management areas; therefore, undermining the efficacy of management strategies should this phenomenon be replicated in a real dataset. Increasing the number of tracers alleviates the impact of non-conservative tracers. Non-conservative tracer behaviour crucially challenges the ability of mixing models to correctly define source contributions, consequently, strategies to better detect tracer non-conservativeness should be a research priority.

The repeated application of the permutation algorithm to a dataset with sequentially increasing corruption (positively and negatively) of one tracer showed that predicted source contributions were severely impacted (Figure 5.2). Current methods to detect tracer non-conservativeness may therefore result in considerable loss of precision. The predicted source contributions contrast between the maximum positive and negative levels of corruption (-90% and +155%), yet in all instances, the GOF (85-100%) is comparable with other acceptable values. Palazón et al. (2015) reported that GOF could not estimate accuracy of results predictions and data presented in this study support that finding.

Assessment of source prediction uncertainty using the permutation algorithm detected the corrupted tracer at less than -50% and greater than +20%. The range of incorrect source predictions are substantially reduced, however, are not fully remedied (Figure 5.2). Uncertainty values associated with the predictions at the minimum and maximum of the narrowed band of detection report a ‘true’ prediction uncertainty, which has been previously un-quantified (Figure 5.3a). Repeating this analysis for -90% and +155% predictions (Figure 5.3b) showed the improved confidence of source predictions as a result of using the FR2000 permutation approach.

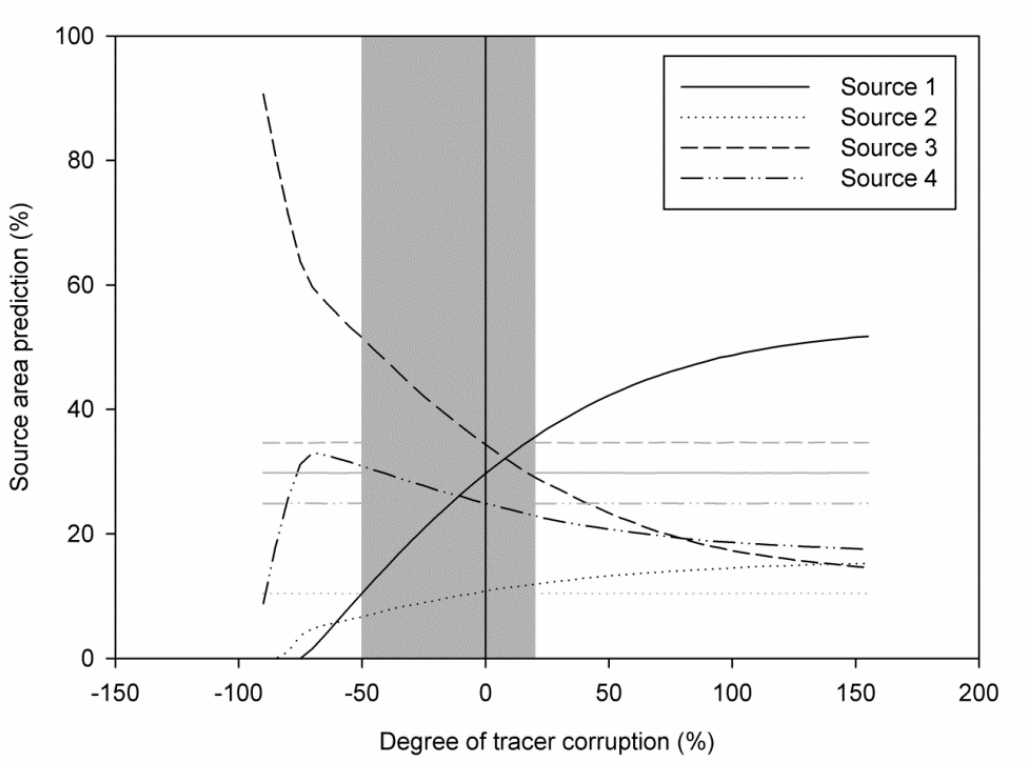

Figure 5.2. Median source predictions resulting from the degree of corruption of one tracer. Grey panel represents the non-detection area of the FR2000 permutation methodology, and grey lines are source predictions following the rejection of the corrupted tracer.

The permutation approach is used here to assess a dataset representative of many previous sediment fingerprinting exercises in relation to input data; number of sources, number of samples, source variability and number of tracers. The scenario of tracer non-conservativeness presented is likely a simplification, i.e., one corrupted tracer and seven perfect tracers; however, the procedure outlines a viable technique for further investigation. The capacity of the algorithm to process large groups of tracers, is limited due to computational requirements and processing time. Automation and expansion is on-going to facilitate further analysis of more complex scenarios (e.g. multiple corrupted tracers).

Tracer correction is a topic requiring greater prominence in sediment fingerprinting studies. The ability of linear correction factors to adequately resolve selectivity processes have been commonly disputed and are suggested to contribute further to inaccuracies (Smith and Blake, 2014). Improvements to the linear correction factor approach to resolve particle size and organic matter selectivity processes have been suggested (Russell *et al.,* 2001; Small *et al.,* 2004). However, the laborious nature of such approaches has prevented their wide scale adoption. The impact of true non-conservative behaviour, through biogeochemical transformations, can be limited by

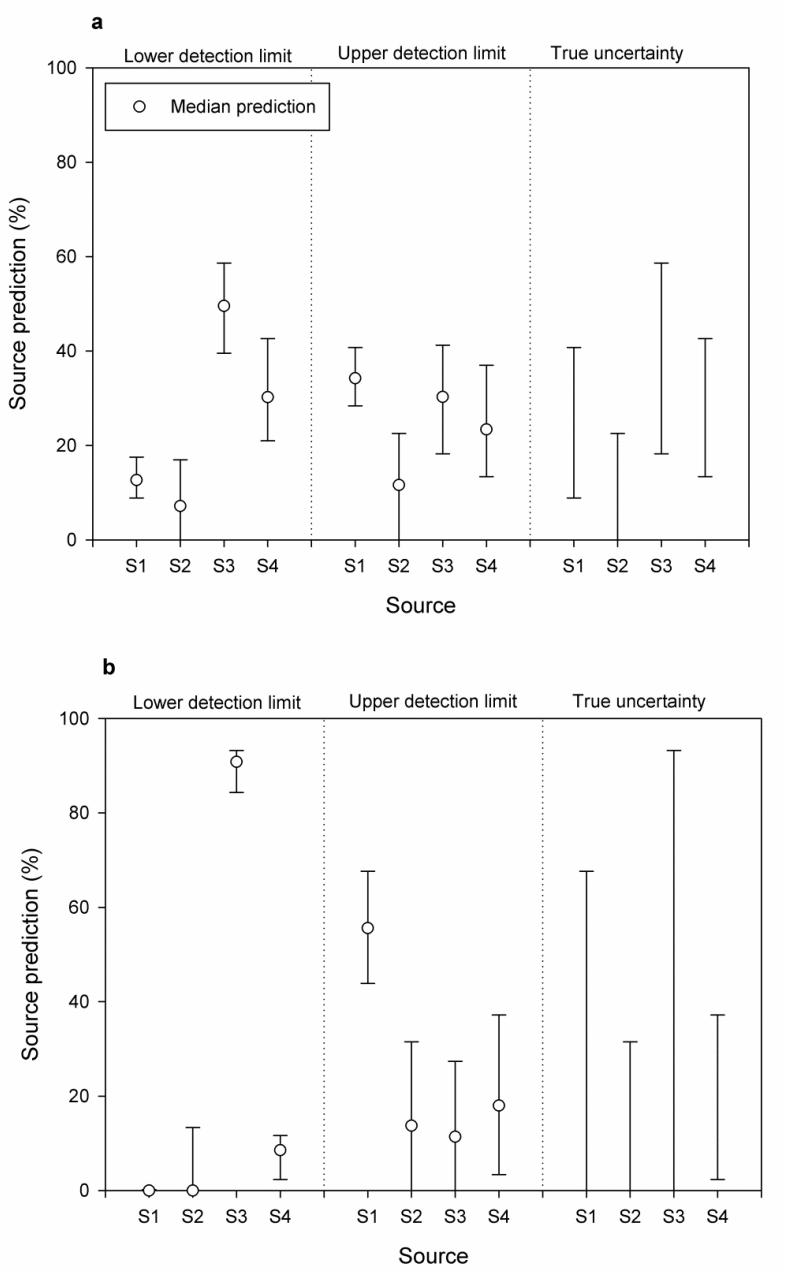

Figure 5.3. True uncertainty of predicted source contributions using a) the FR2000 methodology, and b) a source sample-based tracer selection approach.

selecting chemically conservative tracers. However, the inability to identify or control all catchment processes suggests that bio-geochemical non-conservativeness in tracer behaviour cannot be assured for all eventualities, and therefore cannot be corrected. Statistical approaches to monitor known sources of prediction inaccuracies and uncertainty could be a useful addition to current sediment fingerprinting applications. The permutation approach applied here as a tracer corruption identification algorithm fits within the wider framework of sediment fingerprinting as a quality assurance tool.

5.3.2 Definition of the 'optimum fingerprint'

The optimal fingerprint in an eight tracer dataset was explored using two strategies; tracer reduction using source data (e.g. Collins *et al.,* 1997) and the uncertainty-based permutation algorithm of FR2000 (Franks and Rowan, 2000). The source based approach suggested an optimal six tracer solution for un-mixing. The corrupted target tracer was not rejected as, according to source data, the tracer passed both the Kruskal-Wallis and MDA tests. Two non-corrupted tracers were rejected; one failed the Kruskal-Wallis test and one failed to contribute any source discrimination in the MDA. Conversely the permutation algorithm detected the corrupt tracer and considered the remaining seven tracers as an optimal tracer set. Un-mixing results using the two tracer sets are shown in Figure 5.4. The source optimised prediction of median source contributions are incorrect whereas, using the FR2000 optimisation approach, source predictions are highly accurate. Uncertainty in the permutation-based solution is also improved due to the additional, non-corrupt tracers despite their reduced discrimination capabilities.

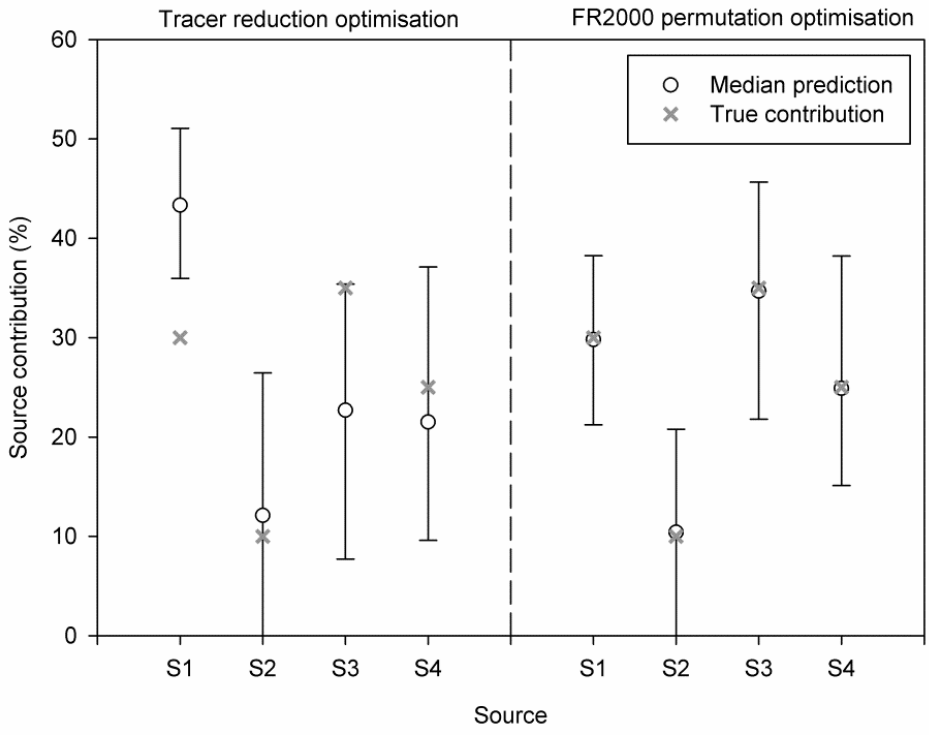

Figure 5.4. Prediction and uncertainty un-mixing results of tracer sets selected by 'tracer reduction' (left) and FR2000 permutation approach (right).

To date, tracer reduction strategies have been widely adopted to define an ‘optimal’ fingerprint (Collins *et al.,* 1997; Collins and Walling, 2002; D’Haen *et al.*, 2012), but have been criticised due to their reliance upon statistical techniques. The use of MDA type analysis is essential to ensure that sources can be adequately distinguished, however, it assumes that additional tracers provide no further value. Multiple uncertainty studies (including data presented here) have expressed the importance of increasing tracer numbers to improve result constraint (Small *et al.,* 2004; Martinez-Carreras *et al.,* 2008) and better identify tracer non-conservativeness. The application of tracer reduction strategies, has potential benefits; the reduction of analytical costs and computer processing time, however, potentially at the expense of uncertainty. Tracers which are inexpensive and rapidly analysed may offer some potential future direction to increase tracer numbers (Guzman *et al.,* 2013). However, employed tracers and statistical selection methodologies must ensure physical relevance to contribute meaningful results which require user experience and considerable knowledge of geochemical catchment process (Fox and Papanicolaou, 2008; Koiter *et al.,* 2013b).

5.3.3 Multiple solutions

The permutation algorithm was successfully applied to explore near-equivalent, or non-unique tracer solution sets termed ‘multiple solutions’ (Figure 5.5). The combinations of tracer sub-sets selected by the model reflected the predetermined source groups and consequently the allocated median source contributions. Due to the smaller number of tracers employed to describe each solution, the uncertainty envelopes are wider than the all tracer solution.

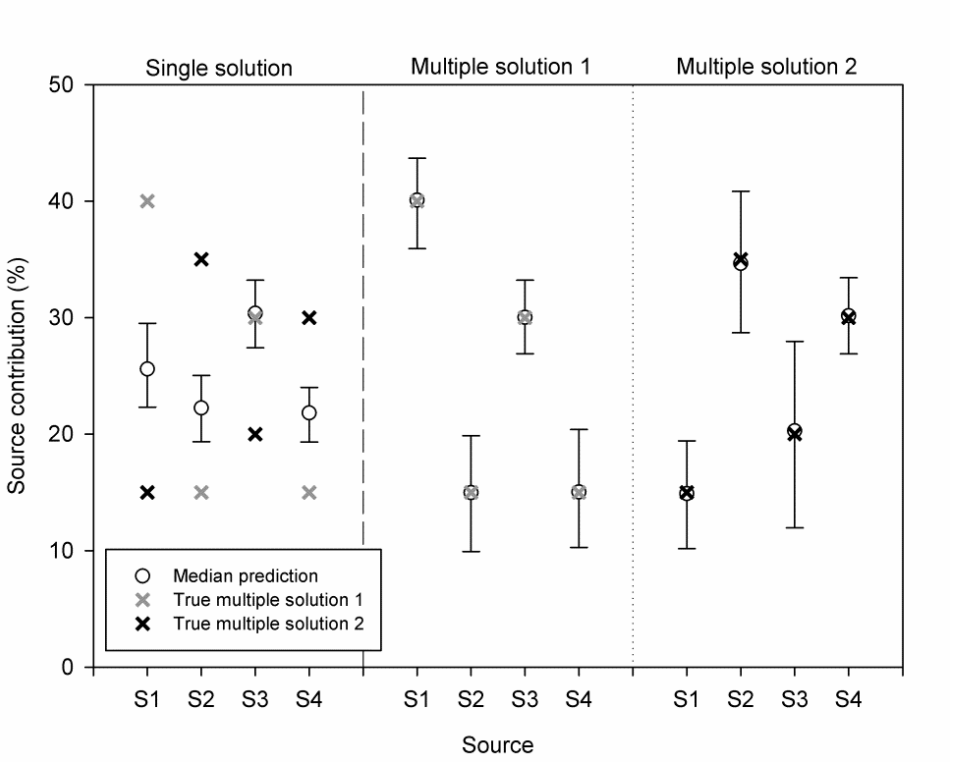

Figure 5.5. Results of uncertainty inclusive un-mixing of multiple solution datasets showing the all tracer solution (left) and multiple solution sets (right).

5.3.4 Identification of tracer corruption and multiple solutions in field data

Fourteen tracers were available for un-mixing analysis however, due to the limitations of computer power, run time and result processing time, a lesser number of tracers was required to conduct the permutation algorithm. Tracers were, therefore, assessed using the source-based tracer selection procedure to reduce the tracer set whilst preserving discrimination capacity. Based on the assessment of the six sampled source groups, the Kruskal-Wallis test showed that all tracers were capable of distinguishing between sources ($p<0.05$). All tracers were further entered into MDA which resulted in 78.9% discrimination between sources (Figure 5.6). An improvement in source discrimination could be made by combining source groups.

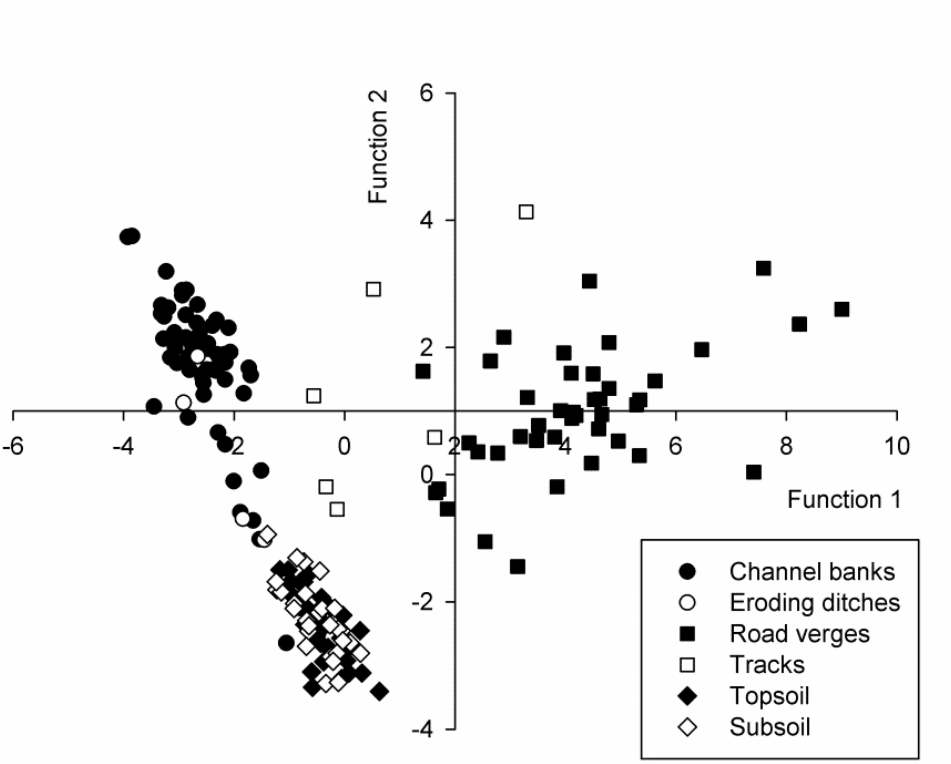

Figure 5.6. Result of multiple discriminant analysis for six sample source groups. For un-mixing, sources were consolidated into three 'parent' groups: channel (cirlces), road (squares) and field (diamonds).

Figure 5.6 shows source samples with similar underlying tracer generation and erosion processes e.g. damaged road verges and tracks, and channel banks and open field ditch banks, occupy similar areas of space using the first two discriminant functions (describing 97% of group centroid variance) therefore ‘road’ and ‘channel’ parent source groups were constructed from the bulked groups. Despite the theoretical differences underlying the generation of tracers at topsoils and subsoils, the tracer array had no capacity to distinguish these sources and were consequently bulked into a ‘field’ parent group. Collins and Walling (2007) were previously able to discriminate topsoils with the combined source of subsurface and channel banks in two agricultural river catchments in the UK. Similar discrimination in the study catchment is negated by a thick layer of marine clay at 2-3 m depth in the catchment lowlands (Mellander *et al.*, 2014). Channel bank height was frequently greater than 2 m, particularly in the mid- to lower sections of the catchment, therefore the clay layer was exposed in the actively eroding area where stream erosivity is greatest. Subsoil samples, captured at 40 cm depth were too shallow to reflect the chemical signature of this layer. Discrimination between topsoils and subsoils could be improved by surface deposited tracers such as caesium-137 which have been valuable in other sediment fingerprinting studies (Gruszowski *et al.*, 2003). Repeated MDA analysis of bulked source groups

considerably improved discriminatory power of the tracer set to 94.7%, which was achieved using a seven tracer dataset (χ_{ARM}, IRM_{soft}, Cd, Co, Cr, Ni and Zn). Where source discrimination is reduced, the resource intensiveness of sample analysis cannot be validated. Good discrimination of fewer source groups should, therefore, be prioritised. Particle size and organic matter correction was not used here in order to investigate raw data trends.

Soil mineral magnetic and geochemical source characteristics of the seven employed tracers (Table 5.4) reflect two main processes; anthropogenic additions and the vertical soil profile. Tracers χ_{ARM}, IRM_{soft}, and Zn were elevated in road sources reflecting the input of magnetic minerals and heavy metals from vehicles (Gruszowski *et al.,* 2003). Appropriately, the channel banks reported the lowest mean value for mineral magnetic parameters due to the dominance of the heavy marine clay layer. The concentrations of Cd, Cu, Cr and Ni are highest in the channel sources, Smith and Blake (2014) related a higher Cr concentration in channel banks to a vertical weathering gradient where subsurface material is enriched in elements relative to surface material due to decreased weathering. This vertical weathering gradient may similarly occur here or, conversely, due to the change in soil type (the surface soil layer as opposed to the marine clay layer).

Field data were processed using the permutation algorithm, firstly to determine any non-conservative behaviour, and secondly to explore multiple solutions. Non-conservative behaviour of Cr was detected in the raw dataset of Feb-13, Jun-13, and Zn at May-12 (Table 5.4) and was removed from analysis as target tracer values were outside the range of source values. Non-conservative behaviour was detected in one sediment sample by the permutation algorithm (May-12) for IRM_{soft}. Although the value was within the range of individual source values, it was outside of the mean value of all sources, therefore, this non-conservative behaviour could have been detected without the algorithm using more stringent source-based methods (*cf.* Collins *et al.,* 2010). The IRM_{soft} tracer represents the proportion of magnetically soft minerals, e.g. magnetite,

Table 5.4. Summary of seven tracer source data (mean and co-efficient of variance) and sediment target sample data collected at the catchment outlet). Note: [a]values were detected as non-conservative in raw dataset, [b]values detected as non-conservative using the permutation algorithm.

	Source samples						**Sediment samples**						
	Channel		Road		Field		Jul-12	Sep-12	Jan-13	Feb-13	Apr-13	May-13	Jun-13
	Mean	CV%	Mean	CV%	Mean	CV%							
χ_{ARM} (10^{-7} Am kg^{-1})	0.08	41	0.23	44	0.17	159	0.07	0.15	0.12	0.13	0.14	0.19	0.13
IRM_{soft} (10^{-5} Am^2 kg^{-1})	123.47	40	688.27	35	150.91	116	44.66[b]	119.31	125.88	130.96	114.36	200.26	237.02
Cd (mg kg^{-1})	0.27	45	0.18	67	0.20	170	0.69	1.51	0.51	1.15	1.38	1.33	1.31
Co (mg kg^{-1})	16.31	22	11.11	23	9.73	42	21.25	22.17	20.50	18.67	22.12	21.29	19.48
Cr (mg kg^{-1})	27.08	34	21.92	32	26.55	42	42.63	33.39	35.82	81.64[a]	37.11	34.09	87.57[a]
Ni (mg kg^{-1})	29.16	30	21.13	24	19.74	43	26.41	41.10	37.91	54.71	40.16	38.31	56.45
Zn (mg kg^{-1})	78.16	22	120.59	31	72.60	108	657.99[a]	197.83	151.20	133.37	154.04	196.44	232.58

shown here to be useful at discriminating road samples from channels and fields. This non-conservative behaviour may be due to a dilution effect due to an influx of magnetically 'hard' minerals. Following the removal of the non-conservative tracers, source discrimination for May-12 using five tracers was 88.3%, Feb-13 and Jun-13 were 93.0%, and all seven tracers resulted in 94.7% discrimination.

The permutation algorithm to detect tracer non-conservativeness occasionally met a well constrained solution at low tracer numbers, i.e. two or three tracers, such that the addition of subsequent tracers increased the uncertainty. Based on tests using synthetic data presented here, this would suggest that all other tracers experience non-conservative behaviour which, considering the array of tracers employed here is unlikely. Interestingly, the rejection of these tracers could be attributed to their source characteristics, for example, due to the increased dimensionality of data. For example, the Sep-12 sediment sample reported a well constrained result using four tracers (IRM_{soft}, Co, Cr and Ni) and referring to Table 5.4 these tracers have the lowest CV% for field sources. The remaining tracers (χ_{ARM}, Cd and Zn) possessed greater CV% for field sources, therefore, the uncertainty was increased through their inclusion. It is plausible that components of uncertainty in the source dataset may impact the capability of non-conservative tracer detection and this is an area requiring further assessment.

Multiple solutions were detected in every target dataset (Table 5.5), the un-mixing results for which are shown in Figure 5.7. The source discrimination capability of tracer sub-sets are reduced 73 - 93% due to the small number of tracers. The parameters forming each tracer set were reasonably consistent; χ_{ARM}, Cd and Zn were frequently grouped together reflecting the grouping of tracers with lower source variability (as previously discussed). Using these tracers, a larger proportion of sediment is attributed to road sources at the expense of the channel source. In all cases both multiple solutions agree that field contributions are negligible. In the Feb-13 sample, Cr is omitted due to non-conservativeness and Ni is instead grouped with χ_{ARM} and Zn indicating that Ni showed better agreement with the predicted source contributions than the alternative well constrained solution set (otherwise the 2+4 multiple solution would have reported the lowest combined error).

Table 5.5. Combined error values for configurations of multiple solutions (optimum solutions are shown in italics), and tracer groupings based on optimal multiple solutions which correspond to multiple solution one and multiple solution two in Figure 5.7.

TISS sample	**Combined error**	**Multiple solution sets**						
		χ_{ARM}	IRM_{soft}	Cd	Co	Cr	Ni	Zn
May-12		1	-	1	1	2	2	-
2+3	*1.4373**							
Sep-12		2	1	2	1	1	1	2
2+5	2.1994							
3+4	*2.1907**							
Jan-13		2	1	2	1	1	1	2
2+5	1.6600							
3+4	*1.6518**							
Feb-13		1	2	1	2	-	2	1
2+4	1.7639							
3+3	*1.7455**							
Apr-13		2	1	2	1	1	1	2
2+5	2.1428							
3+4	*2.1367**							
May-13		2	1	2	1	1	1	2
2+5	2.1441							
3+4	*2.1285**							
Jun-13		2	2	1	1	-	1	1
2+4	*2.1056**							
3+3	2.2274							

Confidence intervals were smaller for the tracer sub-set where source data was more constrained (IRM_{soft}, Co, Cr and Ni). In all cases, the source contributions predicted by this dataset are almost identical to the single solution, suggesting the less constrained tracer set only marginally influences the all tracer solution and the tracer subset provides a highly accurate estimation of sediment sources in the study catchment.

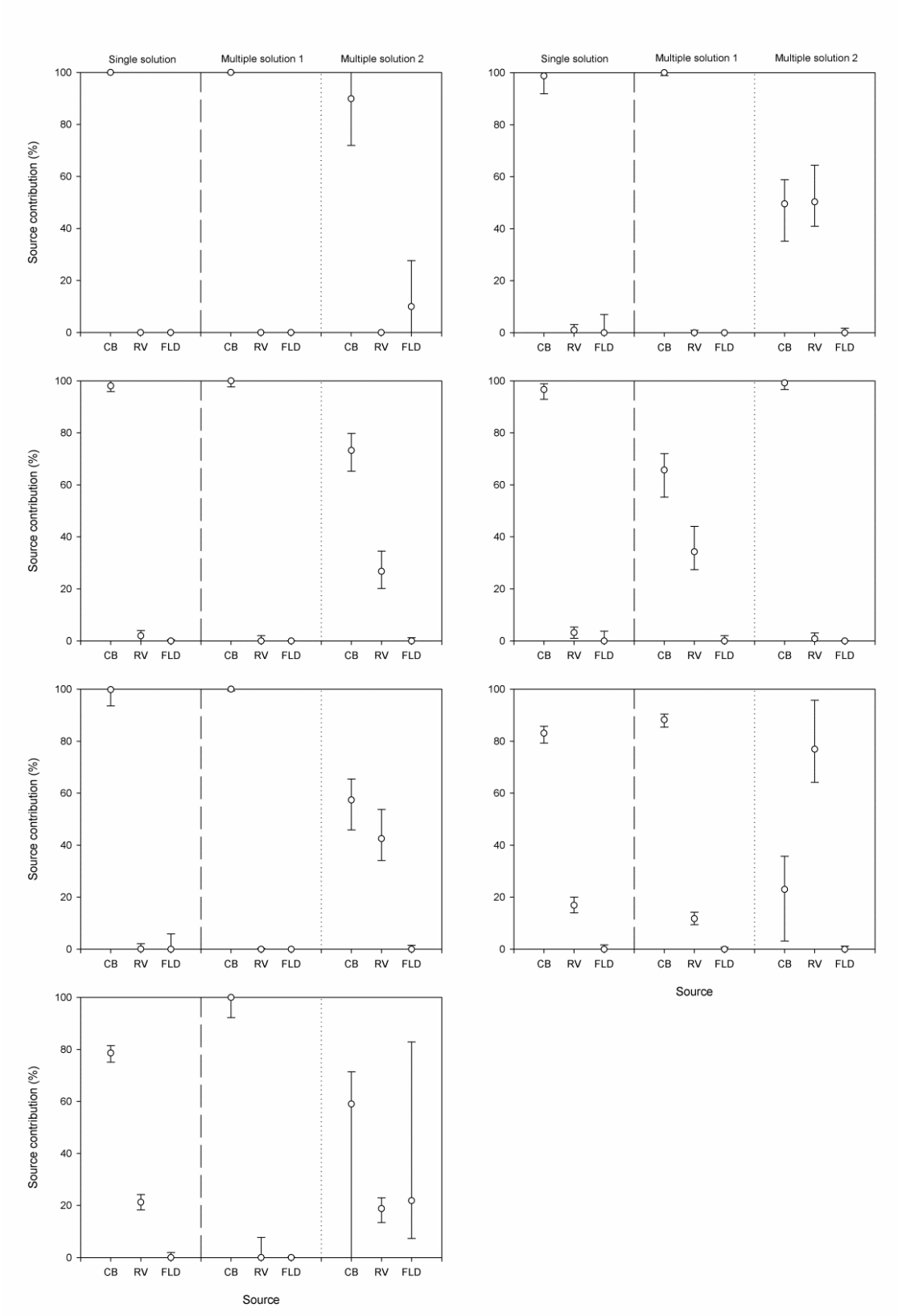

Figure 5.7. Single and multiple solution set results for source samples collected in: a) July 12, b) September 12, c) January 13, d) February 13, e) April 13, f) May 13, g) June, 13. Circle shows median value and bars represent upper and lower 95% confidence intervals; CB, RD, FD indicate channel, road and field sources, respectively.

Previous discussion in this study has suggested that using minimal tracer numbers is not appropriate to achieve constrained source predictions, particularly where tracer corrections have not been formally assessed, a decrease in source discrimination occurs or the physical relevance of tracer configurations cannot be validated. The current capacity of the model to process large datasets unearths difficulties in addressing these issues in the current study. However, the ability of the permutation algorithm to explore non-unique tracer solutions is an important advance for sediment fingerprinting applications to be further investigated. Additionally, in a sediment management context, the multiple and single solutions are in agreement that channels are the dominant sources of sediments. To determine the broad origin of sediment within a small catchment a minimal number of conservative tracers would sufficiently complete the study aim. However, to distinguish between more sources, i.e. the original six sampled sources, the current array of tracers need to be expanded.

5.4 Conclusions

Uncertainty-inclusive sediment fingerprinting studies have facilitated a critical appraisal of current approaches and methodologies. In this study, we have shown that better accuracy and precision of results is achieved through maximising available tracer data. Tracer reduction exercises are disadvantageous toward achieving constrained result predictions and increase the sensitivity of results to non-conservative tracer behaviour. Non-conservative tracer behaviour, and the methods used to correct tracer datasets and validate applied corrections require considerable attention. As the physical and biochemical processes governing tracer enrichment/depletion and transformation are tracer and environment specific, the correction factors require more thorough research. This study supports the notion that particle size and organic matter correction factors that are commonly used may be too coarse to sufficiently correct all tracers, or could introduce further biases into the tracer set.

A Monte-Carlo based uncertainty-inclusive un-mixing algorithm was shown to provide a methodology to assess tracer non-conservativeness more precisely than techniques used to-date for synthetic test data. At a critical degree of corruption, non-conservative tracers could be identified and subsequently rejected according to the constraint of uncertainty afforded on the result. Consequently, the range of possible incorrect predictions was significantly reduced. Further analysis is required to determine the

robustness of the technique when applied to more complex datasets, such as increased tracer and source numbers, or datasets with increased variability.

Near equivalent solutions were explored in synthetic datasets using the permutation algorithm which was successful at selecting the pre-determined source groups. The preferred multiple solutions predicted similar source contributions suggesting that tracers were consistent and likely to group according to source details. Application of the tracer non-conservative and multiple solution methodology to field data showed that tracer non-conservativeness could be detected; however, the capabilities of this algorithm may be affected by source data variability and non-normal distributions of source data. The validity of the multiple solution techniques is, in physical terms, questionable. The ability to analyse tracer groupings and the related un-mixing results has, however, not been approached to date and may improve knowledge of behavioural similarities between tracers.

Measures to standardise the sediment fingerprinting technique in order to constrain resources is problematic and may compromise efficacy. The reduction of samples collected and tracers utilised will likely increase the uncertainty of un-mixing results such that no benefits are obtained over techniques such as catchment surveys. Nevertheless, maximising sample and tracer data can be considerably resource demanding suggesting that in some cases, the cost of robust sediment fingerprinting may outweigh the benefits. Additionally, the advances of statistical approaches to optimise tracer arrays are considered as a deviation from physically-based tracer selection approaches. The benefits of statistical approaches have the potential to be undermined by insufficient assessment of environmental significance; therefore, this is an essential precursor to the application of any statistical method. Finding approaches to corroborate the modelling results (perhaps through use of controlled mixture experiments e.g. Small *et al.*, 2002; 2004) would greatly increase the robustness of evidence for river basin managers to implement mitigation measures.

Efficient mitigation measures are paramount to protect freshwater resources and improve the resilience and sustainability of contributing catchment areas. Sediment provenance techniques can, therefore, offer valuable insights to target cost effective and source specific mitigation strategies. Improved knowledge of underlying

methodological techniques, such as appropriate tracer selection is an essential step to ensure accurate and reliable provenance results are consistently achieved.

5.5 Summary

Reduction of prediction uncertainty is an important step to improve the robustness of sediment fingerprinting results. This study used synthetic and field tracer data to assess the impact of tracer selection methodologies, tracer non-conservativeness on median source predictions and associated uncertainty. Furthermore, the introduced methodology successfully identified the presence of multiple dataset solutions in tracer sets which highlighted the potential of small tracer datasets to apportion contrasting results despite the confirmation of environmental significance and conservative behaviour of tracers.

Nonetheless, the approach used in this chapter to identify tracer non-conservativeness and multiple solutions is not currently suitable for application to large field datasets with variable uncertainty components. However, the reduced uncertainty of result predictions (source contribution) afforded by maximising the number of employed tracers is implementable and will be incorporated into the application of sediment fingerprinting in Chapter 6.

Chapter 6. Sediment fingerprinting as a management tool to identify variability of sediment sources through time in multiple agricultural catchments

6.1 Introduction

Intensive agricultural systems pose risks to aquatic ecosystems though enhanced soil erosion and sediment delivery (Nearing *et al.*, 2004; Delgado and Berry, 2008; Foster *et al.*, 2011). In agricultural catchments, landscape improvements such as artificial drainage are required to manage excess soil moisture, and cultivation of arable crops seeks to increase the extent and productivity of soils. Modifications interact with local heterogeneous catchment attributes (landscape position, slope, soil drainage, antecedent conditions) and rainfall to alter the distribution of soil erosion, connectivity and sediment delivery. Catchment management strategies require identification of sediment sources and an understanding of the spatial and temporal dynamics of physical processes to cost-effectively reduce on-farm soil loss and off-farm downstream sediment supply (Walling *et al.*, 2008).

Auditing individual soil erosion and sediment storage components to assemble a catchment sediment budget demands considerable investigation time and resources (Walling and Collins, 2008). Establishing an evidence-base relating specific agricultural practices to different sediment sources and delivery pathway fluctuations over multiple seasons requires a representatively long study period with observations at an appropriate resolution. Alternative catchment-scale techniques such as sediment fingerprinting have, therefore, emerged as an effective management tool in agricultural catchments (Gruszowski *et al.*, 2003, Rowan *et al.*, 2012; Thompson *et al.*, 2012; Lamba *et al.*, 2015).

The sediment fingerprinting approach (Figure 6.1) assumes that physico-chemical properties of mineragenic sediment can be conserved along a transport pathway, providing the basis to mathematically ‘unmix’ the sedimentary signatures to apportion the relative contribution to their respective upstream sources. Downstream locations represent ‘targets’, spanning storm-derived suspended sediments, or sediment stored in river channels, wetlands, floodplains and lakes. The upstream catchment is subdivided into multiple potential sources (or source group types), for example, according to land

use (Gruszowski *et al.*, 2003; Blake *et al.*, 2012), lithology (Collins *et al.*, 1998), or erosional processes (Fox and Papandicolou, 2008).

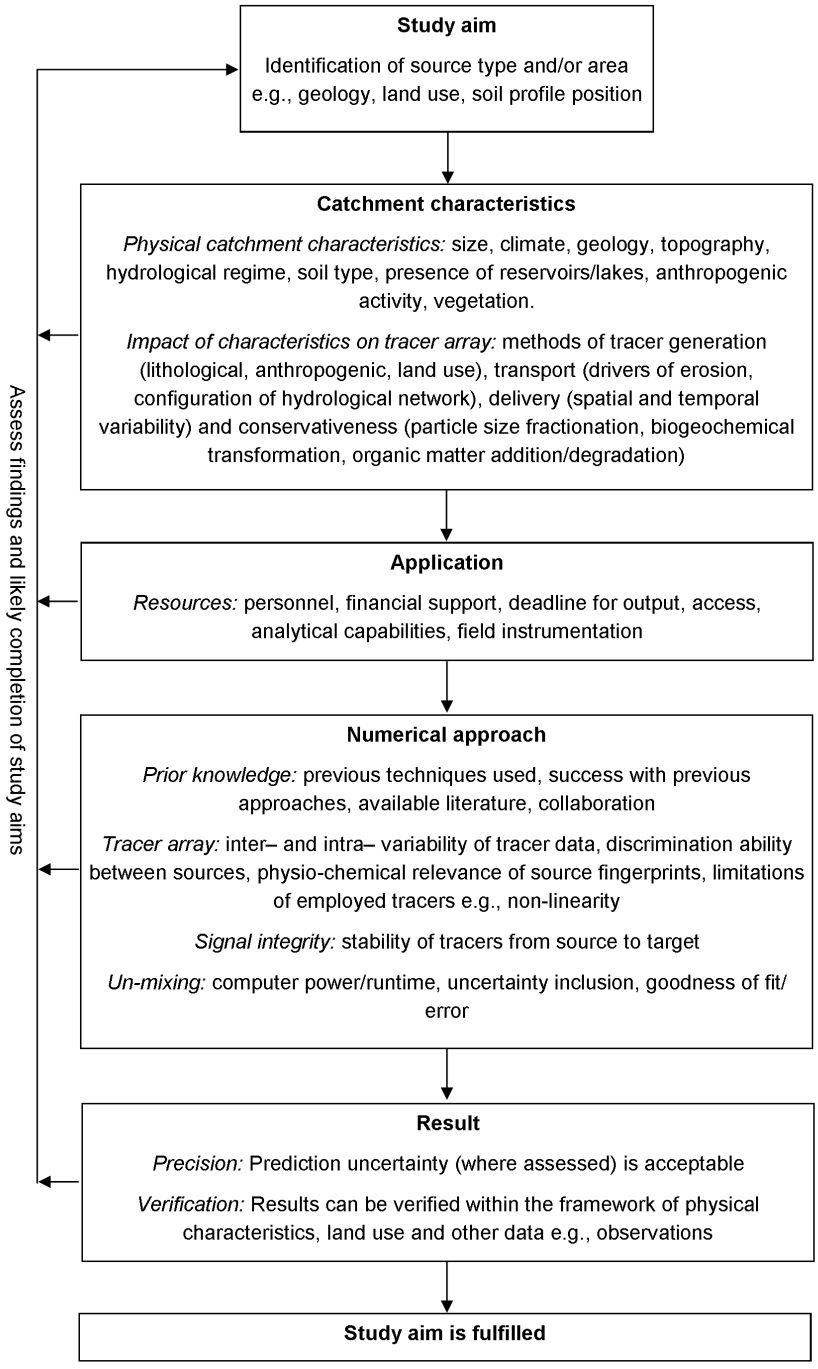

Figure 6.1. Flow chart outlining approach to sediment fingerprinting studies. Adapted from Sherriff *et al.*, (2015b).

Sediment tracers typically employed include geochemistry, mineral magnetics and environmental radionuclides and are potentially numerous considering the capacity of modern analytic equipment. However, selected tracers must be conservative (resistant to chemical transformation) and their environmental significance justified in terms of the ability to discriminate between environmentally relevant sources (Koiter *et al.*, 2013b). Furthermore, the assumption is commonly made that the impact of physical processes (erosion, transport, deposition, and re-entrainment) on tracer concentrations, such as particle size selectivity and organic matter variations, can be numerically corrected. Simple correction factors are commonly used (Collins *et al.*, 2001), but more refined approaches involving particle size fractionation exist (Motha *et al.*, 2004; Small *et al.*, 2004) and the appropriateness of simple correction factors are now disputed (Smith and Blake, 2014). Sediment contributions from each source are determined using statistically-based un-mixing algorithms frequently accompanied by uncertainty estimates (Franks and Rowan, 2000).

The sediment fingerprinting methodology was applied in the three study catchments with the greatest suspended sediment yields (Grassland B, Arable A and Arable B) in order to fulfil the following two objectives:

- Explore sediment sources in catchments with contrasting land use and dominant soil drainage characteristics;
- Assess the seasonal variability of sediment sources in agricultural catchments.

6.2 Methodology

6.2.1 Sample collection

Reconnaissance surveys identified six primary potential sediment sources in the study catchments; grassland topsoils, arable topsoils, damaged road verges, farm tracks, eroding channel banks and eroding ditch banks. The location of fields samples were randomly selected from a spatial dataset (Agricultural Catchments Programme – ACP) stratified by land use type (grassland versus arable) to match the proportion of fields sampled to the overall catchment land use. Each field topsoil sample (0-5 cm) comprised multiple sub-samples from various locations within each field. In Grassland B, Arable A and Arable B, 22 fields (grassland n=16; arable n=6), 25 fields (grassland

n=9, arable n=16) and 30 fields (grassland n=19, arable n=11) were sampled, respectively.

Channel and ditch reaches were surveyed during winter when vegetation cover was low and likelihood of erosion was high and showed field-scale land management was an important control on riparian characteristics (e.g. presence/absence of fencing and hedgerows – Section 4.3.3). Sample collection targeted actively eroding areas (composite of vertical bank section) along the intersection of an individual field with the watercourse, with opposite river banks sampled separately. Channel samples were collected using a plastic trowel resulting in 62 samples from Grassland B, 15 from Arable A and 14 from Arable B. The prevalence of bare channel banks in Grassland B explained the large number of samples collected. Time constraints associated with radionuclide laboratory analysis resulted in a randomly selected sub-set of 30 samples being analysed and were deemed appropriate to characterise the channel sediment source (locations shown in Figure 6.2). Active erosion of ditch (open field drain) channels was observed only in Grassland B (n=4) and sampled consistently with channel banks. Samples of damaged road verges and farm tracks were collected using a plastic trowel. Surface scrapings of readily entrainable soils along a maximum road or track length of approximately 200 m integrating both sides of the road were composited into one sample (Figure 6.2) and GPS co-ordinates recorded.

River sediment samples were collected using time integrated suspended sediment (TISS) samplers (Phillips *et al.*, 2000) located at the outlet of each catchment from May 2012 to May 2014. In Grassland B, two samplers were installed to ensure sufficient sediment was collected for further analysis and bulked into a single sample. One TISS sampler yielded sufficient sample quantity at Arable A and Arable B. Sediment samples were collected at 6-12 week intervals to assess seasonal changes in sediment sources (Table 6.1). Two sediment samples from Arable A were of insufficient quantity to analyse (01/07/13 and 29/19/13), therefore were discarded.

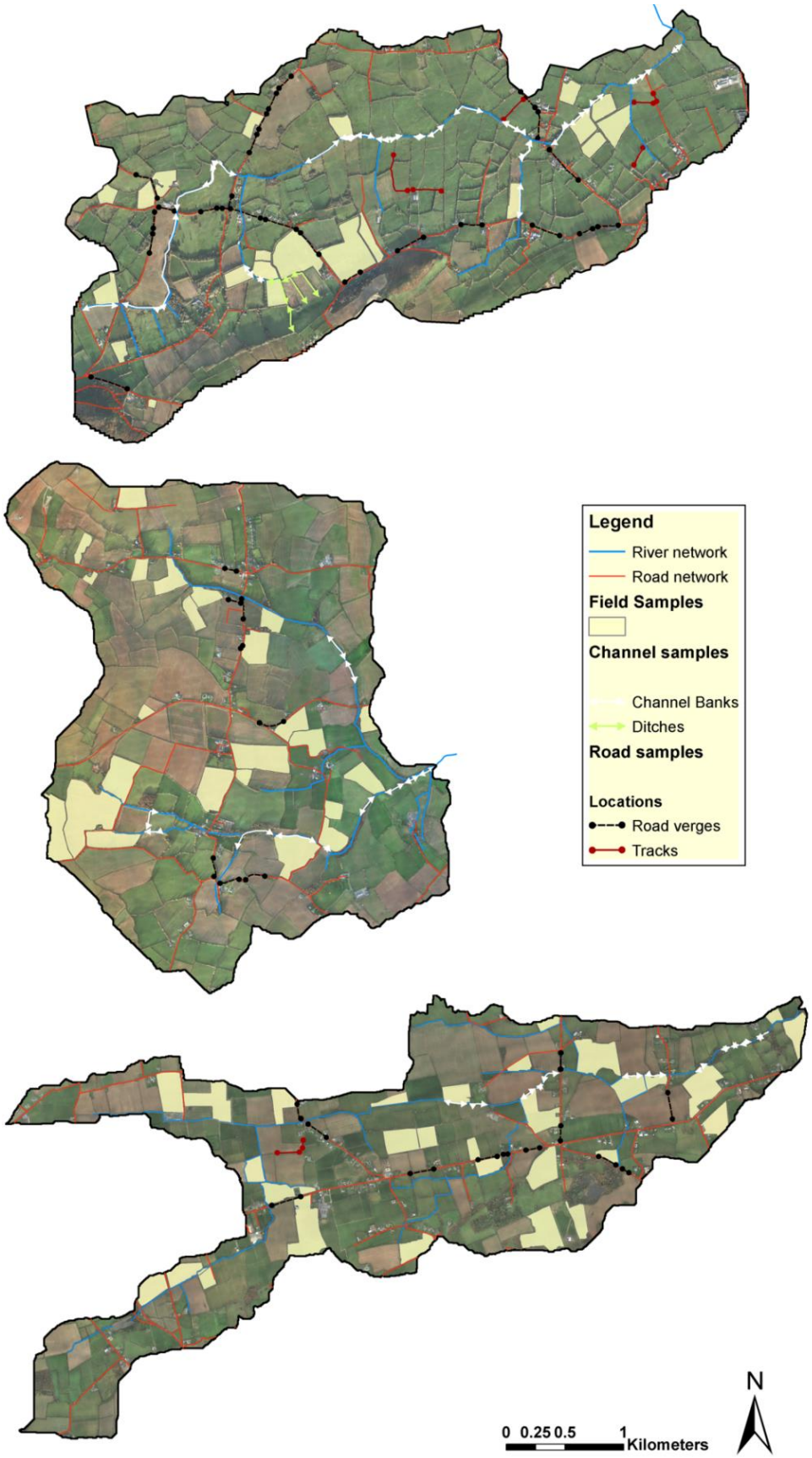

Figure 6.2. Location of source samples in a) Grassland B, b) Arable A and c) Arable B.

Table 6.1. Time integrated sediment sampler collection dates in Grassland B, Arable A and Arable B.

Grassland B	Arable A	Arable B
23/07/2012	11/07/2012	27/07/2012
24/09/2012	01/10/2012	09/10/2012
11/12/2012	09/01/2012	11/12/2012
24/01/2013	12/02/2013	15/01/2013
21/02/2013	05/04/2013	07/02/2013
04/04/2013	13/05/2013	20/03/2013
13/05/2013	01/07/2013	30/04/2013
24/06/2013	29/09/2013	25/06/2013
26/09/2013	30/10/2013	23/09/2013
30/10/2013	16/12/2013	19/11/2013
16/12/2013	28/01/2014	16/01/2014
28/01/2014	13/03/2014	06/03/2014
13/03/2014	22/05/2014	30/04/2014
22/05/2014		21/05/2014

6.2.2 Laboratory analysis

The specific surface area (SSA – $m^2\ kg^{-1}$) of soil and sediment samples were measured using a Malvern Mastersizer Hydro 2000G (range 0.02 to 2000 μm) following pre-treatment with hydrogen peroxide to remove organic matter. Samples were chemically dispersed (Calgon solution 0.4%), homogenised through an auto-sampler unit, then physically dispersed before a triplicate measurement (Fenton *et al.*, 2015). Geochemical, radionuclide and mineral magnetic analysis was conducted on soil and sediment samples. Geochemical elements cadmium (Cd), cobalt (Co), chromium (Cr), copper (Cu), manganese (Mn), nickel (Ni), lead (Pb) and zinc (Zn) were analysed using an Agilent ICP-OES (Santa Clara, US) following microwave assisted acid digestion (USEPA, 1996) to obtain total concentration (mg kg^{-1}).

Radionuclide activity mass concentrations (Bq kg^{-1}) of ^{210}Pb, ^{234}Th, ^{235}U, ^{214}Pb, ^{137}Cs, ^{228}Ac, ^{40}K were measured using a low background Ortec HPGe gamma spectrometer detector (Model no. GEM-FX7025-S) after samples were radon-sealed inside 55 mm petri dishes for a minimum of 30 days to equilibrate ^{210}Pb with ^{222}Rn to determine the unsupported fraction, $^{210}Pb_{unsupp}$, of ^{210}Pb activity (Foster *et al.*, 2007; Rowan *et al.*, 2012). Detector calibration was achieved using a National Physics Laboratory mixed-gamma standard (R08-03) within standardised mass/geometries (1, 2, 5, 10 g). Mineral magnetic measurements, the mass-specific low field susceptibility (χ_{LF} – $10^{-6}\ m^{-3}\ kg^{-1}$), high field susceptibility (χ_{HF} – $10^{-6}\ m^{-3}\ kg^{-1}$), frequency-dependent susceptibility

($\%\chi_{FD}$), anhysteric remanence magnetisation (χ_{ARM} – 10^{-7} Am^2 kg^{-1}), saturation isothermal remanent magnetisation (SIRM at 1 T – 10^{-5} Am^2 kg^{-1}), backfield IRM measurements IRM_{soft} and $bIRM_{hard}$, and ratios SIRM/χ_{LF}, SIRM/χ_{ARM}, χ_{ARM}/χ_{LF} and the H-ratio (0.5 * (SIRM-$bIRM_{40}$)) were calculated. A full description of magnetic measurements is given in Section 5.2.6. Total carbon (TC), total nitrogen (TN) and total organic carbon (TOC – following acid treatment of the inorganic fraction with hydrochloric acid (Massey *et al.*, 2013)) were analysed on a LECO Truspec CN analyser (LECO Corporation, Michigan, USA). The full tracer set is summarised in Table 6.2.

Table 6.2. Summary of measured tracers

Group	Tracers
Geochemistry	Cd, Co, Cr, Cu, Mn, Ni, Pb, Zn
Radionuclides	^{234}Th, ^{235}U, ^{228}Ac, ^{137}Cs, ^{40}K, ^{210}Pb
Mineral magnetics	χ_{LF}, χ_{HF}, $\%\chi_{FD}$, χ_{ARM}, SIRM, IRM_{soft}, IRM_{hard}, SIRM/χ_{LF}, SIRM/χ_{ARM}, χ_{ARM}/χ_{LF}, H-ratio

6.2.3 Statistical analysis

6.2.3.1 Tracer correction, detection of tracer enrichment and non-conservative processes

The contrasts in SSA and organic matter (using TOC as a proxy) between source groups and river sediment samples in each catchment were explored statistically using non-parametric Mann-Whitney U-test (SPSS, v22 – $p<0.05$). Particle size corrections were made on individual samples (corrected tracer concentration = measured tracer concentration/SSA – Gruszowski *et al.*, 2003) rather than deriving source means (Collins *et al.*, 2001; Rowan *et al.*, 2012) as individual values were later input into the un-mixing model. Further correction accounted for organic matter differences between sources and target sediments (corrected tracer concentration = particle size corrected concentration/% organic carbon).

The capability of an individual tracer to distinguish between sources was assessed using the Kruskal-Wallis test (SPSS v22 – $p<0.05$), with tracers passing this test being retained for further analysis. Non-conservative behaviour of tracers from target river sediment samples was identified by comparison with the range of individual source sample values (Mukundan *et al.*, 2010; Smith and Blake, 2014). River sediment tracer

values falling outside of the range provided by the sources were removed from further analysis. All tracers passing the previous steps were subsequently interrogated to justify the environmental significance of tracer contrasts between sources (Koiter *et al.*, 2013b). Next, tracers were entered into Multiple Discriminant Analysis (MDA) to determine the discrimination capability of the complete tracer set. Previous application of the MDA method (Collins *et al.*, 1997) used a stepwise approach to select the minimum number of tracers capable of achieving the maximum source discrimination. Franks and Rowan (2000) and Small *et al.,* (2004) reported that including a greater number of tracers reduced uncertainty, therefore, the MDA was applied only to ensure discrimination was sufficient rather than reduce the tracer set. Source contributions were un-mixed using the uncertainty inclusive FR2000 model as summarised in Section 5.2.1.

6.3 Results and discussion

6.3.1 Environmental and statistical tracer selection

The six sampled source categories could not be discriminated using the employed tracer array. Three composite 'parent' groups were identified and justified as similar processes were likely to control soil loss. The groups were; channels: comprising channel banks and ditches, topsoils: comprising arable and grassland topsoils, and roads: comprising road verges and tracks and were justified as similar processes controlled soil loss (Grassland B – Table 6.3; Arable A – Table 6.4, Arable B– Table 6.5). In Grassland B and Arable B, samples from the road source group were generally elevated for mineral magnetic tracers (χ_{LF},χ_{HF},χ_{ARM},SIRM) and metallic elements Cu, Pb and Zn reflecting inputs from vehicles exhausts. This trend was evident in the geochemical tracers in Arable A but not mineral magnetics likely due to the iron-rich geology which increased the dominance of ferrimagnetic minerals (high IRM_{soft}) in field soils relative to roads. High Mn concentrations were present in Arable A topsoils attributed to the acidic brown earth soils and underlying shales at a minimum depth of 40 cm in catchment uplands.

Surficial sources (fields and roads versus channels) were well defined by atmosphere derived tracers such as ^{137}Cs in Grassland B (Table 6.3) and Arable A (Table 6.4) but were less definitive in Arable B (Table 6.5), where channel sources reported similar values. Elevated average ^{137}Cs concentrations and large standard deviation of Arable B

channel samples compared to other catchments may be attributed to the method of erosion. Bare channel banks in Arable B occasionally corresponded with stock access to the stream and likely transference of surface soils (and associated tracers) to the channel zone. In Grassland B and Arable A, $\%\chi_{FD}$ was higher in field soils but not so in Arable B. Maher (1988) attributed elevated $\%\chi_{FD}$ in topsoils to the production of magnetite grain coatings in poorly-drained soils, however this is not consistent with the drainage characteristics of the study catchments assessed here. Higher concentrations of Cu and Ni in channel compared to topsoil were explained in Grassland B and Arable A due to the reduced weathering (and therefore depletion of element concentration) in topsoils (Smith and Blake, 2014). The same trend is not evident in Arable B, likely due to the heterogeneity of soil types due to quaternary glacio-fluvial sediment deposits (rather than in-situ weathering).

Tracer characteristics of channel samples are frequently indistinguishable from other sub-surface sources such as drains, gullies and tracks which similarly expose the subsoil profile (Collins *et al.*, 2010a). Similarly, in Arable A and Arable B, channel sources are likely a good representation of sub-surface soils; therefore, channel and sub-surface erosion cannot be distinguished here. In Grassland B, however, a thick and low-permeability marine clay subsoil was exposed at 1.5 – 2 m depth along the channel bank (Mellander *et al.*, 2015) and is unlikely to characterise the wider catchment subsoil (to a 1.5 m depth).

Particle size (SSA) and organic matter corrections content were significantly different ($p<0.05$) between source group and river sediment values within each catchment. Average SSA values for channels, fields, roads and river sediments were 1.20, 1.41, 1.11 and 1.59 $m^2\ kg^{-1}$ in Grassland B, 1.29, 1.55, 1.09 and 1.45 $m^2\ kg^{-1}$ in Arable A and 1.06, 1.26, 1.12 and 1.71 $m^2\ kg^{-1}$ in Arable B. Average organic matter (estimated by total organic carbon content) for channels, fields, roads and river sediments were 1.46%, 3.70%, 7.87% and 5.54% in Grassland B, 2.23%, 4.23%, 7.06% and 8.52% in Arable A and 2.94%, 2.89%, 5.25% and 9.64% in Arable B.

Table 6.3. Summary of tracer source data in Grassland B.

Tracer (units defined in text)	**Channel**		**Field topsoils**		**Roads**	
	Mean	Std Dev	Mean	Std Dev	Mean	Std Dev
χ_{LF}	1.73	0.54	2.83	4.18	6.44	2.54
χ_{HF}	1.70	0.53	2.61	3.74	6.24	2.38
$\%\chi_{FD}$	2.38	1.58	5.97	2.87	4.65	5.93
χ_{ARM}	0.08	0.04	0.18	0.30	0.22	0.12
SIRM	296	152	240	253	1207	625
IRM_{soft}	162.90	39.28	105.35	19.54	183.36	56.02
IRM_{hard}	4289	2002	2066	920.3	5797	3132
SIRM/χ_{LF}	0.04	0.01	0.06	0.02	0.04	0.01
SIRM/χ_{ARM}	268.7	145.3	220.9	246.3	1182	623.4
χ_{ARM}/χ_{LF}	122.1	58.02	150.6	192.0	680.6	288.8
H-ratio	27.45	7.90	19.10	7.47	24.63	13.10
Cd	0.23	0.12	0.11	0.05	0.18	0.14
Co	15.78	3.56	8.35	1.70	11.94	2.70
Cr	27.78	10.09	23.78	3.77	22.77	7.67
Cu	23.52	7.35	16.32	3.63	29.10	5.99
Mn	1469	765.1	704.3	348.6	1296	436.3
Ni	28.58	7.01	17.07	2.55	22.11	5.19
Pb	18.17	2.25	23.82	4.79	45.01	58.42
Zn	73.14	14.65	55.63	8.00	123.1	37.24
^{234}Th	171.5	55.82	118.1	31.60	122.1	41.29
^{235}U	163.0	38.12	120.0	41.20	158.1	62.72
^{228}Ac	28.90	8.70	20.39	7.76	24.43	7.81
^{137}Cs	12.10	21.36	88.23	30.28	106.9	98.45
^{228}Ac	377.4	106.9	278.5	67.64	322.3	101.0
^{40}K	54257	5182	49522	4328	50670	5069
$^{210}Pb_{unsupp.}$	102.7	49.77	99.20	70.37	368.0	186.7

Table 6.4. Summary of tracer source data in Arable A.

Tracer (units defined in text)	**Channel**		**Field topsoils**		**Roads**	
	Mean	Std Dev	Mean	Std Dev	Mean	Std Dev
χ_{LF}	2.30	1.76	19.89	13.23	12.65	0.91
χ_{HF}	2.20	1.55	17.71	11.72	11.82	0.90
$\%\chi_{FD}$	2.87	2.53	10.68	0.69	6.60	1.94
χ_{ARM}	0.10	0.10	1.28	0.80	0.60	0.15
SIRM	160.5	101.0	1039	704.4	1258	345.7
IRM_{soft}	74.26	30.53	123.43	210.39	99.32	25.22
IRM_{hard}	1868	601.4	702.4	267.2	2328	1042
SIRM/χ_{LF}	0.04	0.02	7.10	18.65	0.05	0.01
SIRM/χ_{ARM}	142.5	100.1	1026	688.9	1241	342.3
χ_{ARM}/χ_{LF}	101.1	69.92	784.2	671.5	869.0	196.8
H-ratio	17.92	23.68	107.3	257.64	17.28	4.75
Cd	0.17	0.09	0.21	0.09	0.50	0.39
Co	19.67	6.50	13.90	1.83	13.09	2.21
Cr	37.83	5.52	28.21	3.19	26.54	5.49
Cu	29.49	7.24	21.56	3.13	32.79	14.03
Mn	1181	266.6	167	415.8	1377	225.4
Ni	38.76	6.18	22.76	3.32	24.98	4.59
Pb	24.83	5.15	25.66	3.23	34.16	13.47
Zn	92.47	14.11	85.43	8.52	135.1	47.63
^{234}Th	153.0	49.32	150.0	37.65	98.16	39.12
^{235}U	172.4	46.14	162.5	38.85	134.3	53.80
^{228}Ac	39.70	4.31	30.08	7.62	30.95	4.75
^{137}Cs	23.90	22.21	132.4	45.14	132.3	47.92
^{228}Ac	474.0	93.08	397.5	91.32	313.4	70.18
^{40}K	67628	6734	56461	514	5033	3070
$^{210}Pb_{unsupp.}$	67.29	46.02	131.0	55.13	268.0	123.7

Table 6.5. Summary of tracer source data in Arable B.

Tracer (units defined in text)	**Channel**		**Field topsoils**		**Roads**	
	Mean	Std Dev	Mean	Std Dev	Mean	Std Dev
χ_{LF}	2.60	1.84	1.89	0.78	3.94	1.42
χ_{HF}	2.50	1.65	1.79	0.71	3.83	1.41
$\%\chi_{FD}$	2.65	1.91	4.53	1.69	3.13	1.13
χ_{ARM}	0.14	0.05	0.16	0.08	0.17	0.04
SIRM	337.7	118.2	214.5	94.72	533.4	222.0
IRM_{soft}	143.2	25.99	111.7	15.65	131.0	17.43
IRM_{hard}	2540	490.6	1337	229.7	3026	920.4
SIRM/χ_{LF}	0.06	0.01	0.08	0.01	0.05	0.01
SIRM/χ_{ARM}	324.1	116.2	201.5	92.19	518.5	218.6
χ_{ARM}/χ_{LF}	215.4	91.06	135.2	64.74	338.8	138.1
H-ratio	13.62	4.95	12.97	3.40	14.93	5.01
Cd	0.50	0.11	0.48	0.10	0.46	0.08
Co	10.13	1.46	9.02	1.17	11.20	1.06
Cr	27.33	5.48	27.48	2.81	29.30	2.89
Cu	20.88	2.59	23.77	3.88	33.28	5.83
Mn	797.5	325.7	590.1	129.5	718.6	94.07
Ni	33.42	4.56	28.69	3.35	37.29	3.50
Pb	35.73	5.86	37.31	7.35	39.80	8.78
Zn	69.98	7.70	74.58	11.68	117.7	26.65
^{234}Th	121.3	34.71	158.8	44.11	118.8	34.77
^{235}U	112.6	28.11	162.8	38.43	144.9	35.25
^{228}Ac	24.61	8.24	26.62	7.44	26.02	9.65
^{137}Cs	103.5	65.03	121.5	36.53	109.8	59.27
^{228}Ac	325.2	73.41	343.6	75.17	333.6	83.37
^{40}K	53933	6381	51838	5697	56111	4123
$^{210}Pb_{unsupp.}$	97.38	74.77	116.3	45.74	162.7	68.29

6.3.2 Tracer selection

In Grassland B, all tracers passed the Kruskal-Wallis test ($p<0.05$) whereas ^{234}Th and ^{235}U failed in Arable A, and χ_{ARM}, ^{234}Th, ^{228}Ac, and ^{137}Cs failed in Arable B; these tracers were removed from further analysis. Non-conservative behaviour assessment (mass-conservation) of target sediments showed various tracers failed in all catchments but not in river sediment samples (Table 6.6).

Table 6.6. Tracers failing mass conservation tests in target sediment samples in Grassland B, Arable A and Arable B.

Grassland B		**Arable A**		**Arable B**	
Sample	Failed tracer(s)	Sample	Failed tracer(s)	Sample	Failed tracer(s)
23/07/2012	Mn, Zn, ^{234}Th, ^{235}U	11/07/2012	-	27/07/2012	Pb, Zn
24/09/2012	Cd	01/10/2012	-	09/10/2012	Cr, ^{40}K
11/12/2012	-	09/01/2012	-	11/12/2012	-
24/01/2013	%fd	12/02/2013	-	15/01/2013	%fd
21/02/2013	-	05/04/2013	-	07/02/2013	-
04/04/2013	Cd	13/05/2013	Radionuclides	20/03/2013	SIRM/χ_{ARM}
13/05/2013	Cd, Mn	01/07/2013	*	30/04/2013	-
24/06/2013	Cd, Radionuclides	29/09/2013	*	25/06/2013	-
26/09/2013	SIRM/χ_{ARM}, Mn	30/10/2013	Radionuclides SIRM/χ_{ARM}, χ_{ARM}/χ_{LF}	23/09/2013	SIRM/χ_{ARM}, Cd, Cr, ^{40}K
30/10/2013	Cd, Mn	16/12/2013	-	19/11/2013	SIRM/χ_{ARM}, Cd, ^{210}Pb$_{unsupp.}$
16/12/2013	%fd, SIRM/χ_{ARM}, Cd, Mn	28/01/2014	*	16/01/2014	SIRM/χ_{ARM}, Cd
28/01/2014	Cd	13/03/2014	SIRM/ χ_{ARM}	06/03/2014	SIRM/χ_{ARM}, Cd, ^{235}U, ^{40}K
13/03/2014	Cd, ^{234}Th	22/05/2014	Magnetics, radionuclides	30/04/2014	SIRM/χ_{ARM}, Cd
22/05/2014	Cd			21/05/2014	SIRM/χ_{ARM}

* – insufficient sample quantity to analyse tracers

Tracers Cd and Mn frequently displayed non-conservative behaviour in Grassland B, (64% and 36%, respectively) hence these tracers were removed from further analysis. Low sample quantity for samples 01/07/13, 29/09/13 and 28/01/14 collected in Arable A resulted in erroneous values from radionuclide tracers and mineral magnetics for the 13/03/14 sample. Small sample quantities in Arable A were attributed to low sediment export for 01/07/13 and 29/09/13 samples and a blocked TISS device during the 28/01/14 sampling periods. All other failed tracers were removed for the corresponding target sediment only. In Arable B, χ_{ARM}, ^{234}Th, ^{228}Ac and ^{137}Cs failed the Kruskal-

Wallis test and SIRM/χ_{ARM} and Cd river sediment values frequently exceeded acceptable values from source data; these tracers were removed from further analysis in this catchment. The resultant discrimination capacity of employed tracers was 94.2- 97.7% in Grassland B, 95.5-97.7% in Arable A and 94.7-98.2% in Arable B (e.g., Figure 6.3) and qualify against other acceptable values reported elsewhere (Lamba *et al.*, 2015; Theuring *et al.*, 2015).

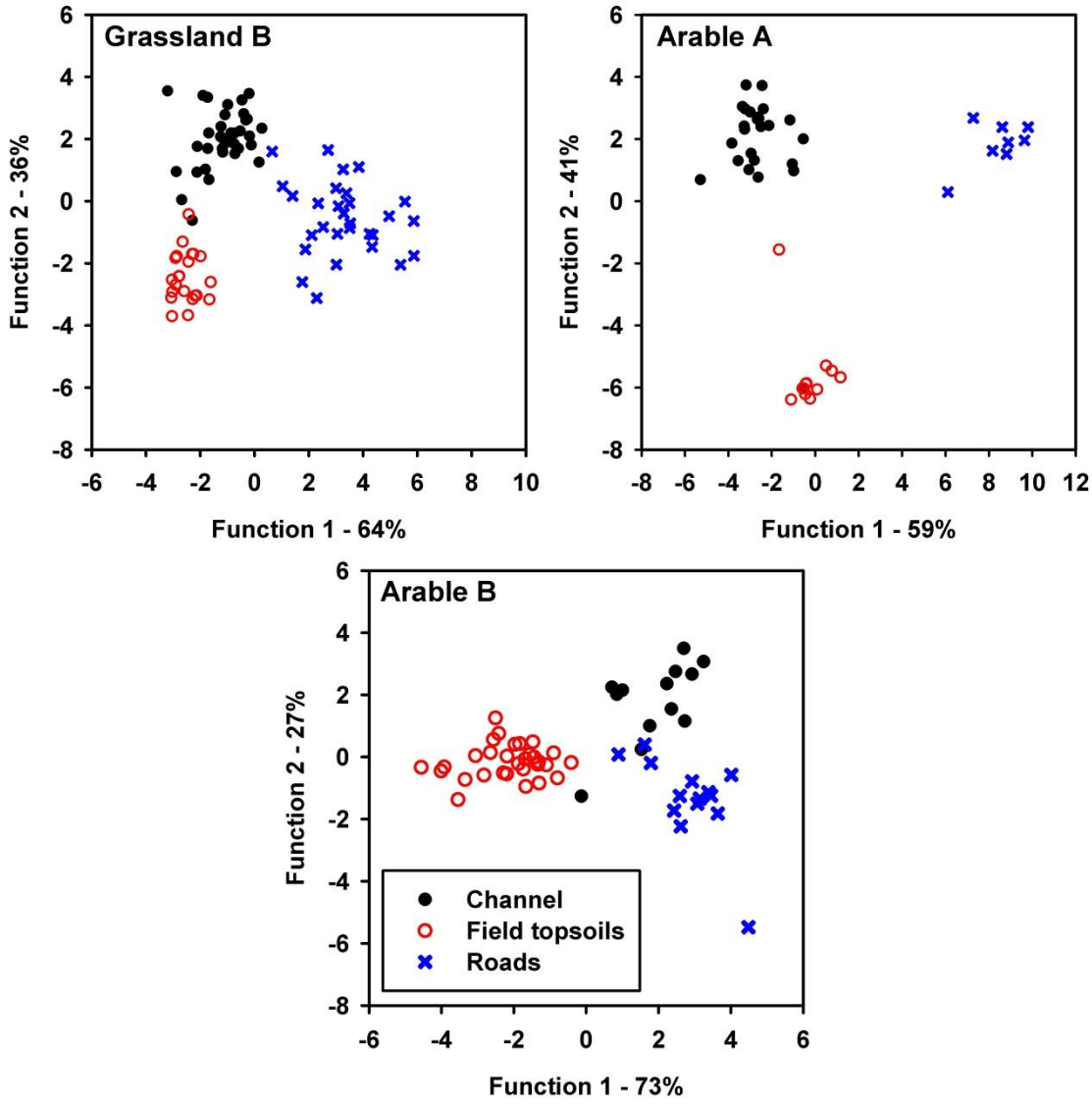

Figure 6.3. Multiple discriminant analysis of full tracer sets at, a) Grassland B, b) Arable A, and c) Arable B.

6.3.3 Sediment fingerprinting

Uncertainty inclusive un-mixing (Figure 6.4) consistently showed larger uncertainty envelopes in Grassland B (average 61%) compared to Arable A (average 50%) and Arable B (average 50%). This is attributed to greater variability (higher standard deviations – Rowan *et al.,* 2012)) of source data in this catchment as observed in Figure 6.3. Sources were least variable over time in Arable B, whereby channel, field and road contributions ranged from 7-25%, 54-89% and 0-21%, respectively. Grassland B, contributions ranged from channel, field and road sources were 55-99%, 0-38% and 0-9%, respectively. Sources were most variable in Arable A, where contributions ranged from 0-60%, 0-22% and 0-49% in channel, field and road sources, respectively. Lower ranges in poorly- and moderately-drained catchments likely reflected the greater sediment connectivity and consequential consistency of hydrological pathways and source availability.

Load specific un-mixing using median predictions indicated channels (eroding channels and ditch banks) were the dominant sediment sources in Grassland B for all samples (Figure 6.5) and overall accounted for 70% of the suspended sediment load (SSL). This confirmed the catchment dynamics previously inferred using hysteresis analysis (Section 4.4.2); rapid delivery of flow from predominantly poorly-drained hillslopes into the featureless (channelised and absent of features promoting roughness and dissipation of flow energy) drainage network which sustains flow velocity and consequent erosion capacity of channel flows which increases the likelihood of channel bank erosion where limited vegetation reduces bank stability. Field topsoils overall contributed 25% to the SSL which confirms that hillslope sediment loss risk is largely reduced by permanent pasture groundcover despite good connectivity. Contributions from field topsoils in individual samples increased with SSLs confirming greater spatial hillslope connectivity following wetter weather (when the majority of sediments are exported – Section 3.5) and subsequent soil erosion and sediment delivery via overland flow pathways. Roads were a negligible sediment source in this catchment.

Sources were predominantly sub-surface (sub-soil or channel banks) in Arable A (59%) with smaller proportions attributed to field topsoils (22%) and roads (19% – Figure 6.5).

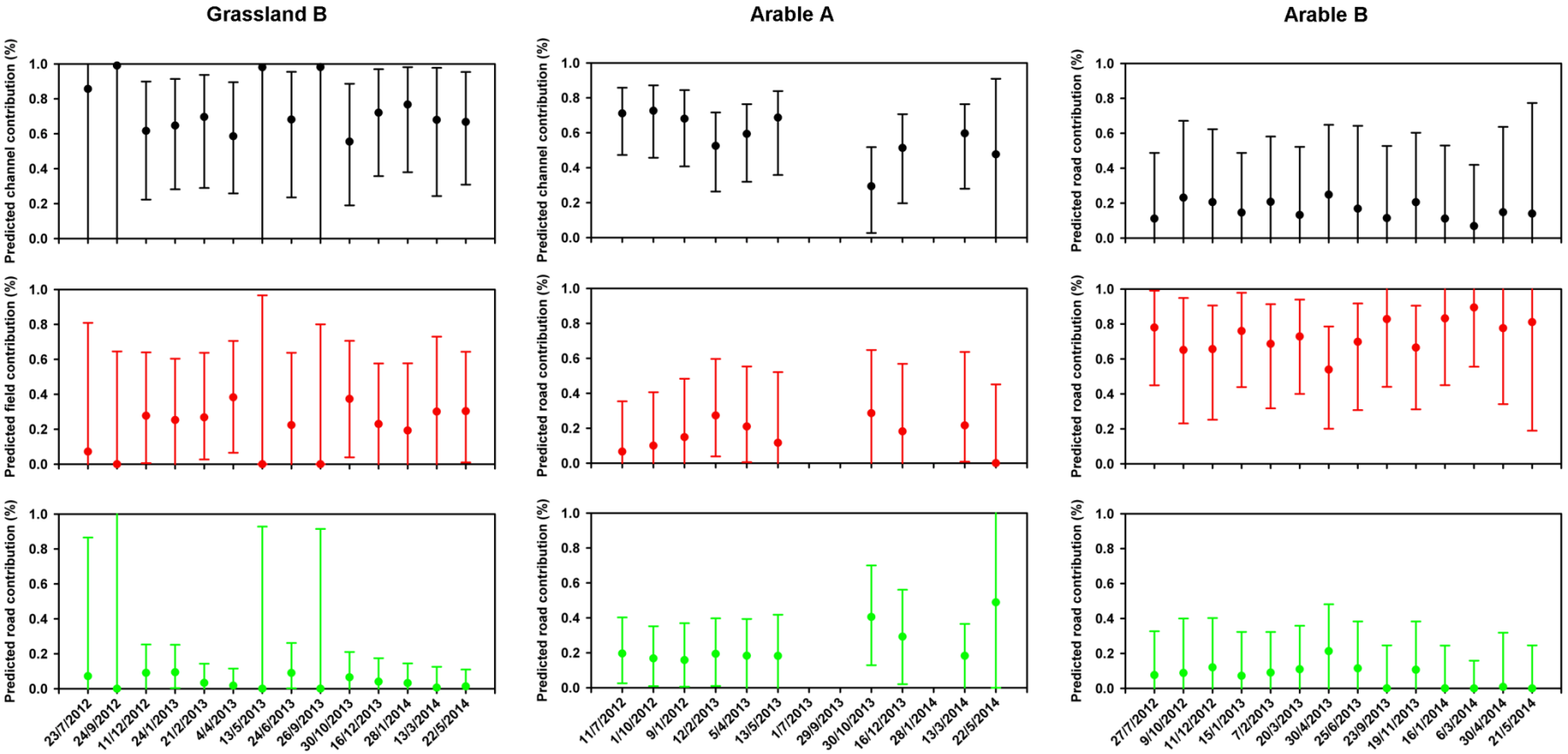

Figure 6.4. Uncertainty inclusive predictions of channel (black), field topsoil (red) and road (green) contributions in a) Grassland B, b) Arable A, and c) Arable B.

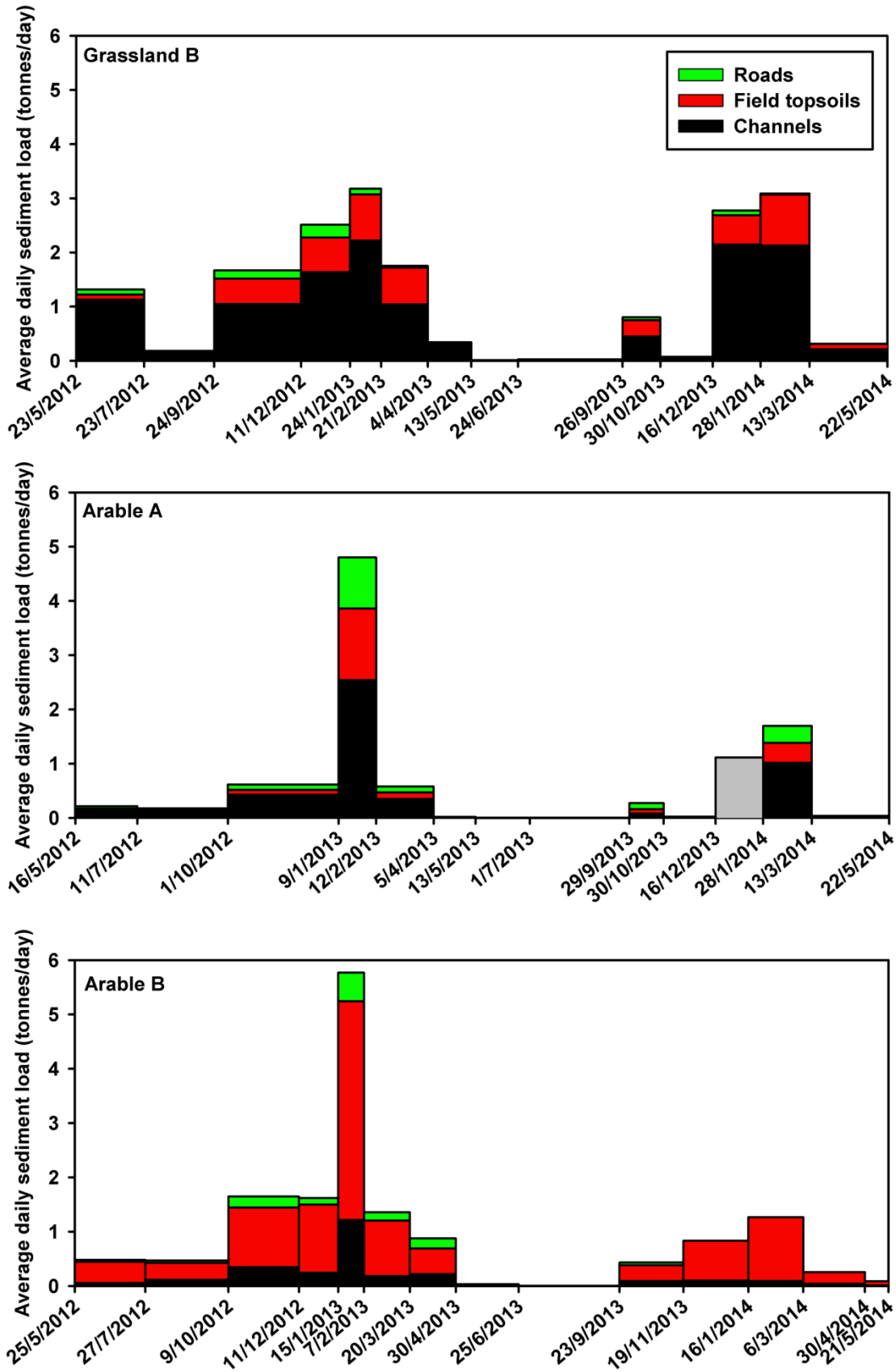

Figure 6.5. Load specific un-mixing of median source predictions in a) Grassland B, b) Arable A, and c) Arable B. Grey bar in Arable A chart corresponds to blocked sediment sampler.

Higher sediment exports (greater than ~2 t/day) per sampling period in Arable A were less frequent than in Grassland B and Arable B, due to the less-flashy hydrological response in Arable A and the influence of event-scale rainfall on the establishment of sediment-associated flow pathways. As previously discussed in Section 4.4.1, a high proportion of the Arable A stream network is dominated by a woodland riparian corridor which reduces channel bank erosion through stabilising soils by root networks (Polvi *et al.*, 2014). Bank sections most susceptible to erosion occur where established riparian vegetation is insufficient to resist undercutting and rotational bank failure (~33% of banks in Arable A) or where watercourse maintenance (two drainage projects were observed during January 2014 on the north-south tributary) temporarily destabilises channel beds and banks until vegetation cover is re-established. Sub-surface sediment sources may have additionally contributed; Deasy *et al.* (2009) attributed sub-surface sediment sources to transmission of flow through tile drains in a predominantly poorly-drained agricultural catchment. However, in-field piped drains to reduce the groundwater table depth and ensure soil productivity are limited to small areas of poorly-drained Groundwater Gleys and Gleyic Brown Earth soils in the riparian corridor in Arable A. Elsewhere in the catchment, high permeability (from fractured bedrock and well-drained soils) is sufficient to maintain agricultural production without artificial drainage and introduces an inherent reduction in sensitivity to sediment loss. Exception may occur during extreme rainfall events (Chapter 4) whereby surface connectivity can be established as is reflected by increased field topsoil contribution during the sampling period with greatest associated yield. Sub-surface sediment transport and erosion may occur through eluviation, and preferential flow pathways such as macropores, however, observation and quantification of these processes is uncommon (Warsta *et al.*, 2013).

Field topsoils dominated sediment sources in Arable B, accounting for 74% of the total yield, with 17% being attributed to channels and 9% to roads (Figure 6.5). Foucher *et al.* (2015) similarly report the dominance of surface sources in a row crop arable catchment in France with widespread sub-surface drainage. Previous inferences using hysteresis analysis (Section 4.4.1) assigned sediment export risk to bare arable fields with good hillslope connectivity (resulting from predominately moderately- and poorly-drained soils) were confirmed with fingerprinting data. Similarly to Arable A, negligible channel contribution likely resulted from increased bank stabilisation from the extensive

root networks of riparian woodland and reduced channel flow velocities due to energy expenditure attributed to the erosion, entrainment and transport of particles from hillslopes. The increased proportion of channel contributions where sediment yield was increased likely resulted from greater lateral channel bank pressure. Ephemeral ditches in the upper catchment, activated following prolonged rainfall and saturation of high permeability but relatively shallow topsoils (Mellander *et al.*, 2012), likely increased the proportion of flow diverted to, and the lateral channel bank pressure (Fox *et al.*, 2005) where riparian vegetation was likely less effective at stabilising channel banks (compared to woodland vegetation alongside the main channel in lower reaches with relatively deeper root depth).

Sediment fingerprinting has confirmed both direct and indirect impacts of agricultural land management on the erosion and transport of sediment. Where low ground cover is combined with good connectivity (consistently in Arable B or sporadically following extreme rainfall events in Arable A), field topsoil contributions were dominant and likely resulted from low ground cover due to cultivation of arable land. In Arable B in particular, consistent losses from field topsoils suggest associated nutrients were also depleted. Supplementary fertilisation is, therefore, required to sustain production which decreases the profitability of a given crop (Quinton *et al.*, 2010). The proportion of topsoil sediments exported from the outlet is also only indicative of sediments delivered to the catchment outlet (resulting from erosion, transport, conveyance losses, channel storage) and cannot quantify actual soil erosion rates. The impact of agriculture on soil erosion and loss of sediment from agricultural fields (field sediment delivery ratio – field-SDR) would require further evaluation using a dedicated methodology including estimation of hillslope soil erosion and sediment redistribution rates using caesium-137 (Collins and Walling, 2004; Walling and Collins, 2008).

Grassland B and Arable A confound previous assumptions (based on the intensity of agriculture) that field-based farming practices were principal sediment sources in intensive agricultural catchment. In Grassland B, channel erosion was likely accelerated by the presence and configuration of drainage systems, whereas in Arable A installation and maintenance of channels (sub-surface drainage, ditches or streams) likely contributed short-term sources. These landscape modifications (aimed to reduce excess soil moisture and increase the utilisable area for agriculture on hillslopes) were likely

responsible for accelerating channel erosion. The proximity of channel sources to the stream network means delivery to the catchment outlet is highly likely, mediated only by indeterminate channel bed storage (within the substrate matrix and surface drapes). In both catchments some ditch networks were seasonally ephemeral in distal network locations (relative to the outlet); therefore, longitudinal connectivity of the drainage network may be an important phenomenon (Fryirs *et al.*, 2007).

Despite relatively high spatial resolution source sampling in relation to the small catchment sizes (~10 km^2), intra-source variability was greater than inter-source variability, thus prevented discrimination of the intended potential sources identified at the outset of the investigation (Rowan *et al.,* 2012). Definition of additional sources (improved dimensionality) such as land use type (arable versus grassland) in Grassland B and Arable B, and sub-surface location (channel versus sub-surface) in Arable A would enable better understanding of interactions between sources and catchment processes to further target sources. For example, in Grassland B, partitioning topsoil contributions between grassland and arable land use types would disentangle the hillslope signal; contributions from high risk but spatially limited and rarely connected arable fields on high permeability soils, or larger areas of poached/overgrazed grassland on low permeability soils. Gruszowski *et al.* (2003) successfully distinguished grassland and arable topsoils using tracersχ_{HF}, χ_{ARM}, IRM_{880}, Fe, Al, Na and Cu. Equivalent tracers measured in this study were, however, not capable of discriminating arable and grassland topsoils and may be attributed to the rotation of arable crops and grassland fields in the study areas. Measurement of additional tracers such as soil enzymes (Nosrati *et al.,* 2011) and crop-specific compound specific stable isotopes (Blake *et al.,* 2012) may be useful to provide greater dimensionality.

Nevertheless, the separation of sediment load into the three sources defined here (field topsoil, channel/subsurface and road) has significantly advanced the scientific understanding of sediment dynamics in Irish agricultural catchments. Previous research in these catchments (Chapter 4, Shore *et al.*, 2014; Mellander *et al.*, 2015; 2016) has confirmed the influence of hydrological connectivity on the delivery of sediment and nutrients at catchment outlets. Identification and mitigation of hillslope sediment loss, of particular importance in Arable B, must therefore target critical source areas to maximise the success of measures (Shore *et al.*, 2013; Thompson *et al.*, 2013; Thomas

et al., 2015). Controls upon bank erosion of natural and artificial channels in the Irish context are required and have been typically overlooked in agri-environmental policy. In particular, investigating erosion thresholds based on flow velocity, bank composition and stability provided by vegetation in relation to channel dimensions, maintenance and recovery is essential to reduce soil erosion. The potential trade-off between reducing hillslope soil moisture to sustain or increase agricultural production and the initiation and acceleration of erosion at the field edge must be fully assessed.

6.4 Conclusion

The successful partitioning of field topsoil, channel and road sources indicated contrasting hillslope versus channel influences in the three catchments, according to source availability and transport pathways. Fingerprinting has additionally confirmed inferences made about soil erosion and sediment dynamics through suspended sediment yield and high resolution sediment-discharge hysteresis in three intensive agricultural catchments. Main conclusions are:

- Grassland B and Arable B exported overall greater sediment load due to the dominance of surface pathways resulting from low landscape permeability;
- Sediment sources were less variable in predominately poorly- or moderately-drained catchments due to the consistency of flow pathways and respective source availability (Grassland B – channels, Arable B – hillslopes);
- Greater sediment export in Arable A corresponded with greater contributions from field topsoils which were attributed to the establishment of surface hydrological connectivity and consequent surface erosion and overland flow transport following extreme rainfall events;
- Contributions from roads sources were low in all catchments;
- Reduced sediment contributions to the catchment outlet from all sources occur in highly permeable catchments likely due to reduced connectivity. However, where connectivity was established, the highest sediment export was recorded and was consistent with a greater proportion of sediments from field topsoils.

Successful sediment mitigation measures must consider hillslope and riparian areas in intensive agricultural catchments and consider the likely impact of hydrological or land use modifications on downstream sediment loss risk. In catchments with arable land use

on low permeability soils, surface hydrological pathways should be intercepted to promote deposition of sediments on the hillslope. Where low permeability soils dominate a catchment and artificial drainage is widespread, the stability of the drainage network may be confounded by high hillslope to channel connectivity. Dissipation of flow energy is required to reduce channel bank vulnerability.

Eradication of sediment export is not the objective of sediment management programmes, as nutrients and organic matter, vital to ecological functioning is delivered with sediments (Foster *et al.*, 2011). However, the disturbance to aquatic ecosystems, particularly those supporting sensitive species, is potentially severe according to the timing, magnitude and duration of sediment delivery events. Therefore, the reduction of the duration and magnitude of sediment transfers into benthic habitats is a priority to sustain water quality.

6.5 Summary

Sediment fingerprinting successfully confirmed the erosional behaviours inferred from sediment-discharge hysteresis analysis in Chapter 4. The interactions between climate, land use and soil drainage resulted in contrasting sources between the three study catchments. Variability of sediment sources through time was detected and demonstrated fluctuations in sediment sources and transport pathways (particularly in the well-drained catchment). Data provided here are valid for management of sediment losses from agricultural systems worldwide where robust sediment fingerprinting research has not been conducted. The sediment fingerprinting method is a reliable tool to determine sources of fine sediments delivered to a catchment outlet and consequently guide sediment management strategies to account for catchment specific sediment loss risk in agricultural catchments.

Questions remain regarding the extent of soil erosion in Irish agricultural catchments and the impact on sustainability of soil resource. This is of particular interest in arable catchments with a long history of high agricultural productivity, but also high soil erosion risk due to extended periods of low ground cover dominate the catchment area. In the final experimental chapter (Chapter 7), this will be explored using field-scale caesium-137 soil erosion assessment methodology.

Chapter 7. Impact of erosional processes on soil and organic carbon losses to indicate soil sustainability in a long-term arable catchment

7.1 Introduction

Soil sustainability is a primary concern for maintaining and increasing food production through intensive agriculture (Tilman *et al.*, 2002). Major threats to soil sustainability in Atlantic Europe include declining soil organic carbon, compaction, contamination and soil erosion (Creamer *et al.*, 2010; Louwagie *et al.*, 2011). Soil erosion can reduce soil quality through the removal of productive, carbon and fertiliser-rich topsoils. Deposition of eroded soil on footslopes may locally augment soil quality by nutrient accumulation (Quinton *et al.*, 2010; Powlson *et al.*, 2011). However, delivery of eroded soils and sediment-associated nutrients into channel networks can degrade the quality of aquatic ecosystems (Kemp *et al.*, 2011; Kjelland *et al.*, 2015).

Increased soil erosion by water from arable-ecosystems is attributed to greater erodibility and efficiency of sheet and rill erosion from runoff on bare soils (Kirkby *et al.*, 2004). This soil erosion risk is variable in space and time, dependent upon the timing of crop drilling and establishment of groundcover post-drilling in relation to rainfall characteristics (Boardman *et al.*, 2009). Tillage practices, on the plot scale, may cause soil erosion due to micro-topography, but on the field scale is a redistribution mechanism due to net downslope displacement (van Oost *et al.*, 2005). Crop harvesting, particularly of root crops, may remove significant volumes of nutrient-rich topsoils which may account for net soil loss, but also nutrient and organic matter losses (Quinton *et al.*, 2010).

The (in)consistency and (dis)connectivity of subsequent transport pathways results in a fraction of the eroded volume being exported from catchment, termed the ‘sediment delivery ratio’, with the remainder of sediment stored within the system (Walling 1983, Fryirs, 2013). At the field-scale, considerable sediment deposition can occur where overland flow velocities are reduced e.g., at low-gradient hillslope sections, interception by barriers such as micro-topographic features, e.g., hedgerows and buffer strips, or when soil conditions no longer support overland flow pathways (Fryirs *et al.*, 2007; Lacoste *et al.*, 2014). Sediment storage in the fluvial system is similarly associated with

conditions or locations where deposition is likely, e.g. floodplains, in-channel on receding event flow or increased channel width (Croke *et al.*, 2013; Shore *et al.*, 2015).

In an intensive, predominantly long-term arable catchment in south-east Ireland (Arable A), quantification of annual catchment suspended sediment export from 2009-2013 (Sherriff *et al.*, 2015a/Chapter 3) and sediment provenance investigations (Chapter 5) suggested a small proportion (22%) of low suspended sediment yields (annual average 12 t km^{-2} yr^{-1}) were attributed to field topsoils. High permeability soils and fractured bedrock dominate the catchment, which support dominating sub-surface hydrological pathways which reduce surface hydrological connectivity, indicative of reduced soil erosion risk. However, high inter-annual variability of annual suspended sediment yield (3-23 t km^{-2} yr^{-1}) and the magnitude of event-scale sediment (Chapter 4) and phosphorus export (Mellander *et al.*, 2012) when field soils are likely connected suggest that the management concern from high permeability catchments cannot be overlooked. Assessment of soil erosion is, therefore, necessary to investigate the impact of contrasting soil erosion mechanisms on soil sustainability and verify catchment sediment dynamics.

Measurement of soil erosion and sediment redistribution using radionuclide tracers, such as caesium-137 (^{137}Cs), present time-averaged erosion rates inclusive of all erosion mechanisms (Walling and Quine, 1990; Brazier, 2004). Nuclear weapons testing in the 1950s and 1960s and the Chernobyl nuclear accident in 1986 transferred and distributed large proportions of ^{137}Cs into the stratosphere (Figure 7.1) which were subsequently

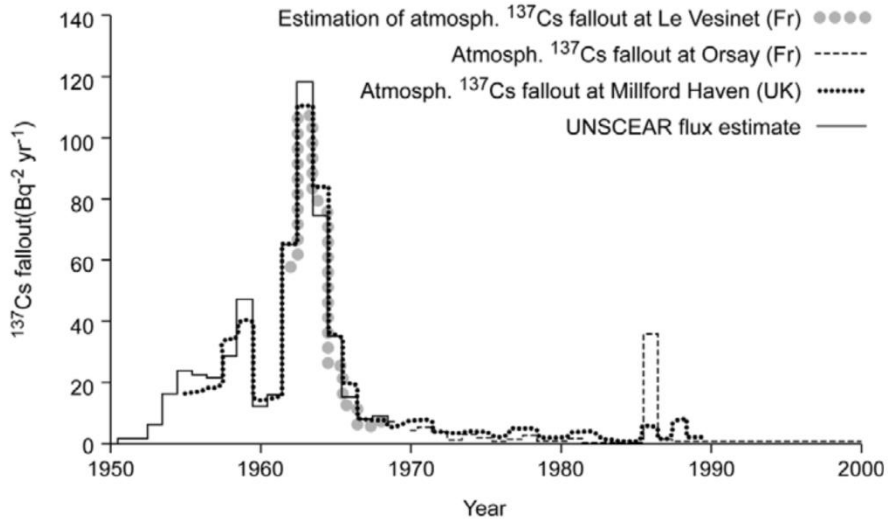

Figure 7.1. Annual ^{137}Cs fallout in France and the United Kingdom (Le Roux and Marshall, 2007)

deposited on land primarily with rainfall (Figure 7.2). Four key assumptions underpin the use of ^{137}Cs tracing for soil erosion and redistribution assessments, i) ^{137}Cs deposition is spatially uniform, ii) fallout is quickly and irreversibly bound to soil particles, iii) redistribution is due to soil movement and iv) ^{137}Cs inventories can be used to infer soil erosion rates (Walling and Quine, 1992).

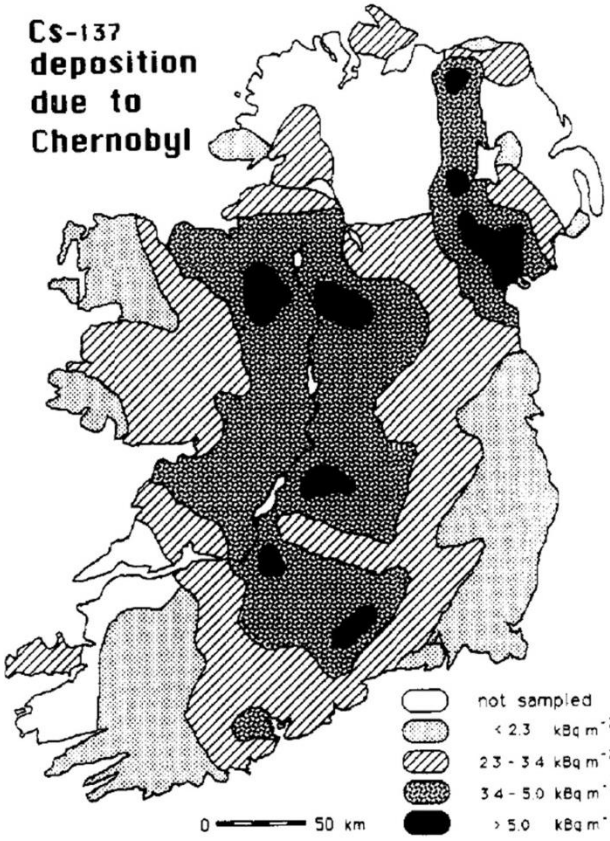

Figure 7.2. Spatial distribution of Chernobyl fallout in Ireland (McAulay and Moran, 1989).

The methodological approach requires an approximation of ^{137}Cs quantity (Bq m^{-2}), termed the 'reference inventory' at a stable location, i.e., where no soil erosion or deposition occurs. Concentrations of ^{137}Cs from field cores collected, (in a grid or transect across a field, hillslope or catchment), are compared to the reference inventory to establish gross erosion (^{137}Cs lower than the reference inventory) or deposition (^{137}Cs higher than reference inventory). Rates of erosion or deposition (t ha^{-1} yr^{-1}) are established, with conversion models tailored to site specific characteristics (Walling *et al.*, 2005). At the scale of analysis, these values are assessed to determine the average net soil erosion rate (erosion minus deposition) from the date of initial ^{137}Cs deposition, i.e., up to 60 years.

Parsons and Foster (2011) challenged many assumptions underlying the ^{137}Cs technique to estimate soil redistribution, which has encouraged consideration of systems components to reduce uncertainties. For example, the spatial variability of ^{137}Cs deposition was assessed by Zhang (2015a) who concluded that individual point cores cannot represent field-scale soil erosion patters. Walling *et al.* (2014) validated a transect approach to field-scale soil erosion assessment. A revised version of this methodology was applied in this study to catchment Arable A to explore the impact of erosion on soil sustainability within the catchment. The aims of this study were to:

- Quantify field-scale soil erosion and re-distribution in a highly productive arable catchment;
- Estimate catchment net soil erosion rates and delivery ratio of the catchment;
- Quantify soil organic carbon and estimate the impact of soil erosion on SOC decline.

7.2 Methodology

7.2.1 Data collection

Mean field slope and maximum downslope field length (MDFL) were derived from a 2 m resolution LiDAR DTM for all fields in the Arable A catchment (n=278). Fields were divided according to slope categories (low: less than 3º, medium: between 3 and 5º, and high: greater than 5º). Within each category, fields were ordered by the deviation from the average maximum downslope length (231 metres), therefore, fields with MDFLs closest to average were prioritised. Thirty fields were selected in total (10 from each category) and aimed to evenly represent grass and arable land uses during 2014 (Figure 7.3).

Soil cores were collected during September 2014 using a percussion drilled soil auger (diameter 60 mm, maximum depth 570 mm). A gridded-transect approach identified sample locations (Figure 7.4); firstly, five hillslope locations (top, upper-mid, mid-slope, lower-mid and bottom) were selected on a downslope transect. At each location, triplicate samples were collected at 3 m intervals perpendicular to the transect direction (total width 6 m) and bulked to reduce the impact of spatial ^{137}Cs variability (Parsons and Foster, 2011; Zhang, 2015a). In total, 450 cores were collected from catchment fields, resulting in 150 bulked samples for analysis. Reference cores were collected

from two locations which were assumed appropriate to represent local background ^{137}Cs variability across the catchment. These locations were selected as soil erosion/sediment deposition was assumed minimal; one a permanent grassland field on high permeability soils, the second a semi-natural grassland site on low permeability soils. Nine cores in total were collected over 1 m^2 at each site and consistently with field cores were composited into three samples (each comprising three cores) for further analysis. Two further cores were collected and sectioned at 50 mm depth intervals to investigate ^{137}Cs depth concentration on a permanent pasture and long-term intensive arable field.

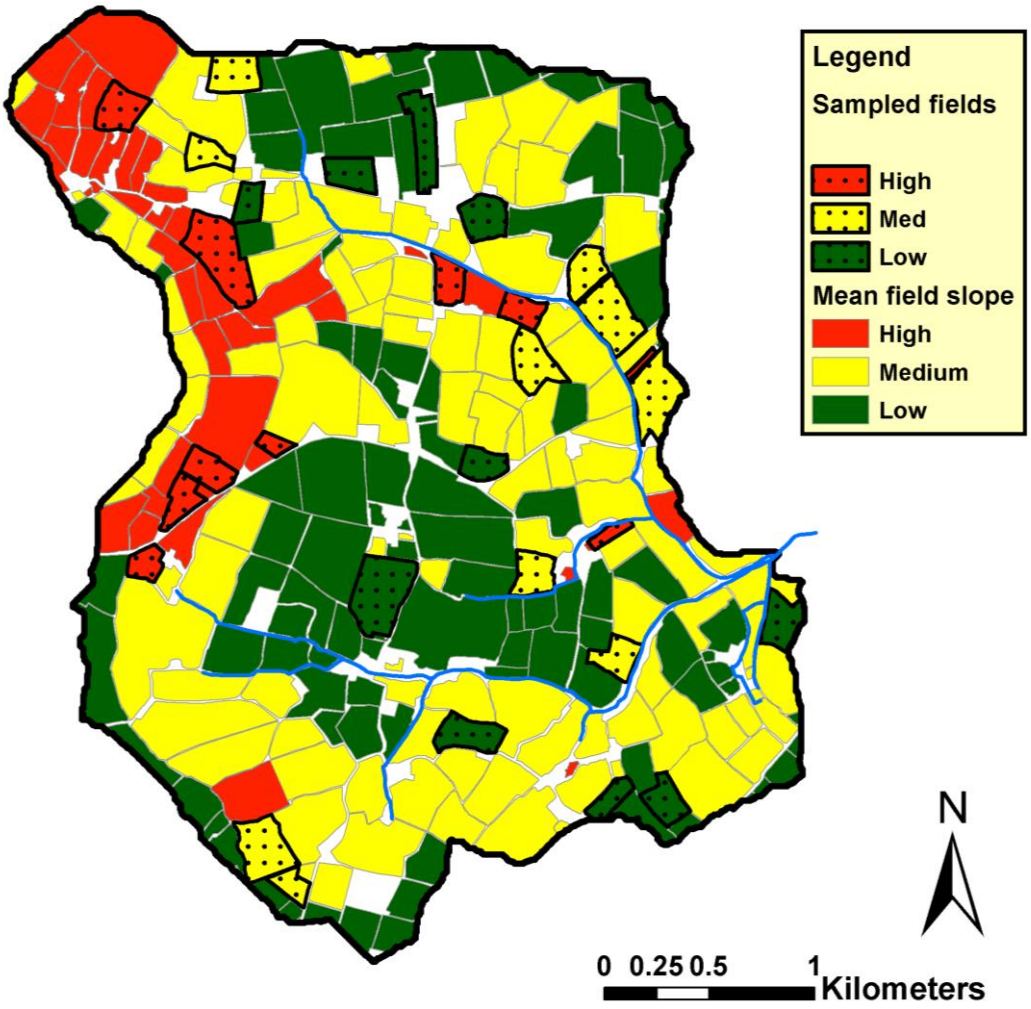

Figure 7.3. Field slope map based on defined categories (low - <3°, medium - 3-5°, high >5°), and sampled fields in Arable A.

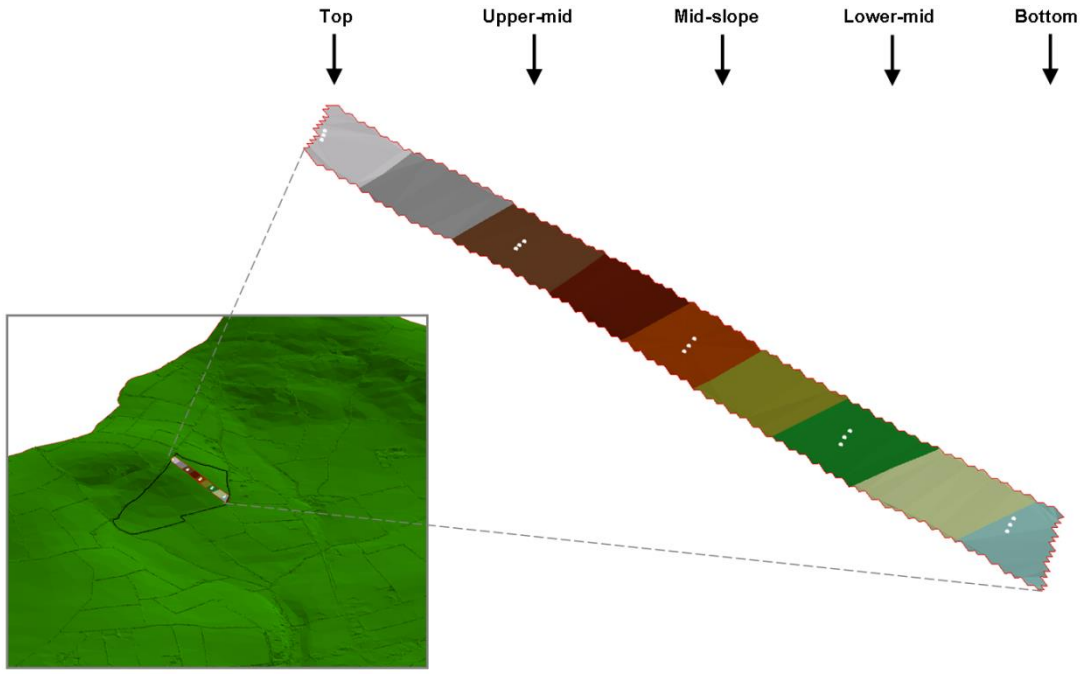

Figure 7.4. Example of field-scale gridded-transect sampling methodology.

7.2.2 Laboratory analysis

Soil cores (field, reference and sectioned) were oven dried at 105°C for minimum 48 hours then mechanically disaggregated and sieved to 2 mm, to remove stones and the <2 mm fraction was retained for further analysis. For ^{137}Cs analysis, field and reference cores were transferred into plastic cylindrical containers. The total mass of reference cores were analysed but due to larger sample mass from bulked field cores, a 900 g sub-sample (assumed representative of the whole sample) was analysed. Caesium-137 was measured from the count activity at 661 keV using GammaVision (version 6.01) software connected to a low background ORTEC HPGe detector gamma spectrometer (ORTEC, Oak Ridge, U.S.). Count times were greater than 30 000 seconds and produced an average error of 15%.

Particle size was measured using a Malvern Mastersizer 2000G with autosampler unit (Fenton *et al.*, 2015). Organic matter was removed using hydrogen peroxide (20 ml at 30%) and chemical dispersant (Calgon solution 0.4%) added pre-analysis. Further physical dispersion (120 seconds at 100% strength) was performed in the Malvern sampling unit before analysis to obtain SSA (mg kg^{-1}). Total carbon and TOC (following acid-digestion of the inorganic carbon using hydrochloric acid 16.5%) were analysed on a LECO Truspec CN analyser (LECO Corporation, Michigan, USA) to obtain the total organic carbon (TOC) fraction (Massey *et al.*, 2013).

7.2.3 Data analysis

Caesium-137 activity concentrations (Bq kg^{-1}) were converted to areal activity concentrations (Bq m^{-2}) using total <2 mm core mass (or bulked core mass) and core surface area (0.0084 m^2 – Porto *et al.*, 2001). Erosion and deposition rates were calculated using existing models used to convert ^{137}Cs concentrations for individual cores into gross soil erosion rates (t ha^{-1} yr^{-1}) and the downslope trend indicates field-scale net erosion (t ha^{-1} yr^{-1}) and the sediment delivery ratio (field-SDR% – Walling and He, 1997) via an excel add-in downloaded from FAO/IAEA (2013). The diffusion and migration (DM) model is commonly used for grassland but rotation between cultivation and grassland was widespread in the catchment, therefore, a model which includes cultivation redistribution of ^{137}Cs is required. Permanent grassland, which did not undergo cultivation, was limited to low-permeability, small fields or those with poor accessibility (which likely discouraged cultivation). Where fields fulfilled these criteria (n=6), the DM model was used. Input parameters were the diffusion coefficient (kg m^{-2} yr^{-1}) and migration rate (kg m^{-2} yr^{-1}) and measured ^{137}Cs samples concentrations and particle size correction. The mass balance model II (MB2) was used for all other fields (n=24) which required the following parameters; proportion factor, relaxation depth, tillage depth, year of tillage commencement in addition to the areal sample concentrations and a particle size correction factor (Figure 7.5). The origin of values is discussed in the following paragraph and results sections.

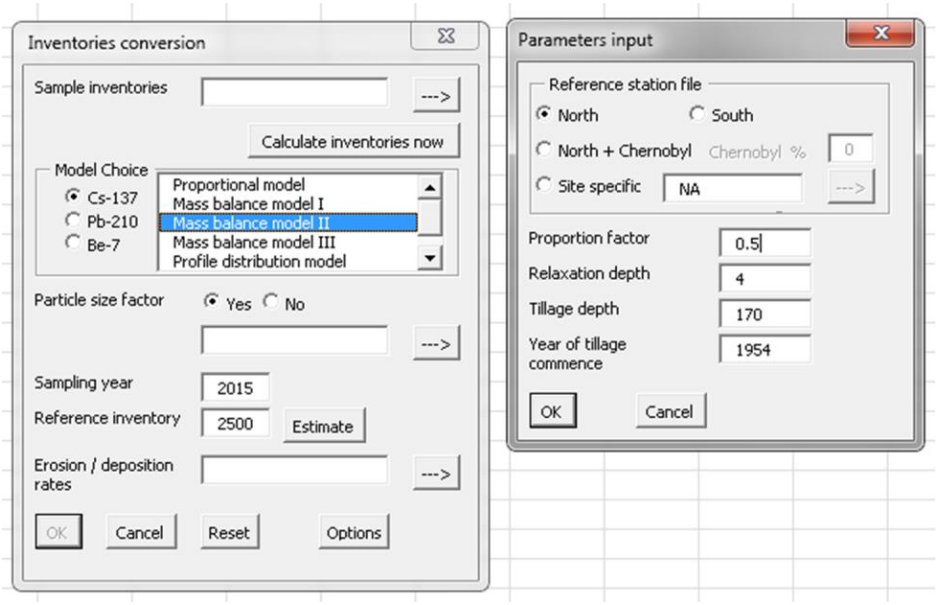

Figure 7.5. Mass Balance 2 model interface detailing input parameters.

The relaxation depth, defined as the mass depth of the initial distribution of fresh fallout (kg m^{-2}) and the tillage depth, the depth to which cultivation causes ^{137}Cs mixing with depth, were estimated using sectioned cores. The proportion factor is estimated based on the likely impact of rainfall and cultivation timing on ^{137}Cs distribution within the soil profile. Monthly 30-year rainfall data (1961-1991) from the Rosslare, Co. Wexford, national synoptic station (52º15'N, 6º21'W) was used to infer the temporal distribution of rainfall conditions. The land use record (Land Parcel Information System – LPIS) from 2000-2013 was used to infer dominant cultivation systems in the study catchment (DAFM, 2013). Particle size correction for erosional (PS) and depositional (PS') sites were calculated using Equation 7.1 and Equation 7.2, respectively.

$$PS = \left(\frac{S_{ms}}{S_{ls}}\right)^{v}$$

Equation 7.1

$$PS' = \left(\frac{S_{ds}}{S_{ls}}\right)^{v}$$

Equation 7.2

Where S_{ms} is the SSA of mobilised sediment ($m^2\ g^{-1}$), S_{ls} is the SSA of the original soil, S_{ds} is the SSA of deposited sediment and v is a constant of 0.65.

7.3 Results

7.3.1 Model parameters

The proportion factor represents the amount of newly deposited ^{137}Cs in a typical year which is available near the soil surface for re-distribution it is determined by the dominant crop type (which indicates timing of cultivation and integration of ^{137}Cs within the plough later) and rainfall characteristics (whereby the majority of sediment and associated ^{137}Cs movement can be assumed to occur where rainfall intensity is highest).

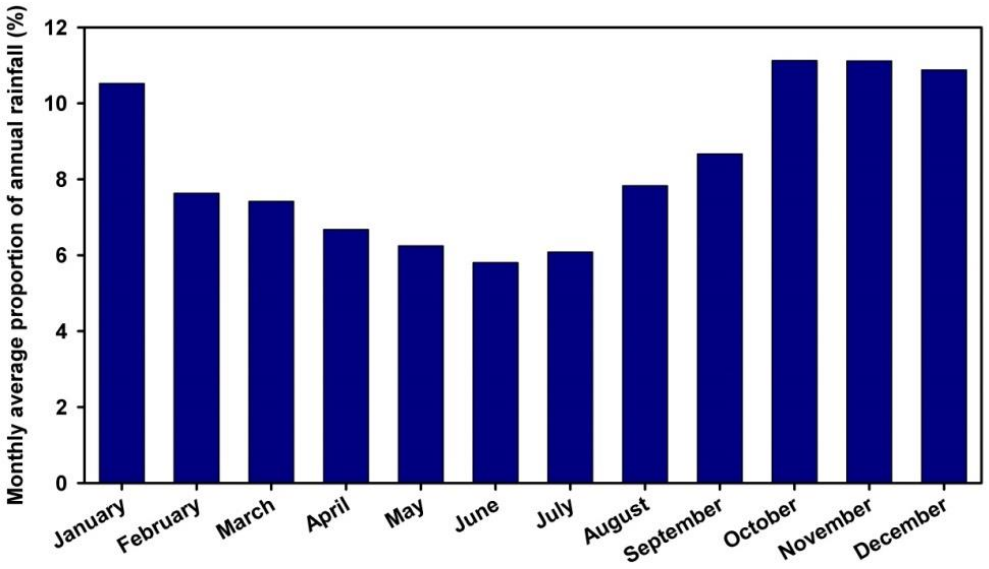

Figure 7.6. Monthly average proportion of annual rainfall at Rosslare national synoptic station (1961-1991).

The majority of rainfall was received from October to January (Figure 7.6) which, on average over 30-years, was responsible for 45% of the annual average rainfall. Grains, predominantly spring barley were most common in this catchment (Figure 7.7). Land use records pre-2000 were unavailable, however, the 2000-2005 land use was assumed representative of the longer-term trend from 1954-2000. From 2005, the cultivated crops do not include sugar beet but other arable crops such as maize, potatoes and oilseed rape become more prominent over time. Cultivation of spring crops, and re-distribution of ^{137}Cs in the soil profile, occurred from late February to late April, i.e.,

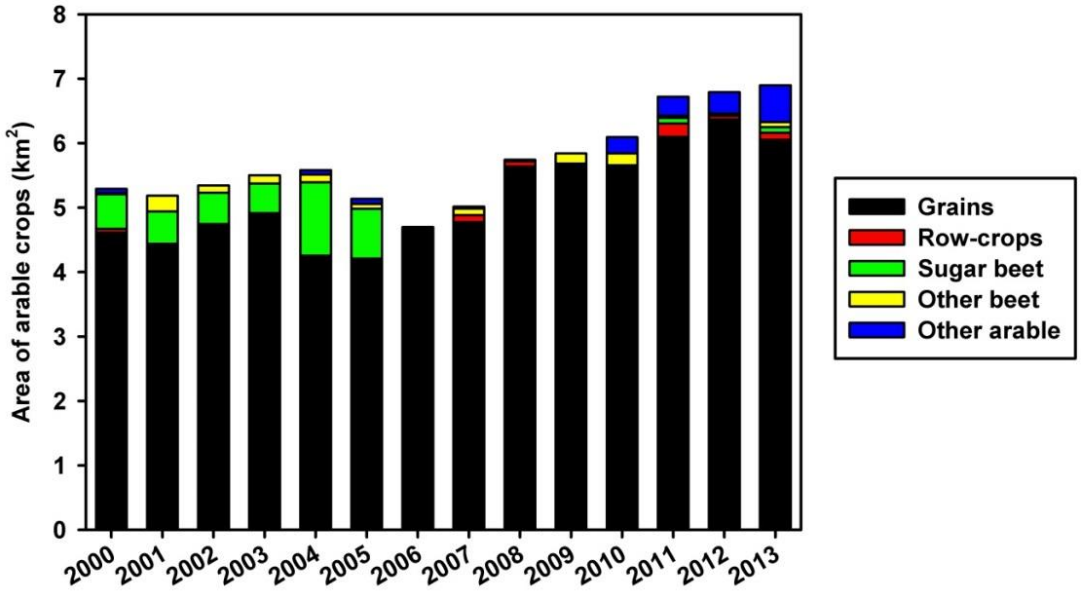

Figure 7.7. Arable crop type from 2000-2013 in the Arable A catchment.

after the main rainfall period. Fresh ^{137}Cs accumulation was, therefore, assumed to remain at or near the soil surface until the main rainfall period as no further cultivations occurred (for the majority of the catchment) until winter. Intercepted ^{137}Cs by plants was assumed to be transferred to the soil by rainfall. Consequently, a proportion factor of 1 was used.

The relaxation depth could not be determined from sectioned cores (Figure 7.8) as neither showed elevated surface values; the default model value of 4 kg m^{-2} was accepted as a plausible. The impact of the relaxation depth on the estimated net field scale soil erosion was relatively small; a 25% increase of the relaxation depth (to 5 kg m^{-2}) resulted in a 7% increase in the field-scale soil erosion rate, and a 25% decrease (to 3 kg m^{-2}) resulted in a 10% decrease in modelled field-scale net soil erosion. Concentrations in the grassland sectioned core were consistently elevated values (4-6 Bq kg^{-1}) from 0-115 kg m^{-2} and depleted values at greater depths. The assertion that grassland fields are likely commonly cultivated is supported here as the mass depth of elevated concentrations is equivalent to the expected tillage depth (approximately 30 cm), therefore, the mass depth 115 kg m^{-2} represented the tillage depth in the model. The arable core was depleted in the top section (up to approximately 90 kg m^{-2}) and elevated concentrations below this (4-6 Bq kg^{-1}). As widespread cultivation of soils was consistent over time, the commencement year equalled the initial fallout year 1954.

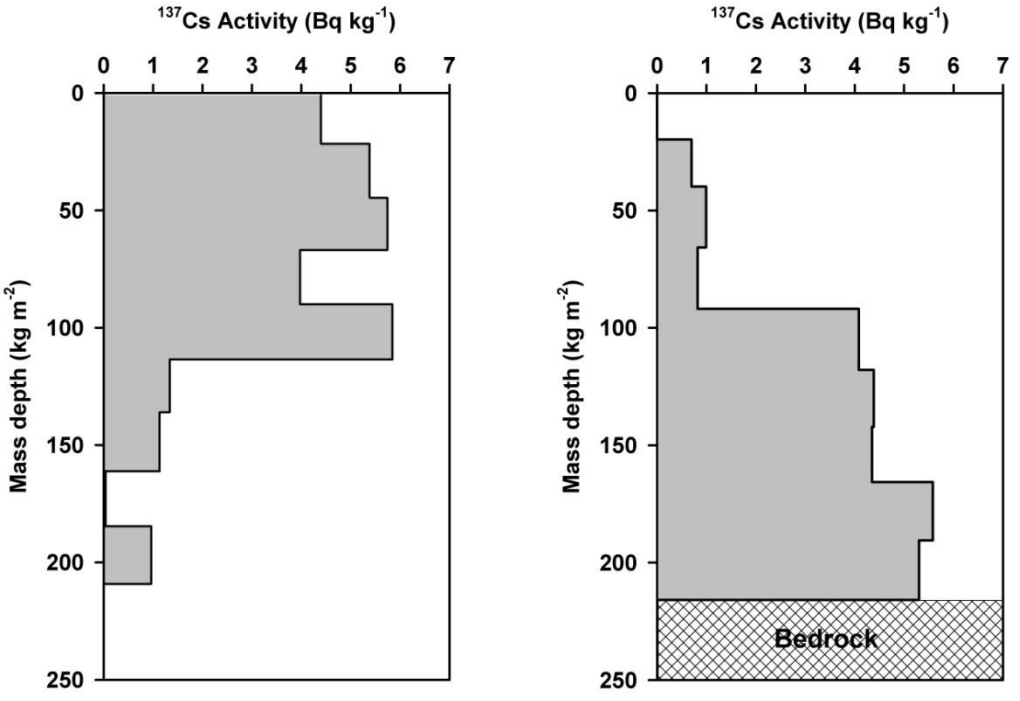

Figure 7.8. Soil cores sectioned with depth in the, a) Grassland and, b) Arable location.

The reference activity ^{137}Cs concentration (1901 Bq m^{-2}) was greater than the majority of field samples (Figure 7.9). At both reference locations, the CV% of the reference inventory of the nine collected cores was 14%. Cores from arable fields had significantly higher ^{137}Cs activity concentrations than grassland fields ($p<0.05$, independent t-test, SPSS v18) but no significant difference occurred between high, medium and low slope groups ($p>0.05$, ANOVA, SPSS v18). Mean ^{137}Cs concentrations for slope-land use categories, as displayed in Figure 7.9, were significantly different only between arable medium slope and grassland medium slope ($p<0.05$, F=2.74, ANOVA).

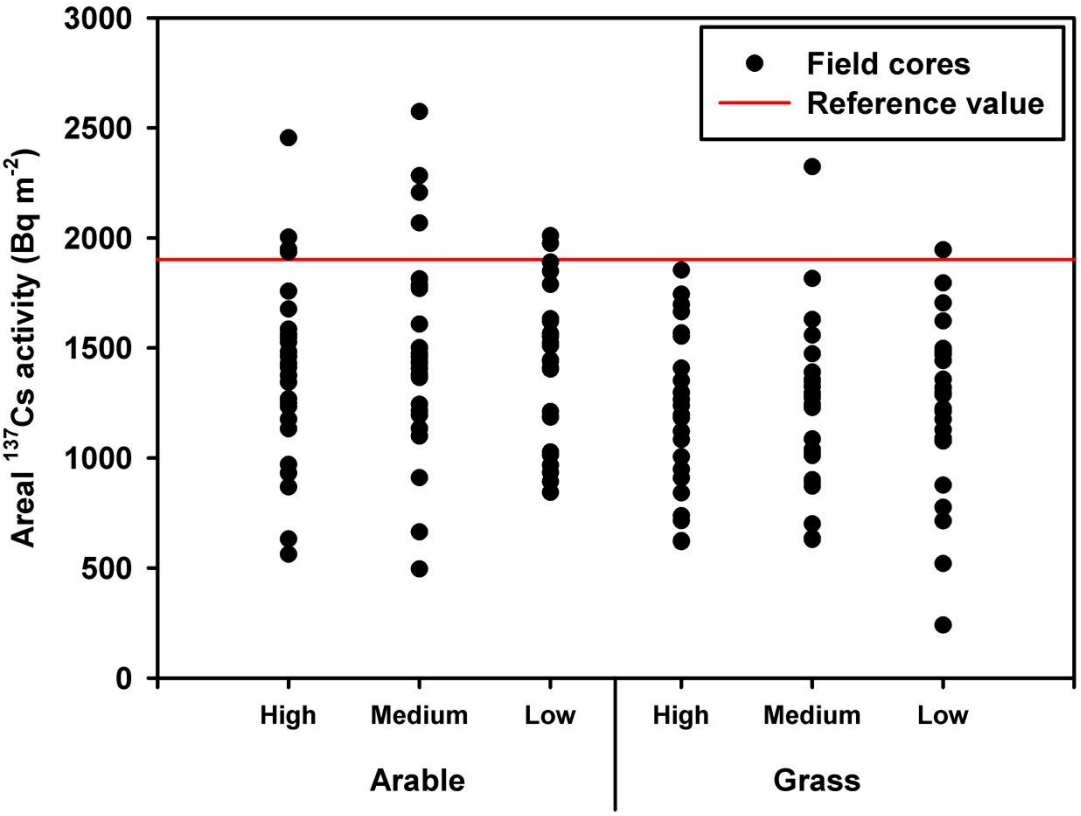

Figure 7.9. Activity concentrations of field and reference cores according to land use by slope groupings.

7.3.2 Soil erosion

Modelled soil erosion/deposition showed individual core points were mostly erosional (93%) with maximum erosion of 34.6 t ha^{-1} yr^{-1} at the upper slope position in a grassland field and maximum deposition of 5.6 t ha^{-1} yr^{-1} in an arable field at lower-mid slope position (Figure 7.10). No consistent downslope trends were evident within fields (Figure 7.9) but the relationship with the slope at each core location shows a highly scattered (R^2=0.19, p=0.280) but positive trend (erosion or deposition rate: y = 0.333*slope + 2.954) at slopes greater than 4 degrees (Figure 7.11). In comparison,

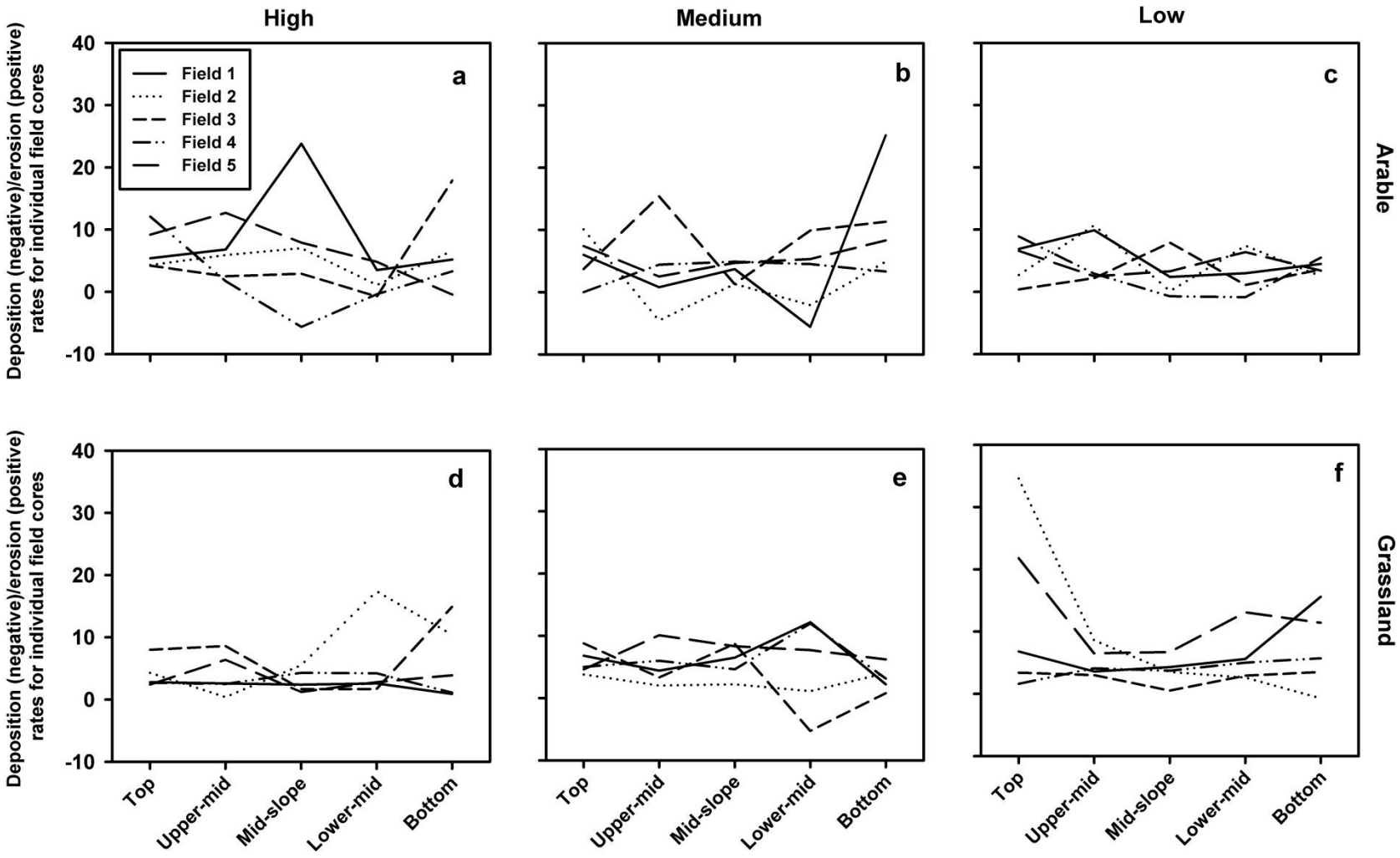

Figure 7.10. Downslope gross erosion/deposition trends in fields separated by land use by slope group; a) arable-high, b) arable-medium, c) arable-low, d) grassland-high, e) grassland-medium, f) grassland-low.

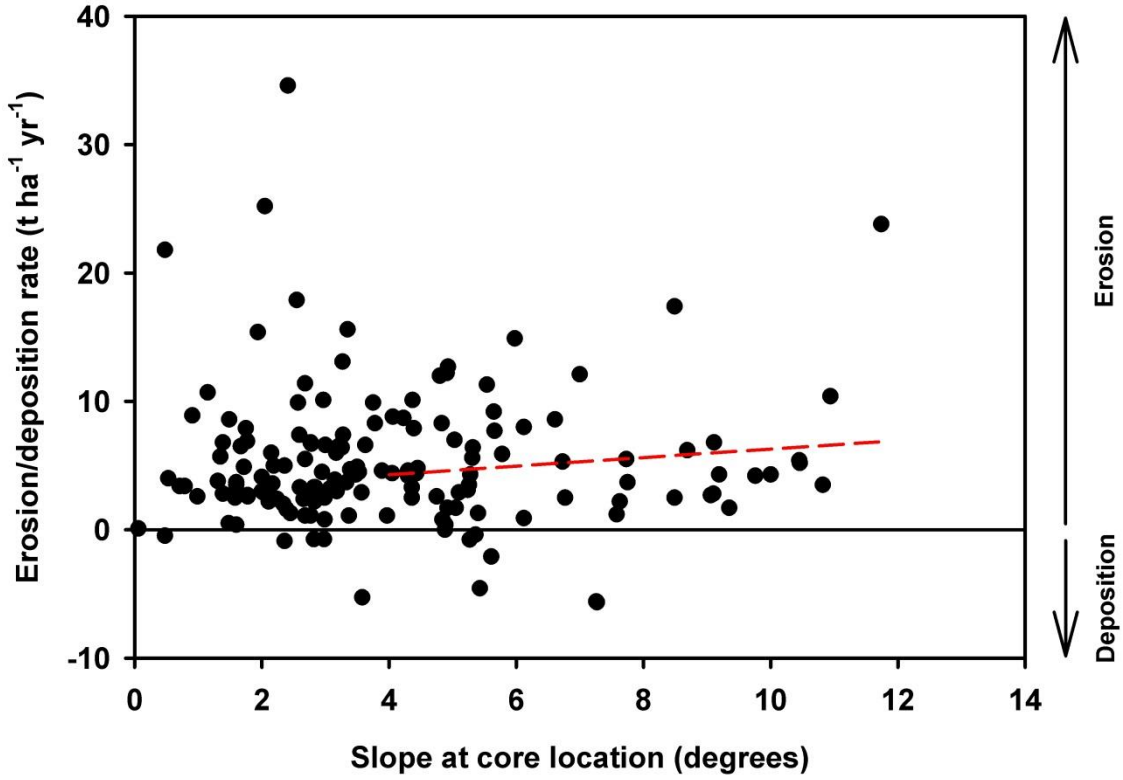

Figure 7.11. Slope and estimated erosion or deposition rate using ^{137}Cs method of bulked cores.

analysis of the complete dataset showed little direction in the regression trend (erosion or deposition rate: y = 0.032*slope + 5.144) and low correlation (R^2=0, p=0.856).

Mean gross erosion rates were 6.9 t ha^{-1} yr^{-1} and high field-scale sediment delivery ratios (average 96%, range 59-100%) resulted in a mean net field erosion rate of 5.4 t ha^{-1} yr^{-1} (minimum 1.9, maximum 11.9). Large within-group variability resulted in negligible differences between the field slope, land use and land use by slope categories. Two fields reported elevated net field erosion due to extremely high erosion rates (21.8 and 34.6 t ha^{-1} yr^{-1}) from cores at 'top-slope' transect locations (Figure 7.10). Net erosion rates from permanent pasture fields were significantly lower ($p<0.05$) than cultivated fields with averages of 3.4 t ha^{-1} yr^{-1} and 5.8 t ha^{-1} yr^{-1}, respectively. All other groups (slope, land use or slope land use were statistically not significantly different). Fields currently under grassland had significantly higher ($p<0.05$) soil erosion than permanent pasture but no differences were significant between arable and cultivated ($p>0.05$). The average net soil erosion rate of rotated and permanent grassland fields (from 2000-2014) were multiplied by the total cultivated and permanent grassland area,

respectively (cultivated – 874 ha, permanent grassland – 106 ha) estimated a medium-term soil erosion rate of 5430 t yr^{-1} or 554 t km^{-2} yr^{-1} for the whole catchment.

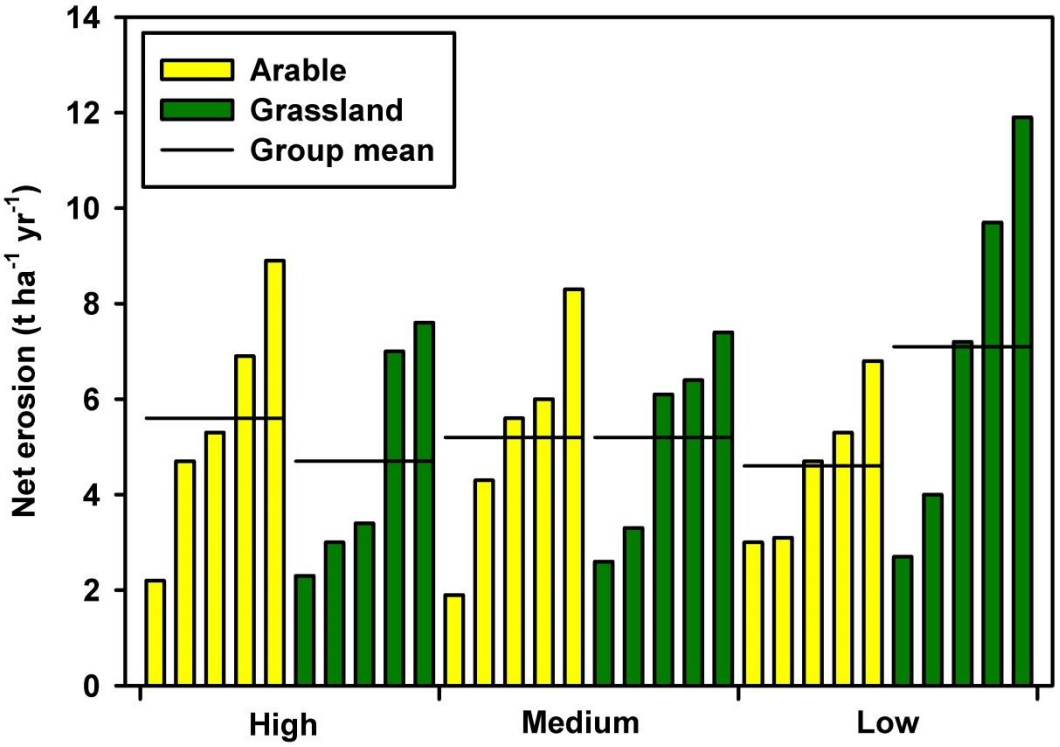

Figure 7.12**.** Net field-scale erosion in each land-use slope type category.

7.3.3 Soil organic carbon

Total organic carbon content was greater in surface soil samples relative to core samples and greater in grassland soils compared to arable ($p<0.05$ – Table 7.1). Grassland low-slope fields were depleted in soil organic carbon in both surface and core samples relative to grassland-medium slope and grassland-high slope fields. Fields currently under grassland had significantly higher TOC than those under long-term grassland (permanent pasture). However, current arable fields had significantly lower TOCs than all fields under cultivation over the last 60 years. Carbon content of fields was estimated using the core concentrations to a standard depth of 30 cm and bulk density of 1.5 g cm^{-3}. Similarly to soil erosion data, little variability occurred between land use by slope categories. Using cultivated and permanent pasture values, catchment TOC storage at 30 cm depth was estimated at 74 x 10^3 tonnes equivalent to 7.5 kg m^{-2}. The concentrations of ^{137}Cs per unit weight and TOC content were significantly correlated (Figure 7.13). The loss of TOC attributed to soil erosion was estimated at 95 – 189 t yr^{-1}

(range using core (lower) and surface (higher) concentrations on mean net soil erosion on area weighted cultivated and permanent grassland categories).

Table 7.1. Summary of total organic carbon content of surface (0-5 cm) and core samples (approximately 50 cm).

	Surface TOC (%)	Core TOC (%)	Organic carbon content to 30 cm depth (t ha^{-1})
Arable	2.8	1.6	72
Arable high	2.5	1.6	72
Arable medium	2.5	1.4	63
Arable low	3.5	1.6	72
Grassland	5.5	1.9	86
Grassland high	5.8	1.9	86
Grassland medium	6.8	2.1	95
Grassland low	2.5	1.7	77
Cultivated	3.2	1.7	74
Permanent pasture	6.5	2.0	88

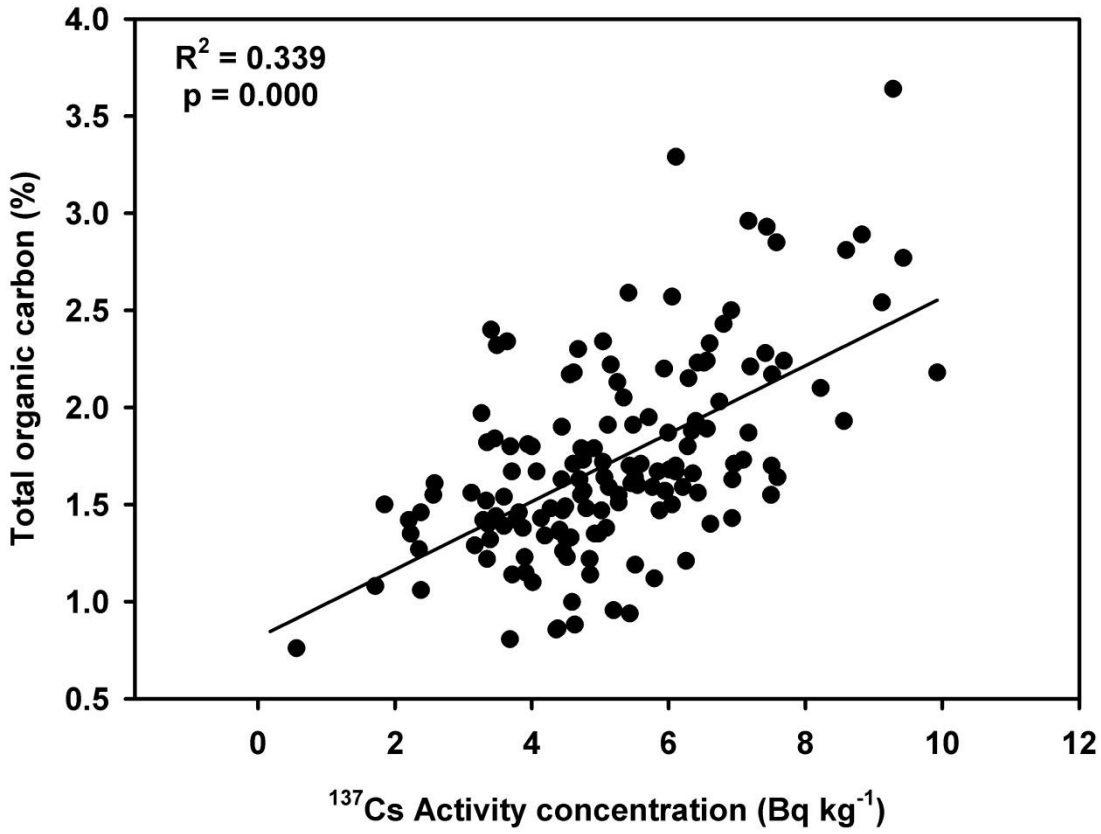

Figure 7.13. ^{137}Cs activity and total organic carbon content in all bulked field samples.

7.4 Discussion

Bulked field cores were predominately depleted in ^{137}Cs relative to the reference concentration indicating widespread gross erosion, net erosion and low in-field sediment retention across the landscape. Estimated total erosion (inclusive of water, wind, and agricultural erosion) from tilled agriculture across Europe was 4.5 – 38.8 t ha^{-1} yr^{-1} (Verheijen *et al.*, 2009). The Arable A average and maximum field scale net erosion (5.8 and 11.9 t ha^{-1} yr^{-1}) were comparably low yet exceeded tolerable soil erosion rates of 0.3 – 1.4 t ha^{-1} yr^{-1} (Verheijen *et al.*, 2009). Reduced soil erosion in Arable A is unsurprising, as large proportions of high permeability catchment soils and underlying fractured bedrock support sub-surface hydrological pathways (Mellander *et al.*, 2015). Such pathways primarily erode sub-surface soils generally depleted in ^{137}Cs, e.g., sub-surface drains and macropores. High ^{137}Cs concentrations in sub-surface drain flow have been reported and occur on low permeability cracked soils which divert ^{137}Cs rich sediments to the sub-surface system (Chapman *et al.*, 2005). However, this process is unlikely to be replicated on high permeability soils where artificial drains and soil cracking are absent. Catchment scale sediment and phosphorus delivery investigations have also indicated reduced sensitivity of highly permeable soils to surface losses from water and sediment fingerprinting results have confirmed the infrequent surface hydrological connectivity of hillslope soils (Mellander *et al.*, 2012; 2014; 2015; Sherriff *et al.*, 2015b; Chapter 6).

Soil erosion rates were, however, much greater than those predicted for water erosion in Ireland: 0.5 t ha^{-1} yr^{-1} estimated by extrapolating plot data (Cerdan *et al.*, 2010) and 0.96 t ha^{-1} yr^{-1} modelled using a revised universal soil loss equation (Panagos *et al.*, 2015) which incorporate soil permeability and land use factors. Also, Arable A net soil erosion exceeded predicted average water erosion on arable land, estimated at 4.4 and 1.32 t ha^{-1} yr^{-1}, respectively by Cerdan *et al.* (2010) and Panagos *et al.* (2015). This suggests either erosion of highly permeable soils was sufficient to export significant quantities of sediment from the field or additional processes are responsible for erosion. Dalgleish and Foster (1996) reported ^{137}Cs applied to soil in a laboratory-based plot experiment adsorbed disproportionately to eroded sediments relative to the original soil volume. Furthermore a proportion of ^{137}Cs was measured in runoff indicating the assumption that irreversible binding to the soil profile may be flawed (Parsons and Foster, 2011) but

likely of greater importance where soils more commonly obtain saturated conditions. Due to the preferential absorption of ^{137}Cs to finer particles, the conversion models used in this study require a particle size correction to obtain estimated sediment redistribution rates. Porto *et al.*, (2003) however concluded that simple correction factors, although useful for preliminary assessments, should be further improved and may be a source of uncertainty in soil redistribution estimates.

Saturation of high permeability soils (whether connected to a watercourse or not) and overland flow can arise from local erosion and redistribution driven by micro-topography, e.g., local deposition in hollows, saturation of variable source areas by antecedent wetness, and infiltration-excess following long duration and high intensity rainfall events particularly on compacted areas (Quinn and Bevan, 1993; Doody *et al.*, 2010; Boardman and Favis-Mortlock, 2014). Low permeability soils in the riparian corridor are more frequently saturated by groundwater and, therefore, have greater hydrological connectivity but the dominance of grass enterprises on low-permeability soils reduces the continuity of overland flow pathways due interception by vegetation, therefore, the sediment connectivity (Cerdan *et al.*, 2004). It is therefore unlikely that water erosion was responsible for the entire measured soil erosion rate.

Downslope ^{137}Cs distributions have previously verified lateral transfer by overland flow (Zhang *et al.*, 2015b). The depletion of soil and associated ^{137}Cs at upper slope positions and enrichment associated with deposition at lower slope positions are also the foundation for positive relationships between soil erosion rate and slope (Verheijen *et al.*, 2009). On arable soils, overland flow pathways were observed to redistribute eroded soil downslope following extreme rainfall events which coincided with low ground cover soil. Significant erosion by overland flow is therefore conditioned by hydrology; sufficient antecedent wetness, rainfall duration, coinciding with unfavourable soil cover conditions which exhibit high inter-annual variability (Boardman and Favis-Mortlock, 2014). However, no such trends in downslope ^{137}Cs enrichment and depletion, or influence of mean field slope category on net soil erosion were apparent in this study.

A tentative relationship between soil erosion/sediment deposition rates and slope at the immediate hillslope section of core collection suggests micro-topography may influence soil erosion, but this is regarded as in-field redistribution rather than erosion process (Fredericks *et al.*, 1988; van Oost *et al.*, 2005; Zhang et al., 2015c). The spatial

resolution of the ^{137}Cs survey was, however, too coarse to further explore these controls on soil erosion and sediment deposition and this is largely considered as redistribution at the field scale rather than erosion (Heckrath *et al.*, 2005). The inconsistency of surface hydrological pathways over space and time on high permeability soils likely resulted in any downslope trends being eradicated by supplementary erosion and redistribution processes (Govers *et al.*, 1996).

At the sub-field scale, Govers *et al*. (1993) attributed 57% of soil erosion to water and 43% to tillage erosion. Tillage erosion, approximated at 3 t ha^{-1} yr^{-1}, can redistribute large quantities of soil and associated ^{137}Cs and alter micro-topographic features by transferring soil from concave to convex slope sections (Govers *et al.*, 1996; van Oost *et al.*, 2006). A ^{137}Cs depth profile consistent with cultivation – ^{137}Cs uniformly mixed to plough depth (DiStefano *et al.*, 1999) on a contemporary grassland field indicated widespread rotation and cultivation of soils and, therefore, the likely impact of tillage erosion. This led to a reclassification of fields to 'cultivated' and 'permanent pasture' categories which revealed elevated net soil erosion from cultivated fields. On the field scale, tillage erosion does not account for net soil removal, i.e., soil is redistributed and not removed, therefore, likely contributed to downslope ^{137}Cs variability but not net soil erosion.

Contemporary arable catchment land use is dominated by spring barley and negligible amounts of other crop types (Melland *et al.*, 2012a). In recent history, crop rotation supported sugar beet cultivation which pre-dated initial ^{137}Cs deposition (1954) until factories were closed and the industry collapsed in 2005. The harvesting of root crops such as sugar beet, potatoes and carrots account for soil erosion rates of between 3.8-11.8 t ha harvest^{-1} through soil attachment to roots (Posen *et al.*, 2001; Ruysschaert *et al.*, 2004; 2007; Tuğrul *et al.*, 2012). Loam soil texture likely decreased harvest soil removal in Arable A relative to clay-dominated soil textures (Ruysschaert *et al.*, 2004) and soils could only support sugar beet on a minimum one in three year rotation due to nematodes (Hbirkou *et al.*, 2011). This rotation likely reduced the frequency and spatial extent of increased soil erosion risk. Late autumn/early winter drilling of sugar beet crops additionally increase the likely efficiency of water erosion during the main annual rainfall period (October to January) compared to spring cereals which are drilled once during, on average, drier months. Dearing *et al.* (1987) reconstructed SSYs from lake

cores in a small (141 ha) catchment in Sweden with similar proportions (62%) of cereal and sugar beet agriculture. Estimated SSY of 2.5 t ha^{-1} yr^{-1} (250 t km^{-2} yr^{-1}) from 1950-1979 indicates severe erosion which were likely influenced by snow-melt hydrology. Accelerated soil erosion rates and high field-SDRs likely resulted from historical land use, i.e., sugar beet harvest erosion and enhanced water erosion between 1954 and 2005 (85% of time period) and are supported by anecdotal evidence from catchment landowners.

These findings are further supported by present sediment flux data. Should net soil erosion rates, as estimated by ^{137}Cs, be indicative of present catchment dynamics, average sediment export (2009-2013 – 12 t km^{-2} yr^{-1}) would account for 2% of soil erosion. Porto *et al.* (2001) validated high field-SDRs with good agreement between net erosion rates and suspended sediment export values in a 1.38 ha low permeability catchment in Italy, however, this comparison cannot be made in this study. Lower catchment-SDRs may be expected in larger catchments due to greater sediment deposition on floodplains and storage in channels (Walling, 1983; Walling and Collins, 2008). Storage of sediments in channels may also encourage conveyance losses of sediments. Quantification of fine sediment (<125 μm) storage in this catchment, however, indicated low availability of readily mobilised sediments in the stream channel and accounted for only 2% of net field losses at the present day. Shore *et al.* (2015) also reported 58% of ditch channels in this catchment were net transfer zones of sediment, attenuation occurred in only 13% of ditch channels. Significant sediment deposition in the riparian zone was not observed and floodplain inundation was extremely rare and limited to lower catchment reaches. The discrepancies between medium-term soil erosion rates and contemporary sediment flux may support the conclusion that alternative off-take mechanisms such as harvest removal as discussed above were previously an important component of soil erosion and led to a significant shift in the catchment sediment budget.

Soil carbon content was elevated in surface soils compared to the total cores in both arable and grassland fields due to increased biological activity (Takanaka *et al.*, 1998). Surface soils were also higher than the TOC threshold required for unimpeded soil functions (2%) in Ireland (Spink *et al.*, 2010). Storage of TOC in arable and grassland soils (74 and 88 t ha^{-1}) was within the range of estimated values for countries in the

United Kingdom (Bradley *et al.*, 2005). Positive correlations between ^{137}Cs and TOC content of soil samples are indicative of similar soil erosion controls (Ritchie and McCarty, 2003). As TOC is replenished more readily than soil erosion, micro-topography and localised flow pathways are likely the dominant controls. Organic carbon losses attributed to soil erosion were likely greater when soils supported sugar beet due to harvest losses and increased efficiency of water erosion.

Current sediment yield and channel bed storage estimates suggest a major change in soil loss rates occurred to justify high soil loss rates from fields averaged over 60 years. The end of sugar beet cultivation likely resulted in a reduction in soil erosion and TOC loss, as soil erosion by crop harvesting was limited to more infrequently cultivated potato and swede root crops and the 'window of opportunity' for erosion no longer coincided with the mean annual rainfall period. Contemporary arable practices in this catchment (spring cereal production) are likely less damaging to soil resources, in turn improving the sustainability of soil resources. However, prevention of soil erosion is still a valid management concern for sustainable intensification as low soil production rates cannot compensate for current soil erosion rates or support the recovery of long-term soil erosion due to farming practices.

Encouraging crop diversification in homogenous arable landscapes through EU 'Greening' measures in CAP may increase winter crop cultivation (e.g., maize, potatoes) and associated soil erosion risk. Significant ecosystem benefits are likely to result from crop diversification including crop productivity and decreased requirement for nutrients and pesticides (Tilman and Downing, 1994; Gurr *et al.*, 2003; Smith *et al.*, 2006), however, positive impacts may occur at the expense of accelerated soil losses and potentially elevated pollutant transport to aquatic ecosystems. Climate change projections include increases in winter rainfall amount and intensity which will enhance the frequency, magnitude and extent of soils saturation, surface runoff and associated soil erosion (Nearing *et al.*, 2004; Steele-Dunne *et al.*, 2008; Mullan, 2013). Alleviation of the impacts of future climate and possible introduction winter-cultivated crops soil erosion risk may include re-configuration based on knowledge of hydrological flow pathways and variable source areas whereby high-risk crops are situated on hydrologically less-risky soils and vice versa.

7.5 Conclusion

Gross erosion, deposition and field-scale net erosion rates of cultivated and permanent pasture field were quantified using ^{137}Cs in a long-term arable catchment in Ireland to estimate catchment soil erosion. Controls upon soil erosion were considered and the impact of past land use on medium-term (60 years) average soil loss rates. The quantity of organic soil carbon was quantified and likely impacts of organic carbon losses due to soil erosion were assessed. Main findings were:

- Gross soil erosion was high and sediment deposition was low resulting in high field-scale sediment delivery ratios;
- In-field redistribution likely resulted from local flow processes driven by micro-topography;
- Net soil erosion from cultivated soils (on predominantly high permeability soils) was greater than from permanent pasture (on predominantly low permeability soils), despite reduced likelihood of the former to initiative overland flow except during extreme rainfall events;
- The past influence of sugar beet with high soil losses attributed primarily to soil removal by crop harvesting, but also water erosion due to coinciding low groundcover following drilling and increased rainfall amounts and intensities during winter months was believed responsible for historically high erosion;
- Current spring cropping land uses likely reduce soil erosion risk and sediment delivery risk and increase the sustainability of soils relative to winter-crops;
- Soil organic carbon in surface soils exceeded the 2% required to support soil functions and correlation with ^{137}Cs concentration suggested similar mechanisms (removal of topsoils by harvest and water erosion following extreme rainfall events) may control its depletion.

These findings highlight the potential for significant increases in soil erosion and sediment delivery to watercourses due to land use changes. Furthermore, it encourages optimisation of agricultural enterprises based on soil permeability to spatially off-set high-risk arable crops to least impacted areas. Reduction of topsoil erosion, by whichever process will retain nutrient and organic matter rich soil in-field, therefore, reducing the requirements for additional soil fertility management.

7.6 Summary

Assessment of soil erosion is essential in intensive agricultural ecosystems to consider the pathways of soil from hillslope to catchment outlet. This study used a novel field-scale ^{137}Cs sampling strategy to quantify soil erosion rates inclusive of all processes (water, tillage and crop harvest erosion). This is the first approximation of field-scale soil erosion rates from agriculture in Ireland and raises important issues associated with changing land use and climate patterns relevant to current European agri-environment schemes.

Chapter 8. Conclusions, further work and implications

8.1 Introduction

The knowledge gaps highlighted in Chapter 1 were investigated in experimental chapters by installing a sediment monitoring platform alongside existing water quality monitoring networks in multiple agricultural catchments in Ireland representing a range of catchment characteristics and land use pressures (Chapter 3, Chapter 4, Chapter 5 and Chapter 6). A summary of the research approach and five study catchment descriptions is included in Chapter 2. Chapter 3 quantified suspended sediment export in five intensive agricultural catchments with contrasting land uses and landscape permeability (according to underlying geology and soil drainage class) to assess the extent of fine sediment delivery. Catchments with the greatest soil loss and sediment delivery risk (three of the five assessed in Chapter 3) were selected for further investigation. In Chapter 4, controls upon storm-event scale sediment delivery were evaluated using a suspended sediment-discharge hysteresis metric and multivariate analysis of potential rainfall stream hydrology, and antecedent rainfall and soil moisture controls. In Chapter 5, the accuracy and uncertainty of sediment fingerprinting un-mixing models is assessed with respect to soil and sediment tracer selection, tracer non-conservativeness and multiple solutions based on synthetic datasets and trialled using field data from one catchment. Sources of suspended sediments were determined in Chapter 6 using sediment fingerprinting of time-integrated catchment samples in the same three catchments. The magnitude and extent of medium-term (60-year) field-scale soil erosion and re-distribution was quantified in the long-term cultivated catchment to evaluate soil sustainability and estimate the hillslope sediment delivery ratio.

8.2 Synopsis of research findings

Quantification of sediment fluxes from five intensive agricultural catchments in Chapter 2 demonstrated that suspended sediment export from Irish catchments were low compared to published values for the UK and mainland Europe. This was attributed to the greater arrangement of micro-topographic landscape features such as hedgerows and open drainage ditches which reduce field sizes and control the hydrological pathways on the surface resulting in diversion or connection. Comparison of sediment export between the catchments showed the impact of landscape permeability and land use.

Catchments with low permeability exported larger suspended sediment yields and concentrations and more frequently transported higher concentrations than those with high permeability. Where arable land use occurred on low permeability soils, such as in Arable B, the highest sediment export was recorded. Despite high proportions of arable land in Arable A, the combination of high permeability soil and fractured bedrock reduced sediment loss risk. High inter-annual variability resulted from rainfall fluctuations. Ex-situ turbidity based suspended sediment measurement, relative to in-situ turbidity monitoring and direct depth-integrated cross-sectional measurements were also validated in Chapter 3. Turbidity datasets were of similar quality and completeness, but sources of error contrasted (in-situ – spurious data, ex-situ – pump blockages) yet resulted in negligible differences in estimated sediment loads. The results indicated that catchment soil erosion risk can be classified according to soil drainage characteristics and land use type.

In Chapter 4, analysis of sediment response following rainfall-runoff events over time revealed the impact of sediment source location and availability, and delivery mechanism fluctuations on sediment export efficiency over time in the three highest yielding catchments (Grassland B, Arable A and Arable B). A novel application of the hysteresis index to all events over two hydrological years, combined with multivariate analysis of delineated rainfall, stream hydrology and antecedent moisture controls, successfully showed the seasonality of hydrological pathways and interaction with fluctuating land cover patterns in the arable catchments. Catchments with reduced drainage (moderate- or low-permeability soils in Arable B and Grassland B, respectively) and, therefore, good connectivity surface hydrological connectivity had contrasting hysteresis responses due to the location of available sources (hillslope versus channel bank). In Grassland B, channel erosion was likely accelerated by high velocity flow resulting from extensive artificial drainage (surface ditches and sub-surface drains). Arable A exported less sediment as high permeability and underlying fractured bedrock promoted sub-surface pathways which reduced surface hydrological connectivity. However, when surface connectivity was established, the largest event sediment load of all catchments occurred. Event sediment export was elevated in arable catchments when low groundcover was coupled with high connectivity, whereas in the Grassland B catchment, export was attributed to wetter weather only. The results indicated the variability of sediment source availability, hydrological transport

pathways, and subsequent sediment exports are variable in time. Effective catchment sediment management strategies must consider both the frequency and magnitude of all catchment sediment pathways.

In Chapter 5, analysis of sediment fingerprinting un-mixing results using the FR2000 uncertainty-inclusive un-mixing model with synthetic datasets showed tracer non-conservativeness in target samples negatively impacted median result predictions rather than uncertainty as previously assumed. Incremental corruption (the artificial equivalent of non-conservativeness), showed a wide range of source prediction results may be accepted due to the inability of current methodologies to detect tracer non-conservatism. The additional FR2000 permutation algorithm was capable of reducing the range of source predictions to improve the robustness of un-mixing results. The permutation algorithm also successfully solved multiple solutions within a tracer dataset. Application of synthetic testing methodologies to field data from Grassland B showed high uncertainties from source data reduced the ability of the algorithm to detect tracer non-conservativeness, therefore, it was not utilised in Chapter 6.

The provenance of suspended sediments collected at Grassland B, Arable A and Arable B catchments were evaluated in Chapter 6. Contributions from field topsoils, channel banks/sub-surface soils and roads were estimated and revealed contrasting dynamics in the three catchments. Low-permeability in Grassland B and Arable B catchments, with more consistent hydrological pathways resulted in less fluctuation between sources. The temporal and spatial sensitivity of surface hydrological connectivity and overland flow pathways in Arable A showed contrasting sources between periods where low- (channel/sub-surface) and high- (field topsoils) surface connectivity was likely. Overall, dominant sources in Grassland B, Arable A and Arable B were channel banks, channel banks/sub-surface soils and field topsoils respectively. Contributions from road sources, including farm tracks, were low in all catchments.

Field-scale assessment of medium-term soil erosion and deposition using ^{137}Cs in Arable A, a long-term predominantly arable catchment, showed net soil erosion was high and exceeded tolerable soil erosion rates. Net erosion, represented as an average over 60 years, was greater from cultivated soils than those under permanent pasture. Erosion from cultivated land was primarily attributed to soil loss from harvesting of root crops, namely sugar beet up to 2005. The presence of winter-crops in the catchment,

although spatially limited due to rotation to prevent nematode damage, also likely increased the efficacy of water erosion. Drilling of the sugar beet crop and the subsequent period of low groundcover until crop establishment coincided with the highest rainfall months (October to January) and likely increased sediment delivery to watercourses and catchment sediment export. The dominance of spring cropping in the current catchment likely reduced soil erosion risk by off-setting increased climate risk and low groundcover periods.

8.3 Implications

Simultaneous achievement of agricultural production and water quality targets (such as Food Wise 2025 and WFD in Ireland) requires effective management of sediment loss risk. However, to date, relatively few studies have sought to quantify and explore the sources and dynamics of sediment at the catchment scale worldwide, likely due to an absence of relevant legislation in this area and the resource intensiveness of gaining high quality numerical evidence to support further policy measures. The increasing body of scientific evidence detailing negative impacts on aquatic ecosystems of accelerated sediment losses, and the crucial role of sediment in phosphorus transfer from soils to watercourses, demonstrates the significance of effective catchment sediment management (Jones *et al.*, 2011b; Kemp *et al.*, 2011; Larsen *et al.*, 2011). The research completed in this thesis defined the dynamic behaviour of sediment loss, transport and delivery in agricultural catchments and which are compelling for sediment management worldwide.

Increased sediment exports from agricultural catchments are commonly attributed to soil erosion from arable land (Walling *et al.*, 1999; Wass and Leeks, 1999; Freebairn *et al.*, 2009; Van Oost *et al.*, 2009; Duvert *et al.*, 2010). However, soil drainage class, which regulated dominant hydrological flow pathways, was the primary control in this study (Chapter 3). Disregarding the influence of dominant hydrological flow pathways on soil loss may, therefore, result in ineffective management. Firstly, the *overestimation* of soil loss risk in high permeability arable catchments (with sub-surface pathways) may result in unsuccessful mitigation of water quality risk from agriculture. Agri-environment payments may not be cost-effective where blanket measures are implemented; for example, arable buffer margins are likely bypassed by sub-surface hydrological pathways (but create wider ecosystem benefits, e.g., biodiversity (Borin *et*

al., 2010)). Field-scale soil erosion estimates showed soil removal due to crop harvesting was likely greater than water erosion losses (Chapter 7) which has implications for soil sustainability and regions where root crops dominate agricultural production.

Underestimation of soil losses from intensively managed grassland on low permeability soils may occur. Land drainage is essential Ireland and other poorly-drained regions with high agricultural production demands to increase water table depth and decrease the extent and duration of saturated soils (O'Sullivan *et al.*, 2015), but can displace soil loss risk from hillslopes to channels (Chapter 6; Mekonnen *et al.*, 2015). Current watercourse (artificial and 'natural') management in agricultural landscapes often promotes water transit by maintaining low sinuosity and high depth:width ratios in channel reaches, resulting in limited in-stream vegetation and reduced bank vegetation (particularly deep rooted trees). Consequently, limited dissipation of flow energy and increased bank erodibility accelerates channel erosion risk. Installation of drainage ditches is regulated through EIAs, but do not consider downstream impact on flow. Optimising drainage installation according to site-specific soil types and groundwater characteristics is encouraged (Tuohy *et al.*, 2013) but no recommendations currently exist for on-going management of channels or the risk from up-catchment modifications. A full assessment of relationships between channel dimensions, flow velocity, up-catchment characteristics, bank erodibility and vegetation type and coverage in relation to management methods is required. As approximately 30% of managed grassland in Ireland is supported by low permeability poorly or imperfectly drained soils (which likely require artificial drainage), the extent of channel bank erosion is potentially extensive. Furthermore, channel bank stability likely influenced total bed sediment storage which was greater in channel reaches with greater modifications (removed vegetation, stock access). Although only a small fraction was readily available, a significant scour event could entrain a significant quantity of sediment (30-127% of the annual average SSY in the three surveyed catchments).

Sediment connectivity has, therefore, been validated as a valuable framework to evaluate soil erosion and sediment yield risk and also to mitigate sediment losses. At the mini-catchment scale, dominant source and transport characteristics were sufficient to explain contrasts between coarse resolution sediment metrics, e.g., annual average

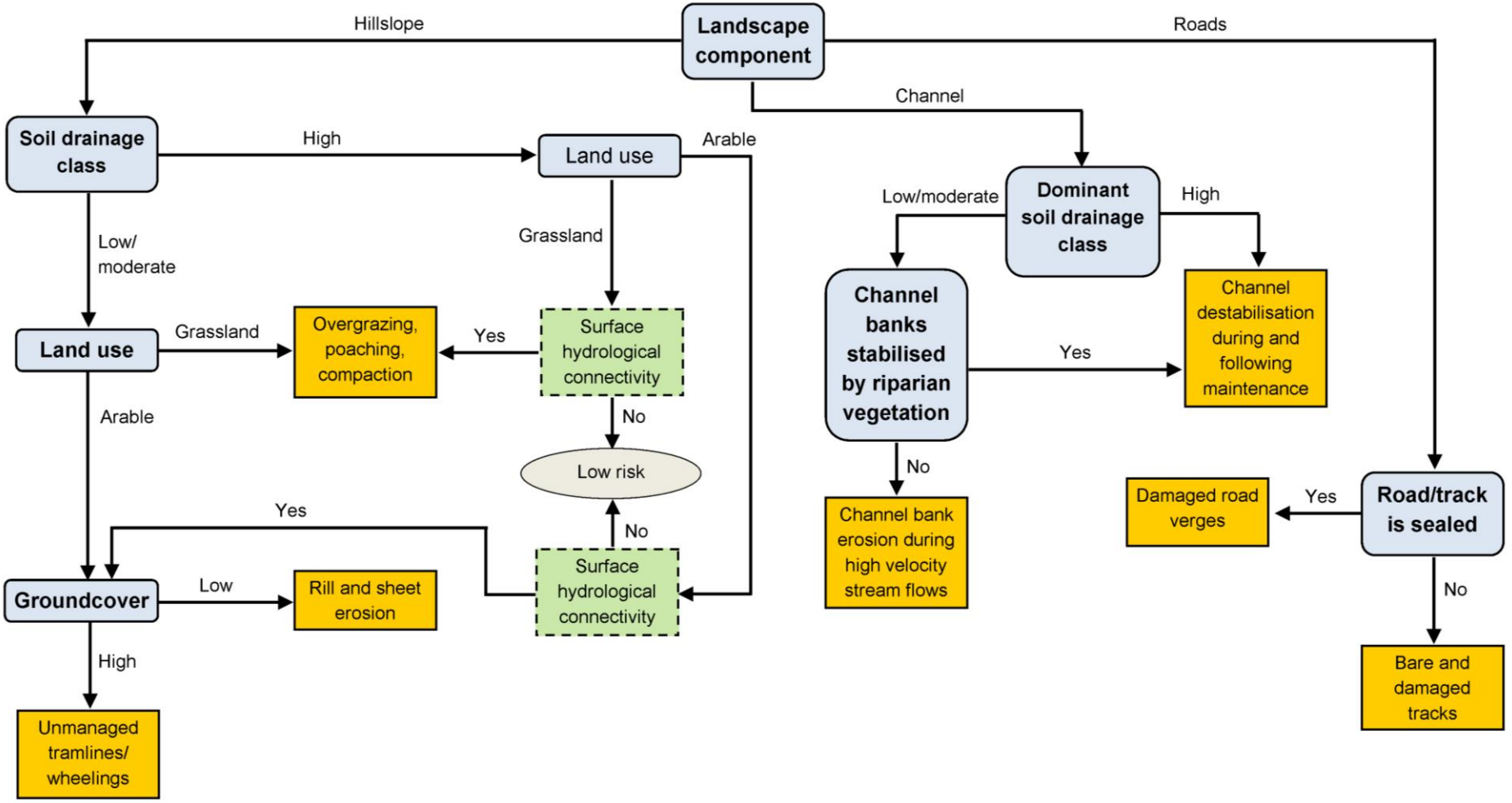

Figure 8.1. Flow chart describing soil loss controls and sediment loss risk in catchments with contrasting land uses and soil drainage class.

suspended sediment yield. Investigations at sub-annual timescales (storm-events and seasonal sediment fingerprinting results) showed hydrological connectivity and the location and availability of sediment, drove seasonal sediment connectivity fluctuations which contrasted between catchments (Chapter 4 and Chapter 6). Underlying controls on catchment sediment loss risk in agricultural catchments with contrasting land use and permeability were identified and are summarised in Figure 8.1.

At present, hydrological connectivity is frequently considered as a static metric for hillslope estimation of critical source areas (Shore *et al.*, 2013; Alder *et al.*, 2015). The extent and duration of surface hydrological connectivity are inherently linked to groundwater storage, the significance of which is gaining increasing recognition (Chapter 4; Bracken *et al.*, 2013). Further verification of such is required with reference to sediment connectivity which is commonly neglects the influence of groundwater dynamics. Other components of hydrological connectivity also exist, e.g., longitudinal connectivity (Braken and Croke, 2007). However, their interactions with sediments and other particulate pollutants are not currently accounted for. For robust management of soil loss risk, mitigation strategies must consider the full range of temporal and spatial connectivity characteristics and interactions between resultant hydrological pathways and sediment availability from multiple landscape components (hillslope and channel).

Low sediment export compared to broadly comparable catchments in Europe (based on climatic region) were attributed to complex landscape features (hedgerows, drainage ditches and small field sizes) which reduced sediment connectivity and sediment yield by decreasing the slope-length of individual fields, intercepting transported sediments which reduces soil erosion potential. Readily available channel sediment storage quantities and fluctuations were low indicating the sediment yield was unlikely to be significantly augmented. Maintenance of landscape structure is, therefore, a priority to prevent acceleration of soil losses from agricultural catchments, particularly under increasing land use pressures to support further intensification. In regions where field amalgamation and removal of landscape features have occurred to support agricultural intensification, accelerated sediment yields may be managed by restoration of landscape complexity.

Mitigation options for sediment loss risk from agricultural catchments must consider the range of sediment connectivity to mitigate for future land use and climate challenges.

On the hillslope, arable land on low permeability soils is a high soil loss risk. Reducing source availability through converting land use to permanent grassland is not necessarily an effective solution as it is likely to promote channel bank erosion as reduced hillslope water erosion increases the erosive capacity of water reaching channels. In-field mitigation measures such as RSuDS and rapid establishment of crop cover after drilling are practical approaches to reduce the space and time that soils are bare. Arable land on high permeability soils requires management where antecedent conditions and/or rainfall amount, duration and intensity are sufficient to saturate soils when groundcover is low. Temporary sediment control measures, e.g., sediment fences, particularly where in-field features are likely to conduit flow, e.g., tramlines. Grassland dominated low permeability catchments primarily require channel mitigation measures. Creation of riparian wetlands through increasing lateral connectivity, widening channels, reducing depth and re-vegetation with deep rooted tree species will dissipate flow energy, decrease erodibility of banks and channel erosion risk.

To support future sustainable intensification of agro-ecosystems, a risk-based management approach inclusive of soil erodibility, spatial and temporal groundcover reductions due to different crop types, likelihood of connectivity (soil drainage class) may be useful to ‘optimise’ catchment land use. For example, the location of high erosion risk crops on well-drained soils (low risk of hydrological connectivity) largely disconnected from the channel network and low-intensity grassland based farming (to ensure consistent groundcover) on poorly-drained soils frequently saturated by groundwater. More efficient use of available land may be a valuable approach for soil erosion, sediment loss and sediment-associated pollutant management strategies.

An innovative sediment monitoring network combined sediment flux and sediment fingerprinting studies in catchments with contrasting physical catchment characteristics and land use pressures. Sediment losses from hillslope and channel landscape components were successfully partitioned and, as previously discussed, confirms the need to assess non-field sediment sources in agricultural catchments. Management strategies are required to reduce the magnitude and duration of fine sediment delivery to aquatic ecosystems particularly in sensitive or high status catchments which support protected species (e.g., freshwater pearl mussel, Atlantic salmon). Despite low annual average sediment yield, this is valid for Irish catchment as marginally increased flux,

duration or timing of sediment transfers may exceed the tolerance threshold of specific aquatic species. Research completed in this thesis supports connectivity is an imperative framework to cost-effectively manage current and future soil erosion and sediment losses in intensively managed agro-ecosystems.

8.4 Further work

The following research needs have been identified through conducting work in this thesis. Firstly, sediment quantification in additional areas, including impacted and non-impacted catchments contributing to aquatic ecosystems supporting priority species is essential to increase the available data on sediment fluxes and yields. The scale dependency of sediment fluxes and yields and influence of increasing physical and land use heterogeneity will also enhance understanding of the relative importance of sources, delivery processes and underlying controls on different spatial scales. Measuring the response of catchment sediment yield to mitigation measures (to assess sediment response lag times) is a challenging endeavour but required by policy makers to validate the efficacy of mitigations measures. Assessment of sediment magnitude, frequency and duration impacts on priority Irish freshwater species and in other aquatic ecosystems worldwide is of significant importance to inform sediment management strategies.

Advances in sediment fingerprinting, for example, to determine storm event scale fingerprints to determine intra-source variations in sediment delivery and confirm sediment connectivity during periods of high source pressures will be particularly useful to develop high-resolution sediment dynamics. Application of sediment fingerprinting to impacted, high-risk or catchments supporting sensitive species is additionally of importance to cost-effectively preserve protected species (e.g., freshwater pearl mussels and salmonid spawning habitats). Also, facilitating the use of sediment fingerprinting as a catchment management tool for non-specialists could have significant benefits but also numerous challenges to ensure underlying principals are not violated.

Greater understanding of catchment sediment budgets and sediment delivery ratios are of particular importance in intensive agricultural catchments with poorly- and moderately-drained soils to determine maximum soil erosion rates for arable and grassland systems. Identification of sub-field scale critical source areas using high-resolution remotely sensed flow pathway data is also essential to pinpoint management

strategies for sediment and sediment-associated pollutants, e.g. P. However, these areas must be validated for soil erosion, for example, using short-term radionuclide tracers (^{7}Be) and need to consider fluctuations in connectivity over time.

Methods to assess channel bank erosion risk, for example, assessing the importance of river velocity, shear stress, channel-cross section, bank stability and root networks are essential to determine the impact of channel modifications on sediment losses in managed drainage networks. The impact of channel banks protection measures on soil loss and sediment delivery are essential to determine if management strategies are successful. In addition, farmer and local authority engagement may be required to address changing perspectives on appropriate channel management. Finally, up-scaling the results of the present study to inform environmentally sensitive farming enterprises will inform a national sustainable intensification plan for Ireland and provide a framework for other countries.

References

Aich, V., Zimmermann, A., Elsenbeer, H. (2014) Quantification and interpretation of suspended-sediment discharge hysteresis patterns: How much data do we need? *Catena* **122**, 120-129.

Alder, S., Prasuhn, V., Liniger, H., Herweg, K., Hurni, H., Candinas, A., Gujer, H.U. (2015) A high-resolution map of direct and indirect connectivity of erosion risk areas to surface waters in Switzerland—A risk assessment tool for planning and policy-making. *Land Use Policy* **48**, 236-249.

Anon. (2013) Chapter 2: Soil and drainscapes. Creamer, R., Ibrahim, T., Fenton, O. In: Teagasc Manual on Drainage and Soil Management. Eds. Moore, M., Fenton, O., Tuohy, P. and Ibrahim, T. Teagasc, Carlow.

Bača, P. (2008) Hysteresis effect in suspended sediment concentration in the Rybárik basin, Slovakia / Effet d'hystérèse dans la concentration des sédiments en suspension dans le bassin versant de Rybárik (Slovaquie). *Hydrological Sciences Journal* **53**, 224-235.

Baessler, C., Klotz, S. (2006) Effects of changes in agricultural land-use on landscape structure and arable weed vegetation over the last 50 years. *Agriculture, Ecosystems & Environment* **115**, 43-50.

Ballantine, D., Walling, D., Leeks, G.L. (2009) Mobilisation and Transport of Sediment-Associated Phosphorus by Surface Runoff. *Water, Air, and Soil Pollution* **196**, 311-320.

Belmont, P., Willenbring, J., Schottler, S., Marquard, J., Kumarasamy, K., Hemmis, J. (2014) Toward generalizable sediment fingerprinting with tracers that are conservative and nonconservative over sediment routing timescales. *Journal of Soils and Sediments* **14**, 1479-1492.

Bende-Michl, U., Verburg, K., Cresswell, H. (2013) High-frequency nutrient monitoring to infer seasonal patterns in catchment source availability, mobilisation and delivery. *Environmental Monitoring and Assessment* **185**, 9191-9219.

Bilotta, G.S., Brazier, R.E. (2008) Understanding the influence of suspended solids on water quality and aquatic biota. *Water Research* **42**, 2849-2861.

Bilotta, G.S., Brazier, R.E., Haygarth, P.M. (2007a) Processes affecting transfer of sediment and colloids, with associated phosphorus, from intensively farmed grasslands: erosion. *Hydrological Processes* **21**, 135-139.

Bilotta, G.S., Brazier, R.E., Haygarth, P.M., (2007b) The Impacts of Grazing Animals on the Quality of Soils, Vegetation, and Surface Waters in Intensively Managed Grasslands, in: Donald, L.S. (Ed.), *Advances in Agronomy*. Academic Press, pp. 237-280.

Bilotta, G.S., Krueger, T., Brazier, R.E., Butler, P., Freer, J., Hawkins, J.M.B., Haygarth, P.M., Macleod, C.J.A., Quinton, J.N. (2010) Assessing catchment-scale erosion and yields of suspended solids from improved temperate grassland. *Journal of Environmental Monitoring* **12**, 731-739.

Blake, W.H., Ficken, K.J., Taylor, P., Russell, M.A., Walling, D.E. (2012) Tracing crop-specific sediment sources in agricultural catchments. *Geomorphology* 139–140, 322-329.

Boardman, J. (2013) The hydrological role of 'sunken lanes' with respect to sediment mobilization and delivery to watercourses with particular reference to West Sussex, southern England. *Journal of Soils and Sediments* **13**, 1636-1644.

Boardman, J. (2015) Extreme rainfall and its impact on cultivated landscapes with particular reference to Britain. Earth Surface Processes and Landforms, doi: 10.1002/esp.3792.

Boardman, J., Shepheard, M.L., Walker, E., Foster, I.D.L. (2009) Soil erosion and risk-assessment for on- and off-farm impacts: A test case using the Midhurst area, West Sussex, UK. *Journal of Environmental Management* **90**, 2578-2588.

Boardman, J., Favis-Mortlock, D.T. (2014) The significance of drilling date and crop cover with reference to soil erosion by water, with implications for mitigating erosion on agricultural land in South East England. *Soil Use and Management* **30**, 40-47.

Borin, M., Passoni, M., Thiene, M., Tempesta, T. (2010) Multiple functions of buffer strips in farming areas. *European Journal of Agronomy* **32**, 103-111.

Bowes, M.J., House, W.A., Hodgkinson, R.A., Leach, D.V. (2005) Phosphorus–discharge hysteresis during storm events along a river catchment: the River Swale, UK. *Water Research* **39**, 751-762.

Bracken, L.J., Croke, J. (2007) The concept of hydrological connectivity and its contribution to understanding runoff-dominated geomorphic systems. *Hydrological Processes* **21**, 1749-1763.

Bracken, L.J., Wainwright, J., Ali, G.A., Tetzlaff, D., Smith, M.W., Reaney, S.M., Roy, A.G. (2013) Concepts of hydrological connectivity: Research approaches, pathways and future agendas. *Earth-Science Reviews* **119**, 17-34.

Bradley, C., Webster, P., Lucey, J., McGarrigle, M., McCreesh, P., Gallagher, T. (2015) Rivers and Canals. In: Byrne, C. and Fanning, A. (eds.) Water quality in Ireland 2010-2012, http://www.epa.ie/pubs/reports/water/waterqua/wqr20102012/#.VlIdpeknzIU [accessed 22.11.15]

Bradley, R.I., Milne, R., Bell, J., Lilly, A., Jordan, C., Higgins, A. (2005) A soil carbon and land use database for the United Kingdom. *Soil Use and Management* **21**, 363-369.

Brazier, R. (2004) Quantifying soil erosion by water in the UK: a review of monitoring and modelling approaches. *Progress in Physical Geography* **28**, 340-365.

Brils, J. (2008) Sediment Monitoring and the Water Framework Directive. *Annali dell'Istituto Superiore di Sanita* **44**, 218-223.

Bryan, R.B. (2000) Soil erodibility and processes of water erosion on hillslope. *Geomorphology* **32**, 385-415.

Central Statistics Office – CSO (2015) *Crops and Livestock Survey June Final Results*, http://www.cso.ie/en/releasesandpublications/er/clsjf/cropsandlivestocksurveyjunefinal2014/. [accessed 22.11.15].

Cerdan, O., Govers, G., Le Bissonnais, Y., Van Oost, K., Poesen, J., Saby, N., Gobin, A., Vacca, A., Quinton, J., Auerswald, K., Klik, A., Kwaad, F.J.P.M., Raclot, D., Ionita,

I., Rejman, J., Rousseva, S., Muxart, T., Roxo, M.J., Dostal, T. (2010) Rates and spatial variations of soil erosion in Europe: A study based on erosion plot data. *Geomorphology* **122**, 167-177.

Chapman, A.S., Foster, I.D.L., Lees, J.A., Hodgkinson, R.A. (2005) Sediment delivery from agricultural land to rivers via subsurface drainage. *Hydrological Processes* **19**, 2875-2897.

Collins, A.L., Anthony, S.G. (2008) Assessing the likelihood of catchments across England and Wales meeting 'good ecological status' due to sediment contributions from agricultural sources. *Environmental Science & Policy* **11**, 163-170.

Collins, A.L., Walling, D.E. (2002) Selecting fingerprint properties for discriminating potential suspended sediment sources in river basins. *Journal of Hydrology* **261**, 218-244.

Collins, A.L., Walling, D.E. (2004) Documenting catchment suspended sediment sources: problems, approaches and prospects. *Progress in Physical Geography* **28**, 159-196.

Collins, A.L., Walling, D.E. (2007) Sources of fine sediment recovered from the channel bed of lowland groundwater-fed catchments in the UK. *Geomorphology* **88**, 120-138.

Collins, A.L., Walling, D.E., Leeks, G.J.L. (1997) Fingerprinting the Origin of Fluvial Suspended Sediment in Larger River Basins: Combining Assessment of Spatial Provenance and Source Type. *Geografiska Annaler: Series A, Physical Geography* **79**, 239-254.

Collins, A.L., Walling, D.E., Leeks, G.J.L. (1998) Use of composite fingerprints to determine the provenance of the contemporary suspended sediment load transported by rivers. *Earth Surface Processes and Landforms* **23**, 31-52.

Collins, A.L., Walling, D.E., Sichingabula, H.M., Leeks, G.J.L. (2001) Suspended sediment source fingerprinting in a small tropical catchment and some management implications. *Applied Geography* **21**, 387-412.

Collins, A.L., Strőmqvist, J., Davison, P.S., Lord, E.I. (2007) Appraisal of phosphorus and sediment transfer in three pilot areas identified for the catchment sensitive farming initiative in England: application of the prototype PSYCHIC model. *Soil Use and Management* **23**, 117-132.

Collins, A.L., Walling, D.E., Stroud, R.W., Robson, M., Peet, L.M. (2010a) Assessing damaged road verges as a suspended sediment source in the Hampshire Avon catchment, southern United Kingdom. *Hydrological Processes* **24**, 1106-1122.

Collins, A.L., Walling, D.E., Webb, L., King, P. (2010b) Apportioning catchment scale sediment sources using a modified composite fingerprinting technique incorporating property weightings and prior information. *Geoderma* **155**, 249-261.

Collins, A.L., Naden, P.S., Sear, D.A., Jones, J.I., Foster, I.D.L., Morrow, K. (2011) Sediment targets for informing river catchment management: international experience and prospects. *Hydrological Processes* **25**, 2112-2129.

Collins, A.L., Williams, L.J., Zhang, Y.S., Marius, M., Dungait, J.A.J., Smallman, D.J., Dixon, E.R., Stringfellow, A., Sear, D.A., Jones, J.I., Naden, P.S. (2013) Catchment source contributions to the sediment-bound organic matter degrading salmonid spawning gravels in a lowland river, southern England. *Science of the Total Environment* **456–457**, 181-195.

Cooper, D., Naden, P., Old, G., Laizé, C. (2008) Development of guideline sediment targets to support management of sediment inputs into aquatic systems, Natural England Research Report NERR008, CEH Wallingford, pp. 96.

Cooper, R.J., Krueger, T., Hiscock, K.M., Rawlins, B.G. (2014) High-temporal resolution fluvial sediment source fingerprinting with uncertainty: a Bayesian approach. *Earth Surface Processes and Landforms* **40**, 78–92.

Creamer, R.E., Brennan, F., Fenton, O., Healy, M.G., Lalor, S.T.J., Lanigan, G.J., Regan, J.T., Griffiths, B.S. (2010) Implications of the proposed Soil Framework Directive on agricultural systems in Atlantic Europe – a review. *Soil Use and Management* **26**, 198-211.

Croke, J., Fryirs, K., Thompson, C. (2013) Channel–floodplain connectivity during an extreme flood event: implications for sediment erosion, deposition, and delivery. *Earth Surface Processes and Landforms* **38**, 1444-1456.

D'Haen, K., Verstraeten, G., Degryse, P. (2012) Fingerprinting historical fluvial sediment fluxes. *Progress in Physical Geography* **36**, 154-186.

Dalgleish, H.Y., Foster, I.D.L. (1996) ^{137}Cs losses from a loamy surface water gleyed soil (Inceptisol): a laboratory simulation experiment. *Catena* **26**, 227-245.

Department of Agriculture, Food and Farming – DAFF (2010) Food Harvest 2020: A Vision for Irish Agri-food and Fisheries. Department of Agriculture, Fisheries and Food, Ireland, Available at: http://www.agriculture.gov.ie/media/migration/agri-foodindustry/foodharvest2020/2020FoodHarvestEng240810.pdf [accessed 22.11.15].

Department of Agriculture, Forestry and the Marine – DAFM (2015) Food Wise 2025: A 10-year Vision for the Irish Agri-food Industry. Department of Agriculture, Forestry and the Marine, Ireland, Available at: http://www.agriculture.gov.ie/media/migration/agri-foodindustry/foodwise2025/report/FoodWise2025.pdf [accessed 03.12.15].

Department of Agriculture, Forestry and the Marine – DAFM (2013) The Second National Forest Inventory Republic of Ireland Field Procedures and Methodology, http://www.agriculture.gov.ie/media/migration/forestry/nationalforestinventory/2012/NFI%20Ireland%20Methodology2013v12%20Final.pdf [accessed 01.11.15]

Darboux, F., Huang, C.-h. (2003) An Instantaneous-Profile Laser Scanner to Measure Soil Surface Microtopography. *Soil Science Society of America Journal* **67**, 92-99.

Davis, C., Fox, J. (2009) Sediment Fingerprinting: Review of the Method and Future Improvements for Allocating Nonpoint Source Pollution. *Journal of Environmental Engineering* **135**, 490-504.

Dearing, J.A., xe, kansson, H., Liedberg, J., xf, nsson, B., Persson, A., Skansj, xf, S., Widholm, D., El-Daoushy, F. (1987) Lake Sediments Used to Quantify the Erosional Response to Land Use Change in Southern Sweden. *Oikos* **50**, 60-78.

Deasy, C., Brazier, R.E., Heathwaite, A.L., Hodgkinson, R. (2009) Pathways of runoff and sediment transfer in small agricultural catchments. *Hydrological Processes* **23**, 1349-1358.

Delgado, J.A., Berry, J.K. (2008) Advances in Precision Conservation, *Advances in Agronomy*. Academic Press, pp. 1-44.

Deverell, R., McDonnell, K., Devlin, G. (2009) The impact of field size on the environment and energy crop production efficiency for a sustainable indigenous bioenergy supply chain in the Republic of Ireland, *Sustainability* **1**, 994-1011.

Di Stefano, C., Ferro, V., Porto, P. (1999) Linking Sediment Yield and Caesium-137 Spatial Distribution at Basin Scale. *Journal of Agricultural Engineering Research* **74**, 41-62.

Doody, D.G., Higgins, A., Matthews, D., Foy, R.H., Pilatova, K., Duffy, O., Watson, C.J. (2010) Overland flow initiation from a drumlin grassland hillslope. *Soil Use and Management* **26**, 286-298.

Duerdoth, C.P., Arnold, A., Murphy, J.F., Naden, P.S., Scarlett, P., Collins, A.L., Sear, D.A., Jones, J.I. (2015) Assessment of a rapid method for quantitative reach-scale estimates of deposited fine sediment in rivers. *Geomorphology* **230**, 37-50.

Duvert, C., Gratiot, N., Evrard, O., Navratil, O., Némery, J., Prat, C., Esteves, M. (2010) Drivers of erosion and suspended sediment transport in three headwater catchments of the Mexican Central Highlands. *Geomorphology* **123**, 243-256.

Eder, A., Strauss, P., Krueger, T., Quinton, J.N. (2010) Comparative calculation of suspended sediment loads with respect to hysteresis effects (in the Petzenkirchen catchment, Austria). *Journal of Hydrology* **389**, 168-176.

Estrany, J., Garcia, C., Batalla, R.J. (2009) Suspended sediment transport in a small Mediterranean agricultural catchment. *Earth Surface Processes and Landforms* **34**, 929-940.

Evans, D.J., Gibson, C.E., Rossell, R.S. (2006) Sediment loads and sources in heavily modified Irish catchments: A move towards informed management strategies. *Geomorphology* **79**, 93-113.

European Environment Agency – EEA (2015) Greening Europe's agriculture http://www.eea.europa.eu/themes/agriculture/greening-agricultural-policy [accessed 22.11.15].

FAO/IAEA (2015) Models and Tool Kits http://www-naweb.iaea.org/nafa/swmn/models-tool-kits.html [accessed 22.11.15].

Fay, D., McGrath, D., Chaosheng, Z., Carrigg, C., O'Flaherty, V., Carton, O.T. and Grennan, E. (2002) Towards a national soil database, Appendix E, Environmental RTDI Programme 2000-2006 (2001-CD/S2-M2). Environmental Protection Agency, Wexford, Ireland.

Fealy, R.M., Buckley, C., Mechan, S., Melland, A., Mellander, P.E., Shortle, G., Wall, D., Jordan, P. (2010) The Irish Agricultural Catchments Programme: catchment selection using spatial multi-criteria decision analysis. *Soil Use and Management* **26**, 225-236.

Fenton, O., Schulte, R.P.O., Jordan, P., Lalor, S.T.J., Richards, K.G. (2011) Time lag: a methodology for the estimation of vertical and horizontal travel and flushing timescales to nitrate threshold concentrations in Irish aquifers. *Environmental Science & Policy* **14**, 419-431.

Fenton, O., Vero, S., Ibrahim, T.G., Murphy, P.N.C., Sherriff, S.C., Ó hUallacháin, D. (2015) Consequences of using different soil texture determination methodologies for soil physical quality and unsaturated zone time lag estimates. *Journal of Contaminant Hydrology* **182**, 16-24.

Florsheim, J.L., Pellerin, B.A., Oh, N.H., Ohara, N., Bachand, P.A.M., Bachand, S.M., Bergamaschi, B.A., Hernes, P.J., Kavvas, M.L. (2011) From deposition to erosion: Spatial and temporal variability of sediment sources, storage, and transport in a small agricultural watershed. *Geomorphology* **132**, 272-286.

Foley, J.A. (2005) Global consequences of land use. *Science* **309**, 570-574.

Foster, I.D.L., Lees, J.A. (2000) Tracers in geomorphology: theory and applications in tracing fine sediments. In: Foster IDL (ed.) *Tracers in Geomorphology*. Wiley, Chichester, pp. 3-20.

Foster, I.D.L., Lees, J.A., Owens, P.N., Walling, D.E. (1998) Mineral magnetic characterization of sediment sources from an analysis of lake and floodplain sediments in the catchments of the Old Mill reservoir and Slapton Ley, South Devon, UK. *Earth Surface Processes and Landforms* **23**, 685-703.

Foster, I.D.L., Boardman, J., Keay-Bright, J. (2007) Sediment tracing and environmental history for two small catchments, Karoo Uplands, South Africa. *Geomorphology* **90**, 126-143.

Foster, I., Collins, A., Naden, P., Sear, D., Jones, J., Zhang, Y. (2011) The potential for paleolimnology to determine historic sediment delivery to rivers. *Journal of Paleolimnology* **45**, 287-306.

Foucher, A., Salvador-Blanes, S., Evrard, O., Simonneau, A., Chapron, E., Courp, T., Cerdan, O., Lefèvre, I., Adriaensen, H., Lecompte, F., Desmet, M. (2014) Increase in soil erosion after agricultural intensification: Evidence from a lowland basin in France. *Anthropocene* **7**, 30-41.

Fox, J.F., Papanicolaou, A.N. (2008) An un-mixing model to study watershed erosion processes. *Advances in Water Resources* **31**, 96-108.

Fox, G.A., Wilson, G.V., Simon, A., Langendoen, E.J., Akay, O., Fuchs, J.W. (2007) Measuring streambank erosion due to ground water seepage: correlation to bank pore water pressure, precipitation and stream stage. *Earth Surface Processes and Landforms* **32**, 1558-1573.

Franks, S.W., Rowan, J.S. (2000) Multi-parameter fingerprinting of sediment sources: Uncertainty estimation and tracer selection. In: Bentley LR, Sykes JF, Gray WG, Brebbia CA, Pinder GF (eds.) *Computational Methods in Water Resources* XIII. Balkema, Rotterdam, pp 1067-1074.

Fredericks, D.J., Norms, V., Perrens, S.J. (1988) Estimating erosion using caesium-137: I. Measuring caesium-137 activity in a soil, *Sediment Budgets* (Proceedings of the Porto

Alegre Symposium, December 1988). IAHS Publication no.174, IAHS, Wallingford, pp. 225-231.

Freebairn, D.M., Wockner, G.H., Hamilton, N.A., Rowland, P. (2009) Impact of soil conditions on hydrology and water quality for a brown clay in the north-eastern cereal zone of Australia. *Soil Research* **47**, 389-402.

Fryirs, K.A., Brierley, G.J., Preston, N.J., Kasai, M. (2007) Buffers, barriers and blankets: The (dis)connectivity of catchment-scale sediment cascades. *Catena* **70**, 49-67.

Fryirs, K. (2013) (Dis)Connectivity in catchment sediment cascades: a fresh look at the sediment delivery problem. *Earth Surface Processes and Landforms* **38**, 30-46.

Gao, P., Josefson, M. (2012) Event-based suspended sediment dynamics in a central New York watershed. *Geomorphology* **139–140**, 425-437.

Gay, A., Cerdan, O., Delmas, M., Desmet, M. (2014) Variability of suspended sediment yields within the Loire river basin (France). *Journal of Hydrology* **519**, Part A, 1225-1237.

Gellis, A.C. (2013) Factors influencing storm-generated suspended-sediment concentrations and loads in four basins of contrasting land use, humid-tropical Puerto Rico. *Catena* **104**, 39-57.

Geraghty, M., Farrelly, I., Claringbold, K., Jordan, C., Meehan, R., and Hudson, M. (1997) Geology of Monaghan-Carlingford. A geological description to accompany the Bedrock Geology 1:100,000 Scale Map Series, Sheet 8/9, Monaghan-Carlingford, Geological Survey of Ireland: Dublin, Ireland.

Giménez, R., Casalí, J., Grande, I., Díez, J., Campo, M.A., Álvarez-Mozos, J., Goñi, M. (2012) Factors controlling sediment export in a small agricultural watershed in Navarre (Spain). *Agricultural Water Management* **110**, 1-8.

Glendell, M., Brazier, R.E. (2014) Accelerated export of sediment and carbon from a landscape under intensive agriculture. *Science of the Total Environment* **476–477**, 643-656.

Glendell, M., Granger, S.J., Bol, R., Brazier, R.E. (2014) Quantifying the spatial variability of soil physical and chemical properties in relation to mitigation of diffuse water pollution. *Geoderma* **214–215**, 25-41.

Govers, G., Quine, T.A., Walling, D.E. (1993) The effect of water erosion and tillage movement on hill slope profile development: a comparison of field observations and model results. In: Wicherek, S. (Ed.), *Farm Land Erosion: In Temperate Plains Environments and Hills*. Elsevier, pp. 285–300.

Govers, G., Quine, T.A., Desmet, P.J.J., Walling, D.E. (1996) The relative contribution of soil tillage and overland flow erosion to soil redistribution on agricultural land. *Earth Surface Processes and Landforms* **21**, 929-946.

Gruszowski, K.E., Foster, I.D.L., Lees, J.A., Charlesworth, S.M. (2003) Sediment sources and transport pathways in a rural catchment, Herefordshire, UK. *Hydrological Processes* **17**, 2665-2681.

Gurr, G.M., Wratten, S.D., Luna, J.M. (2003) Multi-function agricultural biodiversity: pest management and other benefits. *Basic and Applied Ecology* **4**, 107-116.

Guzmán, G., Quinton, J., Nearing, M., Mabit, L., Gómez, J. (2013) Sediment tracers in water erosion studies: current approaches and challenges. *Journal of Soils and Sediments* **13**, 816-833.

Harlow, A., Webb, B.W., Walling, D.E., (2006) Sediment yields in the Exe Basin: a longer-term perspective, in: Rowan, J.S., Duck, R.W., Werrity, A. (Eds.), Sediment Dynamics and the Hydromorphology of Fluvial Systems. IAHS 306, Dundee, UK.

Harrington, S.T., Harrington, J.R. (2013) An assessment of the suspended sediment rating curve approach for load estimation on the Rivers Bandon and Owenabue, Ireland. *Geomorphology* **185**, 27-38.

Hatfield, R., Maher, B., Pates, J., Barker, P. (2008) Sediment dynamics in an upland temperate catchment: changing sediment sources, rates and deposition. *Journal of Paleolimnology* **40**, 1143-1158.

Hatfield, R.G., Maher, B.A. (2009) Fingerprinting upland sediment sources: particle size-specific magnetic linkages between soils, lake sediments and suspended sediments. *Earth Surface Processes and Landforms* **34**, 1359-1373.

Haygarth, P.M., Condron, L.M., Heathwaite, A.L., Turner, B.L., Harris, G.P. (2005) The phosphorus transfer continuum: linking source to impact with an interdisciplinary and multi-scaled approach. *Science of the Total Environment* **344**, 5-14.

Haygarth, P.M., Bilotta, G.S., Bol, R., Brazier, R.E., Butler, P.J., Freer, J., Gimbert, L.J., Granger, S.J., Krueger, T., Macleod, C.J.A., Naden, P., Old, G., Quinton, J.N., Smith, B., Worsfold, P. (2006) Processes affecting transfer of sediment and colloids, with associated phosphorus, from intensively farmed grasslands: an overview of key issues. *Hydrological Processes* **20**, 4407-4413.

Hbirkou, C., Welp, G., Rehbein, K., Hillnhütter, C., Daub, M., Oliver, M.A., Pätzold, S. (2011) The effect of soil heterogeneity on the spatial distribution of Heterodera schachtii within sugar beet fields. *Applied Soil Ecology* **51**, 25-34.

Heckrath, G., Djurhuus, J., Quine, T.A., Van Oost, K., Govers, G., Zhang, Y. (2005) Tillage erosion and its effect on soil properties and crop yield in Denmark. *Journal of Environmental Quality* **34**, 312-324.

Horowitz, A.J. (1991) A Primer in Sediment-Trace Element Chemistry, 2nd edn. Lewis Publishers, Chelsea, MI.

Horowitz, A.J. (2008) Determining annual suspended sediment and sediment-associated trace element and nutrient fluxes. *Science of the Total Environment* **400**, 315-343.

Huang, C.C., O'Connell, M. (2000) Recent land-use and soil-erosion history within a small catchment in Connemara, western Ireland: evidence from lake sediments and documentary sources. *Catena* **41**, 293-335.

Ibrahim, T.G., Fenton, O., Richards, K.G., Fealy, R.M., Healy, M.G. (2013) Spatial and temporal variations of nutrient loads in overland flow and subsurface drainage from a marginal land site in south-east Ireland. *Biology and Environment: Proceedings of the Royal Irish Academy* **113B**, 169-186.

Jansson, M.B. (2002) Determining sediment source areas in a tropical river basin, Costa Rica. *Catena* **47**, 63-84.

Jastram, J.D., Zipper, C.E., Zelazny, L.W., Hyer, K.E. (2010) Increasing Precision of Turbidity-Based Suspended Sediment Concentration and Load Estimates. *Journal of Environmental Quality* **39**, 1306-1316.

Jones, J.I., Murphy, J.F., Collins, A.L., Sear, D.A., Naden, P.S., Armitage, P.D. (2011a) The impact of fine sediment on macro-invertebrates. *River Research and Applications* **28**, 1055-1071.

Jones, J.I., Collins, A.L., Naden, P.S., Sear, D.A. (2011b) The relationship between fine sediment and macrophytes in rivers. *River Research and Applications* **28**, 1006-1018.

Jordan, P., Rippey, B., John Anderson, N. (2002) The 20th century whole-basin trophic history of an inter-drumlin lake in an agricultural catchment. *Science of the Total Environment* **297**, 161-173.

Jordan, P., Menary, W., Daly, K., Kiely, G., Morgan, G., Byrne, P., Moles, R. (2005) Patterns and processes of phosphorus transfer from Irish grassland soils to rivers—integration of laboratory and catchment studies. *Journal of Hydrology* **304**, 20-34.

Jordan, P., Cassidy, R. (2011) Technical Note: Assessing a 24/7 solution for monitoring water quality loads in small river catchments. *Hydrology and Earth System Sciences* **15**, 3093-3100.

Jordan, P., Arnscheidt, A., McGrogan, H., McCormick, S. (2007) Characterising phosphorus transfers in rural catchments using a continuous bank-side analyser. *Hydrology and Earth System Sciences* **11**, 372-381.

Kemp, P., Sear, D., Collins, A., Naden, P., Jones, I. (2011) The impacts of fine sediment on riverine fish. *Hydrological Processes* **25**, 1800-1821.

Kirkby, M.J. (Ed), 1978. *Hillslope Hydrology*. John Wiley and Sons

Kirkby, M.J., Jones, R.J.A., Irvine, B., Gobin, A, Govers, G., Cerdan, O., Van Rompaey, A.J.J., Le Bissonnais, Y., Daroussin, J., King, D., Montanarella, L., Grimm, M., Vieillefont, V., Puigdefabregas, J., Boer, M., Kosmas, C., Yassoglou, N., Tsara, M.,

Mantel, S., Van Lynden, G.J., Huting, J.(2004). European Soil Bureau Research Report No.16, EUR 21176, 18pp. and 1 map in ISO B1 format. Office for Official Publications of the European Communities, Luxembourg.

Kjelland, M., Woodley, C., Swannack, T., Smith, D. (2015) A review of the potential effects of suspended sediment on fishes: potential dredging-related physiological, behavioral, and transgenerational implications. *Environment Systems and Decisions* **35**, 334-350.

Koiter, A.J., Owens, P.N., Petticrew, E.L., Lobb, D.A. (2013a) The behavioural characteristics of sediment properties and their implications for sediment fingerprinting as an approach for identifying sediment sources in river basins. *Earth-Science Reviews* **125**, 24-42.

Koiter, A., Lobb, D., Owens, P., Petticrew, E., Tiessen, K.D., Li, S. (2013b) Investigating the role of connectivity and scale in assessing the sources of sediment in an agricultural watershed in the Canadian prairies using sediment source fingerprinting. *Journal of Soils and Sediments* **13**, 1676-1691.

Krause, A.K., Franks, S.W., Kalma, J.D., Loughran, R.J., Rowan, J.S. (2003) Multi-parameter fingerprinting of sediment deposition in a small gullied catchment in SE Australia. *Catena* **53**, 327-348.

Laceby, J.P., Olley, J. (2015) An examination of geochemical modelling approaches to tracing sediment sources incorporating distribution mixing and elemental correlations. *Hydrological Processes* **29**, 1669-1685.

Lacoste, M., Michot, D., Viaud, V., Evrard, O., Walter, C. (2014) Combining 137Cs measurements and a spatially distributed erosion model to assess soil redistribution in a hedgerow landscape in northwestern France (1960–2010). *Catena* **119**, 78-89.

Lal, R. (1988) Effects of slope length, slope gradient, tillage methods and cropping systems on runoff and soil erosion on a tropical Alfisol: preliminary results. Proceedings of the Porto Alegre Symposium, December 1988, edited by Bordas, M.P. and Walling, D.E. , IAHS Publ., 174, 79-88.

Lamba, J., Karthikeyan, K.G., Thompson, A.M. (2015) Apportionment of suspended sediment sources in an agricultural watershed using sediment fingerprinting. *Geoderma* **239–240**, 25-33.

Langlois, J.L., Johnson, D.W., Mehuys, G.R. (2005) Suspended sediment dynamics associated with snowmelt runoff in a small mountain stream of Lake Tahoe (Nevada). *Hydrological Processes* **19**, 3569-3580.

Läppe, D., and Hennessy, T. (2012) The capacity to expand milk production in Ireland following the removal of milk quotas. *Irish Journal of Agricultural and Food Research* **51**, 1-11.

Larsen, S., Pace, G., Ormerod, S.J. (2011) Experimental effects of sediment deposition on the structure and function of macroinvertebrate assemblages in temperate streams. *River Research and Applications* **27**, 257-267.

Lawler, D.M., Petts, G.E., Foster, I.D.L., Harper, S. (2006) Turbidity dynamics during spring storm events in an urban headwater river system: The Upper Tame, West Midlands, UK. *Science of the Total Environment* **360**, 109-126.

Le Roux, G., and Marshall, W.A. (2011) Constructing recent peat accumulation chronologies using atmospheric fall-out radionuclides, *Mires and Peat* **7**, 1-14.

Lefrançois, J., Grimaldi, C., Gascuel-Odoux, C., Gilliet, N. (2007) Suspended sediment and discharge relationships to identify bank degradation as a main sediment source on small agricultural catchments. *Hydrological Processes* **21**, 2923-2933.

Lenhart, C.F., Verry, E.S., Brooks, K.N., Magnet, J.A. (2012) Adjustment of prairie pothole streams to land use, drainage and climate changes and consequences for turbidity impairment, *River Research and Applications* **28**, 1609-1619.

Lewis, J. (2003) Turbidity-controlled sampling for suspended sediment load estimation, in: Bogen, J., Fergus, T., Walling, D.E. (Eds.), Erosion and Sediment Transport Measurement in Rivers: Technological and methodological advances. IAHS 283, Proc. Oslo Workshop, June 2002, pp. 13-20.

Louwagie, G., Gay, S.H., Sammeth, F., Ratinger, T. (2011) The potential of European Union policies to address soil degradation in agriculture. *Land Degradation & Development* **22**, 5-17.

Mano, V., Nemery, J., Belleudy, P., Poirel, A. (2009) Assessment of suspended sediment transport in four alpine watersheds (France): influence of the climatic regime. *Hydrological Processes* **23**, 777-792.

Martínez-Carreras, N., Krein, A., Gallart, F., Iffly, J.F., Pfister, L., Hoffmann, L., Owens, P.N. (2010) Assessment of different colour parameters for discriminating potential suspended sediment sources and provenance: A multi-scale study in Luxembourg. *Geomorphology* **118**, 118-129.

Massey, P., O'Connor, C., Sills, P., Fenelon, A., Maloney-Finn, L., Stone, D., Reidy, B., Creamer, R. (2013) Irish Soil Information System: Laboratory Standard Operating Procedures, Teagasc Report, Wexford, Ireland.

Massoudieh, A., Gellis, A., Banks, W.S., Wieczorek, M.E. (2013) Suspended sediment source apportionment in Chesapeake Bay watershed using Bayesian chemical mass balance receptor modeling. *Hydrological Processes* **27**, 3363-3374.

Matthaei, C.D., Piggott, J.J., Townsend, C.R. (2010) Multiple stressors in agricultural streams: interactions among sediment addition, nutrient enrichment and water abstraction. *Journal of Applied Ecology* **47**, 639-649.

McAulay, I.R., Moran, D. (1989) Radiocaesium fallout in Ireland from the Chernobyl accident. *Journal of Radiological Protection* **9**, 29.

McConnell B., Philcox, M., and Geraghty, M. (2001) Geology of Meath: A geological description to accompany the bedrock geology 1:100,000 scale map series, Sheet 13, Meath. Geological Survey of Ireland: Dublin, Ireland.

McManus, J., and Duck, R.W. (1996) Regional variations of fluvial sediment yield in eastern Scotland. In: Walling, D.E., and Webb, B.W., (eds.) Proceedings of the Exeter Symposium, Jul 1996, IAHS Publication 236, 157-161.

Medley, K., Okey, B., Barrett, G., Lucas, M., Renwick, W. (1995) Landscape change with agricultural intensification in a rural watershed, southwestern Ohio, U.S.A. *Landscape Ecology* **10**, 161-176.

Mekonnen, M., Keesstra, S.D., Stroosnijder, L., Baartman, J.E.M., Maroulis, J. (2015) Soil Conservation Through Sediment Trapping: A Review. *Land Degradation & Development* **26**, 544-556.

Melland, A.R., Mellander, P.E., Murphy, P.N.C., Wall, D.P., Mechan, S., Shine, O., Shortle, G., Jordan, P. (2012a) Stream water quality in intensive cereal cropping catchments with regulated nutrient management. *Environmental Science & Policy* **24**, 58-70.

Melland, A.R., Ryan, D., Shortle, G., and Jordan, P. (2012b) A cost:benefit evaluation of in-situ high temporal resolution stream nutrient monitoring, World Congress on Water, Climate and Energy, Dublin.

Mellander, P.-E., Melland, A.R., Jordan, P., Wall, D.P., Murphy, P.N.C., Shortle, G. (2012) Quantifying nutrient transfer pathways in agricultural catchments using high temporal resolution data. *Environmental Science & Policy* **24**, 44-57.

Mellander, P.-E., Melland, A.R., Murphy, P.N.C., Wall, D.P., Shortle, G., Jordan, P. (2014) Coupling of surface water and groundwater nitrate-N dynamics in two permeable agricultural catchments. *The Journal of Agricultural Science* **152**, 107-124.

Mellander, P.-E., Jordan, P., Shore, M., Melland, A.R., Shortle, G. (2015) Flow paths and phosphorus transfer pathways in two agricultural streams with contrasting flow controls. *Hydrological Processes* **29**, 3504-3518.

Mellander, P.E., Jordan, P., Shore, M., McDonald, N.T., Wall, D.P., Shortle, G., Daly, K. (2016) Identifying contrasting influences and surface water signals for specific groundwater phosphorus vulnerability. *Science of the Total Environment* **541**, 292-302.

Milliman, J.D., and Syvitski, J.P.M. (1992) Geomorphic/Tectonic control of sediment discharge to the ocean: the importance of small mountainous rivers. *Journal of Geology* **100**, 5, 525-544.

Minella, J.P.G., Walling, D.E., Merten, G.H. (2014) Establishing a sediment budget for a small agricultural catchment in southern Brazil, to support the development of effective sediment management strategies. *Journal of Hydrology* **519**, Part B, 2189-2201.

Motha, J.A., Wallbrink, P.J., Hairsine, P.B., Grayson, R.B. (2003) Determining the sources of suspended sediment in a forested catchment in southeastern Australia. *Water Resources Research* **39**, 1056.

Motha, J.A., Wallbrink, P.J., Hairsine, P.B., Grayson, R.B. (2004) Unsealed roads as suspended sediment sources in an agricultural catchment in south-eastern Australia. *Journal of Hydrology* **286**, 1-18.

Mukundan, R., Radcliffe, D.E., Ritchie, J.C., Risse, L.M., McKinley, R.A. (2010) Sediment Fingerprinting to Determine the Source of Suspended Sediment in a Southern Piedmont Stream. *Journal of Environmental Quality* **39**, 1328-1337.

Mukundan, R., Walling, D.E., Gellis, A.C., Slattery, M.C., Radcliffe, D.E. (2012) Sediment Source Fingerprinting: Transforming From a Research Tool to a Management Tool. *Journal of the American Water Resources Association* **48**, 1241-1257.

Mullan, D. (2013) Soil erosion under the impacts of future climate change: Assessing the statistical significance of future changes and the potential on-site and off-site problems. *Catena* **109**, 234-246.

Murphy, P.N.C., Mellander, P.E., Melland, A.R., Buckley, C., Shore, M., Shortle, G., Wall, D.P., Treacy, M., Shine, O., Mechan, S., Jordan, P. (2015) Variable response to phosphorus mitigation measures across the nutrient transfer continuum in a dairy grassland catchment. *Agriculture, Ecosystems & Environment* **207**, 192-202.

Navratil, O., Esteves, M., Legout, C., Gratiot, N., Nemery, J., Willmore, S., Grangeon, T. (2011) Global uncertainty analysis of suspended sediment monitoring using turbidimeter in a small mountainous river catchment. *Journal of Hydrology* **398**, 246-259.

Nearing, M., Pruski, F.F., O'Neal, M.R. (2004) Expected climate change impacts on soil erosion rates: A review. *Journal of Soil and Water Conservation* **59**, 43-50.

Nosrati, K., Govers, G., Ahmadi, H., Sharifi, F., Amoozegar, M.A., Merckx, R., Vanmaercke, M. (2011) An exploratory study on the use of enzyme activities as sediment tracers: biochemical fingerprints? *International Journal of Sediment Research* **26**, 136-151.

Nosrati, K., Govers, G., Semmens, B.X., Ward, E.J. (2014) A mixing model to incorporate uncertainty in sediment fingerprinting. *Geoderma* **217–218**, 173-180.

O'Sullivan, L., Creamer, R.E., Fealy, R., Lanigan, G., Simo, I., Fenton, O., Carfrae, J., Schulte, R.P.O. (2015) Functional Land Management for managing soil functions: A case-study of the trade-off between primary productivity and carbon storage in response to the intervention of drainage systems in Ireland. *Land Use Policy* **47**, 42-54.

Ockenden, M.C., Deasy, C., Quinton, J.N., Surridge, B., Stoate, C. (2014) Keeping agricultural soil out of rivers: Evidence of sediment and nutrient accumulation within field wetlands in the UK. *Journal of Environmental Management* **135**, 54-62.

Oeurng, C., Sauvage, S., Sánchez-Pérez, J.-M. (2010) Dynamics of suspended sediment transport and yield in a large agricultural catchment, southwest France. *Earth Surface Processes and Landforms* **35**, 1289-1301.

Official Journal of the European Union – OJEU (1991) Council Directive 91/676/EEC of 12 December 1991 concerning the protection of waters against pollution caused by nitrates from agricultural sources, EU, Brussels.

Official Journal of the European Union – OJEU (2000) Establishing a Framework for Community Action in the Field of Water Policy (Water Framework Directive), 2000/60/EC, EU, Brussels.

Official Journal of the European Union – OJEU (2006) Council Directive 2006/44/EC of the 6 September 2006 on the quality of fresh waters needing protection or improvement in order to support fish life, EU, Brussels.

Official Journal of the European Union – OJEU (2013) Council Directive 1305/2013 of 17 December 2013 on support for rural development by the European Agricultural Fund for Rural Development (EAFRD) and repealing Council Regulation (EC) No 1698/2005, EU, Brussels.

Onderka, M., Krein, A., Wrede, S., Martínez-Carreras, N., Hoffmann, L. (2012) Dynamics of storm-driven suspended sediments in a headwater catchment described by multivariable modeling. *Journal of Soils and Sediments* **12**, 620-635.

Owen, G.J., Perks, M.T., Benskin, C.M.H., Wilkinson, M.E., Jonczyk, J., Quinn, P.F. (2012) Monitoring agricultural diffuse pollution through a dense monitoring network in the River Eden Demonstration Test Catchment, Cumbria, UK. *Area* **44**, 443-453.

Owens, P.N., Duzant, J.H., Deeks, L.K., Wood, G.A., Morgan, R.P.C., Collins, A.J. (2007) Evaluation of contrasting buffer features within an agricultural landscape for reducing sediment and sediment-associated phosphorus delivery to surface waters. *Soil Use and Management* **23**, 165-175.

Palazón, L., Latorre, B., Gaspar, L., Blake, W.H., Smith, H.G., Navas, A. (2015) Comparing catchment sediment fingerprinting procedures using an auto-evaluation approach with virtual sample mixtures. *Science of the Total Environment* **532**, 456-466.

Palmer, R.C., Smith, R.P. (2013) Soil structural degradation in SW England and its impact on surface-water runoff generation. *Soil Use and Management* **29**, 567-575.

Panagos, P., Borrelli, P., Poesen, J., Ballabio, C., Lugato, E., Meusburger, K., Montanarella, L., Alewell, C. (2015) The new assessment of soil loss by water erosion in Europe. *Environmental Science & Policy* **54**, 438-447.

Parsons, A.J., Foster, I.D.L. (2011) What can we learn about soil erosion from the use of 137Cs? *Earth-Science Reviews* **108**, 101-113.

Perks, M.T., Owen, G.J., Benskin, C.M.H., Jonczyk, J., Deasy, C., Burke, S., Reaney, S.M., Haygarth, P.M. (2015) Dominant mechanisms for the delivery of fine sediment and phosphorus to fluvial networks draining grassland dominated headwater catchments. *Science of the Total Environment* **523**, 178-190.

Peukert, S., Griffith, B.A., Murray, P.J., Macleod, C.J., Brazier, R.E. (2014) Intensive management in grasslands causes diffuse water pollution at the farm scale. *Journal of Environmental Quality* **43**, 2009-2023.

Phillips, J.M., Russell, M.A., Walling, D.E. (2000) Time-integrated sampling of fluvial suspended sediment: a simple methodology for small catchments. *Hydrological Processes* **14**, 2589-2602.

Poesen, J.W.A., Verstraeten, G., Soenens, R., Seynaeve, L. (2001) Soil losses due to harvesting of chicory roots and sugar beet: an underrated geomorphic process? *Catena* **43**, 35-47.

Porto, P., Walling, D.E., Ferro, V. (2001) Validating the use of caesium-137 measurements to estimate soil erosion rates in a small drainage basin in Calabria, Southern Italy. *Journal of Hydrology* **248**, 93-108.

Porto, P., Walling, D.E., Tamburino, V., Callegari, G. (2003) Relating caesium-137 and soil loss from cultivated land. *Catena* **53**, 4, 303-326.

Powlson, D.S., Gregory, P.J., Whalley, W.R., Quinton, J.N., Hopkins, D.W., Whitmore, A.P., Hirsch, P.R., Goulding, K.W.T. (2011) Soil management in relation to sustainable agriculture and ecosystem services. *Food Policy* **36**, Supplement 1, S72-S87.

Pulley, S., Foster, I., Antunes, P. (2015) The uncertainties associated with sediment fingerprinting suspended and recently deposited fluvial sediment in the Nene river basin. *Geomorphology* **228**, 303-319.

Quinn, P.F., Beven, K.J. (1993) Spatial and temporal predictions of soil moisture dynamics, runoff, variable source areas and evapotranspiration for plynlimon, mid-wales. *Hydrological Processes* **7**, 425-448.

Quinton, J.N., Govers, G., Van Oost, K., Bardgett, R.D. (2010) The impact of agricultural soil erosion on biogeochemical cycling. *Nature Geoscience* **3**, 311-314.

Rachman, A., Anderson, S.H., Gantzer, C.J., Thompson, A.L. (2003) Influence of Long-term Cropping Systems on Soil Physical Properties Related to Soil Erodibility. *Soil Science Society of America Journal* **67**, 637-644.

Raymond, P.A., Oh, N.H., Turner, R.E., Broussard, W. (2008) Anthropogenically enhanced fluxes of water and carbon from the Mississippi River. *Nature* **451**, 449-452.

Regan, J.T., Rodgers, M., Healy, M.G., Kirwan, L., Fenton, O. (2010) Determining Phosphorus and Sediment Release Rates from Five Irish Tillage Soils. *Journal of Environmental Quality* **39**, 185-192.

Regan, J.T., Fenton, O., Healy, M.G. (2012) A review of phosphorus and sediment release from Irish tillage soils, the methods used to quanitfy losses and the current state of mitigation practice. *Biology and Environment: Proceedings of the Royal Irish Academy* **112(B)**, 157-183.

Rehg, K.J., Packman, A.I., Ren, J. (2005) Effects of suspended sediment characteristics and bed sediment transport on streambed clogging. *Hydrological Processes* **19**, 413-427.

Rickson, R.J. (2014) Can control of soil erosion mitigate water pollution by sediments? *Science of the Total Environment* **468–469**, 1187-1197.

Ritchie, J.C., McCarty, G.W. (2003) 137Cesium and soil carbon in a small agricultural watershed. *Soil and Tillage Research* **69**, 45-51.

Rowan, J.S., Black, S., Franks, S.W. (2012) Sediment fingerprinting as an environmental forensics tool explaining cyanobacteria blooms in lakes. *Applied Geography* **32**, 832-843.

Russell, M.A., Walling, D.E., Hodgkinson, R.A. (2001) Suspended sediment sources in two small lowland agricultural catchments in the UK. *Journal of Hydrology* **252**, 1-24.

Ruysschaert, G., Poesen, J., Verstraeten, G., Govers, G. (2004) Soil loss due to crop harvesting: significance and determining factors. *Progress in Physical Geography* **28**, 467-501.

Ruysschaert, G., Poesen, J., Verstraeten, G., Govers, G. (2007) Soil loss due to harvesting of various crop types in contrasting agro-ecological environments. *Agriculture, Ecosystems & Environment* **120**, 153-165.

Sanjari, G., Yu, B., Ghadiri, H., Ciesiolka, C.A.A., Rose, C.W. (2009) Effects of time-controlled grazing on runoff and sediment loss. *Soil Research* **47**, 796-808.

Schulte, R.P.O., Diamond, J., Holden, N.M., Brereton, A.J. (2005) Predicting the soil moisture conditions of Irish grasslands. *Irish Journal of Agricultural and Food Research* **44**, 95-110.

Schulte, R.P.O., Creamer, R.E., Donnellan, T., Farrelly, N., Fealy, R., O'Donoghue, C., O'hUallachain, D. (2014) Functional land management: A framework for managing soil-based ecosystem services for the sustainable intensification of agriculture. *Environmental Science & Policy* **38**, 45-58.

Sherriff, S.C., Rowan, J.R., Franks, S.W., Walden, J., Melland, A.R., Jordan, P., Ó hUallacháin, D. (2014) Sediment Fingerprinting. *TResearch*, Summer 2014, 40-41.

Sherriff, S.C., Rowan, J.S., Melland, A.R., Jordan, P., Fenton, O., Ó hUallacháin, D. (2015a) Investigating suspended sediment dynamics in contrasting agricultural catchments using ex situ turbidity-based suspended sediment monitoring *Hydrology and Earth System Sciences* **19**, 3349–3363.

Sherriff, S., Franks, S., Rowan, J., Fenton, O., Ó'hUallacháin, D. (2015b) Uncertainty-based assessment of tracer selection, tracer non-conservativeness and multiple solutions in sediment fingerprinting using synthetic and field data. *Journal of Soils and Sediments* **15**, 2101-2116.

Shore, M., Murphy, P.N.C., Jordan, P., Mellander, P.E., Kelly-Quinn, M., Cushen, M., Mechan, S., Shine, O., Melland, A.R. (2013) Evaluation of a surface hydrological connectivity index in agricultural catchments. *Environmental Modelling & Software* **47**, 7-15.

Shore, M., Jordan, P., Mellander, P.E., Kelly-Quinn, M., Wall, D.P., Murphy, P.N.C., Melland, A.R. (2014) Evaluating the critical source area concept of phosphorus loss from soils to water-bodies in agricultural catchments. *Science of the Total Environment* **490**, 405-415.

Shore, M., Jordan, P., Mellander, P.E., Kelly-Quinn, M., Melland, A.R. (2015) An agricultural drainage channel classification system for phosphorus management. *Agriculture, Ecosystems & Environment* **199**, 207-215.

Silgram, M., Jackson, D.R., Bailey, A., Quinton, J., Stevens, C. (2010) Hillslope scale surface runoff, sediment and nutrient losses associated with tramline wheelings. *Earth Surface Processes and Landforms* **35**, 699-706.

Sleeman, A.G., and Pracht, M. (1995) Geology of South Cork, Sheet 25. Geological Survey of Ireland: Dublin, Ireland.

Small, I.F., Rowan, J.S., Franks, S.W. (2002) Quantitative sediment fingerprinting using a Bayesian uncertainty estimation framework. In: Dyer FJ, Thoms MC, Olley JM (eds.) The structure, function and management implications of fluvial sedimentary systems, IAQHS Publications no. 276. IAHS, Wallingford, pp 443-450.

Small, I.F., Rowan, J.S., Franks, S.W., Wyatt, A., Duck, R.W. (2004) Bayesian sediment fingerprinting provides a robust tool for environmental forensic geoscience applications. Geological Society, London, Special Publications 232, 207-213.

Smith, H.G., Blake, W.H. (2014) Sediment fingerprinting in agricultural catchments: A critical re-examination of source discrimination and data corrections. *Geomorphology* **204**, 177-191.

Smith, T. B., Owens, P.N. (2014) Flume- and field-based evaluation of a time-integrated suspended sediment sampler for the analysis of sediment properties. *Earth Surface Processes and Landforms* **39**, 1197-1207.

Smith, R., Gross, K., Robertson, G.P. (2008) Effects of Crop Diversity on Agroecosystem Function: Crop Yield Response. *Ecosystems* **11**, 355-366.

Soane, B.D., Ball, B.C., Arvidsson, J., Basch, G., Moreno, F., Roger-Estrade, J. (2012) No-till in northern, western and south-western Europe: A review of problems and opportunities for crop production and the environment. *Soil and Tillage Research* **118**, 66-87.

Spink, J., Hackett, R., Forrestal, D. and Creamer, R. (2010) Soil Organic Carbon: A review of ‘critical levels and practices to increase levels in tillage Land in Ireland Teagasc, Oak Park, Crops Research Centre, Co Carlow. (http://www.teagasc.ie/publications/2010/982/SoilOrganicCarbon.pdf).

Steegen, A., Govers, G., Nachtergaele, J., Takken, I., Beuselinck, L., Poesen, J. (2000) Sediment export by water from an agricultural catchment in the Loam Belt of central Belgium. *Geomorphology* **33**, 25-36.

Steele-Dunne, S., Lynch, P., McGrath, R., Semmler, T., Wang, S., Hanafin, J., Nolan, P. (2008) The impacts of climate change on hydrology in Ireland. *Journal of Hydrology* **356**, 28-45.

Takenaka, C., Onda, Y., Hamajima, Y. (1998) Distribution of cesium-137 in Japanese forest soils: Correlation with the contents of organic carbon. *Science of the Total Environment* **222**, 193-199.

Teagasc (2015) Good Agricultural & Environmental Condition (GAEC), http://www.teagasc.ie/environment/cross_compliance/GAEC.asp [accessed 22.11.15].

Theuring, P., Collins, A.L., Rode, M. (2015) Source identification of fine-grained suspended sediment in the Kharaa River basin, northern Mongolia. *Science of the Total Environment* **526**, 77-87.

Thomas, I., Jordan, P., Mellander, P.-E., Fenton, O.,, Shine, O., Ó hUallacháin D., Dunlop, P., Murphy, P.N.C. (2015) Identifying hydrologically sensitive areas using LiDAR DEMs to mitigate critical source areas of diffuse pollution: a policy-applicable index. Catchment Science into Policy Conference, 23rd-25th September, Wexford, Ireland.

Thompson, J., Cassidy, R., Doody, D.G., Flynn, R. (2013) Predicting critical source areas of sediment in headwater catchments. *Agriculture, Ecosystems & Environment* **179**, 41-52.

Thompson, J., Cassidy, R., Doody, D.G., Flynn, R. (2014) Assessing suspended sediment dynamics in relation to ecological thresholds and sampling strategies in two Irish headwater catchments. *Science of the Total Environment* **468–469**, 345-357.

Tietzsch-Tyler, D., Sleeman, A.G., McConnell, B.J., Daly, E.P., Flegg A.M., O'Connor P.J., Warren W.P. (1994) Geology of Carlow-Wexford, Sheet 19. Geological Survey of Ireland: Dublin, Ireland.

Tilman, D., Downing, J.A. (1994) Biodiversity and stability in grasslands. *Nature* **367**, 363-365.

Tilman, D., Cassman, K.G., Matson, P.A., Naylor, R., Polasky, S. (2002) Agricultural sustainability and intensive production practices. *Nature* **418**, 671-677.

Trimble, S.W., Mendel, A.C. (1995) The cow as a geomorphic agent — A critical review. *Geomorphology* **13**, 233-253.

Tuğrul, K.M., İçöz, E., Perendeci, N.A. (2012) Determination of soil loss by sugar beet harvesting. *Soil and Tillage Research* **123**, 71-77.

Tuohy, P., Fenton, O., O'Loughlin, J., Humphreys, J. (2013) Land Drainage – A farmer's practical guide to draining grassland in Ireland. Teagasc, Moorepark.

Tuohy, P., Humphreys, J., Holden, N.M., Fenton, O. (2015) Mole drain performance in a clay loam soil in Ireland. *Acta Agriculturae Scandinavica, Section B — Soil & Plant Science* **65**, 2-13.

USEPA (1996) SW-846 Method 3052: microwave assisted acid digestion of siliceous and organically based matricies. U.S. Gov. Print Office, Washington.

Van Oost, K., Van Muysen, W., Govers, G., Deckers, J., Quine, T.A. (2005) From water to tillage erosion dominated landform evolution. *Geomorphology* **72**, 193-203.

Van Oost, K., Govers, G., De Alba, S., Quine, T.A. (2006) Tillage erosion: a review of controlling factors and implications for soil quality. *Progress in Physical Geography* **30**, 443-466.

Van Oost, K., Quine, T.A., Govers, G., De Gryze, S., Six, J., Harden, J.W., Ritchie, J.C., McCarty, G.W., Heckrath, G., Kosmas, C., Giraldez, J.V., da Silva, J.R.M., Merckx, R. (2007) The Impact of Agricultural Soil Erosion on the Global Carbon Cycle. *Science* **318**, 626-629.

Van Oost, K., Cerdan, O., Quine, T.A. (2009) Accelerated sediment fluxes by water and tillage erosion on European agricultural land. *Earth Surface Processes and Landforms* **34**, 1625-1634.

Vanmaercke, M., Poesen, J., Verstraeten, G., de Vente, J., Ocakoglu, F. (2011) Sediment yield in Europe: Spatial patterns and scale dependency. *Geomorphology* **130**, 142-161.

Vanmaercke, M., Poesen, J., Radoane, M., Govers, G., Ocakoglu, F., Arabkhedri, M. (2012) How long should we measure? An exploration of factors controlling the inter-annual variation of catchment sediment yield. *Journal of Soils and Sediments* **12**, 603-619.

Veihe, A., Jensen, N.H., Schiøtz, I.G., Nielsen, S.L. (2011) Magnitude and processes of bank erosion at a small stream in Denmark. *Hydrological Processes* **25**, 1597-1613.

Verheijen, F.G.A., Jones, R.J.A., Rickson, R.J., Smith, C.J. (2009) Tolerable versus actual soil erosion rates in Europe. *Earth-Science Reviews* **94**, 23-38.

Vero, S.E., Ibrahim, T.G., Creamer, R.E., Grant, J., Healy, M.G., Henry, T., Kramers, G., Richards, K.G., Fenton, O. (2014) Consequences of varied soil hydraulic and meteorological complexity on unsaturated zone time lag estimates. *Journal of Contaminant Hydrology* **170**, 53-67.

Verstraeten, G., Poesen, J. (2001) Factors controlling sediment yield from small intensively cultivated catchments in a temperate humid climate. *Geomorphology* **40**, 123-144.

Vinten, A.J.A., Loades, K., Addy, S., Richards, S., Stutter, M., Cook, Y., Watson, H., Taylor, C., Abel, C., Baggaley, N., Ritchie, R., Jeffrey, W. (2014) Reprint of: Assessment of the use of sediment fences for control of erosion and sediment phosphorus loss after potato harvesting on sloping land. *Science of the Total Environment* **468–469**, 1234-1244.

Vongvixay, A., Grimaldi, C., Gascuel-Odoux, C., Laguionie, P., Faucheux, M., Gilliet, N., Mayet, M., (2010) Analysis of suspended sediment concentration and discharge relations to identify particle origins in small agricultural watersheds, Sediment Dynamics for a Changing Future: Proceedings of the ICCE symposium held at Warsaw University of Life Sciences-SGGW, Poland, pp. 14-18.

Vought, L.M., Lacoursière, J., (2010) Restoration of Streams in the Agricultural Landscape, in: Eiseltová, M. (Ed.), Restoration of Lakes, Streams, Floodplains, and Bogs in Europe. Springer Netherlands, pp. 225-242.

Wall, D., Jordan, P., Melland, A.R., Mellander, P.E., Buckley, C., Reaney, S.M., Shortle, G. (2011) Using the nutrient transfer continuum concept to evaluate the European Union Nitrates Directive National Action Programme. *Environmental Science & Policy* **14**, 664-674.

Walling, D.E. (1983) The sediment delivery problem. *Journal of Hydrology* **65**, 209-237.

Walling, D.E. (2005) Tracing suspended sediment sources in catchments and river systems. *Science of the Total Environment* **344**, 159-184.

Walling, D. (2013) The evolution of sediment source fingerprinting investigations in fluvial systems. *Journal of Soils and Sediments* **13**, 1658-1675.

Walling, D., Collins, A. (2008a) The catchment sediment budget as a management tool. *Environmental Science & Policy* **11**, 136-143.

Walling, D.E., Collins, A.L. (2008b) The catchment sediment budget as a management tool. *Environmental Science & Policy* **11**, 136-143.

Walling, D.E., He, Q. (1997) Use of fallout 137Cs in investigations of overbank sediment deposition on river floodplains. *Catena* **29**, 263-282.

Walling, D.E., Leeks, G.J.L. (1999) River Basin Sediment Dynamics and Interactions within the UK Land-Ocean Interaction Study : The Context. *Hydrological Processes* **13**, 931-934.

Walling, D.E., Quine, T.A. (1990) Calibration of caesium-137 measurements to provide quantitative erosion rate data. *Land Degradation & Development* **2**, 161-175.

Walling, D. E., Quine, T.A. (1992) The use of caesium-137 measurements in soil erosion surveys, IAHS Publ no. 210, IAHS, Wallingford, pp. 143–152.

Walling, D.E., Webb, B.W., (1988) The reliability of rating curve estimates of suspended sediment yield: some further comments, in: Bordas, M., Walling, D.E. (Eds.), Sediment budgets, Porto Alegre, pp. 337-350.

Walling, D.E., Woodward, J.C., Nicholas, A.P. (1993) A multi-parameter approach to fingerprinting suspended-sediment sources. In: Peters NE, Hoehn E, Leibundgut C, Tase N, wallding DE (eds.) *Tracers in Hydrology*, IAHS Publication no.215, IAHS, Wallingford, pp. 329-337.

Walling, D.E., Owens, P.N., Leeks, G.J.L. (1999) Fingerprinting suspended sediment sources in the catchment of the River Ouse, Yorkshire, UK. *Hydrological Processes* **13**, 955-975.

Walling, D. E., Russell, M. A., Hodgkinson, R. A., Zhang, Y. (2002) Establishing sediment budgets for two small lowland agricultural catchments in the UK. *Catena* **47**, 323–353.

Walling, D.E., Zhang, Y, He, Q. (2005) Models for Converting Measurements of Environmental Radionuclide Inventories (^{137}Cs, Excess ^{210}Pb and ^{7}Be) to Estimates of Soil Erosion and Deposition Rates (Including Software for Model Implementation. University of Exeter.

Walling, D. E., Webb, B., Shanahan, J. (2007) Investigations into the use of critical sediment yields for assessing and managing fine sediment inputs into aquatic ecosystems. *Natural England Research Reports, Number 007*.

Walling, D.E., Collins, A.L., Stroud, R.W. (2008) Tracing suspended sediment and particulate phosphorus sources in catchments. *Journal of Hydrology* **350**, 274-289.

Walling, D.E., Porto, P., Zhang, Y., Du, P. (2014) Upscaling the Use of Fallout Radionuclides in Soil Erosion and Sediment Budget Investigations: Addressing the Challenge. *International Soil and Water Conservation Research* **2**, 1-21.

Warsta, L., Taskinen, A., Koivusalo, H., Paasonen-Kivekäs, M., Karvonen, T. (2013) Modelling soil erosion in a clayey, subsurface-drained agricultural field with a three-dimensional FLUSH model. *Journal of Hydrology* **498**, 132-143.

Wass, P.D., Leeks, G.J.L. (1999) Suspended sediment fluxes in the Humber catchment, UK. *Hydrological Processes* **13**, 935-953.

Wilkinson, S.N., Wallbrink, P.J., Hancock, G.J., Blake, W.H., Shakesby, R.A., Doerr, S.H. (2009) Fallout radionuclide tracers identify a switch in sediment sources and transport-limited sediment yield following wildfire in a eucalypt forest. *Geomorphology* **110**, 140-151.

Wilkinson, S.N., Hancock, G.J., Bartley, R., Hawdon, A.A., Keen, R.J. (2013) Using sediment tracing to assess processes and spatial patterns of erosion in grazed rangelands, Burdekin River basin, Australia. *Agriculture, Ecosystems & Environment* **180**, 90-102.

Williams, G.P. (1989) Sediment concentration versus water discharge during single hydrologic events in rivers. *Journal of Hydrology* **111**, 89-106.

Wilson, C.G., Kuhnle, R.A., Bosch, D.D., Steiner, J.L., Starks, P.J., Tomer, M.D., Wilson, G.V. (2008) Quantifying relative contributions from sediment sources in Conservation Effects Assessment Project watersheds. *Journal of Soil and Water Conservation* **63**, 523-532.

Wiskow, E., van der Ploeg, R.R. (2003) Calculation of drain spacings for optimal rainstorm flood control. *Journal of Hydrology* **272**, 163-174.

Withers, P.J.A., Hodgkinson, R.A., Bates, A., Withers, C.M. (2006) Some effects of tramlines on surface runoff, sediment and phosphorus mobilization on an erosion-prone soil. *Soil Use and Management* **22**, 245-255.

Zabaleta, A., Martínez, M., Uriarte, J.A., Antigüedad, I. (2007) Factors controlling suspended sediment yield during runoff events in small headwater catchments of the Basque Country. *Catena* **71**, 179-190.

Zhang, X., Zhang, Y., Wen, A., Feng, M. (2003) Assessment of soil losses on cultivated land by using the 137Cs technique in the Upper Yangtze River Basin of China. *Soil and Tillage Research* **69**, 99-106.

Zhang, X.C., Zhang, G.H., Wei, X., Guan, Y.H. (2015a) Evaluation of cesium-137 conversion models and parameter sensitivity for erosion estimation. *Journal of Environmental Quality* **44**, 789-802.

Zhang, X.C. (2015b) New Insights on using Fallout Radionuclides to Estimate Soil Redistribution Rates. *Soil Science Society of America Journal* **79**, 1-8.

Zhang, X.C., Zhang, G.H., Wei, X. (2015c) How to make 137Cs erosion estimation more useful: An uncertainty perspective. *Geoderma* **239–240**, 186-194.

Appendix 1

Hydrol. Earth Syst. Sci., 19, 3349–3363, 2015
www.hydrol-earth-syst-sci.net/19/3349/2015/
doi:10.5194/hess-19-3349-2015

Hydrology and Earth System Sciences

Investigating suspended sediment dynamics in contrasting agricultural catchments using ex situ turbidity-based suspended sediment monitoring

S. C. Sherriff[1,2], J. S. Rowan[2], A. R. Melland[3], P. Jordan[4,5], O. Fenton[1], and D. Ó hUallacháin[1]

[1]Johnstown Castle Research Centre, Teagasc, Wexford, Ireland
[2]School of the Environment, University of Dundee, Dundee, DD1 4HN, Scotland, UK
[3]National Centre for Engineering in Agriculture, University of Southern Queensland, Toowoomba, Australia
[4]School of Environmental Sciences, Ulster University, Coleraine, Co. Derry, BT52 1SA, UK
[5]Agricultural Catchments Programme, Johnstown Castle Research Centre, Teagasc, Wexford, Ireland

Correspondence to: S. C. Sherriff (sophie.sherriff@teagasc.ie)

Received: 12 February 2015 – Published in Hydrol. Earth Syst. Sci. Discuss.: 3 March 2015
Revised: 6 July 2015 – Accepted: 9 July 2015 – Published: 3 August 2015

Abstract. Soil erosion and suspended sediment (SS) pose risks to chemical and ecological water quality. Agricultural activities may accelerate erosional fluxes from bare, poached or compacted soils, and enhance connectivity through modified channels and artificial drainage networks. Storm-event fluxes dominate SS transport in agricultural catchments; therefore, high temporal-resolution monitoring approaches are required, but can be expensive and technically challenging. Here, the performance of in situ turbidity sensors, conventionally installed submerged at the river bankside, is compared with installations where river water is delivered to sensors ex situ, i.e. within instrument kiosks on the riverbank, at two experimental catchments (Grassland B and Arable B). The in situ and ex situ installations gave comparable results when calibrated against storm-period, depth-integrated SS data, with total loads at Grassland B estimated at 12 800 and 15 400 t, and 22 600 and 24 900 t at Arable B, respectively. The absence of spurious turbidity readings relating to bankside debris around the in situ sensor and its greater security make the ex situ sensor more robust. The ex situ approach was then used to characterise SS dynamics and fluxes in five intensively managed agricultural catchments in Ireland which feature a range of landscape characteristics and land use pressures. Average annual suspended sediment concentration (SSC) was below the Freshwater Fish Directive (78/659/EEC) guideline of 25 mg L^{-1}, and the continuous hourly record demonstrated that exceedance occurred less than 12 % of the observation year. Soil drainage class and proportion of arable land were key controls determining flux rates, but all catchments reported a high degree of inter-annual variability associated with variable precipitation patterns compared to the long-term average. Poorly drained soils had greater sensitivity to runoff and soil erosion, particularly in catchments with periods of bare soils. Well drained soils were less sensitive to erosion even on arable land; however, under extreme rainfall conditions, all bare soils remain a high sediment loss risk. Analysis of storm-period and seasonal dynamics (over the long term) using high-resolution monitoring would be beneficial to further explore the impact of landscape, climate and land use characteristics on SS export.

1 Introduction

Excessive supply of fine sediments (<125 µm) and sediment-associated pollutants are detrimental to aquatic ecosystems (Wood and Armitage, 1997; Collins et al., 2011; Kemp et al., 2011). Elevated suspended sediment (SS) concentrations decrease light penetration and can reduce primary productivity. Deposition of sediments onto river channel beds also degrades habitat quality for benthic species and spawning fish (Bilotta and Brazier, 2008). In the European Union, the Water Framework Directive (WFD – OJEU, 2000) requires that

Published by Copernicus Publications on behalf of the European Geosciences Union.

water quality meet a "good" standard, but no binding environmental standards yet exist for SS across member states (Brils, 2008; Collins and Anthony, 2008). In rivers, the EU Freshwater Fish Directive (FFD – OJEU, 2006) introduced a mean annual threshold of 25 mg L^{-1}, but this was subsequently repealed. Phosphorus (P) targets are, however, binding and because of its strong affinity for particulate transport, catchment sediment fluxes are an essential area of research.

Agriculture is commonly linked with elevated rates of soil erosion (Foster et al., 2011; Glendell and Brazier, 2014), but the degree to which sediment exports from catchments can be attributed to specific land-management practices is challenging to measure (Rowan et al., 2012). Catchments exhibit complex responses to different land uses, (e.g. arable or grazing practices) which are further influenced by climate, landscape setting and topographic controls (Wass and Leeks, 1999). A comprehensive evaluation of the extent of erosion and elevated sediment supply, therefore, requires a robust determination of sediment flux (Navratil et al., 2011), knowledge of the sources and fate of fine sediments within the system (Walling, 2005), and an appreciation of the risks that elevated concentrations present to aquatic ecosystems (Bilotta and Brazier, 2008). This evidence base can be used to better inform integrated land, water and sediment management strategies.

Sediment losses from agricultural areas are commonly attributed to arable practices (Walling et al., 1999; Wass and Leeks, 1999; Freebairn et al., 2009; Van Oost et al., 2009; Duvert et al., 2010), especially where bare or freshly tilled soils are exposed to rainfall-runoff processes (Regan et al., 2012). Arable farming typically involves the mechanical redistribution of soil through ploughing and seed bed preparation, and via erosion from compacted and/or bare fields and down-slope tramlines (Chambers and Garwood, 2000; Withers et al., 2006; Boardman et al., 2009; Silgram et al., 2010; Regan et al., 2012; Soane et al., 2012). Over-grazed grassland soils are also an important sediment source (Bilotta et al., 2010) and critical to the transport of particle-bound pollutants, such as P (Haygarth et al., 2006). Poaching of soils by livestock, particularly cattle wintered outside, results in loss of soil structure and compaction around gates, drinking troughs and, where access is not restricted, channel banks (Trimble and Mendel, 1995; Evans et al., 2006).

Erosion risk is conditioned by physical catchment characteristics (soil type and hydrology), and erodibility determined by physiography (slope length, steepness and shape, ground cover and soil management). Soil drainage class, for example, is dictated by landscape position whereby well drained soils, such as Brown Earths and Podzols commonly located on hillslopes, contribute sediment predominantly through sub-surface pathways such as relocation of fine surface sediments vertically and/or horizontally through the soil profile, and preferential flow through macropores (Chapman et al., 2001; Deasy et al., 2009). Conversely, poorly drained soils, such as Gleys (surface and groundwater) and silt and clay dominated alluvial soils in proximity to watercourses, are at greater risk of overland-flow generation and surface soil erosion due to reduced infiltration capacity. The installation of surface and sub-surface drains can also alter natural flow pathways (Ibrahim et al., 2013). Drainage installation and maintenance, for example, can result in faster quick-flow, resulting in an increased likelihood of more frequent, higher magnitude and short duration sediment transfers associated with storm runoff (Wiskow and van der Ploeg, 2003; Deasy et al., 2009; Florsheim et al., 2011).

To accurately quantify sediment fluxes from complex catchments, field monitoring programmes require three considerations. Firstly, robust flow and suspended sediment concentration (SSC) data capable of accurately describing short-term fluxes (Navratil et al., 2011). Secondly, the duration of the measurements must be sufficiently long to be "representative" of either stationary long-term averages (inclusive of natural variability), or to reveal temporal trends of increasing or decreasing loads or concentrations. Capturing crucial high-magnitude, low-frequency events is, therefore, vital to generating meaningful flux determinations (Walling and Webb, 1988; Wass and Leeks, 1999). Thirdly, monitoring programmes need to be operationally cost-effective.

Sediment load estimation based on SSC-discharge rating curves has been widely superseded by catchment outlet and near-continuous turbidity monitoring (Lewis, 2003; Jarstram et al., 2010; Melland et al., 2012a). The latter requires turbidity sensors, loggers and infrastructure that cope with issues such as debris interference, bio-fouling, power outages and equipment/data security (Wass and Leeks, 1999; Jordan et al., 2007; Owen et al., 2012). Assessment of new monitoring strategies, compared to traditional in situ turbidity-SSC monitoring programmes, is essential to assess improvements and limitations, and to validate their implementation.

There have been relatively few sediment flux investigations in Ireland (Melland et al., 2012a; Harrington and Harrington, 2013; Thompson et al., 2014). Initially regulated and managed through the Nitrates Directive (OJEU, 1991, 2007), the transfer of diffuse agricultural pollutants across the EU is now primarily integrated into obligations under the WFD. In Ireland, soil conservation issues also fall under the Nitrates Directive regulations, but the impact of SS in rivers is commonly compared to the repealed FFD target due to the absence of explicit sediment targets within the WFD.

As part of an experiment to evaluate the Nitrates Directive in Ireland, a common experimental design across six agricultural catchments included high temporal-resolution measurements of river nutrient and sediment exports (Wall et al., 2011). Using these catchments and data, the aims of this study were (1) to assess the efficacy of a novel ex situ SS monitoring technique in two catchments and (2) to investigate annual average sediment concentrations and loads in relation to soil drainage class and land use in five monitored catchments. One catchment situated in low-relief karst terrain was omitted from this study due to intermittent runoff

combined with very low SS concentrations (cf. Mellander et al., 2012).

2 Study location

Suspended sediment monitoring was conducted in five catchments (Table 1) across Ireland (Fig. 1). Catchments were selected to represent the main intensive agricultural land use types in Ireland and dominant hydrological pathways (surface or sub-surface) at a scale where headwater to channel hydrological process were detectable (Fealy et al., 2010). The characteristics of individual catchments are summarised as follows.

Grassland A catchment (7.9 km^2) is located in south-western Ireland (51°38′ N, 8°47′ W). Catchment soils are predominantly shallow well drained Brown Earths and Podzols with loam dominating the texture of A- and B-horizons, and smaller areas of Surface Water Gleys at the base of hillslopes. A coarse loamy drift with siliceous stone subsoil is underlain by Devonian old red sandstones and mudstones from the Toe Head and Castlehaven formations (Sleeman and Pracht, 1995), which form an unconfined productive aquifer (Mellander et al., 2014). Sub-surface water pathways are therefore dominant. Land is predominantly grazed by cattle for intensive dairy production and smaller areas of beef production with an average catchment stocking rate of 1.98 livestock units (LU) ha^{-1}; additionally, minor areas of arable land use are present (Table 1).

Grassland B catchment (11.0 km^2) is located in south-eastern Ireland (52°36′ N, 6°20′ W). Soil type is predominantly poorly drained Groundwater Gleys in the catchment lowlands with a clay loam texture in A- and B-horizons resulting from a clayey calcareous Irish Sea till subsoil. The uplands contain smaller areas of well drained Brown Earths; these soils are underlain by drift deposits with siliceous stones. The underlying geology is permeable, dominated by Ordovician volcanics and metasediments of the Campile formation (Tietzsch-Tyler et al., 1994), which form a productive aquifer with faults (Mellander et al., 2012). Artificial drainage is a key feature including open drains, defined here as ditches, and closed, sub-surface piped drains (predominantly 80 mm diameter). Grassland B is considered to be dominated by overland flow pathways (Mellander et al., 2012; Shore et al., 2013) except for areas of well drained soils featuring sub-surface transport pathways. Land is predominantly grass-based for dairy and beef cattle grazing, and also sheep enterprises (Shore et al., 2013) with a stocking rate of 1.04 LU ha^{-1}. Arable crops such as spring barley are common on the well drained soils which are unmanaged between harvest and ploughing for the following crop.

Grassland C catchment (3.3 km^2) is located in north-eastern Ireland (54°01′ N, 6°51′ W). Soils are mainly deep and moderately to poorly drained, characterised by a loam A-horizon texture and clay loam B-horizon and areas of shallow well drained soils in the upper catchment areas underlain predominately by Lower Palaeozoic shale tills. The geology is Silurian metasediments and volcanics of the Shercock Formation (Geraghty et al., 1997), which create an unproductive aquifer. Overland flow and near-surface pathways are, therefore, dominant here. Land use is principally grass based for dairy cattle, sheep and beef cattle grazing (stocking rate 1.00 LU ha^{-1}).

Arable A catchment (11.2 km^2) is located in south-eastern Ireland (52°34′ N, 6°36′ W). Soils are predominantly shallow well drained Brown Earths with loam texture dominating the A- and B-horizons, and limited areas of poorly drained groundwater Gleys around the stream corridor to the east of the catchment (Melland et al., 2012a). Subsoils predominantly comprise fine loamy drift with siliceous stones over slate and silt stones of the Oaklands Formation (Tietzsch-Tyler et al., 1994), which produces a poorly productive aquifer. The well drained soils result in below-ground hydrological transfers, particularly bedrock fissure flow (Mellander et al., 2012). Artificial drainage is limited to the poorly drained soil areas and comprises open ditches and sub-surface piped drainage. Land use is dominated by spring barley (land is unmanaged between cropping cycles and crop rotation is limited) with areas of permanent grassland for beef cattle and sheep grazing in more poorly drained areas (Melland et al., 2012a) at 0.40 LU ha^{-1}.

Arable B catchment (9.5 km^2) is located in north-eastern Ireland (53°49′ N, 6°27′ W). The soil type is a complex pattern of poorly to moderately drained soils (Melland et al., 2012a). Loam soil texture dominates the A-horizon and clay loams are dominant in the B-horizon. Subsoil is dominated by fine till containing siliceous stones with fluvioglacial sediments located near-channel. Soils are underlain by calcareous greywacke and banded mudstone geology (McConnell et al., 2001) and produce a poorly productive aquifer (Mellander et al., 2012). Hydrologically, surface pathways dominate; however, below-ground pathways may also be important, especially during winter (Melland et al., 2012a; Mellander et al., 2012). Artificial drainage is dominant, particularly in the poorly drained catchment areas. Arable land is dominated by winter-sown cereals, but also comprises maize and potatoes. These areas are unmanaged between cropping cycles; however, crop rotation is more common than at Arable A due to the wider range of crop types. Additional areas of permanent grassland are utilised for dairy cattle, beef cattle, and sheep grazing (0.77 LU ha^{-1}).

3 Materials and methods

3.1 Suspended sediment monitoring

Monitoring for SS at catchment outlets was initiated in 2009 for Grassland B, Arable A and Arable B catchments and 2010 for Grassland A and Grassland C catchments. All catch-

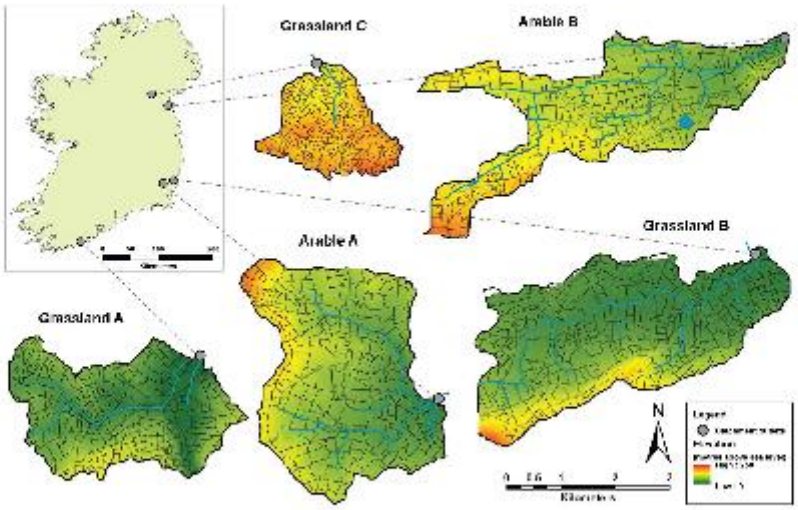

Figure 1. Map of catchment monitoring locations and study catchments with topographic and field size information.

ments had identical instrumentation deployed for temporally high-resolution nutrient, conductivity, temperature and turbidity data capture using bankside analysers mains powered at 230 V (Fig. 2; Wall et al., 2011; Jordan et al., 2012; Melland et al., 2012b). Turbidity (T) data were collected using a turbidity sensor (Solitax, Hach-Lange, Germany; range 0–4000 NTU; factory calibrated to 1000 NTU) and SC1000 controller at 10 min intervals. The sensors were located out-of-stream (ex situ) in a rapidly and continuously circulating header tank with river water delivered from the channel by an in-stream pump (30 $m^3 h^{-1}$) located on the channel bed. The instrument tank was assumed well mixed as no particulate deposition occurred. Turbidity probes were fitted with wipers to prevent biological fouling, and checked monthly against deionised water (0 NTU) and a 20 NTU Formazin turbidity standard. Synchronised discharge data (Q – $m^3 s^{-1}$) were calculated from vented pressure-transducer stage measurements (OTT Orpheus-mini; OTT Germany). Stage height was converted to Q using velocity-area measurements (OTT Acoustic Doppler Current meter; OTT Germany) collected over non-standard flat-v weirs (custom made, Corbett Concrete, Ireland) and WISKI-SKED software (Grassland A, $R^2 = 0.96$, $n = 272$; Grassland B, $R^2 = 1$, $n = 166$ (Mellander et al., 2015); Grassland C, $R^2 = 0.95$ and 0.97, $n = 316$; Arable A, $R^2 = 1$, $n = 376$ (Mellander et al., 2015); Arable B, $R^2 = 0.94$ and 1, $n = 493$). Both Grassland C and Arable B had changing controls at higher discharges and WISKI-SKED provided two parts to the curves with two R^2 coefficients.

Turbidity units (NTU) were field-calibrated to SSC (mg L^{-1}) using a combination of regular low-flow samples (at least fortnightly since programme initiation) and intensive sampling during high magnitude flow events with elevated SSCs. In all cases, water samples were collected from the instrument tank either manually, or using a programmable automatic water sampler (ISCO 6712; ISCO Inc. USA) with a 1 m pumping tube (pump capacity ~ 0.9 m s^{-1}) at predefined intervals of 30 or 60 min according to the specific storm characteristics. High SSC data capture was further targeted in Grassland B and Arable B using a turbidity-stratified sampling programme, whereby collection of 1000 mL samples was triggered when T measurements were within threshold turbidity bands of 140 to 160 NTU, 240 to 260 NTU, 480 to 530 NTU and 700 to 800 NTU. This circumvented the need to pre-set water samplers according to forecasted event characteristics. Water samples were stored at 4 °C on return to the laboratory before a sub-sample (minimum 100 mL) was processed for SSC. Whatman GF/C glass-fibre filter papers (1.2 µm) were pre-dried at 105 °C for 1 h, cooled in a desiccator and weighed before being used for vacuum filtration. Sediment concentrations were calculated from the weight of residue retained on the filter post-filtration once dried > 12 h at 105 °C and cooled in a desiccator.

3.2 Method comparison

In order to compare the ex situ sampling methodology described above with the conventional in situ monitoring approach, additional instrumentation to measure T was in-

Table 1. Summary of study catchments.

Catchment	Size	30-year average rainfall[a]	Median slope	Dominant soil		Land use	Landscape complexity features			
				Drainage class *Hydrological flow pathway*			Average field size	Average maximum downslope length	Hedgerow density	Ditch density
	(km^2)	($mm\ yr^{-1}$)	(°)					(m)	($km\ km^{-2}$)	($km\ km^{-2}$)
Grassland A	7.9	1228	4	Well drained *Sub-surface*		89 % grassland predominantly for dairy cattle; 5 % arable	2.00	170	0.061	1.7
Grassland B	11.5	906	3	Poorly drained *Surface*		77 % grassland for dairy cattle, beef cattle and sheep; 12 % spring crops; 2 % winter crops	3.04	189	0.011	5.7[b]
Grassland C	3.3	960	6	Moderately to poorly drained *Surface*		94 % grassland for beef cattle, dairy cattle and sheep	1.12	114	0.044	2.6
Arable A	11.2	906	3	Well drained *Sub-surface*		54 % arable predominantly spring crops; 39 % grassland mainly for beef cattle and sheep	3.32	194	0.011	1.3[b]
Arable B	9.4	758	3	Poorly drained *Surface*		42 % arable crops; 29 % grazing for beef cattle and sheep; 19 % dairy cattle grazing	2.70	200	0.011	2.3

[a] 1981–2010 mean annual rainfall; [b] from Shore et al. (2013)

Figure 2. Picture of in situ and ex situ suspended sediment and discharge instrumentation at Grassland B.

stalled in Grassland B and Arable B from September to December 2012, and December 2012 to March 2013, respectively. A turbidimeter (T_{IN}) (Analite, McVan, Australia, range 0–1000 NTU) fitted with a wiper blade to prevent biological fouling and automatic pumping sampler ($ISCO_{IN}$) intake were positioned in situ, adjacent to the channel edge, in proximity to the bankside analyser pump intake (1 m and 4 m upstream, respectively, in both catchments), but sufficiently distant not to affect, or to be affected by, the ex situ instrumentation. The turbidity sensor T_{IN} and the $ISCO_{IN}$ intake at Grassland B were approximately 20 cm above the channel bed and 15 cm from the bank edge. At Arable B, T_{IN} and the $ISCO_{IN}$ intake were positioned approximately 10 cm from the bank edge and 10 cm above the channel bed. T_{IN} and $ISCO_{IN}$ sample collection was synchronised to replicate the ex situ turbidity sensor (T_{OUT}) and pumping sampler ($ISCO_{OUT}$) programme as described above. T-SSC rating curves were developed for each sensor using water samples collected at the respective positions ($ISCO_{OUT}$ and $ISCO_{IN}$) and applied to the raw turbidity set. Low-quality data capture attributed to spurious readings (a short-term increase in T output not associated with a known environmental process such as accompanying rise in Q or equipment maintenance) and saturation of the T_{IN} sensor or missing data at

Table 2. Turbidity-suspended sediment calibration data-set summary and rating curve equations and fit parameters.

Catchment	Data points	Calibrated turbidity range (NTU)	Maximum measured turbidity in NTU (number of data points outside calibrated range)*	Calibration equation	MSE
Grassland A	247	0–725	1074 ($n = 7$)	$SSC = 0.6636\,T^{1.1045}$	495
Grassland B	443	1–577	1179 ($n = 37$)	$SSC = 0.5657\,T^{1.1109}$	580
Grassland C	339	1–154	1225 ($n = 207$)	$SSC = 0.4341\,T^{1.2148}$	38
Arable A	231	1–767	2730 ($n = 30$)	$SSC = 0.4119\,T^{1.1456}$	891
Arable B	242	1–1853	1853 ($n = 0$)	Where $T < 432.2$ $SSC = 1.1320\,T$ Where $T > 432.2$ $SSC = 0.5288 + 0.6032T$	1335

* Number of data points at 10 min resolution.

T_{OUT} due to delivery system blockages did not undergo correction such that comparisons between methodologies could be made. Five storm-flow events were captured in Grassland B and two in Arable B for T-SSC calibration. Due to the location settings, the in situ automatic water sampler was fitted with a 7 m long intake tube in both catchments.

Depth-integrated water samples were manually collected ($n = 171$) from a bridge over each investigated channel during flood events, using a depth-integrating SS sampler (US DH-48, Rickly Hydrological; USA). These samples were used firstly to investigate the cross-sectional variability in sediment transportation, and secondly to provide a validation data set to assess and compare the efficacy of estimated SSC using in situ and ex situ T sensors. Samples were collected using two strategies: (1) depth-integrated samples taken at 20 cm intervals across the channel width in rapid succession, and (2) samples taken at coarser widths with roughly 1 m intervals. All samples were processed for SSC as described above. Due to the sampling approach used, consecutive depth-integrated samples reflected the event trend (either the rising or falling sedigraph limb) plus the cross-sectional trend. The event effect was de-trended using SSC estimated from the ex situ turbidimeter. The average change in SSC during transect sampling at T_{OUT}, or the event trend, was 9 % (range 1 % at 175 mg L^{-1} to 19 % at 442 mg L^{-1}); the average transect time was 22 min.

Where sufficient sample volume and sediment concentration existed, samples were analysed for particle size distribution using laser diffraction (Malvern Mastersizer 2000G, Malvern, UK). Samples were circulated for 2 min (pump speed 2000 rpm, stirrer speed 800 rpm) before analysis with no pre-treatment, i.e. physical or chemical dispersant, to broadly replicate the "effective particle size" measured by the turbidity sensor. To assess the effect of automatic sampler tube length, laboratory prepared SSC samples were collected using the two intake pump lengths (1 and 7 m) used in-field. Ten 500 mL sub-samples (at 5, 10, 25, 50, 100, 250, 500, 750 and 1000 mg L^{-1}) were collected from homogenised 10 L mixtures using each pump length and processed for SSC. A non-parametric Mann–Whitney U test was conducted to compare SSC values collected at $ISCO_{IN}$ (SSC $ISCO_{IN}$) and $ISCO_{OUT}$ (SSC $ISCO_{OUT}$), and particle size characteristics at the two study sites.

3.3 Suspended sediment rating curve construction

Data pairs for T-SSC calibration for each individual site (each catchment outlet over a complete time series) and method comparison investigations were statistically assessed using SAS 9.3 (SAS Institute Inc., USA). Two regression equations, power (Eq. 1) and two-section linear split at a threshold T′ (Eq. 2), were assessed using the mean square error (MSE) of the SSC predictions.

$$\text{Power SSC} = aT^b \quad (1)$$

$$\text{Split linear SSC} = aT \text{ Where } T < T'$$
$$SSC = c(b_1 - b_2) + b_2 T \text{ Where } T > T'. \quad (2)$$

The intercept was set at zero for all regressions and was considered not to compromise fit at the upper end of the data set (cf. Thompson et al., 2014). Power relationships provided the best fit in Grassland A, Grassland B, Grassland C and Arable A, whereas the split linear relationship considerably improved fit at Arable B (Table 2). Using the selected curves, continuous turbidity measurements were computed to SSC and, using discharge data, were converted to instantaneous sediment load (SSL – t s^{-1}) and yield (SSY – t km^{-2} yr^{-1}).

4 Results and discussion

4.1 Method comparison

Data-set completeness was similar in both T records (98–99 %); however, the timing and nature of spurious and/or missing T data were dissimilar (Fig. 3). Spurious data at T_{IN} coincided with random peaks possibly relating to local debris interference around the sensor, which is a frequent problem

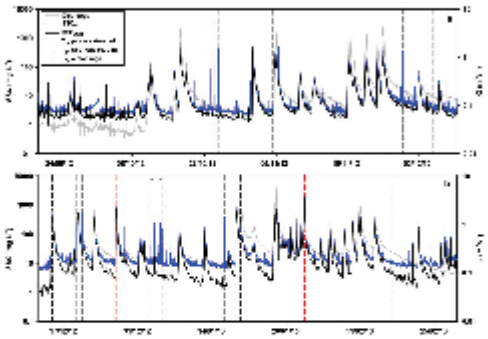

Figure 3. Raw turbidity output of T_{IN} and T_{OUT} sensors (converted to SSC) and discharge at **(a)** Grassland B and **(b)** Arable B. Periods of missing data are annotated by dashed lines.

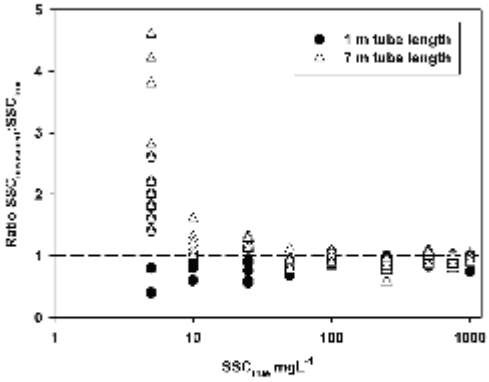

Figure 4. Suspended sediment concentration of samples collected from known concentration mixtures (SSC_{true}) using ISCO water samplers with 1 and 7 m tube lengths.

in T analysis (Lewis and Eads, 2001). This effect was not recorded at T_{OUT}, suggesting that the ex situ approach was less vulnerable to local in-stream debris interference (Jansson, 2002). Missing data at T_{IN} during periods of high sediment concentration were attributed to sensor saturation at Arable B. The T_{OUT} probe estimated 5 % of the total sediment load was delivered whilst T_{IN} was saturated. Sporadically, pump blockages occurred in T_{OUT} at Arable B due to extreme debris transport in the channel (Melland et al., 2012b); data collection was ordinarily restored in less than 2 h. At T_{IN} 6 % of the total load was delivered during this period. The ex situ turbidity monitoring may be at greater risk of delivery system blockages, especially during key periods of elevated turbidity and sediment transfer. These short periods are critical for sediment transport as they are responsible for the majority of the annual sediment load (Walling and Webb, 1988; Lawler et al., 2006; Estrany et al., 2009; Navratil et al., 2011). Other key issues such as bio-fouling trends were not found in either data set, reflecting the subweekly frequency of maintenance at these sites.

Estimated sediment metrics (Table 3) during both monitoring periods showed discrepancies between the two measurement locations. Suspended sediment load estimated by ex situ equipment was 83 % and 91 % of in situ at Grassland B and Arable B, respectively, and mean SSC at SSC_{OUT} was 85 % of SSC_{IN} at both locations. Differences in raw T output between the sensors were negated by calibration with SSC; however, the SSC of water samples from in situ (SSC $ISCO_{IN}$) and ex situ (SSC $ISCO_{OUT}$) measurement locations showed consistent differences. Samples at SSC $ISCO_{OUT}$ were 90 and 94 % of SSC $ISCO_{IN}$ at Grassland B and Arable B catchments, respectively. The differences in SSC and loads between the two approaches were not statistically significant, as confirmed by the non-parametric Mann–Whitney U test between SSC $ISCO_{OUT}$ and SSC $ISCO_{IN}$ ($p > 0.05$).

Particle size analysis of event samples showed that the proportion of silt and sand particles changed through the events, whereas clay remained consistent. The greater density of sand particles compared to silts and clays can impact SSC and be oversampled by pumped samples such as the $ISCO_{IN}$ approach (Horowitz, 2008). The percentage of sand (or sand-sized aggregates) between SSC $ISCO_{IN}$ and SSC $ISCO_{OUT}$ did not differ significantly ($p > 0.05$). Additionally, the ratio of the sand-sized fraction between simultaneous samples at $ISCO_{IN}$ and $ISCO_{OUT}$ showed no consistent evidence of over- or under-collection by either collection method. The hypothesis that inadequate sample collection could affect the differences between SSCs at $ISCO_{IN}$ and $ISCO_{OUT}$ is unlikely, as contrasts between the sand-sized fractions seemed to be event specific.

Differences between SSC $ISCO_{IN}$ and SSC $ISCO_{OUT}$ could not be directly attributed to diverging particle size of the collected samples ($p > 0.05$), the pump length of the water sample collection ($p > 0.05$; Fig. 4), or the position of the sample intake within the cross section (Fig. 5). It is possible that the proximity of the $ISCO_{IN}$ pump intake to the channel bank could influence the relationship; however, differences could additionally result from methodological dissimilarities which could not be tested in isolation, i.e. the piped delivery of river water to the ex situ instrument tank. The impact of elevated SSCs from $ISCO_{IN}$, compared to $ISCO_{OUT}$ on the calibration of turbidity sensors T_{IN} and T_{OUT}, and the consequential prediction of high-resolution turbidity-based SSC record is discussed below.

4.2 Method validation

Samples collected from the channel cross section were used to test the accuracy of predicted SSC using calibrated tur-

Table 3. Suspended sediment metrics estimated using in situ and ex situ turbidity-based SSC estimation methods.

Catchment	Total load (t)[a]		Mean concentration (mg L^{-1})		Max concentration (mg L^{-1})	
	SSL_{OUT}	SSL_{IN}	SSC_{OUT}	SSC_{IN}	SSC_{OUT}	SSC_{IN}
Grassland B	128 ± 28	154 ± 35	14	16	1010	1188
Arable B	225 ± 54	248 ± 52	29	34	2043	823[b]

[a] Confidence intervals are the coefficient of variance of the mean prediction.
[b] T_{IN} sensor saturated at 1000 NTU.

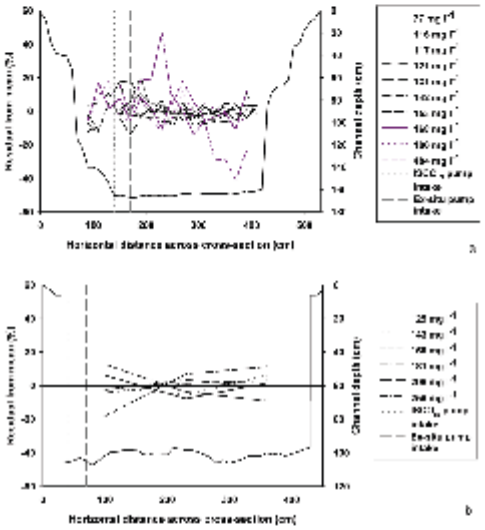

Figure 5. Variability of instantaneous depth-integrated SSC measurements across the channel cross section compared to the mean transect SSC using a US DH-48 sediment sampler at **(a)** Grassland B and **(b)** Arable B.

bidity sensors at in situ and ex situ locations. The average SSC from each cross-sectional, depth-integrated set of measurements was plotted onto the rating curve over the method comparison monitoring period (Fig. 6). At Grassland B, measured SSCs largely plot within the 95 % confidence intervals of predicted SSC using both methodologies using the simultaneous T values. This trend is repeated for the majority of samples at Arable B; however, some data points plot outside of the 95 % confidence intervals for both in situ and ex situ method data sets. In the case that these out of range values were consistently higher or lower than the predicted values, this may suggest a systematic error due to sampling strategy; however, both upper and lower confidence limits were exceeded by the SSC values (Fig. 6c and d). Therefore, the error associated with the measurement method was generally less than that encapsulated within the 95 % prediction intervals of the T to SSC calibration curve and, consequently, both measurement approaches can be accepted as accurate for the estimation of SS metrics in these catchments. The suitability of ex situ water monitoring equipment installation must consider programme-specific research objectives. Melland et al. (2012b) stated that for policy evaluation studies including multiple water quality parameters in addition to SSC, the improved resolution, accuracy and precision, in particular for hydrologically dynamic catchments, justified the increased financial costs of initial installation of ex situ instrumentation.

4.3 Suspended sediment metrics in five agricultural catchments

High-magnitude SSCs were of short duration in all five catchments (e.g. Fig. 3 for Grassland B and Arable B), but such periods are typically critical to cumulative annual SSY (Fig. 7b – Walling and Webb, 1988; Navratil et al., 2011). Grassland B and Arable B had a large proportion (80 % of the monitoring period) of sediment transported at SSCs between 1 and 10 mg L^{-1}, and shorter periods of concentrations $\geq$ 10 mg L^{-1} for 15 and 20 % of the monitoring period, respectively (Fig. 7). In the remaining catchments, low concentrations of $<$ 1 mg L^{-1} were more common and occurred between 25 and 40 % of the time. High concentrations ($\geq$10 mg L^{-1}) were limited to less than 10 % of the monitoring period. Overall, however, the FFD average annual SSC guideline was not exceeded in any monitoring year in any of the catchments (Table 4). The highest mean SSCs were recorded at Grassland B (up to 14 mg L^{-1}) and Arable B (up to 17 mg L^{-1}) and the remaining catchments reported very low values of $<$ 6 mg L^{-1}. Accordingly, the instantaneous exceedance of the FFD guideline (Table 4) occurred during extremely short time periods (1–11 % of sampled time per year). The values here are similar to those reported by Thompson et al. (2014) in two other intensively managed grassland catchments in Ireland; 8 % exceedance was reported in a moderately drained catchment in Co. Down and 18 % exceedance in a poorly drained catchment in Co. Louth. Although the instantaneous exceedance of the FFD metric has been reported in other sediment studies (Glendell et al., 2014; Peukert et al., 2014; Thompson et al., 2014),

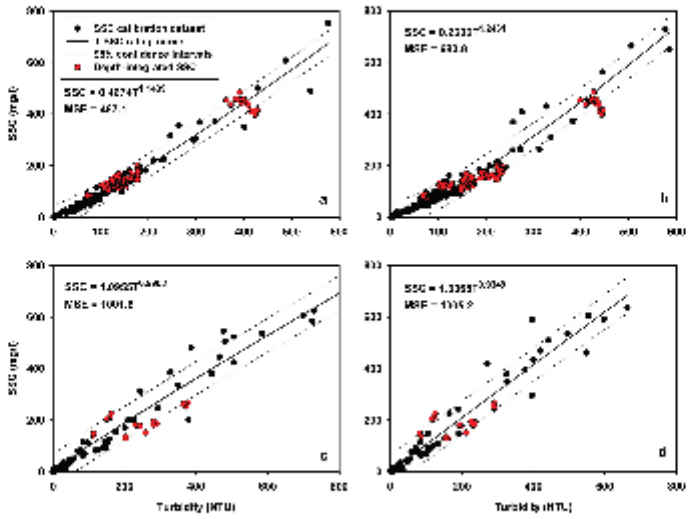

Figure 6. Turbidity-suspended sediment concentration rating curves, confidence intervals, calibration data and cross-sectional depth-integrated suspended sediment concentration samples for **(a)** Grassland B T_{OUT}, **(b)** Grassland B T_{IN}, **(c)** Arable B T_{OUT}, and **(d)** Arable B T_{IN}.

the transferability of this coarse threshold (compliance to which requires an undefined annual sample number) to high-resolution SS data is questionable.

Average SSYs in the five catchments were 9, 25, 12, 12 and 24 t km^{-2} yr^{-1} at Grassland A, Grassland B, Grassland C, Arable A and Arable B, respectively. Figure 8 illustrates average annual SSYs from Ireland, the United Kingdom (UK) and the wider Atlantic climatic region of Europe (Vanmaercke et al., 2011). The variability of average SSYs may be partly described by catchment size (x axis) but furthermore according to physical attributes such as soil type, which controls soil erodibility. Values from catchments assessed in this study align with existing data on SSY in Ireland (cf. Huang and O'Connell, 2000; Jordan et al., 2002; Harrington and Harrington, 2013; Thompson et al., 2014), and are consistently low compared with the UK and Europe. Considering the agricultural intensity of these catchments (for example, Grassland A is within the highest region of milk yield in Ireland; Läppe and Hennessy, 2012), and that crop yields across Ireland are internationally high (Melland et al., 2012a), these values are particularly low.

Catchment observations suggest high landscape complexity, comprising small and irregularly shaped fields, separated by a dense network of hedgerows and vegetated ditches (Table 1) reduced water and sediment connectivity potential between hillslopes and the channel network. Efficient drainage can be considered to reduce the spatial extent and temporal stability of connected areas and, considering the over-engineered nature of these ditch networks, encouraged sediment deposition (Shore et al., 2014). Furthermore, lower slope lengths reduce the hillslope erosion potential (Lal, 1988), and sediment trapping and soil erosion prevention by root binding of hedgerows were observed. However, at the catchment scale, greater efficiency of hillslope drainage can increase the erosivity of streams, in turn accelerating erosion from in-channel sources such as channel banks (Belmont et al., 2011; Massoudieh et al., 2013).

In the UK, Cooper et al. (2008) suggested annual average "target" and threshold "investigation" SSY values be based upon drainage class and catchment terrain characteristics. Grassland A and Arable A qualify as lowland well drained catchments and, on average, fall well below target and investigation SSY of 20 and 50 t km^{-2} yr^{-1}, respectively. Grassland B, Grassland C and Arable B, categorised as lowland predominantly poorly drained catchments, on average, fall below target and investigation thresholds of 40 and 70 t km^{-2} yr^{-1}, respectively. Total SSY data for individual years (Table 4), however, indicate variability and exceeded respective SSY target values at Grassland B in 2009, Arable A in 2012 and Arable B in 2012.

Higher average SSC, intra-annual period of FFD exceedance, and average SSY in catchments Grassland B and Arable B are suggested to result from poorer soil drainage. During rainfall events, soils are rapidly saturated and critical overland flow pathways established, and consequently, eroded particles within these connected areas are transported

Table 4. Annual rainfall, discharge and suspended sediment flux summary for five catchments. Monitoring years correspond to hydrologic years (October to September).

	Grassland A			Grassland B				Grassland C			Arable A			Arable B		
Year	2010	2011	2012	2009	2010	2011	2012	2010	2011	2012	2009	2010	2011	2012	2009	2010	2011	2012
Rainfall (mm yr^{-1})	1045	1139	1097	1278	800	1155	920	965	1234	969	1240	763	1102	827	896	742	1049	844
Runoff (mm yr^{-1})	443	633	608	643	330	504	382	424	727	575	750	366	517	473	383	319	521	542
Mean SSC (mg L^{-1})	5	4	5	14	5	8	12	4	4	3	6	3	4	6	9	10	10	18
Max SSC (mg L^{-1})	707	467	966	1020	426	882	707	419	813	462	773	224	737	2141	494	707	688	1120
>25 mg L^{-1} (% of ST*)	3	2	3	11	5	6	8	2	2	2	4	1	2	3	6	6	6	11
SSY (tonnes km^{-2} yr^{-1})	3.95	6.61	14.92	48.39	6.65	13.46	30.08	6.07	22.28	6.52	17.44	2.11	5.22	23.10	15.59	15.97	24.20	41.81

*ST = sampled time.

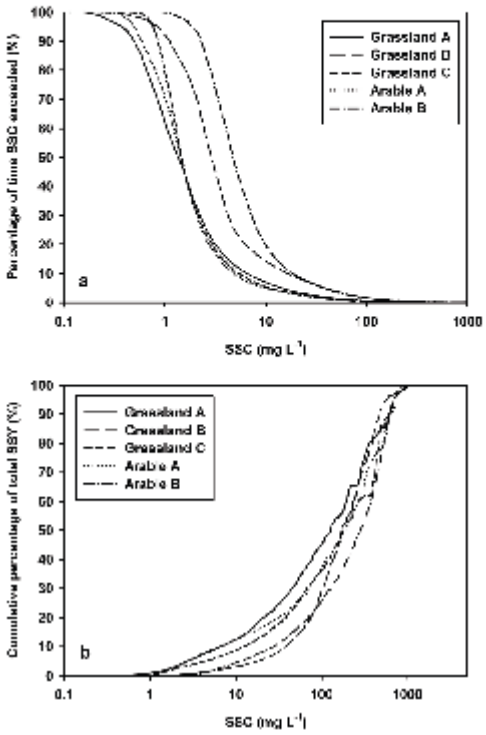

Figure 7. Frequency-duration graphs of (a) suspended sediment concentration exceedance with time and (b) cumulative percentage of suspended sediment yield with exceedance of suspended sediment concentration.

through the catchment (Mellander et al., 2012; Shore et al., 2013). The SSC responses here suggest, as in other catchments with impeded drainage, that high overland-flow potential is also associated with a notable proportion of sediment delivered at lower concentrations over a longer period, through surface and sub-surface flow pathways such as through macropores and tile drains (e.g. Deasy et al., 2009; Melland et al., 2012a; Ibrahaim et al., 2013; Mellander et al., 2015) resulting in increased average SSCs. In catchments Grassland A and Arable A, sub-surface flow pathways dominate, due to well drained soils reducing the likelihood of overland flow and consequently surface soil losses. Furthermore, at Arable A, Mellander et al. (2015) found that weathered bedrock formed groundwater pathways, further decreasing surface pathway initiation. Consequently, SSCs, the intra-annual period of FFD exceedance, and SSYs were low. Conversely, Grassland C more accurately reflects the sediment characteristics of the well drained catchments de-

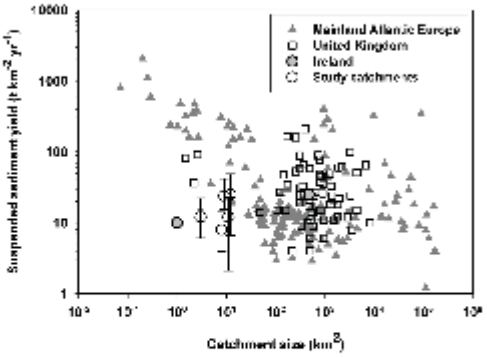

Figure 8. Catchment size and suspended sediment yield of European river catchments; study catchments displayed with inter-annual range. Sources: Foster et al. (1986); Milliman and Syvitski (1992); McManus and Duck (1996); Wass and Leeks (1999); Huang and O'Connell (2000); Verstraeten and Poesen (2001); Jordan et al. (2002); Walling et al. (2002); Harlow et al. (2006); Oeurng et al. (2010); Zabaleta et al. (2007); Gay et al. (2014).

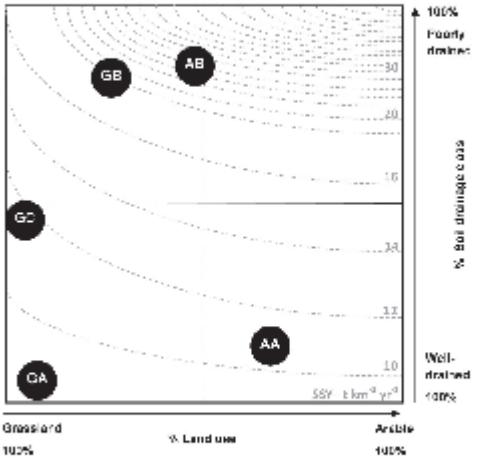

Figure 9. Conceptual diagram of suspended sediment yield as represented by iso-lines according to land use and dominant soil drainage class. Catchment abbreviations: GA – Grassland A; GB – Grassland B; GC – Grassland C; AA – Arable A; AB – Arable B.

spite the moderately to poorly drained soils. Near-complete cover of permanent pasture here was considered to sufficiently reduce sediment source availability and transport of sediment to the watercourse.

Generalisations can be made in relation to the overriding controls on SSY across the monitored catchments (Fig. 9). Inter-catchment comparisons here used data from hydrological years 2010 to 2013, where data were available for all five catchments. Sediment delivery was enhanced by the combined effect of an overland-flow dominated transport system (poorly drained soils) and, to a lesser extent, source availability (arable soils with potentially lengthy periods of bare ground cover (Regan et al., 2012) or seasonally thinly vegetated grassland soils; cf. Bilotta et al., 2010). Catchments that possess better drainage characteristics and/or permanent crop cover have greater resilience to extreme sediment losses. In catchments such as Arable A, where good drainage is combined with high source availability, the risk associated with sediment transport during extreme rainfall events and years was, nevertheless, high. Similarly, poorly drained soils stabilised by permanent pasture should be maintained and periods of bare cover should be avoided.

High inter-annual variability was evident, particularly with regard to SSY (Table 4). The annual SSY coefficients of variation (CV %) were 67, 76, 79, 83 and 50 % in Grassland A, Grassland B, Grassland C, Arable A and Arable B, respectively. Notably, in the Grassland B and Arable B catchments, the inter-annual SSY ranges of 42 and 26 t km^{-2} yr^{-1}, respectively, were greater than the average annual inter-catchment SSY of approximately 24 t km^{-2} yr^{-1} for both sites. The variability found within each of the five monitoring catchments was comparable to the results of Vanmaercke et al. (2012), who reported CV % ranging from 6 to 313 % (median 75 %) in 726 catchments worldwide. The catchment with the lowest inter-annual SSY (11 t km^{-2} yr^{-1}), Grassland A, received the least variable rainfall input and total discharge.

Inter-annual SSY variability results from strong seasonality due to the timing and character of rainfall events, soil moisture deficit and land management which conditions sediment availability in critical source areas. Analysis of shorter-term sediment losses, i.e. at seasonal, monthly and event scales, would also provide empirical evidence to inform both high-level policy considerations and local decision making. Additionally, assessment of seasonal transfers are likely to have greater ecological significance as mean annual thresholds such as SSC (through the FFD), and SSY may underestimate the seasonal fluctuations of risk of sediments to aquatic ecosystems (Thompson et al., 2014). Sensitivity to sediment is species-specific and dependent upon life stage (Collins et al., 2011); therefore, shorter-term metrics such as the timing, magnitude, duration and frequency of sediment transfers are important concepts to consider. Existing static thresholds may, therefore, be considered ecologically irrelevant, particularly when utilised as an instantaneous threshold for high-resolution data. Future discussion regarding sediment targets requires an assessment of multiple species and habitat quality. This task is particularly complicated where ecological condition is subject to multiple stressors such as nutrients (Bilotta and Brazier, 2008), bed substrate quality (Kemp et

al., 2011) and time lag of water quality response to pollutant mitigation measures (Fenton et al., 2011; Vero et al., 2014).

Overall, annual average sediment metrics from small catchments (~ 10 km^2) with dominant land uses representative of main land use types in Ireland reported here are internationally low. Considering the spatial dominance and intensity of agricultural land use and high effective rainfall in the study catchments, this is perhaps unexpected, particularly considering the small scale of study. As previously discussed, the complexity of landscape features (e.g. fields, hedgerows, ditches) which are representative of the wider Irish agricultural landscape (Deverell et al., 2009) can be expected to decrease the likelihood of field-scale soil erosion, and/or increase the opportunity for interception and deposition of mobile particles on land or within the hydrological network. The Irish landscape may, therefore, improve the resilience of agricultural soils to soil loss. However, even with modest SSY, the potential for other specific risks to ecologically sensitive habitats, from SS deposition in rivers for example, will need a cautionary approach. Therefore, identification of the specific mechanisms promoting soil conservation or sediment retention in multiple catchments with contrasting physical and land use characteristics is important. This is particularly relevant for water and agricultural policy, as the prevention of environmental degradation and maintenance and/or sustainable intensification of agricultural production are simultaneously considered. Furthermore, other sediment sources, for example, from channel banks and road networks, may contribute significant proportions of the annual load (Rowan et al., 2012; Collins et al., 2013; Sherriff et al., 2014), particularly where strategies to reduce sediment loss on the hillslope scale such as sub-surface drainage may accelerate losses from channel sediment sources at the catchment scale. Assessment of such sources could be a useful insight to prioritise sediment management strategies (Wilson et al., 2008).

5 Conclusions

This study assessed the accuracy and reliability of an ex situ, turbidity-based methodology to estimate suspended sediment fluxes in multiple monitored catchments. Applying the method, annual SSC, FFD exceedance and SSY data in five catchments were further investigated in relation to physical catchment characteristics and land management. The key findings are:

- Suspended sediment metrics between in situ and ex situ methodologies were not significantly different from in-stream cross-sectional, depth-integrated samples in two monitoring catchments.
- The ex situ methodology reported less sensitivity to spurious data peaks; however, periods of extreme large debris transport increased the sensitivity of the ex situ instrumentation to short-term blockages.
- All catchments reported mean annual SSCs of less than the FFD threshold of 25 $mg L^{-1}$ and short-term exceedance of 1–11 % of sampled time.
- Inter-annual variability of SSY was strong due to the timing and character of rainfall events in relation to land management.
- Average annual SSYs in all five Irish catchments reported here were low in comparison to similar catchment and landscape settings elsewhere in Europe. Farming practices favouring relatively small fields, a high density of field boundaries including ditches, with low consequent connectivity are likely to explain this.
- Within the study catchments, SSY was higher in catchments dominated by poorly drained soils than those with well drained soils. Furthermore, on poorly drained soils, catchments with a greater proportion of arable land use reported the highest annual average SSY.
- Well drained soils dominated by arable crops did, however, show the potential to supply significant quantities of sediment.
- Complexity of landscape features (hedgerows, drainage ditches and irregular field sizes) may provide resilience to hillslope soil erosion and/or sediment transport despite spatial dominance and intensity of agriculture and these will be important considerations for future management (such as sustainable intensification) and/or SS mitigation in Ireland and elsewhere.

These findings illustrate that interactions between climate, landscape and land use regulate the supply of sediments from Irish agricultural catchments. Whilst the current SSYs are low by international standards, key questions still remain regarding the impact of land use on the magnitude and frequency characteristics of sediment transfers at shorter timescales. Seasonal and storm-event scale sediment transfers may better inform erosion risk due to better detection of sediment pulses moving into the channel network particularly within ecologically sensitive periods. Further to this, seasonal sediment provenance and field-scale soil loss assessments within this land management and landscape framework are crucial to quantify the contributions made from specific agricultural and other sediment sources.

Acknowledgements. This study was funded by the Walsh Fellowship Programme, Teagasc, Ireland allied to the University of Dundee, UK, and the Teagasc Agricultural Catchments Programme (funded by the Department of Agriculture, Food and the Marine, Ireland). We thank Hugo McGrogan (Ulster University) for supplying and programming additional turbidity and pump-sampling equipment and Agricultural Catchments Programme colleagues for technical support. We finally acknowledge support from the farmers and landowners of the study catchments and two reviewers for comments on the manuscript.

Edited by: C. Stamm

References

Belmont, P., Gran, K. B., Schottler, S. P., Wilcock, P. R., Day, S. S., Jennings, C., Lauer, J. W., Viparelli, E., Willenbring, J. K., Engstrom, D. R., and Parker, G.: Large shift in source of fine sediment in the Upper Mississippi River, Environ. Sci. Technol., 45, 8804–8810, 2011.

Bilotta, G. S. and Brazier, R. E.: Understanding the influence of suspended solids on water quality and aquatic biota, Water Res., 42, 2849–2861, 2008.

Bilotta, G. S., Krueger, T., Brazier, R. E., Butler, P., Freer, J., Hawkins, J. M. B., Haygarth, P. M., Macleod, C. J. A., and Quinton, J. N.: Assessing catchment-scale erosion and yields of suspended solids from improved temperate grassland, J. Environ. Monit., 12, 731–739, 2010.

Boardman, J., Shepheard, M. L., Walker, E., and Foster, I. D. L.: Soil erosion and risk-assessment for on- and off-farm impacts: A test case using the Midhurst area, West Sussex, UK, J. Environ. Manage., 90, 2578–2588, 2009.

Borselli, L., Cassi, P., and Torri, D.: Prolegomena to sediment and flow connectivity in the landscape: A GIS and field numerical experiment, Catena, 75, 268–277, 2008.

Brils, J.: Sediment Monitoring and the European Water Framework Directive, Annali dell'Istituto Superiore di Sanita 44, 218–223, 2008.

Chambers, B. J., and Garwood, T. W. D.: Monitoring of water erosion on arable farms in England and Wales, 1990–1994, Soil Use Manag., 16, 93–99, 2000.

Collins, A. L. and Anthony, S. G.: Assessing the likelihood of catchments across England and Wales meeting 'good ecological status' due to sediment contributions from agricultural sources, Environ. Sci. Policy, 11, 163–170, 2008.

Collins, A. L., Naden, P. S., Sear, D. A., Jones, J. I., Foster, I. D. L., and Morrow, K.: Sediment targets for informing river catchment management: international experience and prospects, Hydrol. Process., 25, 2112–2129, 2011.

Collins, A. L., Williams, L. J., Zhang, Y. S., Marius, M., Dungait, J. A. J., Smallman, D. J., Dixon, E. R., Stringfellow, A., Sear, D. A., Jones, J. I., and Naden, P. S.: Catchment source contributions to the sediment-bound organic matter degrading salmonid spawning gravels in a lowland river, southern England, Sci. Total Environ., 456–457, 181–195, 2013.

Cooper, D., Naden, P., Old, G., and Laizé, C.: Development of guideline sediment targets to support management of sediment inputs into aquatic systems, Natural England Research Report NERR008, CEH Wallingford, 96 pp., 2008.

Deasy, C., Brazier, R. E., Heathwaite, A. L., and Hodgkinson, R.: Pathways of runoff and sediment transfer in small agricultural catchments, Hydrol. Process., 23, 1349–1358, 2009.

Deverell, R., McDonnell, K., and Devlin, G.: The impact of field size on the environment and energy crop production efficiency for a sustainable indigenous bioenergy supply chain in the Republic of Ireland, Sustainability, 1, 994–1011, 2009.

Duvert, C., Gratiot, N., Evrard, O., Navratil, O., Némery, J., Prat, C., and Esteves, M.: Drivers of erosion and suspended sediment transport in three headwater catchments of the Mexican Central Highlands, Geomorphology, 123, 243–256, 2010.

Estrany, J., Garcia, C., and Batalla, R. J.: Suspended sediment transport in a small Mediterranean agricultural catchment, Earth Surf. Process. Landf., 34, 929–940, 2009.

Evans, D. J., Gibson, C. E., and Rossell, R. S.: Sediment loads and sources in heavily modified Irish catchments: A move towards informed management strategies, Geomorphology, 79, 93–113, 2006.

Fealy, R. M., Buckley, C., Mechan, S., Melland, A. R., Mellander, P.-E., Shortle, G., Wall, D., and Jordan, P.: The Irish Agricultural Catchment Programme: catchment selection using spatial multi-criteria decision analysis, Soil Use Manage., 26, 225–236, 2010.

Fenton, O., Schulte, R. P. O., Jordan, P., Lalor, S. T. J., and Richards, K. G.: Time lag: a methodology for estimation of vertical and horizontal travel and flushing timescales to nitrate threshold concentrations in Irish aquifers, Environ. Sci. Policy, 14, 419–431, 2011.

Florsheim, J. L., Pellerin, B. A., Oh, N. H., Ohara, N., Bachand, P. A. M., Bachand, S. M., Bergamaschi, B. A., Hernes, P. J., and Kavvas, M. L.: From deposition to erosion: Spatial and temporal variability of sediment sources, storage, and transport in a small agricultural watershed, Geomorphology, 132, 272–286, 2011.

Foster, I. D. L., Dearing, J. A., and Appleby, P. G.: Historical trends in catchment sediment yields: a case study from lake-sediment records in Warwickshire, UK, Hydrol. Sci. J., 31, 427–443, 1986.

Foster, I., Collins, A., Naden, P., Sear, D., Jones, J., and Zhang, Y.: The potential for paleolimnology to determine historic sediment delivery to rivers, J. Paleolimnol., 45, 287–306, 2011.

Freebairn, D. M., Wockner, G. H., Hamilton, N. A., and Rowland, P.: Impact of soil conditions on hydrology and water quality for a brown clay in the north-eastern cereal zone of Australia, Aust. J. Soil Res., 47, 389–402, 2009.

Gay, A., Cerdan, O., Delmas, M., and Desmet, M.: Variability of suspended sediment yields within the Loire river basin (France), J. Hydrol., 519, 1225–1237, 2014.

Geraghty, M., Farrelly, I., Claringbold, K., Jordan, C., Meehan, R., and Hudson, M.: Geology of Monaghan-Carlingford. A geological description to accompany the Bedrock Geology 1:100,000 Scale Map Series, Sheet 8/9, Monaghan-Carlingford, Geological Survey of Ireland: Dublin, Ireland, 1997.

Glendell, M. and Brazier, R. E.: Accelerated export of sediment and carbon from a landscape under intensive agriculture, Sci. Total Environ., 476–477, 643–656, 2014.

Glendell, M., Extence, C., Chadd, R., and Brazier, R. E.: Testing the pressure-specific invertebrate index (PSI) as a tool for determining ecologically relevant targets for reducing sedimentation in streams, Freshwater Biol., 59, 353–367, 2014.

Grangeon, T., Legout, C., Esteves, M., Gratiot, N., and Navratil, O.: Variability of the particle size of suspended sediment during highly concentrated flood events in a small mountainous catchment, J. Soils Sed., 12, 1549–1558, 2012.
Harlow, A., Webb, B. W., and Walling, D. E.: Sediment yields in the Exe Basin: a longer-term perspective, Sediment Dynamics and the Hydromorphology of Fluvial Systems, Dundee, UK, 12–20, 2006.
Harrington, S. T. and Harrington, J. R.: An assessment of the suspended sediment rating curve approach for load estimation on the Rivers Bandon and Owenabue, Ireland, Geomorphology, 185, 27–38, 2013.
Haygarth, P. M., Bilotta, G. S., Bol, R., Brazier, R. E., Butler, P. J., Freer, J., Gimbert, L. J., Granger, S. J., Krueger, T., Macleod, C. J. A., Naden, P., Old, G., Quinton, J. N., Smith, B., and Worsfold, P.: Processes affecting transfer of sediment and colloids, with associated phosphorus, from intensively farmed grasslands: an overview of key issues, Hydrol. Process., 20, 4407–4413, 2006.
Horowitz, A. J.: Determining annual suspended sediment and sediment-associated trace element and nutrient fluxes, Sci. Total Environ., 400, 315–343, 2008.
Huang, C. C. and O'Connell, M.: Recent land-use and soil-erosion history within a small catchment in Connemara, western Ireland: evidence from lake sediments and documentary sources, Catena, 41, 293–335, 2000.
Ibrahim, T. G., Fenton, O., Richards, K. G., Fealy, R. M., and Healy, M. G.: Spatial and temporal variations of nutrient loads in overland flow and subsurface drainage from a marginal land site in south-east Ireland, Biol. Environ., 113B, 169–186, 2013.
Jansson, M. B.: Determining sediment source areas in a tropical river basin, Costa Rica, Catena, 47, 63–84, 2002.
Jastram, J. D., Zipper, C. E., Zelazny, L. W., and Hyer, K. E.: Increasing Precision of Turbidity-Based Suspended Sediment Concentration and Load Estimates, J. Environ. Qual., 39, 1306–1316, 2010.
Jordan, P., Rippey, B., and John, A. N.: The 20th century whole-basin trophic history of an inter-drumlin lake in an agricultural catchment, Sci. Total Environ., 297, 161–173, 2002.
Jordan, P., Arnscheidt, A., McGrogan, H., and McCormick, S.: Characterising phosphorus transfers in rural catchments using a continuous bank-side analyser, Hydrol. Earth Syst. Sci., 11, 372–381, doi:10.5194/hess-11-372-2007, 2007.
Jordan, P., Melland, A. R., Mellander, P. E., Shortle, G., and Wall, D.: The seasonality of phosphorus transfers from land to water: Implications for trophic impacts and policy evaluation, Sci. Total Environ., 434, 101–109, 2012.
Kemp, P., Sear, D., Collins, A., Naden, P., and Jones, I.: The impacts of fine sediment on riverine fish, Hydrol. Process., 25, 1800–1821, 2011.
Lal, R.: Effects of slope length, slope gradient, tillage methods and cropping systems on runoff and soil erosion on a tropical Alfisol: preliminary results, Proceedings of the Porto Alegre Symposium, December 1988, edited by: Bordas, M. P. and Walling, D. E., IAHS Publ., 174, 79–88, 1988.
Läppe, D. and Hennessy, T.: The capacity to expand milk production in Ireland following the removal of milk quotas, Irish J. Agr. Food Res., 51, 1–11, 2012.
Lawler, D. M., Petts, G. E., Foster, I. D. L., and Harper, S.: Turbidity dynamics during spring storm events in an urban headwater river system: The Upper Tame, West Midlands, UK, Sci. Total Environ., 360, 109–126, 2006.
Lewis, J.: Turbidity-controlled sampling for suspended sediment load estimation, edited by: Bogen, J., Fergus, T., and Walling, D. E., Proceedings of the Oslo Symposium, June 2002, IAHS Publication 337, 13–20, 2003.
Lewis, J., and Eads, R.: Turbidity threshold sampling for suspended sediment load estimation, in: Proceedings of the seventh federal interagency sedimentation conference, Technical committee of the subcommittee on sedimentation, Reno, 25-29th March 2001, 8 pp., 2001.
Massoudieh, A., Gellis, A., Banks, W. S., and Wieczorek, M. E.: Suspended sediment source apportionment in Chesapeake Bay watershed using Bayesian chemical mass balance receptor modeling, Hydrol. Process., 27, 3363–3374, 2013.
McManus, J. and Duck, R. W.: Regional variations of fluvial sediment yield in eastern Scotland, edited by: Walling, D. E. and Webb, B. W., Proceedings of the Exeter Symposium, July 1996, IAHS Publication 236, 157–161, 1996.
McConnell B., Philcox, M., and Geraghty, M.: Geology of Meath: A geological description to accompany the bedrock geology 1:100,000 scale map series, Sheet 13, Meath. Geological Survey of Ireland: Dublin, Ireland, 2001.
Melland, A. R., Mellander, P. E., Murphy, P. N. C., Wall, D. P., Mechan, S., Shine, O., Shortle, G., and Jordan, P.: Stream water quality in intensive cereal cropping catchments with regulated nutrient management, Environ. Sci. Policy, 24, 58–70, 2012a.
Melland, A. R., Ryan, D., Shortle, G., and Jordan, P.: A cost:benefit evaluation of in-situ high temporal resolution stream nutrient monitoring, World Congress on Water, Climate and Energy, Dublin, 13–18 May 2012b.
Mellander, P.-E., Melland, A. R., Jordan, P., Wall, D. P., Murphy, P. N. C., and Shortle, G.: Quantifying nutrient transfer pathways in agricultural catchments using high temporal resolution data, Environ. Sci. Policy, 24, 44–57, 2012.
Mellander, P.-E., Melland, A. R., Murphy, P. N. C., Wall, D. P., Shortle, G., and Jordan, P.: Coupling of surface water and groundwater nitrate-N dynamics in two permeable agricultural catchments, J. Agr. Sci., 152, 107–124, 2014.
Milliman, J. D. and Syvitski, J. P. M.: Geomorphic/Tectonic control of sediment discharge to the ocean: the importance of small mountainous rivers, J. Geol., 100, 525–544, 1992.
Navratil, O., Esteves, M., Legout, C., Gratiot, N., Nemery, J., Willmore, S., and Grangeon, T.: Global uncertainty analysis of suspended sediment monitoring using turbidimeter in a small mountainous river catchment, J. Hydrol., 398, 246–259, 2011.
Oeurng, C., Sauvage, S., and Sánchez-Pérez, J.-M.: Dynamics of suspended sediment transport and yield in a large agricultural catchment, southwest France, Earth Surf. Process. Landf., 35, 1289–1301, 2010.
OJEU: Council Directive 91/676/EEC of 12 December 1991 concerning the protection of waters against pollution caused by nitrates from agricultural sources, EU, Brussels, 1991.
OJEU: Establishing a Framework for Community Action in the Field of Water Policy (Water Framework Directive), 2000/60/EC, EU, Brussels, 2000.
OJEU: Council Directive 2006/44/EC of the 6 September 2006 on the quality of fresh waters needing protection or improvement in order to support fish life, EU, Brussels, 2006.

OJEU: Commission Decision 2007/697/EC of 22 October 2007 granting a derogation requested by Ireland pursuant to Council Directive 91/676/EEC concerning the protection of water against pollution caused by nitrates from agricultural sources, EU, Brussels, 2007.

Owen, G. J., Perks, M. T., Benskin, C. M. H., Wilkinson, M. E., Jonczyk, J., and Quinn, P. F.: Monitoring agricultural diffuse pollution through a dense monitoring network in the River Eden Demonstration Test Catchment, Cumbria, UK, Area, 44, 443–453, 2012.

Peukert, S., Griffith, B. A., Murray, P. J., Macleod, C. J. A., and Brazier, R. E.: Intensive Management in Grasslands Causes Diffuse Water Pollution at the Farm Scale, J. Environ. Qual., 43, 2009–2023, 2014.

Regan, J. T., Fenton, O., and Healy, M. G.: A review of phosphorus and sediment release from Irish tillage soils, the methods used to quantify losses and the current state of mitigation practice, Biol. Environ., 112B, 1–25, 2012.

Rowan, J. S., Black, S., and Franks, S. W.: Sediment fingerprinting as an environmental forensics tool explaining cyanobacteria blooms in lakes, Appl. Geogr., 32, 832–843, 2012.

Sherriff, S. C., Rowan, J. R., Franks, S. W., Walden, J., Melland, A. R., Jordan, P., and ÓhUallacháin, D.: Sediment Fingerprinting, TResearch, Summer 2014, 40–41, 2014.

Shore, M., Murphy, P. N. C., Jordan, P., Mellander, P. E., Kelly-Quinn, M., Cushen, M., Mechan, S., Shine, O., and Melland, A. R.: Evaluation of a surface hydrological connectivity index in agricultural catchments, Environ. Model. Softw., 47, 7–15, 2013.

Shore, M., Jordan, P., Mellander, P.-E., Kelly-Quinn, M., and Melland, A. R.: An agricultural drainage channel classification system for phosphorus management, Agr. Ecosystems Environ., 199, 207–215, 2014.

Silgram, M., Jackson, D. R., Bailey, A., Quinton, J., and Stevens, C.: Hillslope scale surface runoff, sediment and nutrient losses associated with tramline wheelings, Earth Surf. Process. Landf., 35, 699–706, 2010.

Sleeman, A. G. and Pracht, M.: Geology of South Cork, Sheet 25, Geological Survey of Ireland: Dublin, Ireland, 1995.

Soane, B. D., Ball, B. C., Arvidsson, J., Basch, G., Moreno, F., and Roger-Estrade, J.: No-till in northern, western and south-western Europe: A review of problems and opportunities for crop production and the environment, Soil Till. Res., 118, 66–87, 2012.

Thompson, J., Cassidy, R., Doody, D. G., and Flynn, R.: Assessing suspended sediment dynamics in relation to ecological thresholds and sampling strategies in two Irish headwater catchments, Sci. Total Environ., 468–469, 345–357, 2014.

Tietzsch-Tyler, D., Sleeman, A. G., McConnell, B. J., Daly, E. P., Flegg A. M., O'Connor P. J., and Warren W. P.: Geology of Carlow-Wexford, Sheet 19. Geological Survey of Ireland: Dublin, Ireland, 1994.

Trimble, S. W. and Mendel, A. C.: The cow as a geomorphic agent – A critical review, Geomorphol., 13, 233–253, 1995.

Van Oost, K., Cerdan, O., and Quine, T. A.: Accelerated sediment fluxes by water and tillage erosion on European agricultural land, Earth Surf. Process. Landf., 34, 1625–1634, 2009.

Vanmaercke, M., Poesen, J., Verstraeten, G., de Vente, J., and Ocakoglu, F.: Sediment yield in Europe: Spatial patterns and scale dependency, Geomorphol., 130, 142–161, 2011.

Vanmaercke, M., Poesen, J., Radoane, M., Govers, G., Ocakoglu, F., and Arabkhedri, M.: How long should we measure? An exploration of factors controlling the inter-annual variation of catchment sediment yield, J. Soils Sed., 12, 603–619, 2012.

Vero, S. E., Ibrahim, T. G., Creamer, R. E., Grant, J., Healy, M. G., Henry, T., Kramers, G., Richards, K. G., and Fenton, O.: Consequences of varied soil hydraulic and meteorological complexity on unsaturated zone time lag estimates, J. Contam. Hydrol., 170, 53–67, 2014.

Verstraeten, G. and Poesen, J.: Factors controlling sediment yield from small intensively cultivated catchments in a temperate humid climate, Geomorphology, 40, 123–144, 2001.

Wall, D., Jordan, P., Melland, A. R., Mellander, P. E., Buckley, C., Reaney, S. M., and Shortle, G.: Using the nutrient transfer continuum concept to evaluate the European Union Nitrates Directive National Action Programme, Env. Sci. Policy, 14, 664–674, 2011.

Walling, D. E.: Tracing suspended sediment sources in catchments and river systems, Sci. Total Environ., 344, 159–184, 2005.

Walling, D. E. and Webb, B. W.: The reliability of rating curve estimates of suspended sediment yield: some further comments, Sediment budgets, Porto Alegre, 337–350, 1988.

Walling, D. E., Owens, P. N., and Leeks, G. J. L.: Fingerprinting suspended sediment sources in the catchment of the River Ouse, Yorkshire, UK, Hydrol. Process., 13, 955–975, 1999.

Walling, D. E., Russell, M. A., Hodgkinson, R. A., and Zhang, Y.: Establishing sediment budgets for two small lowland agricultural catchments in the UK, Catena, 47, 323–353, 2002.

Wass, P. D. and Leeks, G. J. L.: Suspended sediment fluxes in the Humber catchment, UK, Hydrol. Process., 13, 935–953, 1999.

Wilson, C. G., Kuhnle, R. A., Bosch, D. D., Steiner, J. L., Starks, P. J., Tomer, M. D., and Wilson, G. V.: Quantifying relative contributions from sediment sources in Conservation Effects Assessment Project watersheds, J. Soil Water Conserv, 63, 523–532, 2008.

Wiskow, E. and van der Ploeg, R. R.: Calculation of drain spacings for optimal rainstorm flood control, J. Hydrol., 272, 163–174, 2003.

Withers, P. J. A., Hodgkinson, R. A., Bates, A., and Withers, C. M.: Some effects of tramlines on surface runoff, sediment and phosphorus mobilization on an erosion-prone soil, Soil Use Manage., 22, 245–255, 2006.

Wood, P. J. and Armitage, P. D.: Biological effects of fine sediment in the lotic environment, Environ. Manage., 21, 203–217, 1997.

Zabaleta, A., Martinez, M., Uriarte, J. A., and Antigüedad, I.: Factors controlling suspended sediment yield during runoff events in small headwater catchments of the Basque Country, Catena, 71, 179–190, 2007.

Appendix 2

Environmental Science & Technology

Article

pubs.acs.org/est

Storm Event Suspended Sediment-Discharge Hysteresis and Controls in Agricultural Watersheds: Implications for Watershed Scale Sediment Management

Sophie C. Sherriff,[*,†,‡] John S. Rowan,[‡] Owen Fenton,[†] Philip Jordan,[§] Alice R. Melland,[∥] Per-Erik Mellander,[⊥] and Daire Ó hUallacháin[†]

[†]Crops, Environment and Land Use Programme, Teagasc, Johnstown Castle, Wexford, Ireland

[‡]Geography, School of Social Sciences, University of Dundee, Dundee, DD1 4HN, Scotland, U.K.

[§]School of Geography and Environmental Sciences, Ulster University, Coleraine, Co. Derry, BT52 1SA, U.K.

[∥]National Centre for Engineering in Agriculture, University of Southern Queensland, Toowoomba, Australia

[⊥]Agricultural Catchments Programme, Crops, Environment and Land Use Programme, Teagasc, Johnstown Castle, Wexford, Ireland

S *Supporting Information*

ABSTRACT: Within agricultural watersheds suspended sediment-discharge hysteresis during storm events is commonly used to indicate dominant sediment sources and pathways. However, availability of high-resolution data, qualitative metrics, longevity of records, and simultaneous multiwatershed analyses has limited the efficacy of hysteresis as a sediment management tool. This two year study utilizes a quantitative hysteresis index from high-resolution suspended sediment and discharge data to assess fluctuations in sediment source location, delivery mechanisms and export efficiency in three intensively farmed watersheds during events over time. Flow-weighted event sediment export was further considered using multivariate techniques to delineate rainfall, stream hydrology, and antecedent moisture controls on sediment origins. Watersheds with low permeability (moderately- or poorly drained soils) with good surface hydrological connectivity, therefore, had contrasting hysteresis due to source location (hillslope versus channel bank). The well-drained watershed with reduced connectivity exported less sediment but, when watershed connectivity was established, the largest event sediment load of all watersheds occurred. Event sediment export was elevated in arable watersheds when low groundcover was coupled with high connectivity, whereas in the grassland watershed, export was attributed to wetter weather only. Hysteresis analysis successfully indicated contrasting seasonality, connectivity and source availability and is a useful tool to identify watershed specific sediment management practices.

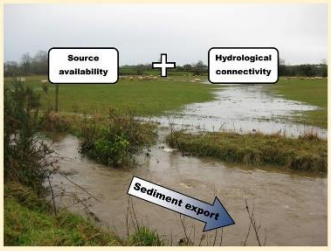

■ INTRODUCTION

Excessive supply of suspended sediment (SS) to rivers or deposition on channel beds can degrade ecological functioning.[1,2] Negative ecological impacts can also result from sediment-associated nutrients such as phosphorus, which is regulated by national or trans-boundary legislation.[3] Therefore, assessing the processes of sediment loss from potential sources such as agricultural landscapes to aquatic ecosystems is of critical importance for developing effective soil erosion and sediment management strategies.[4] Annual SS metrics are useful for prioritizing management strategies between basins, but they provide limited understanding of within watershed sediment sources and processes, and the respective controls upon soil erosion, sediment loss, and delivery.[5]

Methodologies such as sediment fingerprinting,[4,6−9] sediment budgets,[10−14] and modeling[15] are used to target sediment sources in agricultural watersheds. However, the resource intensiveness of field data collection and model validation can restrict multiwatershed comparisons and high temporal resolution investigations. Analysis of watershed suspended sediment concentration (SSC) and discharge (Q) hysteresis following rainfall-runoff are, however, inherently high-resolution. Interpretation of SS-Q hysteresis can provide insights into spatial and temporal dynamics of sediment source availability, sediment storage, and hydrological pathways.[16,17]

The use of SS-Q hysteresis as a sediment management tool has been limited by the inconsistent use of qualitative hysteresis categories, the difficulty of interpreting sediment pathways for complex hysteresis storms, and the scale-dependency of sediment pathways in relation to watershed size.[18] Recent developments in quantitative hysteresis parameters, for example, the Hysteresis Index (HI)[19,20] and the availability and improved reliability of high resolution SS data sets,[5]

Received: September 18, 2015
Revised: January 15, 2016
Accepted: January 19, 2016

DOI: 10.1021/acs.est.5b04573
Environ. Sci. Technol. XXXX, XXX, XXX−XXX

Table 1. Summary of Study Watershed Geology, Soil Type, Hydrological Pathways, Land Use, and Hydrology

	poorly drained	well-drained	moderately drained
size (km^2)	11.5	11.2	9.4
geology	moderate permeability rhyolitic volcanics and slate with fractures	low permeability slate and siltstone	low permeability calcareous greywacke and banded mudstone
soil type: dominant	poorly drained groundwater gleys	well-drained brown earths	poorly drained gleyic soils (groundwater and surface water gleys)
minor	*well-drained brown earths*	*poorly drained groundwater gleys*	*well-drained brown earths and podzols*
hydrological pathways: dominant	surface−lowlands	subsurface−hillslopes	surface−lowlands and southerly uplands
minor	*subsurface−uplands*	*surface−riparian corridor*	*subsurface−northern upland hillslopes*
land use	77% grassland 12% arable	54% arable 39% grassland	48% grassland 42% arable
30-year average annual rainfall (mm)[a]	1060	1060	758
annual average runoff (mm)[b]	465	527	441

[a]1981−2010 mean annual rainfall. [b]2009−2013.

facilitates the analysis of consecutive events in multiple watersheds over time. Long-term event-scale monitoring is commonly analyzed using multivariate statistics to attribute sediment response (either hysteresis type or numeric sediment metrics such as event SS yield, maximum SSC, mean SSC) to potential rainfall, discharge, and antecedent soil condition controls.[17,21−24] The evolution of HI in a watershed over time, however, has the potential to indicate seasonal variability in sediment dynamics, thus facilitating a conceptual understanding of watershed structural and functional hydrological connectivity,[25] transport pathways and sediment availability by combined analysis of contrasting hysteresis responses and their hydroclimatic controls. A conceptual diagram summarizes the hydrologic and geomorphic processes responsible for contrasting hysteresis types (Supporting Information Figure S1). Improved understanding of sediment loss is critical, particularly in agricultural watersheds which are intensively managed using land drainage and fertilization to increase agronomic outputs (crop and milk yields), to improve knowledge of diffuse pollutants under a range of flow conditions and to rigorously assess the causes of, and management options for, sediment export.[26]

In general, greater sediment losses are experienced from arable land.[17] However, in a study of five intensively managed agricultural watersheds in Ireland comprising a range of soil drainage (poor-, moderately-, and well-drained) and land use (predominantly arable or grassland) types, watersheds spatially dominated by arable land were not necessarily the highest yielding.[5] Ground-water flow pathways reduced surface connectivity of arable soils by limiting the surface quickflow component;[27] therefore, soil drainage class was suggested to have a stronger control on annual suspended sediment yield (SSY) than land use type. Conversely, a predominantly grassland watershed (low sediment source availability) with poorly drained soils (increased connectivity) exported a greater yield than the well-drained arable watershed described above. Elevated sediment fluxes from intensively managed grasslands have also been reported in the UK.[28] In the Irish study, the greatest SSY occurred from an arable watershed with poorly drained soils and a significant proportion of arable land. Significant interannual variability was present in the sediment response (as found in other international watersheds[29]) and has similarly been reported in storm-event hydrological flow-pathways[27] indicating that seasonal- and event-scale responses, driven by hydrology and land management, likely impact sediment erosion, entrainment, resuspension, and transport.

There is a need, therefore, to develop an overarching understanding of SS controls for agricultural watersheds to develop management plans and targeted mitigation options. Analysis of long-term SS and Q time-series data was investigated for this purpose in this study. The aim of the study was to develop conceptual models of SS transfer dynamics across and within multiple intensively managed agricultural watersheds to increase understanding and aid with watershed management. The objectives were to

(1) Develop an understanding of dominant hydrological and sediment pathways using storm resolution SS and Q data.
(2) Investigate the temporal evolution of watershed sediment transport processes and contributing areas through SS-Q hysteresis loop analysis.

MATERIALS AND METHODS

Study Sites. Three small (<12 km^2) study watersheds named here as poorly drained, moderately drained and well-drained, consistent with their dominant soil drainage classes, were used for this study (Supporting Information Figure S2).[30] All watersheds are intensively agricultural and considered to be undergoing land-use disturbance representative of longer-term intensification. Watersheds possess complex landscape configurations with dense landscape features (hedgerows and artificial drainage channels) resulting in small field sizes and reduced slope-lengths.[5] Full descriptions of study watersheds are reported elsewhere,[15] a brief summary is included below and in Table 1.

The poorly drained watershed is dominated by lowland groundwater gley soils underlain by a clay subsoil[31] primarily manifesting as poorly drained soils where perched groundwater saturates well-drained topsoils. These soils are predominantly utilized for grassland-based agriculture, namely grazing for dairy, beef, and sheep (1.28 LU/ha). Smaller areas of well-drained brown earth soils in the watershed uplands are used for arable crops and are not artificially drained. Slopes ≤1° and >5° occur in 25% and 25% of the watershed, respectively (2 m DEM). The well-drained watershed is predominantly utilized for spring crops on high permeability Brown Earth soils underlain by fractured bedrock. Poorly drained groundwater gley soils, prone to runoff in the riparian corridor, are more commonly utilized for grazing of beef cattle and sheep (average

DOI: 10.1021/acs.est.5b04573
Environ. Sci. Technol. XXXX, XXX, XXX−XXX

stocking rate 0.40 LU/ha). Slopes ≤1° and >5° occur in 10% and 21% of the watershed, respectively. The moderately drained watershed is primarily utilized for arable winter-sown crops and permanent grassland (stocking rate 0.77 LU/ha) over a spatially complex pattern of poor- (groundwater and surface water gleys) and moderately- (stagnic brown earths and gleyic luvisols) drained soils.[31] Slopes ≤1° and >5° occur in 20% and 23% of the watershed, respectively.

Data Collection. Suspended sediment data were collected at each watershed outlet using high-resolution (10 min) turbidity (T) (Solitax, Hach-Lange, Germany) and Q measurements. Turbidity was calibrated to SSC using a rating curve (poorly drained, $R^2 = 0.96$, $n = 443$; well-drained, $R^2 = 0.96$, $n = 231$; moderately drained, $R^2 = 0.94$ and 0.88, $n = 242$ (two-part regression))[5] constructed from event and nonevent samples collected manually or with an automatic water sampler (ISCO 6712, ISCO Inc.). This approach for SS estimation was validated by direct depth-integrated and cross-sectional samples and no differences in T-SSC relationship occurred between event and nonevent samples.[5] Water level (m), collected at 10 min intervals, was monitored by a vented pressure-transducer (OTT Orpheus-mini, OTT, Germany) in a stilling well rated to discharge over a nonstandard Corbett flat-v weir (Corbett Concrete, Cahir, Ireland) using the velocity-area method for gauging instantaneous discharge (OTT Acoustic Doppler Current-meter, OTT, Germany). Rating relationships were calculated using WISKI-SKED software.[5,27]

Meteorological data were collected from a lowland weather stations (BWS200, Campbell Scientific) measuring 10 min resolution rainfall, air temperature, relative air humidity, radiation and wind-speed. Higher-altitude rainfall depth and rainfall intensity were also measured with an additional upland rain gauge. Ground cover of dominant crop types in each watershed were estimated using monthly observations from multiple locations and 70% ground cover was defined as the threshold required to reduce soil erosion risk.[32]

Data Analysis. Individual storm events from October 2011 to September 2013 were extracted according to watershed specific hydro-sedimentary characteristics.[21] In the well-drained and poorly drained watersheds, annual total rainfall of 2011 (841 mm) was lower and 2012 and 2013 (1172 mm and 880 mm) relatively close to the long-term annual average rainfall of 1060 mm (Johnstown Castle, Met Éireann (Table 1)). In the moderately drained watershed, 2011, 2012, and 2013 (672 mm, 850 mm and 764 mm, respectively) were relatively close to the long-term annual average of 758 mm (Dublin Airport, Met Éireann). In all watersheds 2012 was characterized by a wet summer with rain exceeding the long-term average while 2013 had a dry summer with lower rainfall than normal for the area. In the poorly drained watershed, storm event initiation was defined where the rate of change between consecutive 10 min measurements of Q and SSC exceeded 0.005 m^3/sec and 2 mg/L, respectively, and consistent decreases between consecutive 10 min measurements in Q of <0.012 m^3/sec and SSC of 1 mg/L defined event termination. In the well-drained watershed, event initiation was defined where Q increased by >0.003 m^3/sec and SSC by 2 mg/L between consecutive 10 min measurements, and termination where Q decreased by <0.007 m^3/sec and SSC by 1 mg/L. In the moderately drained watershed, event initiation was defined where Q increased by >0.005 m^3/sec and SSC by >2 mg/L and termination where Q decreased by <0.003 m^3/sec and SSC by <1 mg/L between consecutive 10 min measurements. Where multiple SSC and Q peaks in the stream record could be related to separate rainfall bands they were divided and assessed as single events. Poorly drained, well-drained and moderately drained watersheds comprised 88, 67, and 90 storm events over the study period, respectively.

Events were classified according to hysteresis categories[16] and a HI.[19] Biplots of Q and SSC indicated the hysteresis loop direction to qualitatively assign hysteresis type; clockwise where SSC peaks before Q, anticlockwise where Q peaks before SSC, no hysteresis where peaks are simultaneous, figure-8 patterns which feature both clockwise and anticlockwise characteristics and complex hysteresis where a clear relationship between SSC and Q is difficult to define.

The HI is a numerical indicator of hysteresis[19] calculated using Q and SSC data from each storm event; first the midpoint of Q (Q_{mid}) must be determined:

$$Q_{mid} = 0.5(Q_{max} - Q_{min}) + Q_{min} \quad (1)$$

where Q_{min} and Q_{max} are the initial peak event Q readings. The corresponding SSC values at Q_{mid} on the rising (SSC_{RL}) and falling (SSC_{FL}) hydrological limbs are then assessed:

Where $SSC_{RL} > SSC_{FL}$:

$$HI = (SSC_{RL}/SSC_{FL}) - 1 \quad (2)$$

And where $SSC_{RL} < SSC_{FL}$:

$$HI = (-1/(SSC_{RL}/SSC_{FL})) + 1 \quad (3)$$

Higher HI magnitudes in either direction indicate greater asynchronous behavior between SSC and Q. Positive HI values indicate clockwise hysteresis, where HI ∼ 0 hysteresis is absent a simultaneous SSC and Q response occurs, and negative HI values indicate anticlockwise hysteresis. The HI, calculated at a single Q value, that is, Q_{mid}, cannot reveal Figure-8 and complex hysteresis categories. To aid further discussion, clockwise responses and positive HI metrics are referred to as "proximal" responses and are broadly defined as sediment derived from sources local to the monitoring point and/or subject to a rapid transport pathway. Negative HIs and hysteresis categories are referred as "distal" sediment responses may conversely indicate a spatially distal sediment source, and/or subject to a delayed transport mechanism.

Data were separated by hysteresis category (clockwise, anticlockwise, no-hysteresis, figure-8 and complex) to investigate controls in each watershed.[8] Eighteen potential hydrological event controls were collated for each event. Discharge parameters: maximum discharge (m^3/sec), total event discharge (m^3), event duration (min) flood intensity (($Q_{max} - Q_{min}$)/time of rise), and rainfall-runoff ratio (%). Precipitation parameters: total event precipitation (mm), duration of rainfall event (min), maximum precipitation intensity at 10- and 30 min resolutions (mm/h), and average precipitation intensity (mm/h). Antecedent parameters: antecedent rainfall at 1, 3, 5, and 10 days before event initiation (mm) and antecedent soil wetness at 1, 3, 5, and 10 days before event initiation (mm). Soil wetness was calculated using the effective drainage component of a soil moisture deficit (SMD) model which represents infiltration and runoff components calculated by subtracting the surplus rainfall after potential actual evapotranspiration and filling of a typical soil moisture profile.[33]

The event-SSC_{fw} (total event SS load divided by total event flow volume−mg/L) was selected as the sediment response variable. Flow-weighted concentration metrics are more

DOI: 10.1021/acs.est.5b04573
Environ. Sci. Technol. XXXX, XXX, XXX−XXX

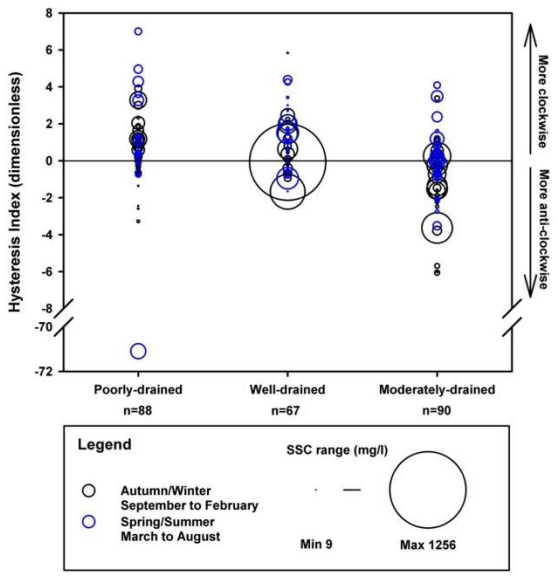

Figure 1. Flow-weighted event suspended sediment concentrations (circle size: magnitude of sediment response) and hysteresis index for hydro-sedimentary events during spring/summer (March to August) in blue circles and autumn/winter (September to February) in black circles in the poorly drained, well-drained and moderately drained watersheds from first October 2011 to 30th September 2013.

indicative of source availability by reducing the influence of contrasting watershed hydrology[34] and also removes any potential autocorrelation with the discharge parameters used to calculate SSC. Principal components analysis (PCA) was performed (SAS JMP v9) and potential controls defined as those occupying similar areas of the PCA loading graph with event-SSC_{fw}.

RESULTS

Storm Event Hysteresis. Over two years the HI showed events that had positive, negative and no-hysteresis in all three watersheds (Figure 1). Events in the poorly drained watershed were predominantly positive and these exported greater event-SSC_{fw} compared to events where HI $\leq$ 0. One event in the poorly drained watershed had an extremely negative HI (−71.1) and high magnitude event-SSC_{fw}. In the well-drained watershed, more positive than negative events occurred and event-SSC_{fw} largest where HI was further from zero (positive or negative), except for one event at HI ~ 0 which reported the highest value (1256 mg/L) for any watershed. The moderately drained watershed had the largest HI range but was overall dominated by negative HI events which exported greater sediment quantities. All watersheds had lower event-SSC_{fw} during spring/summer than autumn/winter.

Fluctuations of HI showed contrasting seasonal trends between watersheds (Figure 2). In the poorly drained watershed, high (>70%) ground cover was maintained throughout the monitoring period, negative HIs corresponded to periods of lower weekly rainfall values (January to March 2012 and June to July 2013). Periods of high weekly rainfall had positive HI, although scatter was greater at these times. Switches in HI direction (positive to negative or vice versa) occurred in Jan 2012 and May 2012. The well-drained watershed showed that during wetter periods (e.g., April 2012 to January 2013), positive HI was more common, but similarly to the poorly drained watershed, the magnitude of positive HIs decreased as such conditions continued. Decreasing weekly rainfall totals (November 2011 to April 2012) coincided with a negative to positive HI switch. Event-SSC_{fw} was larger where ground cover was less than 70% in the arable watersheds ($p < 0.05$). Consistently high weekly rainfall totals corresponded with a change in direction from positive to negative HI in the moderately drained watershed (April 2012 to September 2012) and as wet conditions continued, until February 2013, negative HI was sustained. Increased weekly rainfall then decreased from March 2013 onward and coincided with HI returning toward zero.

Examples of all qualitative hysteresis categories were displayed in the three watersheds (Figure 3), but analysis of "no-hysteresis" events could not be analyzed in the poorly drained and moderately drained watersheds as they were too infrequent ($n = 1$ and $n = 2$, respectively). The contribution of each event hysteresis type to the total event load was not dependent upon the frequency of the type of hysteresis that occurred in any watershed. In the poorly drained watershed, clockwise hysteresis was the most frequent (60%) and contributed the greatest proportion (59%) of the total event SS load. Anticlockwise hysteresis occurred for 14% of events, but only contributed to 2% of the event SS load. The total SS event load in the well-drained watershed was dominated by

DOI: 10.1021/acs.est.5b04573
Environ. Sci. Technol. XXXX, XXX, XXX−XXX

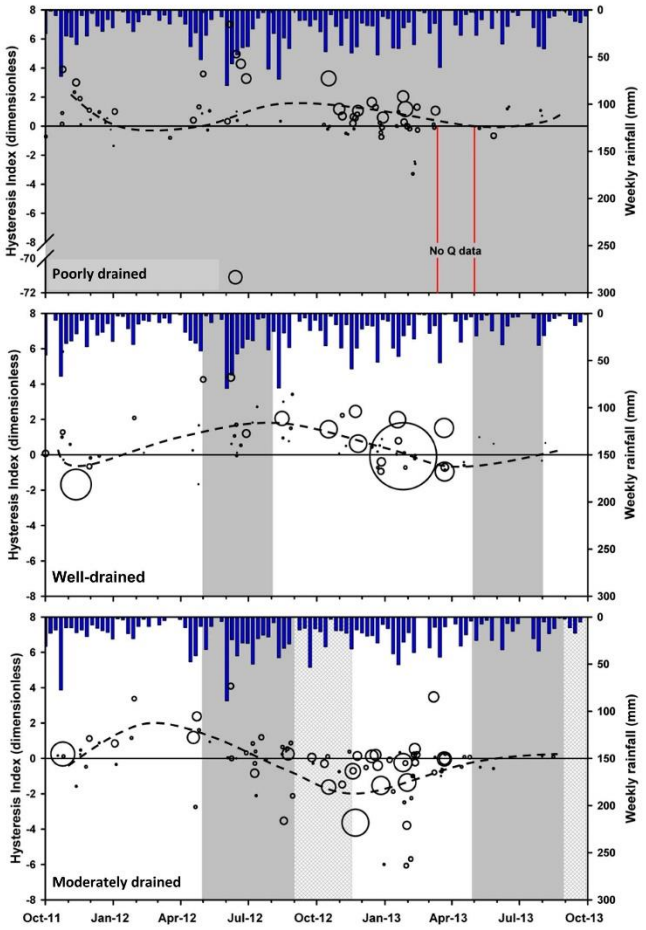

Figure 2. Hysteresis index, weekly rainfall and magnitude of flow-weighted suspended sediment concentration response (indicated by size of circle) over monitoring period in the poorly drained, well-drained and moderately drained watersheds. Gray panel: high ground cover (>70%), gray-white panel: a reduced proportion of fields had high ground cover, dashed line indicates seasonal trend.

events with no hysteresis (47%) but this hysteresis type occurred only 11% of the time. Similarly to the poorly drained watershed, clockwise was the dominant hysteresis type in the well-drained watershed (39%) and had a similar proportion of SS load contribution (35%). In the moderately drained watershed, anticlockwise was most frequent (36%) but contributed 23% of the total event SS load. Contrastingly, figure-8 events comprised 21% of events in the moderately drained watershed but contributed 43% of the total event SS load.

Storm Event SS Controls. Variables correlated with event-SSC_{fw} for each hysteresis category are presented in Figure 4, Supporting Information Figures S3, S4, and S5. Events with clockwise HI in the poorly drained watershed were correlated with discharge parameters, precipitation total and 30 min precipitation intensity. Clockwise events in the well-drained watershed were controlled by the same discharge variables and total precipitation, but also precipitation duration. In the moderately drained watershed, clockwise event-SSC_{fw} was controlled by precipitation variables only. Events with anticlockwise hysteresis were primarily correlated by discharge, precipitation amount, and precipitation intensity in the well- and moderately drained watersheds. Anticlockwise events in the poorly drained watershed, similarly to clockwise hysteresis

DOI: 10.1021/acs.est.5b04573
Environ. Sci. Technol. XXXX, XXX, XXX−XXX

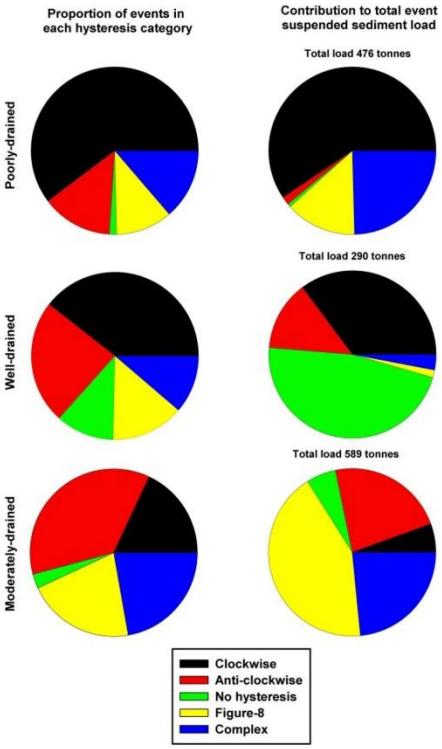

Figure 3. Proportion of events categorized by hysteresis type (left), and the contribution of hysteresis type to total event load over monitoring period (right) in poorly drained, well-drained and moderately drained watersheds.

events were correlated with precipitation amount and most discharge parameters. Figure-8 hysteresis events were controlled by discharge and precipitation controls in the arable watersheds, reflecting the combined clockwise, and anticlockwise hysteresis variable list. In the poorly drained watershed controlling variables for figure-8 hysteresis were maximum discharge, flood intensity, average precipitation intensity, and total precipitation. Complex hysteresis events in the poorly drained watershed were correlated with discharge, precipitation and 10-day antecedent rainfall and soil wetness. Similarly in the moderately drained watershed, discharge and total precipitation were best correlated to event-SSC_{fw}. The well-drained watershed did not show any correlations with event-SSC_{fw} for complex hysteresis events. No-hysteresis events in the well-drained watershed were highly correlated with discharge and precipitation.

■ DISCUSSION

Structural Connectivity and Dominant Sediment Pathways. In the poorly drained watershed, predominantly positive HIs (aligned with clockwise hysteresis) were primarily controlled by stream hydrology, suggesting sediments were channel derived, despite good surface hydrological connectivity[35] driven by perched groundwater on poorly drained lowland soils.[27] Permanent grassland likely reduced the sediment availability (and sediment connectivity) from hillslopes resulting in infrequent and lower yielding distal sediment hysteresis responses. Availability of sediment in- or near-channels was confirmed by observed channel bank erosion and sediment storage in lower stream reaches (see method in Supporting Information and Figure S6), and sediment fingerprinting data.[36] High energy surface runoff from lowland soils and emergent flow from well-drained upland soils is rapidly diverted through extensive subsurface and surface (drainage ditch) artificial drainage networks.[27] In agricultural watersheds, channels are typically artificially straightened, deepened and widened, subsequently increasing the magnitude and erosivity of high flows and reduced base flows which encourages sediment deposition.[37]

In the well-drained watershed, subsurface hydrological pathways resulting from infiltration dominated well-drained soils overlain upon fractured bedrock reduces surface hydrological connectivity.[27] This structural disconnectivity on hillslopes effectively reduces soil loss risk where the spatial and temporal sediment risk is greatest (watershed features the highest proportion and longest period of low ground cover). Proximal sediment hysteresis, controlled predominantly by stream hydrology, was therefore most frequent but unlike the poorly drained watershed, riparian woodland at lower stream reaches likely increased channel bank stability. In- or near-channel storage likely controlled the proximal response influenced by the accumulation of intermediate subsurface storage (referred to here as displacement of water stored in the unsaturated zone due to infiltrating drainage from rainfall) due to inefficient particulate transport through well-drained soils[38] and rapid flood recession causing deposition of entrained sediment. Channel and subsurface sediment stores were likely resuspended and entrained where flow transport capacity was sufficient, resulting in the predominantly proximal response.[22]

A wider HI range in the moderately drained watershed likely resulted from the complexity of soil types and consequential variability of hydrological flow pathways. Moderate- to poorly-drained soils, featuring low storage capacities, increase the likelihood of surface flow pathways upslope of the channel network and resulted in surficially derived sediments (indicated by rainfall erosivity parameters) in all hysteresis categories.[17] The absence of hydrological controls for positive (or clockwise) events and lower event-SSC_{fw} supports low stream channel storage (Supporting Information Table S2 and S3) and limited bank erosion due to a riparian woodland corridor along lower stream reaches. Near-channel poached areas or highly connected features such as unmetalled roads[39] may regulate the proximal response.[22,40] The configuration of drainage channels (high network density to watershed size ratio) likely reduced the hillslope to stream transit time and increased the proportion of the drainage network contributing to proximal and distal sediment responses.[18]

Temporal Hysteresis Evolution, Functional Connectivity and Sediment Availability. Seasonality of the hysteresis response was revealed using the HI which, when combined with control analysis, indicated fluctuations in the hydro-geomorphic processes controlling sediment supply. Scatter around the seasonal trend in all watersheds likely

DOI: 10.1021/acs.est.5b04573
Environ. Sci. Technol. XXXX, XXX, XXX−XXX

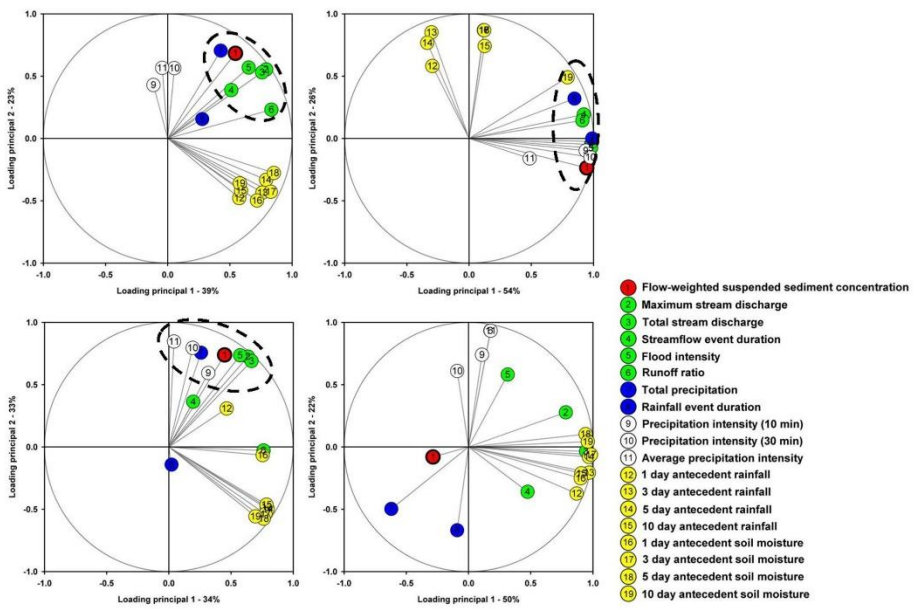

Figure 4. Example of determination of controls on event-SSCfw using PCA loading diagrams. Clockwise from top left: clockwise events in the poorly drained watershed, no-hysteresis events in the well-drained watershed, complex events in the well-drained watershed and figure-8 events in the moderately drained watershed.

resulted from shorter-term fluctuations in connectivity, depletion of available sources, inter-event channel sediment accumulation (Supporting Information Table S2 and S3) and event specific characteristics (rainfall intensity, duration, and spatial variability).[22,41,42] During relatively low rainfall conditions, hysteresis responses were predominantly proximal in all three watersheds. Consequently, restricted connectivity of the majority of the watershed resulted in local (spatially proximal) processes governing storm responses and reduced influence from wider watershed-scale processes. In the poorly- and well-drained watersheds, stream hydrology controls dominated suggesting resuspension of sediment in storage in the lower reaches (Supporting Information Table S2 and S3) but surficial controls in the moderately drained watershed indicated near-channel sediment or rapidly connected soils (e.g., poached soils or compacted grassland soils and tramlines or field margins in arable fields)[21,40,43] were available throughout the year.

The onset and continuation of higher rainfall altered the hysteresis responses, causing increased and sustained proximity of sediment supply in the poorly drained watershed, initial proximity increase was followed by a decrease in the well-drained watershed, and consistently decreasing proximity in the moderately drained watershed. Under continued high rainfall conditions, the poorly drained and moderately drained watersheds may be expected to experience increased surface soil erosion due to greater hydrological connectivity, surface flow pathways, and antecedent storage despite widespread artificial drainage.[17] This is confirmed in the moderately drained watershed by increasingly negative HIs and controls indicating surficially derived sediments particularly during low groundcover periods, where connectivity coincided with source availability. However, in the poorly drained watershed, predominant grassland land use decreased hillslope sediment erodibility and limited distal hysteresis responses despite good connectivity. The rapid delivery of sediment depleted runoff through artificial drainage (subsurface and surface) likely elevated stream flows, encouraged bank erosion, and resuspension of stored channel sediments, therefore, enhancing the proximal response. As in other regions such as the U.S. midwest where flat and poorly drained soils occur, lateral pressure gradients due to confined groundwater conditions further exacerbate channel bank erosion and proximal hysteresis responses.[44,45]

In the well-drained watershed, despite increased rainfall and high distal source availability relative to the moderately drained watershed (larger extent and longer period of low groundcover), proximal hysteresis responses occurred likely due to infiltration on predominantly well-drained soils which disconnected field sources.[27,46] Gradual reduction of positive HI magnitudes with sustained wetter conditions likely indicated depletion of sediment stored in the lower channel reaches (Supporting Information Table S2 and S3). Greater hillslope connectivity and sediment loss during events with distal hysteresis did not necessarily yield higher sediment quantities. The greatest event-$SSC_{fw,}$ defined as the maximum sediment transfer potential (ST_{max}) occurred following an extreme

DOI: 10.1021/acs.est.5b04573
Environ. Sci. Technol. XXXX, XXX, XXX−XXX

rainfall event, (31 mm rainfall, 2.11 mm/h average precipitation intensity) resulting in an intense (0.57 m^3/sec discharge increase per hour of rising limb) and long duration (13 h) no-hysteresis stream hydrology event. Simultaneous sediment and discharge peaks suggested widespread connectivity and this coincided with low groundcover. Comparatively, ST_{max} was more frequent in the moderately drained watershed as connectivity was better maintained.

Management of Sediment Sources and Pathways. Reduction of soil loss and sediment export requires watershed specific management strategies that account for spatial and temporal source availability and landscape connectivity; however, sediment contribution rather than the frequency of hysteresis type must be used to prioritize management strategies. In the poorly drained watershed, sediment losses from lowland hillslope overland flow pathways are effectively reduced by permanent crop cover and thus must be maintained to prevent distal source activation. Channel bank erosion results from high flow energy in the channel network. Management options are therefore, dissipation of flow velocities through improving lateral connectivity (reduction of channel side slope gradient, establishing riparian wetlands), introducing channel geomorphic complexity such as construction of artificial riffle-pool sequences and remeandering, and establishing vegetated and woodland riparian corridors to stabilize banks.[37,47] Management of the stream corridor will likely reduce the magnitude of positive hysteresis responses and sediment loss.

Conversion of arable soils to permanent grassland in the moderately drained watershed will effectively reduce hillslope source availability; however, in postconversion, increased channel flow velocities as in the poorly drained watershed may result as less energy is expended on the erosion and transport of hillslope particulates. The sediment loss risk may consequently be offset particularly in upland and midchannel reaches where no woodland riparian corridor is present. Reducing hillslope connectivity by increasing subsurface pathways through appropriate subsurface drainage[48] or increasing soil water storage capacity by aeration[24] may reduce surface flows but efficacy over time is spatially variable.[48] Interception of surface pathways through buffer strips encourage deposition of sediments and reduction of flow pathways, but can require agricultural land to be set-aside from production.[47] Therefore, rural sustainable drainage systems (RSuDS) are a viable alternative to minimize the area set-aside where land use pressure exists.[49]

Natural disconnectivity in the well-drained watershed effectively reduces soil loss risk from low groundcover on hillslopes. Extreme rainfall was capable of exceeding infiltration capacities, activating surface pathways and exporting large sediment quantities but was infrequent. Temporary sediment control measures such as sediment fences[50] may be a practical solution on fields with high soil erosion risk when extreme rainfall events are predicted. Large scale conversion to grassland is unlikely to reduce sediment export effectively and would be impractical where maintenance of agricultural productivity is an objective.[46]

Climate change projections suggest changes in hydrometeorological patterns and, for this study area, increased winter and reduced summer rainfall and streamflow.[50] Assessment of hysteresis dynamics over time encapsulates dynamic and complex system functions such that impacts on hydrological and sediment pathways can be projected in the study watersheds. Natural disconnectivity in the well-drained watershed is likely more frequently exceeded in winter, increasing hillslope connectivity and the achievement of ST_{max} during low ground cover periods. Surface sources will continue to dominate in the moderately drained watershed with more frequent and higher magnitude distal responses and greater sediment export during low groundcover periods. In the poorly drained watershed the dominant hysteresis response would likely be unchanged but, similarly to the moderately drained watershed the magnitude, in this case the proximal responses (and associated sediment export) will likely increase as stream channels are more frequently inundated. Intermittent negative hysteresis may become more frequent as well-drained upland soils are connected following prolonged wet conditions.

Management of hydrological connectivity is becoming more widely recognized as an effective approach to watershed pollutant management strategies. Novel analysis using high-resolution, robust suspended sediment data and hysteresis methods, as in this study, provide an internationally applicable framework to indicate hydro-geomorphological processes controlling fluctuating connectivity over time. Valuable information for watershed managers is proposed, that is, reducing sediment loss risk by managing fluctuating sediment connectivity specific to physical watershed characteristics. These principals were explored in watersheds with contrasting physical conditions, land use, and land management pressures, and provide a template for similar watersheds elsewhere. Projections of future sediment connectivity variations with changing hydrological regimes associated with climate change can additionally inform future watershed management plans. Consequently, adaptive measures to support sustainable intensification of agricultural systems can be more robustly and cost-effectively designed to mitigate current and future sediment loss risk.

■ ASSOCIATED CONTENT

Supporting Information

The Supporting Information is available free of charge on the ACS Publications website at DOI: 10.1021/acs.est.5b04573.

Additional information as noted in the text (PDF)

■ AUTHOR INFORMATION

Corresponding Author

*Phone: +353 53 9171200; fax: +353 53 9142213; e-mail: s.c.sherriff@dundee.ac.uk.

Notes

The authors declare no competing financial interest.

■ ACKNOWLEDGMENTS

Funding was provided by the Walsh Fellowship Programme, Teagasc, Ireland allied to the University of Dundee, UK, and the Teagasc Agricultural Catchments Programme (funded by the Department of Agriculture, Food and the Marine, Ireland). We thank Agricultural Catchments Programme colleagues for technical support and acknowledge farmers and landowners of the study watersheds.

■ REFERENCES

(1) Glendell, M.; Granger, S. J.; Bol, R.; Brazier, R. E. Quantifying the spatial variability of soil physical and chemical properties in relation to mitigation of diffuse water pollution. *Geoderma* **2014**, *214−215*, 25−41.

DOI: 10.1021/acs.est.5b04573
Environ. Sci. Technol. XXXX, XXX, XXX−XXX

(2) Kjelland, M.; Woodley, C.; Swannack, T.; Smith, D. A review of the potential effects of suspended sediment on fishes: potential dredging-related physiological, behavioral, and transgenerational implications. *Environ. Syst. Decis.* **2015**, *35* (3), 334−350.
(3) Ballantine, D.; Walling, D. E.; Leeks, G. J. L. Mobilisation and Transport of Sediment-Associated Phosphorus by Surface Runoff. *Water, Air, Soil Pollut.* **2009**, *1*, 311−320.
(4) Rowan, J. S.; Black, S.; Franks, S. W. Sediment fingerprinting as an environmental forensics tool explaining cyanobacteria blooms in lakes. *Appl. Geogr.* **2012**, *32* (2), 832−843.
(5) Sherriff, S. C.; Rowan, J. S.; Melland, A. R.; Jordan, P.; Fenton, O.; Ó hUallacháin, D. Investigating suspended sediment dynamics in contrasting agricultural catchments using ex situ turbidity-based suspended sediment monitoring. *Hydrol. Earth Syst. Sci.* **2015**, *19*, 3349−3363.
(6) Gellis, A. C.; Walling, D. E., Sediment Source Fingerprinting (Tracing) and Sediment Budgets as Tools in Targeting River and Watershed Restoration Programs. In *Stream Restoration in Dynamic Fluvial Systems*; Simon, A., Bennett, S. J., Castro, J. M., Eds.; American Geophysical Union: Washington D.C., 2011; pp 544.
(7) Koiter, A. J.; Owens, P. N.; Petticrew, E. L.; Lobb, D. A. The behavioural characteristics of sediment properties and their implications for sediment fingerprinting as an approach for identifying sediment sources in river basins. *Earth-Sci. Rev.* **2013**, *125*, 24−42.
(8) Belmont, P.; Willenbring, J. K.; Schottler, S. P.; Marquard, J.; Kumarasamy, K.; Hemmis, J. M. Toward generalizable sediment fingerprinting with tracers that are conservative and nonconservative over sediment routing timescales. *J. Soils Sediments* **2014**, *14*, 1479−1492.
(9) Smith, H. G.; Blake, W. H. Sediment fingerprinting in agricultural catchments: a critical re-examination of source discrimination and data corrections. *Geomorphol.* **2014**, *204*, 177−191.
(10) Smith, H. G.; Dragovich, D. Sediment budget analysis of slope-channel coupling and in-channel sediment storage in an upland catchment, southeastern Australia. *Geomorphol.* **2008**, *101*, 643−654.
(11) Walling, D. E.; Collins, A. L. The catchment sediment budget as a management tool. *Environ. Sci. Policy* **2008**, *11* (2), 136−143.
(12) Notebaert, B.; Verstraeten, G.; Rommens, T.; Vanmonfort, B.; Govers, G.; Poesen, J. Establishing a Holocene sediment budget for the river Dijle. *Catena* **2009**, *77* (2), 150−163.
(13) Belmont, P.; Gran, K. B.; Schottler, S. P.; Wilcock, P. R.; Day, S. S.; Jennings, C.; Wesley Lauer, J.; Viparelli, E.; Willenbring, J. K.; Engstrom, D. R.; Parker, G. Large shirt in source of fine sediment in the Upper Mississippi river. *Environ. Sci. Technol.* **2011**, *45* (20), 8804−8810.
(14) Minella, J. P. G.; Walling, D. E.; Merten, G. H. Establishing a sediment budget for a small agricultural catchment in southern Brazil, to support the development of effective sediment management strategies. *J. Hydrol.* **2014**, *519* (Part B), 2189−2201.
(15) Collins, A. L.; Strőmqvist, J.; Davison, P. S.; Lord, E. I. Appraisal of phosphorus and sediment transfer in three pilot areas identified for the catchment sensitive farming initiative in England: application of the prototype PSYCHIC model. *Soil Use Manage.* **2007**, *23*, 117−132.
(16) Williams, G.P. Sediment concentration versus water discharge during single hydrological events in rivers. *J. Hydrol.* **1989**, *111*, 89−106.
(17) Duvert, C.; Gratiot, N.; Evrary, O.; Navratil, O.; Némery, J.; Prat, C.; Esteves, M. Drivers of erosion and suspended sediment transport in three headwater catchments of the Mexican Central Highlands. *Geomorphol.* **2010**, *3−4*, 243−256.
(18) Gao, P.; Josefson, M. Event-based suspended sediment dynamics in a central New York watershed. *Geomorphol.* **2012**, *139−140*, 425−437.
(19) Lawler, D. M.; Petts, G. E.; Foster, I. D. L.; Harper, S. Turbidity dynamics during spring storm events in an urban headwater river system: The Upper Tame, West Midlands, UK. *Sci. Total Environ.* **2006**, *360*, 109−126.
(20) Aich, V.; Zimmermann, A.; Elsenbeer, H. Quantification and interpretation of suspended-sediment discharge hysteresis patterns: How much data do we need? *Catena* **2014**, *122*, 120−129.
(21) Zabaleta, A.; Martínez, M.; Uriarte, J. A.; Antigüedad, I. Factors controlling suspended sediment yield during runoff events in small headwater catchments of the Basque Country. *Catena* **2007**, *71* (1), 179−190.
(22) Oeurng, C.; Sauvage, S.; Sánchez-Pérez, J.-M. Dynamics of suspended sediment transport and yield in a large agricultural catchment, southwest France. *Earth Surf. Processes Landforms* **2010**, *35* (11), 1289−1301.
(23) Giménez, R.; Casalí, J.; Grande, I.; Díez, J.; Campo, M. A.; Álvarez-Mozos, J.; Goñi, M. Factors controlling sediment export in a small agricultural watershed in Navarre (Spain). *Agric. Water Manage.* **2012**, *110*, 1−8.
(24) Perks, M. T.; Owen, G. J.; Benskin, C. M. H.; Jonczyk, J.; Deasy, C.; Burke, S.; Reaney, S. M.; Haygarth, P. M. Dominant mechanisms for the delivery of fine sediment and phosphorus to fluvial networks draining grassland dominated headwater catchments. *Sci. Total Environ.* **2015**, *523*, 178−190.
(25) Bracken, L. J.; Wainwright, J.; Ali, G. A.; Tetzlaff, D.; Smith, M. W.; Reaney, S. M.; Roy, A. G. Concepts of hydrological connectivity: Research approaches, pathways and future agendas. *Earth-Sci. Rev.* **2013**, *119*, 17−34.
(26) Bowes, M. J.; House, W. A.; Hodgkinson, R. A.; Leach, D. V. Phosphorus−discharge hysteresis during storm events along a river catchment: the River Swale, UK. *Water Res.* **2005**, *39* (5), 751−762.
(27) Mellander, P.-E.; Jordan, P.; Shore, M.; Melland, A. R.; Shortle, G. Flow paths and phosphorus transfer pathways in two agricultural streams with contrasting flow controls. *Hydrol. Process.* **2015**, *29*, 3504−3518.
(28) Bilotta, G. S.; Krueger, T.; Brazier, R. E.; Butler, P.; Freer, J.; Hawkins, J. M. B.; Haygarth, P. M.; Macleod, C. J. A.; Quinton, J. N. Assessing catchment-scale erosion and yields of suspended solids from improved temperate grassland. *J. Environ. Monit.* **2010**, *12* (3), 731−739.
(29) Vanmaercke, M.; Maetens, W.; Poesen, J.; Jankauskas, B.; Jankauskiene, G.; Verstraeten, G.; de Vente, J. A comparison of measured catchment sediment yields with measured and predicted hillslope erosion rates in Europe. *J. Soils Sediments* **2012**, *12* (4), 586−602.
(30) Wall, D.; Jordan, P.; Melland, A. R.; Mellander, P. E.; Buckley, C.; Reaney, S. M.; Shortle, G. Using the nutrient transfer continuum concept to evaluate the European Union Nitrates Directive National Action Programme. *Environ. Sci. Policy* **2011**, *14* (6), 664−674.
(31) Melland, A. R.; Mellander, P. E.; Murphy, P. N. C.; Wall, D. P.; Mechan, S.; Shine, O.; Shortle, G.; Jordan, P. Stream water quality in intensive cereal cropping catchments with regulated nutrient management. *Environ. Sci. Policy* **2012**, *24*, 58−70.
(32) Sanjari, G.; Yu, B.; Ghadiri, H.; Ciesiolka, C. A. A.; Rose, C. W. Effects of time-controlled grazing on runoff and sediment loss. *Aust. J. Soil Res.* **2009**, *47* (8), 796−808.
(33) Schulte, R. P. O.; Diamond, J.; Holden, N. M.; Brereton, A. J. Predicting the soil moisture conditions of Irish grasslands. *Irish Journal of Agricultural and Food Research* **2005**, *44* (1), 95−110.
(34) Jordan, P.; Menary, W.; Daly, K.; Kiely, G.; Morgan, G.; Byrne, P.; Moles, R. Patterns and processes of phosphorus transfer from Irish grassland soils to rivers—integration of laboratory and catchment studies. *J. Hydrol.* **2005**, *304* (1−4), 20−34.
(35) Mellander, P.-E.; Melland, A. R.; Jordan, P.; Wall, D. P.; Murphy, P. N. C.; Shortle, G. Quantifying nutrient transfer pathways in agricultural catchments using high temporal resolution data. *Environ. Sci. Policy* **2012**, *24*, 44−57.
(36) Sherriff, S. C.; Rowan, J. R.; Franks, S. W.; Walden, J.; Melland, A. R.; Jordan, P.; Ó hUallacháin, D. Sediment Fingerprinting. *TResearch* **2014**, *Summer 2014*, 40−41.
(37) Vought, L. M.; Lacoursière, J., Restoration of Streams in the Agricultural Landscape. In *Restoration of Lakes, Streams, Floodplains,*

DOI: 10.1021/acs.est.5b04573
Environ. Sci. Technol. XXXX, XXX, XXX−XXX

and Bogs in Europe; Eiseltová, M., Ed.; Springer: Netherlands, 2010; Vol. 3, pp 225−242.
(38) Warsta, L.; Taskinen, A.; Koivusalo, H.; Paasonen-Kivekäs, M.; Karvonen, T. Modelling soil erosion in a clayey, subsurface-drained agricultural field with a three-dimensional FLUSH model. *J. Hydrol.* **2013**, *498*, 132−143.
(39) Collins, A. L.; Walling, D. E.; Stroud, R. W.; Robson, M.; Peet, L. M. Assessing damaged road verges as a suspended sediment source in the Hampshire Avon catchment, southern United Kingdom. *Hydrol. Processes* **2010**, *24* (9), 1106−1122.
(40) Mano, V.; Nemery, J.; Belleudy, P.; Poirel, A. Assessment of suspended sediment transport in four alpine watersheds (France): influence of the climatic regime. *Hydrol. Processes* **2009**, 23 (5), 777−792.
(41) Steegen, A.; Govers, G.; Nachtergaele, J.; Takken, I.; Beuselinck, L.; Poesen, J. Sediment export by water from an agricultural catchment in the Loam Belt of central Belgium. *Geomorphol.* **2000**, 33 (1−2), 25−36.
(42) Boardman, J.; Shepheard, M. L.; Walker, E.; Foster, I. D. L. Soil erosion and risk-assessment for on- and off-farm impacts: A test case using the Midhurst area, West Sussex, UK. *J. Environ. Manage.* **2009**, *90* (8), 2578−2588.
(43) Bilotta, G. S.; Brazier, R. E.; Haygarth, P. M., The Impacts of Grazing Animals on the Quality of Soils, Vegetation, and Surface Waters in Intensively Managed Grasslands. In *Advances in Agronomy*; Donald, L. S., Ed.; Academic Press, 2007; Vol. *94*, pp 237−280.
(44) Fox, G. A.; Wilson, G. V.; Simon, A.; Langendoen, E. J.; Akay, O.; Fuchs, J. W. Measuring streambank erosion due to ground water seepage: correlation to bank pore water pressure, precipitation and stream stage. *Earth Surf. Processes Landforms* **2007**, *32* (10), 1558−1573.
(45) Lenhart, C. F.; Verry, E. S.; Brooks, K. N.; Magner, J. A. Adjustment of prairie pothole streams to land-use, drainage and climate changes and consequences for turbidity impairment. *River Res. Appl.* **2012**, *28*, 1609−1619.
(46) Shore, M.; Murphy, P. N. C.; Jordan, P.; Mellander, P. E.; Kelly-Quinn, M.; Cushen, M.; Mechan, S.; Shine, O.; Melland, A. R. Evaluation of a surface hydrological connectivity index in agricultural catchments. *Environ. Model. Software* **2013**, *47*, 7−15.
(47) Ockenden, M. C.; Deasy, C.; Quinton, J. N.; Surridge, B.; Stoate, C. Keeping agricultural soil out of rivers: Evidence of sediment and nutrient accumulation within field wetlands in the UK. *J. Environ. Manage.* **2014**, *135*, 54−62.
(48) Tuohy, P.; Humphreys, J.; Holden, N. M.; Fenton, O. Mole drain performance in a clay loam soil in Ireland. *Acta Agric. Scand., Sect. B* **2015**, *65* (sup1), 2−13.
(49) Owens, P. N.; Duzant, J. H.; Deeks, L. K.; Wood, G. A.; Morgan, R. P. C.; Collins, A. J. Evaluation of contrasting buffer features within an agricultural landscape for reducing sediment and sediment-associated phosphorus delivery to surface waters. *Soil Use Manage.* **2007**, *23*, 165−175.
(50) Vinten, A. J. A.; Loades, K.; Addy, S.; Richards, S.; Stutter, M.; Cook, Y.; Watson, H.; Taylor, C.; Abel, C.; Baggaley, N.; Ritchie, R.; Jeffrey, W. Reprint of: Assessment of the use of sediment fences for control of erosion and sediment phosphorus loss after potato harvesting on sloping land. *Sci. Total Environ.* **2014**, *468−469*, 1234−1244.
(51) Steele-Dunne, S.; Lynch, P.; McGrath, R.; Semmler, T.; Wang, S.; Hanafin, J.; Nolan, P. The impacts of climate change on hydrology in Ireland. *J. Hydrol.* **2008**, *356* (1−2), 28−45.

DOI: 10.1021/acs.est.5b04573
Environ. Sci. Technol. XXXX, XXX, XXX−XXX

Appendix 3

J Soils Sediments (2015) 15:2101–2116
DOI 10.1007/s11368-015-1123-5

ADVANCES IN SEDIMENT FINGERPRINTING

Uncertainty-based assessment of tracer selection, tracer non-conservativeness and multiple solutions in sediment fingerprinting using synthetic and field data

Sophie C. Sherriff[1,2,3] · Stewart W. Franks[3] · John S. Rowan[2] · Owen Fenton[1] · Daire Ó'hUallacháin[1]

Received: 8 August 2014 / Accepted: 19 March 2015 / Published online: 2 April 2015

Abstract
Purpose Modification of sediment properties used in fingerprinting applications occurs along transport pathways as a result of particle size and organic matter enrichment/depletion, and geochemical transformations. Statistical approaches have been widely used to correct for enrichment and depletion, but detection of, and the un-mixing errors and uncertainties that arise from non-conservative behaviour remains under-recognised. Additionally, the over-determined nature of sediment fingerprint un-mixing models results in a range of potential solutions which are yet to be formally assessed.
Materials and methods Synthetic source data comprising 50 tracers and four sources were 'mixed' to generate known target tracer compositions. Firstly, both conservative and deliberately corrupted tracer behaviours were processed by repeated un-mixing from the minimum permissible number of tracers (n=3) to the maximum (n=50) using the FR2000 model. Secondly, using a smaller synthetic dataset, one tracer was deliberately corrupted in a controlled way to determine the impact on results and the ability of the permutation version of the Monte-Carlo FR2000 un-mixing model to detect non-conservative behaviour. Finally, this approach, and the particular case of near equivalent (or equifinal) solutions, was applied to data from on-going sediment provenance studies in Ireland.
Results and discussion Uncertainty in source predictions was better reduced by increasing, rather than decreasing the number of tracers, therefore questioning the justification for tracer reduction strategies. Non-conservative behaviour negatively affected the accuracy of mean source predictions but had no significant effect on uncertainty. The degree of tracer corruption (−90 to +155 %) from the 'perfect' target value resulted in a wide range of source predictions. The applied permutation un-mixing model was successful at detecting and rejecting the corrupted tracer below −50 % and above +20 % corruption. The true corruption (the uncertainty bounds reported by prediction at the upper and lower levels) was, therefore, significantly improved. The methodology to examine multiple solutions identified reasonably consistent source predictions when applied to field data. The suitability of this technique on data with limited tracers and no particle-size or organic matter correction is, however, questionable and warrants further investigation.
Conclusions Tracer selection is a key stage in reliable sediment fingerprinting applications. Non-conservative behaviour results in inaccurate source group prediction. Existing studies may therefore require critical evaluation, particularly where small sample numbers are collected in systems where enrichment/depletion of source group signatures (particle size, organic effects and geochemical alteration) results in non-conservative tracer behaviour (corruption) during entrainment and transport or storage within sediment sinks.

Keywords Non-conservativeness · Provenance · Sediment fingerprinting · Uncertainty · Un-mixing

Responsible Editor: Hugh Smith

✉ Sophie C. Sherriff
sophie.sherriff@teagasc.ie

[1] Johnstown Castle Environment Research Centre, Teagasc, Wexford, Ireland

[2] School of the Environment, University of Dundee, Dundee DD1 4HN, Scotland, UK

[3] School of Engineering, University of Tasmania, Hobart, Tasmania, Australia

1 Introduction

Excessive fine sediment delivery to freshwaters can result in significant degradation of ecosystem quality in rivers and lakes worldwide (Bilotta and Brazier 2008). Cost-effective soil erosion and sediment mitigation strategies are required in contributing catchment areas to meet legislative water quality guidelines, e.g. the Water Framework Directive 2000/60/EC (European Union 2000). The efficacy of standard mitigation approaches can, however, be undermined by the presence of multiple sediment sources within the contributing catchment area (Walling 2005). Multiple factors including soil type, slope, precipitation, connectivity, hydrology and land-use influence the erosion, transport and delivery of sediments (Davis and Fox 2009; Vigiak et al. 2012; Fryirs 2013). Direct measurement of soil erosion and sediment transport processes is, however, resource intensive (Regan et al. 2012) and difficult to accurately scale-up to the catchment unit (Deasy et al. 2011). Identification of sediment provenance through sediment fingerprinting techniques offers an alternative empirical approach to guide soil and sediment management strategies (Foster and Lees 2000; Mukundan et al. 2010; Collins et al. 2012; Rowan et al. 2012). Sediment fingerprinting applications have increased rapidly over recent years (Koiter et al. 2013a; Walling 2013), to a range of environments, and spatial (<10 m^2 to >100, 000 km^2) and temporal scales (Pittam et al. 2009; D'Haen et al. 2012; Cooper et al. 2015).

The sediment fingerprinting approach assumes that the physical and chemical properties of soil particles are relatable between sources and the sediment mixture delivered downstream, i.e. the 'target', such as storm-derived suspended sediments, or local accumulations in sediment stores such as wetlands, floodplains and lakes. The upstream catchment is subdivided into multiple potential sources (or source group types), for example, land use (Gruszowski et al. 2003; Blake et al. 2012), lithology (Collins et al. 1998) or erosional processes (Fox and Papanicolaou 2008). Characterising the physico-chemical properties of sediment, or tracers, provides the basis to identify distinct signatures to statistically discriminate between different source groups (Foster and Lees 2000). Sediment tracers typically employed include geochemistry, mineral magnetics and environmental radionuclides. The contributions from each source are determined using statistically based un-mixing algorithms.

Predictions of source contributions are accompanied by an inherent uncertainty; a consequence of multiple uncertainty components such as the number of tracers, dimensionality, intra- versus inter-source variability and tracer analytical uncertainty (Franks and Rowan 2000; Small et al. 2002, 2004). The propagation of uncertainties through to the result prediction is made possible by Monte-Carlo-based modelling techniques (Franks and Rowan 2000; Cooper et al. 2015). The recognition of, and capacity to fully assess, these components of uncertainty has encouraged discussion and evaluation of research priorities to improve robustness of un-mixing results (Rowan et al. 2012; Laceby and Olley 2015; Nosrati et al. 2014). Two outstanding uncertainty components are the identification of an optimal tracer set for un-mixing and the impact of multiple solutions within a tracer set on source predictions.

The array of tracers available to a sediment fingerprinting application has increased as a result of improved analytical capabilities (more samples can be analysed for a greater number of tracers more rapidly), the benefit of using a multi-parameter approach and the endeavour to develop new tracer properties to improve source resolution (Walling et al. 1993; Martínez-Carreras et al. 2010; Blake et al. 2012; Walling 2013). Selection of the most valuable tracers (based on their physical relevance between source groups and reliability over the scale of assessment) offers opportunities to improve the cost-effectiveness of sediment fingerprinting and, hence, validate it as a routine management tool. Tracer generation, transport and conservativeness are, however, largely catchment specific, and to date, this has encouraged the use of statistical tracer reduction techniques to select an optimal un-mixing tracer set.

A widely adopted two-step tracer selection approach defines an 'optimal' tracer set for un-mixing based on source data (Collins et al. 1997). Firstly, the capacity of an individual tracer to differentiate between sources is statistically verified using, for example, the Kruskal-Wallis test. Furthermore, discriminant analysis determines the discrimination potential of multiple tracers to optimise the tracer set. Such statistical approaches have been criticised due to their statistical reliability and lack of physical relevance (Koiter et al. 2013b) that, however, remains an integral component of tracer selection strategies. Source optimisation does not assess target tracer values and is, therefore, at risk of being significantly impacted by non-conservative tracer issues. The veracity of source group contributions and associated uncertainty may, therefore, be negatively impacted.

Non-conservativeness between tracer values in sources compared to downstream target sediments can be separated into two categories. The first arise from particle-size effects involving both selective entrainment of fines and preferential deposition of the coarser fraction along the transport pathway and, therefore, incur no bio-geochemical alteration of tracer concentrations (Davis and Fox 2009; Koiter et al. 2013a; Walling 2013). The second equates to a true non-conservativeness, whereby biogeochemical processes alter the tracer concentration associated with particles (Mukundan et al. 2012). Physical processes, such as erosion and transport of particles, can selectively transport specific particle size classes and organic matter. Due to the greater specific surface area of finer particles and organic substances, these fractions are chemically more reactive and, therefore, can contain higher tracer

concentrations. This has been highlighted for geochemical (Horowitz 2003), mineral magnetic (Foster et al. 1998; Hatfield and Maher 2009) and radionuclide properties (Wilkinson et al. 2009; Parsons and Foster 2011).

In many studies, tracer signal integrity is assumed providing that the underlying selectivity processes can be quantified (Foster and Lees 2000). The impact of particle size selectivity is commonly reduced by restricting the particle size distribution (e.g. to <63 μm) by sieving to exclude the coarsest fraction. Uncertainty-based assessment by Small et al. (2004) determined the effect of particle size enrichment/depletion on individual tracer concentrations between source and target sediment samples, and tracer values were corrected according to tracer-specific surface area associations. Other studies have targeted specific particle size classes (Hatfield et al. 2008; Wilkinson et al. 2009) or chosen tracers which show less particle size dependency. While such investigations have contributed important insights into uncertainty reduction, their application has been limited by the comparative simplicity of linear correction factors (Collins et al. 1998) despite debates surrounding their appropriateness (Russell et al. 2001; Motha et al. 2004; Small et al. 2004; Smith and Blake 2014).

Biogeochemical transformation of tracers or 'true' non-conservativeness is suggested to introduce further uncertainty into source predictions. The likelihood of a tracer to undergo transformation is dependent upon its reactivity to biogeochemical processes, e.g. sorption, dissolution, precipitation, oxidation, reduction and the presence of environmental conditions facilitating transformation. Highly reactive elements, such as phosphorus and nitrogen, are readily cycled and/or subject to human amendments and are consequently unsuitable tracers. Robust, conservative tracers such as heavy metals are less susceptible to biogeochemical transformations, which, therefore, are more reliable tracers. A review of the processes underlying tracer transformations by Koiter et al. (2013a) highlighted the catchment and environment-specific nature of tracer generation and transformation potential, and therefore, the difficulties involved in assessing tracer data at the catchment scale. Additionally, Smith and Owens (2014) detected non-conservative behaviour of As and Se in sediments collected using time-integrated sediment samplers relative to local bed sediment samples. It is clear that the detection of non-conservative behaviour is problematic but of great importance to confidently determine sediment sources.

Existing approaches to identify non-conservative tracer behaviour compare target tracer values to source data. Target values have been assumed non-conservative where they fall outside of the range of individual source sample values (Mukundan et al. 2010; Smith and Blake 2014). A more stringent test by Collins et al. (2010) required target values to be within the range mean source values. Similarly, Collins et al. (2013) required target values, which had been pre-corrected for tracer discriminatory power, to lie within median source values. Additional limitations include the requirement for average tracer values, where multiple targets have been collected, to be contained by mean source values (Wilkinson et al. 2013). Smith and Blake (2014) removed tracers from analysis based on target tracer values exceeding the range of source tracer values. These non-conservative tracers were attributed to organic enrichment resulting from peaty soils and, in the case of Fe, Mn and Zn, to contamination from mining activity. The suitability of these methods is, however, unknown as it is plausible that non-conservative behaviour remains where tracers have been modified by an unquantifiable process, are uncorrected or wrongly corrected, or are affected by an undetectable error, i.e. analytical or sample contamination.

Franks and Rowan (2000) introduced a permutation algorithm based on Bayesian principles to identify non-informative tracers within a solution set. Tracers were considered non-informative or 'corrupt', where they did not contribute to a constrained solution; therefore, it considers uncertainty of the source predictions as well as model fit to select the most informative tracers. The procedure was applied to a synthetic dataset, whereby a target tracer value was artificially corrupted (to replicate random tracer non-conservative behaviour), successfully detected by the model and subsequently rejected by the user as a non-informative tracer. Krause et al. (2003) later applied the model to field data, whereby three tracers (Pb, Mn and Fe) were rejected by the model and determined non-conservative. Despite the dependence upon statistical methods, the rejection or inclusion of a tracer is user dependent; therefore, tracers identified for rejection can be assessed according to potential underlying physical processes or transformations. The utility of this algorithm for the detection of tracer non-conservativeness has since received little attention, however, but has potential to benefit tracer selection routines.

The permutation approach also provides an opportunity to assess the range of predictions possible within a large tracer set. The over-determined nature of un-mixing models means that subsets of the original tracer set provide multiple potential solutions. The uncertainties present in each tracer may result in multiple and equally likely subsets (i.e. similar model fit or similarly constrained results) but contrasting solutions (Rowan et al. 2000). These non-unique (also referred to as equifinal) solutions present the user with the need to justify the content of a tracer solution set and validate the predicted solution. Many authors have advocated the need to increase the number of tracers employed in un-mixing models (Small et al. 2004; Martínez-Carreras et al. 2008), which may require multiple solutions arising to be considered. The investigation of multiple solutions has not been approached systematically to date.

In this study, we use the FR2000 un-mixing model and the permutation algorithm (Franks and Rowan 2000) to determine

the impact of non-conservative tracers on source predictions and uncertainty, and assess tracer optimisation approaches. A methodology is also introduced to identify multiple solutions and to determine the impact of these on predictions of source contributions and associated uncertainty. Firstly, this was completed using a constrained synthetic dataset and, secondly, using field data.

2 Materials and methods

2.1 FR2000 un-mixing model

The FR2000 algorithm un-mixing approach is summarised as:

$$\begin{bmatrix} \bar{x}_{1,1} & \bar{x}_{1,2} & \cdots & \bar{x}_{1,n} \\ \bar{x}_{2,1} & \bar{x}_{2,2} & \cdots & \cdots \\ \cdots & \cdots & \cdots & \cdots \\ \bar{x}_{m,1} & \cdots & \cdots & \bar{x}_{m,n} \end{bmatrix} \begin{bmatrix} A_1 \\ A_2 \\ \vdots \\ A_n \end{bmatrix} = \begin{bmatrix} X_1 \\ X_2 \\ \vdots \\ X_m \end{bmatrix} + \begin{bmatrix} \varepsilon_1 \\ \varepsilon_2 \\ \vdots \\ \varepsilon_m \end{bmatrix} \quad (1)$$

and constrained by

$$\sum_{j=1}^{n} A_j = 1 \quad \text{where} 0 \le A_j \le 1 \quad (2)$$

where $\bar{x}_{i,j}$ is the estimated population mean, i is the trace property, j is the source group, n is the number of sources and m is the number of tracers, A_j is the fractional contribution of each source group, and ε_i is the sum of the least squares error associated with the prediction of the mixture tracer characteristic, X_i. Eq. (2) constrains the solution such that individual source contribution (A_j) must between 0 and 1, and all sources sum to 1.

The uncertainty in estimation of source contributions was described by the variance component of the Student's t-distribution $(\bar{\sigma}^2)$,

$$\bar{\sigma}^2 = \left(\frac{S}{\sqrt{d}} \right)^2 \quad (3)$$

where S is the sample standard deviation and d is the number of independent samples.

Uncertainties of sample means were propagated using Monte Carlo sampling. A mean probability distribution for each tracer value in the source groups and target sediment was derived from the input dataset. Source contributions were solved using the source and target probability distributions and solved using a least-squares SIMPLEX optimisation routine for 1000 realisations to obtain an optimised source group prediction distribution. The median source contribution was estimated, and 95% confidence intervals were calculated from the optimised frequency distribution.

2.2 Permutation algorithm

Identification of optimal tracer solution sets was approached using a permutation version of the FR2000 model. All possible tracer combinations that satisfy the minimum tracer number requirement, $m \ge n$-1, where m is the number of tracers required and n is the number of source to be un-mixed, were calculated within the algorithm. In the previous development of the tracer selection algorithm (Franks and Rowan 2000; Krause et al. 2003), all potential tracers were included in the first model permutation. Repetition of the algorithm with the sequential removal of each tracer, i.e. all combinations of m-1 tracers, was evaluated according to the sum of least squares error components of all realisations within a permutation:

$$\varepsilon_R = \sum_{i=1}^{m} \varepsilon_i \text{ where } \varepsilon_P = \sum_{k=1}^{K} \varepsilon_R \quad (4)$$

where ε_R is the total error of a realisation, ε_i is the sum of the least squares error for each sediment trace property and ε_P is the error associated with a specific permutation where K is the number of realisations. The preferential solution within a permutation realises the lowest ε_R. Consequently, the removal of the tracer which afforded this reduction is a candidate tracer for removal resulting from an improved least squares fit.

Comparison of solutions derived using tracers sets with decreasing tracer numbers is problematic because as the error term is not comparable between permutations with different numbers of tracers; consequently, an uncertainty index was developed to assess the relative uncertainty (U) of the derived source predictions for different tracer permutations:

$$U = \sum_{j=1}^{m} \left(\left(1 + q^{j}_{1-(0.5\alpha)} \right) - \left(1 + q^{j}_{(0.5\alpha)} \right) \right) / \left(1 + q^{j}_{0.5} \right) \quad (5)$$

where $q^{j}_{1-(0.5\alpha)}$ and $q^{j}_{(0.5\alpha)}$ are the $(1-\alpha)$% upper and lower confidence quantiles, and $q^{j}_{0.5}$ is the median quantile of predicted source contribution A_j. A constant is added to each quantile to negate the inflation of U where the median value approaches zero. Where U is reduced due to the removal of a tracer, the result is more constrained, and the tracer is permanently removed. If U increases due to the removal of a tracer, the result is less constrained, and therefore, the tracer cannot be rejected from the solution set. The process is repeated with m-2, m-3… tracers until U no longer decreases; this is the optimum tracer set.

In this study, the metrics first defined by Franks and Rowan (2000) were approached in a reversed structure. The first permutation included the minimum possible number of tracers to define the sources (m) with additional tracers sequentially added (m+1) into the solution set. Improvement on model fit (ε_P) and consequential impact on the uncertainty of target

sediment estimations (U) were used for verification, consistent with the previous approach. Where an added tracer contributed to a solution with the lowest mean square error and U is reduced as a result of its addition, it was retained. Subsequent permutations increase tracer number (m+2, m+3…) until the result possessed the lowest constraint, i.e. the addition of further tracers cause U to increase. Tracers not included in the optimal solution set were considered as corrupt as they contributed additional uncertainty to the solution set. The cause of this uncertainty could be further explored in relation to source characteristics or non-conservative behaviour.

2.3 Synthetic datasets

An input dataset comprising 50 tracers was synthetically assembled (Table 1). A range of mean source values (minimum and maximum) were entered into a random number generator; four random numbers within this range were assigned as the mean values for four sources, respectively. Similarly, the coefficient of variance (CV%) was randomly allocated within a range of values from 8 to 73 % (average 36 %). Normal Gaussian distributions describing the relevant mean and CV% were used to create individual samples. This normality assumption, although not realistic of sampled data in the majority of existing sediment fingerprinting studies, was considered as suitable to test model function with controlled input data. The number of samples at each source was similarly variable; sources 1–4 comprised 10, 21, 18 and 15 samples, respectively. Target values for each tracer were calculated according to pre-determined synthetic contributions: A_1=30 %, A_2=10 %, A_3=35 % and A_4=25 % and average source values according to Eq. (1). The un-mixing model, FR2000, was run multiple times employing initially three tracers and gradually increasing the number of tracers to the maximum number of 50 tracers with a 'perfect' solution. The target tracer value of one random tracer was subsequently 'corrupted', i.e. artificially modified to represent falsely corrected, or an uncorrected non-conservative tracer within the range of the relevant mean source tracer values and the un-mixing repeated.

A smaller dataset, comprising eight of the above 50 tracers, was processed using the permutation algorithm to determine the ability of the algorithm to detect non-conservative behaviour. The value of one tracer at the target was sequentially corrupted in steps of 5 % in positive and negative directions. The minimum and maximum level of corruption was constrained by the range of mean source values, i.e. where other techniques would be capable of detecting the non-conservative behaviour (Collins et al. 2010). Consequently, the range of corruption was −90 to +155 % of the original tracer value. For each result, the 'optimum' solution and associated uncertainty were recorded. The goodness of fit (GOF) was calculated for each corruption step using Eq. (6):

$$\mathrm{GOF} = \left\{1-\left(\left|C_i-\sum_{s=1}^{m} P_s S_{si}\right|\right)/C_i\right\}*100 \qquad (6)$$

The tracer selection procedure proposed by Collins et al. (1997) was additionally performed on the eight tracer dataset (with corrupted target tracer) and also using the FR2000 methodology to achieve optimum tracer sets. The Kruskal-Wallis H-test (SPSS v22) examined the discrimination capabilities of each tracer to distinguish between sources. Tracers that

Table 1 A 50 tracer synthetic dataset of randomly assigned mean source and coefficient of variance (CV%) values, perfect target tracer values and corrupted tracer value (tracer 3)

Tracer	Source 1		Source 2		Source 3		Source 4		Perfect target value (corrupt)
	Mean	CV%	Mean	CV%	Mean	CV%	Mean	CV%	
1	0.1	60.1	0.1	29.1	0.1	26.6	0.3	61.0	0.1
2	336.8	52.6	131.6	16.5	283.4	35.2	146.9	43.8	250.1
3	1.6	20.3	3.9	29.5	3.5	39.5	2.8	48.0	2.8 (3.1)
4	12.8	26.8	5.2	38.3	14.1	11.4	10.6	24.8	112.0
5	1127.3	38.5	281.6	29.0	486.4	27.1	1187.1	40.7	819.7
6	32.9	26.3	30.6	33.7	41.5	49.0	37.5	55.5	36.8
7	7.7	16.5	5.1	43.7	3.4	19.4	3.3	56.7	4.8
8	7.9	32.4	1.2	28.2	0.2	35.5	2.1	31.8	1.8
⋮	⋮	⋮	⋮	⋮	⋮	⋮	⋮	⋮	⋮
48	26.9	31.9	40.6	51.9	16.4	31.6	22.6	58.1	23.5
49	1.2	41.7	1.0	23.2	1.0	19.6	0.8	33.9	1.0
50	47.7	29.5	50.6	33.6	16.2	57.6	21.9	54.2	30.5

Testing of dataset with three tracers refers to tracer 1–3, five tracers 1–5, eight tracers 1–8, etc

exceeded a critical H-value of 7.598, dependent upon the number of sources and confidence interval, were retained for further statistical verification. Multiple discriminant analysis (MDA), step two, was performed on the remaining seven tracers passing stage one (SPSS v22). The stepwise test obtains an optimum set of tracers by minimising Wilks' Lambda. Default values were used for the partial F inclusion 3.84 and removal 2.71. The procedure continues until the maximum amount of discrimination can be obtained from the input tracers. Those retained are deemed the optimal tracer solution set for subsequent un-mixing.

2.4 Multiple solution methodology

Multiple solutions were explored using a simplistic four source, eight tracer synthetic dataset. In order to test the permutation algorithm, two solution sets were predetermined: Solution one, relating to tracers 1 to 4, had target values calculated according to contributions A_1=40 %, A_2=15 %, A_3=30 %, and A_4=15 %; and solution two, relating to tracers 5–8 and target values, was calculated according to contributions A_1=15 %, A_2=35 %, A_3=20 %, and A_4=30 % (Table 2). Each source contained 10 samples from a Gaussian distribution (CV=10 %).

All potential multiple solution combinations, assuming a maximum of two solutions, were explored. Each solution set must qualify against the minimum tracer requirement for source definition, i.e. $m \geq n$-1 (Table 3), and each tracer can only belong to one solution set. Combinations of multiple solutions were judged according to the combined solution error ε_S, i.e. the sum of error (ε_F) for each solution. Consistent with the FR2000 method, the combination with the lowest combined error is deemed the candidate multiple solution arrangement. By ensuring the combined error is the lowest, the model fit is preserved.

Table 2 Synthetic dataset with two pre-determined solutions

Tracer no.	Source 1	Source 2	Source 3	Source 4	Target
Subset 1	40 %	15 %	30 %	15 %	
1	0.49	0.22	0.33	0.13	0.35
2	1.95	1.21	0.76	1.61	1.43
3	5.57	2.19	8.72	4.03	5.78
4	42.98	49.63	39.88	73.16	47.57
Subset 2	15 %	35 %	20 %	30 %	
5	27.40	15.74	10.99	24.41	19.14
6	610.21	215.07	296.38	1172.45	577.82
7	50.11	17.54	33.47	26.80	28.39
8	118.30	178.90	128.44	163.20	155.01

Source values are true population means, and target tracer values are calculated according to pre-defined contribution ratios: solution one (tracers 1–4) and solution two (tracers 5–8)

Table 3 Examples of tracer subgroup combinations for common source and tracer numbers in un-mixing applications

		Tracers			
		6	7	8	9
Sources	3	3+3	3+4	4+4	4+5
		2+4	2+5	3+5	3+6
				2+2+2	2+7
	4	3+3	3+4	4+4	4+5
				3+5	3+6

Source prediction results using each multiple solution and the single solution (prediction reported by using all available tracers) were compared. Tracer subsets which reported contrasting source predictions from each other and the single solution were accepted as containing multiple solutions. Where these conditions are not met, i.e., both tracer subsets report similar source predictions to each other and the all tracer solution, the tracers can be assumed to be in agreement, and therefore, the single solution accepted as the most appropriate array of tracers.

2.5 Field data

Samples were collected from a small (~11 km^2) agricultural river catchment in south-east Ireland (described in detail as Grassland B in Shore et al. 2013). Sources were sampled according to prevalent land use characteristics: topsoils (n=34), subsoils (n=32), eroding channel banks (n=59), eroding open field drain banks (n=4), damaged road verges (n=43) and farm tracks (n=6). Target samples were collected using time integrated suspended sediment (TISS) samplers (Phillips et al. 2000) in the stream network at 6–12-week intervals from May 2012 to June 2013. In total, seven TISS samples were collected in July 12, September 12, January 13, February 13, April 13, May 13 and June 13. Samples were dried at <40 °C and source samples dry-sieved to standardise samples and approximately replicate in-stream suspended particle size (Walling et al. 2002). Particle size data from a selection of suspended sediment samples collected from the study catchment reported that the 90th percentile of the suspended sediment distribution was frequently over 63 μm (maximum 103 μm); therefore, samples were sieved to 125 μm.

For mineral magnetic analysis, samples were immobilised into 10-cc plastic containers using cling film and cotton wool. Magnetic susceptibility (χ), or concentration of magnetic minerals, was measured using a Bartington MS3B Dual Frequency sensor (Oxford, UK) at low (0.47 kHz) and high (4. kHz) frequency to report the mass-specific low field susceptibility (χ_{LF}), and frequency-dependent susceptibility ($\%\chi_{FD}$;$(\chi_{HF}-\chi_{LF})\times100$). Anhysteretic remanent magnetisation

(ARM) was induced using a Molspin AF demagnetiser (Newcastle, UK) with ARM attachment and normalised by the biasing field (31.84 Am^{-1}) to obtain the mass-specific ARM susceptibility (χ_{ARM}). Isothermal remanent magnetisation (IRM) was induced using a Magnetic Measurements 10 T Pulse Magnetiser (Aughton, UK). Samples for ARM and IRM were subsequently analysed using a Molspin 1A fluxgate magnetometer (Newcastle, UK). IRM was measured at a forward field of 1 T, here defined as the saturation isothermal remanent magnetisation (SIRM) and reverse fields of 40 mT, 100 mT and 300 mT. IRM data were converted into mass-specific measurements (10^{-5} Am^2 kg^{-1}). In total, six magnetic parameters were analysed: χ_{LF}, $\%\chi_{FD}$, χ_{ARM}, SIRM, IRM_{soft}, and IRM_{hard} (Table 4). IRM_{soft} and IRM_{hard} datasets were transformed to ensure all data were positive before statistical analysis. Geochemical elements Cd, Co, Cr, Cu, Mn, Ni, Pb and Zn were analysed using an Agilent ICP-OES (Santa Clara, US) following microwave-assisted acid-digestion (USEPA 1996).

3 Results and discussion

3.1 Impact of tracer non-conservativeness

Predicted source contributions, represented by the median and 95 % confidence intervals in perfect and corrupted synthetic datasets, are shown in Fig. 1. Where tracer numbers are limited, inaccurate predictions are reported for all four source groups for perfect and corrupted datasets. Predicted source contributions converge towards the pre-determined source proportions (represented by the dashed line) due to the increasing number of tracers used for un-mixing. In the perfect dataset, the uncertainty in the result prediction is solely a consequence of the source tracer data. As target tracer values were calculated as an exact value, additional uncertainty components, e.g. target variability or non-conservative tracer behaviour, were eliminated. The addition of further tracers, therefore, improves source dimensionality and definition which is beneficial to reduce prediction uncertainty (Small et al. 2004; Martínez-Carreras et al. 2008).

Confidence intervals of perfect and corrupt datasets at a specific tracer number indicate that the inclusion of a single corrupt tracer, even in large datasets, does not contribute a substantial increase in uncertainty. The cumulative uncertainty of all sources does increase despite individual sources showing more constrained solutions for the corrupt dataset compared to the perfect result. The median source predictions between perfect and corrupted datasets differ greatly at sources 1 and 3 which possess the largest proportion of the target sample. The impact of these results in a sediment management context should also be considered. Source 1, predetermined to be the dominant sediment source, is predicted to have a lesser contribution than all other sources until over 30 tracers (29 correct and one corrupt) are used. A corrupted 10 tracer dataset would indicate that sources two and three are priority management areas, therefore undermining the efficacy of management strategies should this phenomenon be replicated in a real dataset. Increasing the number of tracers is shown to alleviate the impact of non-conservative tracers. Non-conservative tracer behaviour crucially challenges the ability of mixing models to correctly define source contributions; consequently, strategies to better detect tracer non-conservativeness should be a research priority.

The repeated application of the permutation algorithm to a dataset with sequentially increasing corruption (positively and negatively) of one tracer showed that predicted source contributions were severely impacted (Fig. 2). Current methods to detect

Table 4 Summary of seven tracer source data (mean and coefficient of variance) and sediment target sample data collected at the catchment outlet of the 11 km^2 Grassland B study catchment (Ireland)

	Source samples						Sediment samples						
	Channel		Road		Field		July 12	September 12	January 13	February 13	April 13	May 13	June 13
	Mean	CV%	Mean	CV%	Mean	CV%							
χ_{ARM} (10^{-7} Am kg^{-1})	0.08	41	0.23	44	0.17	159	0.07	0.15	0.12	0.13	0.14	0.19	0.13
IRM_{soft} (10^{-5} Am^2 kg^{-1})	123.47	40	688.27	35	150.91	116	44.66[b]	119.31	125.88	130.96	114.36	200.26	237.02
Cd (mg kg^{-1})	0.27	45	0.18	67	0.20	170	0.69	1.51	0.51	1.15	1.38	1.33	1.31
Co (mg kg^{-1})	16.31	22	11.11	23	9.73	42	21.25	22.17	20.50	18.67	22.12	21.29	19.48
Cr (mg kg^{-1})	27.08	34	21.92	32	26.55	42	42.63	33.39	35.82	81.64[a]	37.11	34.09	87.57[a]
Ni (mg kg^{-1})	29.16	30	21.13	24	19.74	43	26.41	41.10	37.91	54.71	40.16	38.31	56.45
Zn (mg kg^{-1})	78.16	22	120.59	31	72.60	108	657.99[a]	197.83	151.20	133.37	154.04	196.44	232.58

[a] Values were detected as non-conservative in raw dataset

[b] Values detected as non-conservative using the permutation algorithm

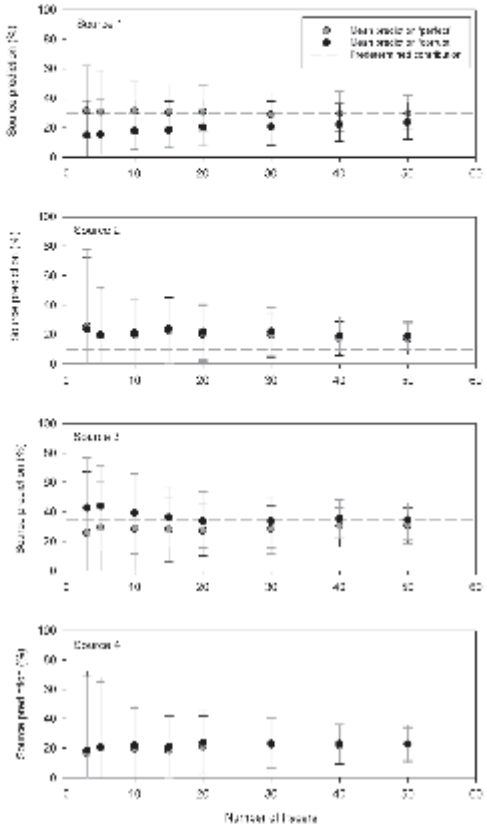

Fig. 1 Result predictions and 95 % confidence intervals for 'perfect' and 'corrupted' datasets using the FR2000 un-mixing model

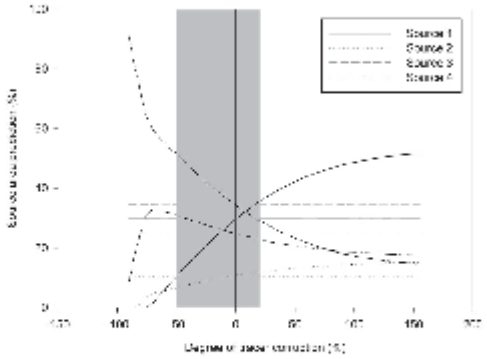

Fig. 2 Median source predictions resulting from the degree of corruption of one tracer. *Grey panel* represents the non-detection area of the FR2000 permutation methodology, and *grey lines* are source predictions following the rejection of the corrupted tracer

tracer non-conservativeness may therefore still expose source predictions to considerable loss of precision. The predicted source contributions are significantly different between the maximum positive and negative levels of corruption (−90 and +155 %), yet in all instances, the GOF (85–100 %) is comparable with other acceptable values in the literature (Motha et al. 2003; Thompson et al. 2013; Smith and Blake 2014).

Assessment of source prediction uncertainty using the permutation algorithm detected the corrupted tracer at less than −50 % and greater than +20 %. The range of incorrect source predictions is substantially reduced and, however, is not fully remedied (Fig. 2). Uncertainty values associated with the predictions at the minimum and maximum of the narrowed band of detection report a true prediction uncertainty, which has been previously un-quantified (Fig. 3a). Repeating this analysis for −90 and 155 % predictions (Fig. 3b) showed the improved confidence of source predictions as a result of using the FR2000 permutation approach.

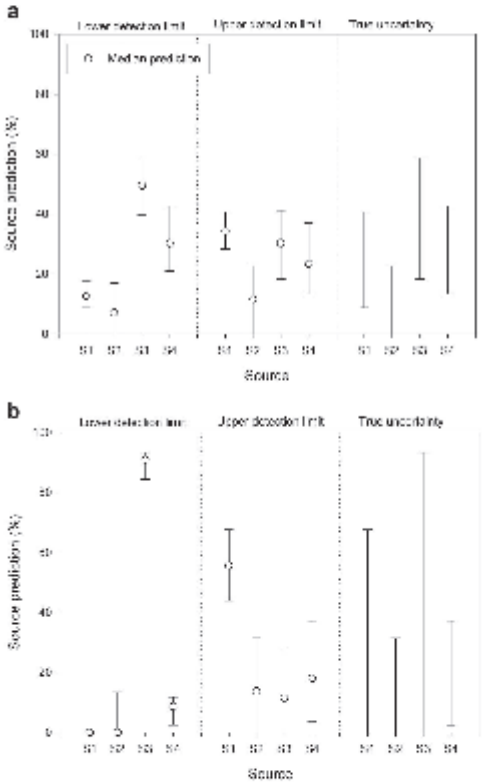

Fig. 3 True uncertainty of predicted source contributions using **a** FR2000 methodology and **b** a source sample-based tracer selection approach

The permutation approach is used here to assess a dataset representative of many previous sediment fingerprinting exercises in relation to input data, number of sources, number of samples, source variability and number of tracers. The scenario of tracer non-conservativeness presented is likely a simplification, i.e. one corrupted tracer and seven perfect tracers; however, the procedure outlines a viable technique for further investigation. The capacity of the algorithm to process large groups of tracers is limited due to computational requirements and processing time. Automation and expansion are on-going to facilitate further analysis of more complex scenarios (e.g. multiple corrupted tracers).

Tracer correction is a topic requiring greater prominence in sediment fingerprinting studies. The abilities of linear correction factors to adequately resolve selectivity processes have been commonly disputed and are suggested to contribute further to inaccuracies (Smith and Blake 2014). Improvements to the linear correction factor approach to resolve particle size and organic matter selectivity processes have been suggested (Russell et al. 2001; Small et al. 2004). However, the laborious nature of such approaches has prevented their wide-scale adoption. The impact of true non-conservative behaviour, through biogeochemical transformations, can be limited by selecting chemically conservative tracers. However, the inability to identify or control all catchment processes suggests that bio-geochemical non-conservativeness in tracer behaviour cannot be assured for all eventualities and therefore cannot be corrected. Statistical approaches to monitor known sources of prediction inaccuracies and uncertainty could be a useful addition to current sediment fingerprinting applications. The permutation approach applied here as a tracer corruption identification algorithm

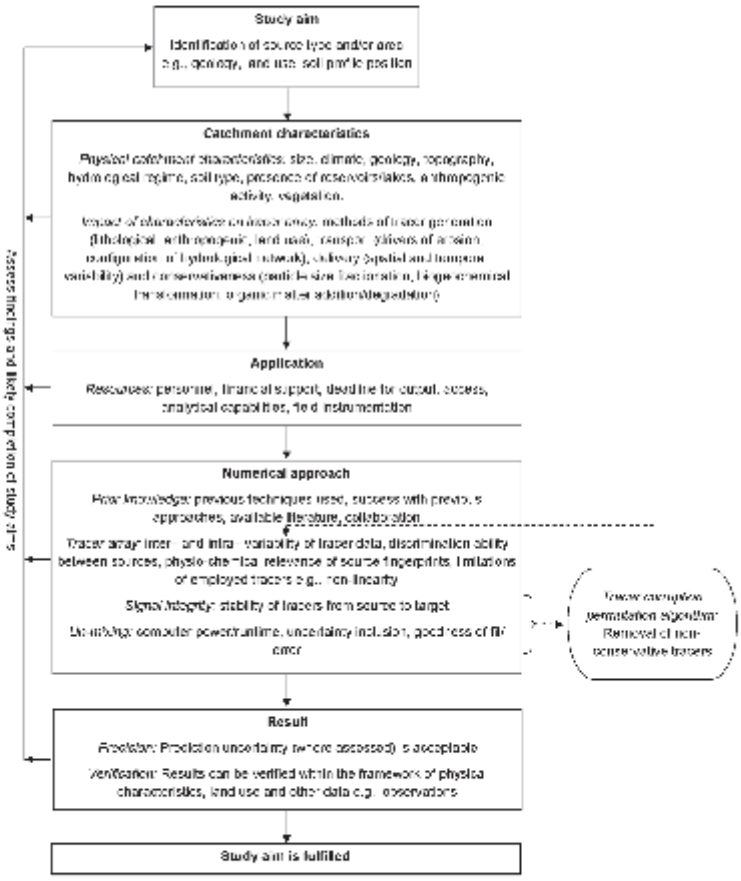

Fig. 4 Flow chart showing the role of the tracer corruption permutation algorithm within the wider sediment fingerprinting procedure

fits within the wider framework of sediment fingerprinting as a quality assurance tool (Fig. 4).

3.2 Definition of the 'optimum fingerprint'

The optimal fingerprint in an eight tracer dataset was explored using two strategies: tracer reduction using source data (e.g. Collins et al. 1997) and the uncertainty-based permutation algorithm of FR2000 (Franks and Rowan 2000). The source-based approach suggested an optimal six tracer solution for un-mixing. The corrupted target tracer was not rejected as, according to source data, the tracer passed both the Kruskal-Wallis and MDA tests. Two non-corrupted tracers were rejected; one failed the Kruskal-Wallis test and one failed to contribute any source discrimination in the MDA. Conversely, the permutation algorithm detected the corrupt tracer and considered the remaining seven tracers as an optimal tracer set. Un-mixing results using the two tracer sets are shown in Fig. 5. The source optimised predictions of median source contributions are incorrect, whereas, using the FR2000 optimisation approach, source predictions are highly accurate. Uncertainty in the permutation-based solution is also improved due to the additional, non-corrupt tracers despite their reduced discrimination capabilities.

To date, tracer reduction strategies have been widely adopted to define an optimal fingerprint (Collins et al. 1997; Collins and Walling 2002; D'Haen et al. 2012) but have been criticised due to their reliance upon statistical techniques. The use of MDA type analysis is essential to ensure that sources can be adequately distinguished; however, it assumes that additional tracers provide no further value. Multiple uncertainty studies (including data presented here) have expressed the importance of increasing tracer numbers to improve result constraint (Small et al. 2004; Martínez-Carreras et al. 2008) and better identify tracer non-conservativeness. The application of tracer reduction strategies has potential benefits; the reduction of analytical costs and computer processing time, however, potentially at the expense of uncertainty. Tracers which are inexpensive and rapidly analysed may offer some potential future direction to increase tracer numbers (Guzmán et al. 2013). However, employed tracers and statistical selection methodologies must ensure physical relevance to contribute meaningful results which require user experience and considerable knowledge of geochemical catchment process (Fox and Papanicolaou 2008; Koiter et al 2013b).

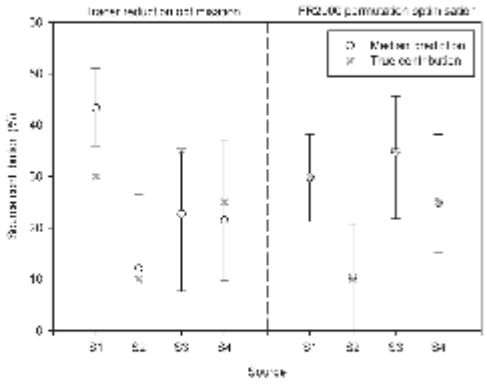

Fig. 5 Prediction and uncertainty un-mixing results of tracer sets selected by 'tracer reduction' (*left*) and FR2000 permutation approach (*right*)

3.3 Multiple solutions

The permutation algorithm was successfully applied to explore near-equivalent, or non-unique tracer solution sets termed 'multiple solutions' (Fig. 6). The combinations of tracer subsets selected by the model reflected the predetermined source groups and, consequently, the allocated median source contributions. Due to the smaller number of tracers employed to describe each solution, the uncertainty envelopes are wider than the all tracer solution.

3.4 Identification of tracer corruption and multiple solutions in field data

Fourteen tracers were available for un-mixing analysis; however, due to the limitations of computer power, run time and result processing time, a lesser number of tracers were required to conduct the permutation algorithm. Tracers were, therefore, assessed using the source-based tracer selection procedure to reduce the tracer set whilst preserving discrimination capacity. Based on the assessment of the six sampled source groups, the Kruskal-Wallis test showed that all tracers were

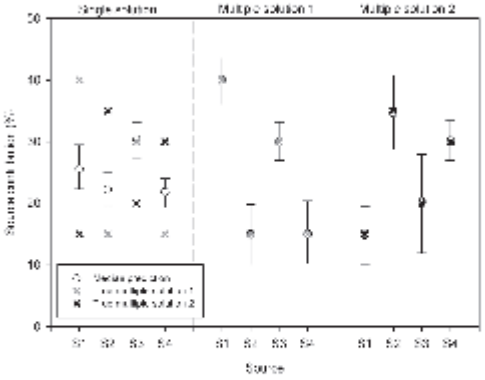

Fig. 6 Results of uncertainty inclusive un-mixing of multiple solution dataset showing the all tracer solution (*left*) and multiple solution sets (*right*)

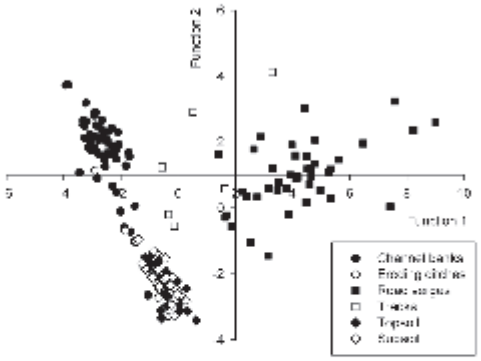

Fig. 7 Result of multiple discriminant analysis for six samples source groups. For un-mixing, sources were consolidated into three 'parent' groups: channel (*circles*), road (*squares*) and field (*diamonds*)

capable of distinguishing between sources ($p<0.05$). All tracers were further entered into MDA which resulted in 78.9 % discrimination between sources (Fig. 7). An improvement in source discrimination could be made by combining source groups.

Figure 7 shows source samples with similar underlying tracer generation and erosion processes—e.g. damaged road verges and tracks, and channel banks and open field ditch banks—that occupy similar areas of space using the first two discriminant functions (describing 97 % of group centroid variance). Therefore, 'road' and 'channel' parent source groups were constructed from the bulked groups. Despite the theoretical differences underlying the generation of tracers at topsoils and subsoils, the tracer array had no capacity to distinguish these sources and were consequently bulked into a 'field' parent group. Collins and Walling (2007) were previously able to discriminate topsoils with the combined source of subsurface and channel banks in two agricultural river catchments in the UK. Similar discrimination in the study catchment is negated by a thick layer of marine clay at 2–3-m depth in the catchment lowlands (Mellander et al. 2014). Channel bank height was frequently >2 m, particularly in the mid to lower sections of the catchment; therefore, the clay layer was exposed in the actively eroding area where stream erosivity was greatest. Subsoil samples, captured at 40-cm depth, were too shallow to reflect the chemical signature of this layer. Discrimination between topsoils and subsoils could be improved by surface deposited tracers such as caesium-137 which have been valuable in other sediment fingerprinting studies (Gruszowski et al. 2003). Repeated MDA analysis of bulked source groups considerably improved discriminatory power of the tracer set to 94.7 %, which was achieved using a seven tracer dataset (χ_{ARM}, IRM_{soft}, Cd, Co, Cr, Ni and Zn). Particle size and organic matter correction were not used here in order to investigate raw data trends.

Soil mineral magnetic and geochemical source characteristics of the seven employed tracers (Table 4) reflect two main processes: anthropogenic additions and the vertical soil profile. The tracers χ_{ARM}, IRM_{soft}, and Zn were elevated in road sources reflecting the input of magnetic minerals and heavy metals from vehicles (Gruszowski et al. 2003). Appropriately, the channel banks reported the lowest mean value for mineral magnetic parameters due to the dominance of the heavy marine clay layer. The concentrations of Cd, Cu, Cr and Ni are highest in the channel sources; Smith and Blake (2014) related a higher Cr concentration in channel banks to a vertical weathering gradient where subsurface material is enriched in elements relative to surface material due to decreased weathering. This vertical weathering gradient may similarly occur here or, conversely, due to the change in soil type (the surface soil layer as opposed to the marine clay layer).

Field data were processed using the permutation algorithm, firstly to determine any non-conservative behaviour and secondly to explore multiple solutions. Non-conservative behaviour of Cr was detected in the raw dataset of February 13, June 13, and Zn at May 12 (Table 4) and was removed from analysis, as target tracer values were outside the range of source values. Non-conservative behaviour was detected in one sediment sample by the permutation algorithm (May 12) for IRM_{soft}. Although the value was within the range of individual source values, it was outside of the mean value of all sources; therefore, this non-conservative behaviour could have been detected without the algorithm using more stringent source-based methods (cf. Collins et al. 2010). The IRM_{soft} tracer represents the proportion of magnetically soft minerals, e.g. magnetite, shown here to be useful at discriminating road samples from channels and fields. This non-conservative behaviour may be due to a dilution effect due to an influx of magnetically 'hard' minerals. Following the removal of the non-conservative tracers, source discrimination for May 12 using five tracers was 88.3 %, February 13 and June 13 were 93.0 %, and all seven tracers resulted in 94.7 % discrimination.

The permutation algorithm to detect tracer non-conservativeness occasionally met a well constrained solution at low tracer numbers, i.e. two or three tracers, such that the addition of subsequent tracers increased the uncertainty. Based on tests using synthetic data presented here, this would suggest that all other tracers experience non-conservative behaviour which, considering the array of tracers employed here, is unlikely. Interestingly, the rejection of these tracers could be attributed to their source characteristics, for example, due to the increased dimensionality of data. For example, the September 12 sediment sample reported a well-constrained result using four tracers (IRM_{soft}, Co, Cr and Ni), and referring to Table 4, these tracers have the lowest CV% for field sources. The remaining tracers (χ_{ARM}, Cd and Zn) possessed greater CV% for field sources; therefore, the uncertainty was increased through their inclusion. It is plausible that

components of uncertainty in the source dataset may impact the capability of non-conservative tracer detection, and this is an area requiring further assessment.

Multiple solutions were detected in every target dataset (Table 5), and the un-mixing results for which are shown in Fig. 8a–g. The source discrimination capability of tracer subsets is reduced to 73–93 % due to the small number of tracers. The parameters forming each tracer set were reasonably consistent; χ_{ARM}, Cd and Zn were frequently grouped together reflecting the grouping of tracers with lower source variability (as previously discussed). Using these tracers, a larger proportion of sediment is attributed to road sources at the expense of the channel source. In all cases, both multiple solutions agree that field contributions are negligible. In the February 13 sample, Cr is omitted due to non-conservativeness, and Ni is instead grouped with χ_{ARM} and Zn indicating that Ni showed better agreement with the predicted source contributions than the alternative well-constrained solution set (otherwise, the 2+4 multiple solution would have reported the lowest combined error).

Confidence intervals were smaller for the tracer subset where source data were more constrained (IRM_{soft}, Co, Cr and Ni). In all cases, the source contributions predicted by this dataset are almost identical to the single solution, suggesting that the less constrained tracer set only marginally influences the all tracer solution and the tracer subset provides a highly accurate estimation of sediment sources in the study catchment.

Previous discussion in this study has suggested that using minimal tracer numbers is not appropriate to achieve constrained source predictions, particularly where tracer corrections have not been formally assessed, a decrease in source discrimination occurs or the physical relevance of tracers configurations cannot be validated. The current capacity of the model to process large datasets unearths difficulties in addressing these issues in the current study. However, the ability of the permutation algorithm to explore non-unique tracer solutions is an important advance for sediment fingerprinting applications to be further investigated. Additionally, in a sediment management context, the multiple and single solutions are in agreement that channels are the dominant sources of sediments. To determine the broad origin of sediment within a small catchment, a minimal number of conservative tracers would sufficiently complete the study aim. However, to distinguish between more sources, i.e. the original six sampled sources, the current array of tracers needs to be expanded.

Table 5 Combined error values for configurations of multiple solutions (optimum solutions are shown in italics) and tracer groupings based on optimal multiple solutions which correspond to multiple solution one and multiple solution two in Fig. 8a–g

TISS sample[a]	Combined error	Multiple solution sets						
		χ_{ARM}	IRM_{soft}	Cd	Co	Cr	Ni	Zn
May 12								
2+3	*1.4373**	*1*	*–*	*1*	*1*	*2*	*2*	*–*
September 12								
2+5	2.1994	2	1	2	1	1	1	2
3+4	*2.1907**							
January 13								
2+5	1.6600	2	1	2	1	1	1	2
3+4	*1.6518**							
February 13								
2+4	1.7639	1	2	1	2	–	2	1
3+3	*1.7455**							
April 13								
2+5	2.1428	2	1	2	1	1	1	2
3+4	*2.1367**							
May 13								
2+5	2.1441	2	1	2	1	1	1	2
3+4	*2.1285**							
June 13								
2+4	2.1056*	2	2	1	1	–	1	1
3+3	*2.2274*							

[a] Time-integrated sediment sampler

Fig. 8 Single and multiple solution sets results for source samples collected in: **a** July 12, **b** September 12, **c** January 13, **d** February 13, **e** April 13, **f** May 13 and **g** June 13. *Circle* shows median value and *bars* represent upper and lower 95 % confidence intervals; *CB*, *RD* and *FD* indicate channel, road and field sources, respectively

4 Conclusions

Uncertainty-inclusive sediment fingerprinting studies have facilitated a critical appraisal of current approaches and methodologies. In this study, we have shown that better accuracy and precision of results are achieved through maximising available tracer data. Tracer reduction exercises are disadvantageous towards achieving constrained result predictions and increase the sensitivity of results to non-conservative tracer behaviour. Non-conservative tracer behaviour and the methods used to correct tracer datasets and validate applied corrections require considerable attention. As the physical and biochemical processes governing tracer enrichment/depletion and transformation are tracer and environment specific, the correction factors require more thorough research. This study supports the notion that particle size and organic matter correction factors that are commonly used may be too coarse to sufficiently correct all tracers or could introduce further biases into the tracer set.

A Monte Carlo-based uncertainty-inclusive un-mixing algorithm was shown to provide a methodology to assess tracer non-conservativeness more precisely than techniques used to date for synthetic test data. At a critical degree of corruption, non-conservative tracers could be identified and subsequently rejected according to the constraint of uncertainty afforded on

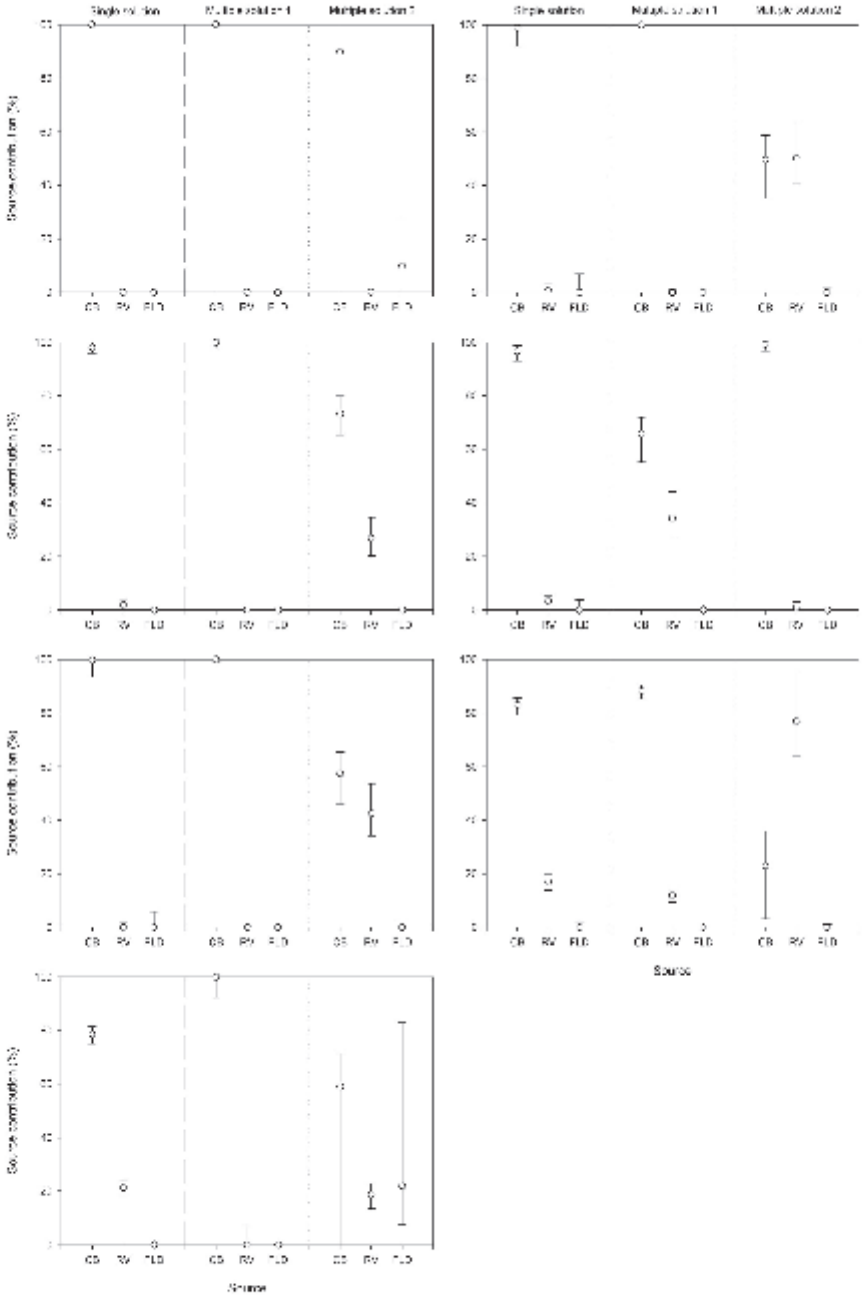
CB
RV
FLD
Source

the result. Consequently, the range of possible incorrect predictions was significantly reduced. Further analysis is required to determine the robustness of the technique when applied to more complex datasets, such as increased tracer and source numbers, or datasets with increased variability.

Near equivalent solutions were explored in synthetic datasets using the permutation algorithm which was successful at selecting the pre-determined source groups. The preferred multiple solutions predicted similar source contributions suggesting that tracers were consistent and likely to group according to source details. Application of the tracer non-conservative and multiple solution methodology to field data showed that tracer non-conservativeness could be detected; however, the capabilities of this algorithm may be affected by source data variability and non-normal distributions of source data. The validity of the multiple solution techniques is, in physical terms, questionable. The ability to analyse tracer groupings and the related un-mixing results has, however, not been approached to date and may improve knowledge of behavioural similarities between tracers.

Measures to standardise the sediment fingerprinting technique in order to constrain resources are problematic and may compromise efficacy. The reduction of samples collected and tracers utilised will likely increase the uncertainty of unmixing results such that no benefits are obtained over techniques such as catchment surveys. Nevertheless, maximising sample and tracer data can be considerably resource demanding suggesting that, in some cases, the cost of robust sediment fingerprinting may outweigh the benefits. Additionally, the advances of statistical approaches to optimise tracer arrays are considered as a deviation from physically based tracer selection approaches. The benefits of statistical approaches have the potential to be undermined by insufficient assessment of environmental significance; therefore, this is an essential precursor to the application of any statistical method. Finding approaches to corroborate the modelling results (perhaps through use of controlled mixture experiments e.g. Small et al. 2002, 2004) would greatly increase the robustness of evidence for river basin managers to implement mitigation measures.

Efficient mitigation measures are paramount to protect freshwater resources and improve the resilience and sustainability of contributing catchment areas. Sediment provenance techniques can, therefore, offer valuable insights to target cost-effective and source-specific mitigation strategies. Improved knowledge of underlying methodological techniques, such as appropriate tracer selection, is an essential step to ensure accurate and reliable provenance results that are consistently achieved.

Acknowledgments This study was funded by the Walsh Fellowship Programme, Teagasc, Ireland, allied to the University of Dundee, UK. Overseas placements facilitating this study were supported by the Walsh Fellowship Overseas Training Award, the Australian Bicentennial Scholarship Fund (Menzies Centre for Australian Studies, Kings College London), University of Tasmania, the University of Dundee and Dr. John Walden (University of St Andrews). Prof. Phil Jordan (Ulster University) and Dr. Alice Melland (University of Southern Queensland) are thanked for their comments and Linda Moloney-Finn (Teagasc) for performing geochemical analysis. We acknowledge support from the Teagasc Agricultural Catchments Programme (funded by the Department of Agriculture, Food and the Marine, Ireland) and the farmers and landowners of the study catchment. Thanks are extended to Prof. Des Walling and one anonymous reviewer for comments which greatly improved the manuscript.

References

Bilotta GS, Brazier RE (2008) Understanding the influence of suspended solids on water quality and aquatic biota. Water Res 42:2849–2861

Blake WH, Ficken KJ, Taylor P, Russell MA, Walling DE (2012) Tracing crop-specific sediment sources in agricultural catchments. Geomorphology 139–140:322–329

Collins AL, Walling DE (2002) Selecting fingerprint properties for discriminating potential suspended sediment sources in river basins. J Hydrol 261:218–244

Collins AL, Walling DE (2007) Sources of fine sediment recovered from the channel bed of lowland groundwater-fed catchments in the UK. Geomorphology 88:120–138

Collins AL, Walling DE, Leeks GJL (1997) Fingerprinting the origin of fluvial suspended sediment in larger river basins: combining assessment of spatial provenance and source type. Geogr Ann Ser A 79: 239–254

Collins AL, Walling DE, Leeks GJL (1998) Use of composite fingerprints to determine the provenance of the contemporary suspended sediment load transported by rivers. Earth Surf Process Landf 23:31–52

Collins AL, Walling DE, Webb L, King P (2010) Apportioning catchment scale sediment sources using a modified composite fingerprinting technique incorporating property weightings and prior information. Geoderma 155:249–261

Collins AL, Zhang Y, McChesney D, Walling DE, Haley SM, Smith P (2012) Sediment source tracing in a lowland agricultural catchment in southern England using a modified procedure combining statistical analysis and numerical modelling. Sci Total Environ 414:301–317

Collins AL, Williams LJ, Zhang Y, Marius M, Dungait JAJ, Smallman DJ, Dixon ER, Stringfellow A, Sear DA, Jones JI, Naden PS (2013) Catchment source contributions to the sediment-bound organic matter degrading salmonid spawning gravels in a lowland river, southern England. Sci Total Environ 456–457:181–195

Cooper RJ, Krueger T, Hiscock KM, Rawlins BG (2015) High-temporal resolution fluvial sediment source fingerprinting with uncertainty: a Bayesian approach. Earth Surf Process Landf 40:78–92

D'Haen K, Verstraeten G, Degryse P (2012) Fingerprinting historical fluvial sediment fluxes. Prog Phys Geogr 36:154–186

Davis C, Fox J (2009) Sediment fingerprinting: review of the method and future improvements for allocating nonpoint source pollution. J Environ Eng 135:490–504

Deasy C, Baxendale SA, Heathwaite AL, Ridall G, Hodgkinson R, Brazier RE (2011) Advancing understanding of runoff and sediment transfers in agricultural catchments through simultaneous observations across scales. Earth Surf Process Landf 36:1749–1760

European Union (2000) Establishing a framework for Community action in the field of water policy (Water Framework Directive) 2000/60/EC, EU, Brussels, L327

Foster IDL, Lees JA (2000) Tracers in geomorphology: theory and applications in tracing fine sediments. In: Foster IDL (ed) Tracers in geomorphology. Wiley, Chichester, pp 3–20
Foster IDL, Lees JA, Owens PN, Walling DE (1998) Mineral magnetic characterization of sediment sources from an analysis of lake and floodplain sediments in the catchments of the Old Mill reservoir and Slapton Ley, South Devon, UK. Earth Surf Process Landf 23:685–703
Fox JF, Papanicolaou AN (2008) An un-mixing model to study watershed erosion processes. Adv Water Resour 31:96–108
Franks SW, Rowan JS (2000) Multi-parameter fingerprinting of sediment sources: uncertainty estimation and tracer selection. In: Bentley LR, Sykes JF, Gray WG, Brebbia CA, Pinder GF (eds) Computational methods in water resources XIII. Balkema, Rotterdam, pp 1067–1074
Fryirs K (2013) (Dis)Connectivity in catchment sediment cascades: a fresh look at the sediment delivery problem. Earth Surf Process Landf 38:30–46
Gruszowski KE, Foster IDL, Lees JA, Charlesworth SM (2003) Sediment sources and transport pathways in a rural catchment, Herefordshire, UK. Hydrol Process 17:2665–2681
Guzmán G, Quinton J, Nearing M, Mabit L, Gómez J (2013) Sediment tracers in water erosion studies: current approaches and challenges. J Soils Sediments 13:816–833
Hatfield RG, Maher BA (2009) Fingerprinting upland sediment sources: particle size-specific magnetic linkages between soils, lake sediments and suspended sediments. Earth Surf Process Landf 34:1359–1373
Hatfield R, Maher B, Pates J, Barker P (2008) Sediment dynamics in an upland temperate catchment: changing sediment sources, rates and deposition. J Paleolimnol 40:1143–1158
Horowitz AL (2003) A primer on sediment-trace element chemistry, 2nd edn, USGS Report 91-76, p 136
Koiter AJ, Owens PN, Petticrew EL, Lobb DA (2013a) The behavioural characteristics of sediment properties and their implications for sediment fingerprinting as an approach for identifying sediment sources in river basins. Earth-Sci Rev 125:24–42
Koiter AJ, Lobb DA, Owens PN, Petticrew EL, Tiessen KD, Li S (2013b) Investigating the role of connectivity and scale in assessing the sources of sediment in an agricultural watershed in the Canadian prairies using sediment source fingerprinting. J Soils Sediments 13:1676–1691
Krause AK, Franks SW, Kalma JD, Loughran RJ, Rowan JS (2003) Multi-parameter fingerprinting of sediment deposition in a small gullied catchment in SE Australia. Catena 53:327–348
Laceby JP, Olley J (2015) An examination of geochemical modelling approaches to tracing sediment sources incorporating distribution mixing and elemental correlations. Hydrol Process 29:1669–1685
Martinez-Carreras N, Gallart F, Iffly JF, Pfister L, Walling DE, Krein A (2008) Uncertainty assessment in suspended sediment fingerprinting based on tracer mixing models: a case study from Luxembourg. In: Schmidt J, Cochrane T, Phillips T, Elliot C, Davies T, Basher L (eds) Sediment dynamics in changing environments, IAHS Publ 325. IAHS Press, Wallingford, pp 94–105
Martinez-Carreras N, Krein A, Gallart F, Iffly JF, Pfister L, Hoffmann L, Owens PN (2010) Assessment of different colour parameters for discriminating potential suspended sediment sources and provenance: a multi-scale study in Luxembourg. Geomorphology 118:118–129
Mellander P-E, Melland AR, Murphy PNC, Wall DP, Shortle G, Jordan P (2014) Coupling of surface water and groundwater nitrate-N dynamics in two permeable agricultural catchments. J Agric Sci 152:107–124
Motha JA, Wallbrink PJ, Hairsine PB, Grayson RB (2003) Determining the sources of suspended sediment in a forested catchment in southeastern Australia. Water Resour Res 39:1056
Motha JA, Wallbrink PJ, Hairsine PB, Grayson RB (2004) Unsealed roads as suspended sediment sources in an agricultural catchment in south-eastern Australia. J Hydrol 286:1–18
Mukundan R, Radcliffe DE, Ritchie JC, Risse LM, McKinley RA (2010) Sediment fingerprinting to determine the source of suspended sediment in a southern Piedmont stream. J Environ Qual 39:1328–1337
Mukundan R, Walling DE, Gellis AC, Slattery MC, Radcliffe DE (2012) Sediment source fingerprinting: transforming from a research tool to a management tool. JAWRA J Am Water Resour Assoc 48:1241–1257
Nosrati K, Govers G, Semmens BX, Ward EJ (2014) A mixing model to incorporate uncertainty in sediment fingerprinting. Geoderma 217–218:173–180
Parsons AJ, Foster IDL (2011) What can we learn about soil erosion from the use of ^{137}Cs? Earth-Sci Rev 108:101–113
Phillips JM, Russell MA, Walling DE (2000) Time-integrated sampling of fluvial suspended sediment: a simple methodology for small catchments. Hydrol Process 14:2589–2602
Pittam N, Foster I, Mighall T (2009) An integrated lake-catchment approach for determining sediment source changes at Aqualate Mere, Central England. J Paleolimnol 42:215–232
Regan JT, Fenton O, Healy MG (2012) A review of phosphorus and sediment release from Irish tillage soils, the methods used to quantify losses and the current state of mitigation practice. Biol Environ 112B:1–25
Rowan JS, Goodwill P, Franks SW (2000) Uncertainty estimation in fingerprinting suspended sediment sources. In: Foster IDL (ed) Tracers in geomorphology. Wiley, Chichester, pp 3–20
Rowan JS, Black S, Franks SW (2012) Sediment fingerprinting as an environmental forensics tool explaining cyanobacteria blooms in lakes. Appl Geogr 32:832–843
Russell MA, Walling DE, Hodgkinson RA (2001) Suspended sediment sources in two small lowland agricultural catchments in the UK. J Hydrol 252:1–24
Shore M, Murphy PNC, Jordan P, Mellander P-E, Kelly-Quinn M, Cushen M, Mechan S, Shine O, Melland AR (2013) Evaluation of a surface hydrological connectivity index in agricultural catchments. Environ Model Softw 47:7–15
Small IF, Rowan JS, Franks SW (2002) Quantitative sediment fingerprinting using a Bayesian uncertainty estimation framework. In: Dyer FJ, Thoms MC, Olley JM (eds) The structure, function and management implications of fluvial sedimentary systems, IAHS Publ 27. IAHS Press, Wallingford, pp 443–450
Small IF, Rowan JS, Franks SW, Wyatt A, Duck RW (2004) Bayesian sediment fingerprinting provides a robust tool for environmental forensic geoscience applications. Geol Soc Lond Spec Publ 232:207–213
Smith HG, Blake WH (2014) Sediment fingerprinting in agricultural catchments: a critical re-examination of source discrimination and data corrections. Geomorphology 204:177–191
Smith TA, Owens PN (2014) Flume- and field-based evaluation of a time-integrated suspended sediment sampler for the analysis of sediment properties. Earth Surf Process Landf 39:1197–1207
Thompson J, Cassidy R, Doody DG, Flynn R (2013) Predicting critical source areas of sediment in headwater catchments. Agric Ecosyst Environ 179:41–52
USEPA (1996) SW-846 Method 3052: microwave assisted acid digestion of siliceous and organically based matricies. U.S. Gov. Print Office, Washington DC
Vigiak O, Borselli L, Newham LTH, McInnes J, Roberts AM (2012) Comparison of conceptual landscape metrics to define hillslope-scale sediment delivery ratio. Geomorphology 138:74–88
Walling DE (2005) Tracing suspended sediment sources in catchments and river systems. Sci Total Environ 344:159–184
Walling DE (2013) The evolution of sediment source fingerprinting investigations in fluvial systems. J Soils Sediments 13:1658–1675

Walling DE, Woodward JC, Nicholas AP (1993) A multi-parameter approach to fingerprinting suspended-sediment sources. In: Peters NE, Hoehn E, Leibundgut C, Tase N, Walling DE (eds) Tracers in hydrology, IAHS Publ 215. IAHS Press, Wallingford, pp 329–337

Walling DE, Collins AL, McMellin GK (2002) Provenance of interstitial sediment retrieved from salmonid spawning gravels in England and Wales: a reconnaissance survey based on the fingerprinting approach. Environment Agency Technical Report W2-046/TR3, Environment Agency, Bristol, UK

Wilkinson SN, Wallbrink PJ, Hancock GJ, Blake WH, Shakesby RA, Doerr SH (2009) Fallout radionuclide tracers identify a switch in sediment sources and transport-limited sediment yield following wildfire in a eucalypt forest. Geomorphology 110:140–151

Wilkinson SN, Hancock GJ, Bartley R, Hawdon AA, Keen RJ (2013) Using sediment tracing to assess processes and spatial patterns of erosion in grazed rangelands, Burdekin River basin, Australia. Agric Ecosyst Environ 180:90–102